Endocytic Regulation of JAK/STAT Signalling

Katja L. Vogt

Submitted for the Degree
of Doctor of Philosophy at the
Biomedical Science Department,
University of Sheffield

February 2014

Table of Contents

List of Figures

List of Tables

Acknowledgements

I would like to thank both Professor Elizabeth Smythe and Doctor Martin P. Zeidler for allowing me to undertake this PhD Thesis within the frame of a collaborative effort between both of their laboratories at the Universities Sheffield. To Professor Smythe I wish to express my appreciation for the valuable opportunity to join her laboratory, offering me a topic of investigation at the cutting edge of biology. Importantly, I appreciate her belief on my intellectual and technical abilities through out the project. Also, I am grateful to her for the professional and personal guidance and support she has provided me with during this period. Likewise, I wish to express my gratitude to Doctor Zeidler for his help and advise undertaking my *in vivo* work and his expertise in JAK/STAT signalling.

I furthermore would like to thank my Advisors Professor David Strutt and Doctor Mohammed Nassar for our fruitful discussions and helpful suggestions regarding the project and the writing of this thesis. Our Advisor meetings and "Fly-meetings" helped me immensely not only to communicate my science, but also to critically think and analyse my data. My gratitude goes also to the whole fly-community at the University of Sheffield and beyond, for sharing reagents, protocols and expertise, especially the members of the Zeidler and Strutt lab, for their enormous patience, explaining *Drosophila* genetics and dissection methods to me.

The fantastic working atmosphere in the Smythe laboratories deserves so much more than the "Thank you guys" words I can express here. It has been priceless to come everyday to the laboratory not only because I love what I do, but also because it is great working within such a friendly team.

Special gratitude shall be awarded to my entire family for their believe in me, my parents for always standing behind me and encouraging me to write this Thesis, my grandparents and brothers for their permanent support and interest. I would like to express my special thanks to Avi for making me being part of your family and supporting me with all means you possess.

Thank you, Jorge, for your indefatigable devotion and enthusiasm in all aspects of our life. Your support and love is one of the most valuable things I possess. The other one is the joy of our son. Otto-Knox, I am so thankful that you are in my life. Your joyfulness enabled me to write this thesis.

Für mein Engelchen Otto-Knox

"Life is old there, older than the trees, younger than the mountains, blowing like a breeze"

John Denver

Abstract

A fundamental concept of the organisation and regulation of cellular communication is the control of signalling by endocytosis. The process of endocytic membrane trafficking is intimately and bidirectionally linked to cell signalling. Crucially, spatial compartmentalisation enables the cell to shuttle distinct signalling complexes into specific intracellular locations in order to elicit specific responses. This may be via the distribution of signals in subsets of endosomes and also their distinct localisation in micro-/ sub- domains (signalosomes). These signalosomes can influence distinct receptor signalling via a variety of exclusive downstream signalling pathways.

Within this thesis I investigated the role of endocytosis *in vivo* and showed that the knockdown of the Rab5 GEFs, RME-6 and Rabex5 distinctively influenced wing vein development. Unfortunately, I was not able to find a suitable *in vivo* system to address if endocytosis influences signalling differentially. Therefore, I established *in vitro* assays to measure Upd2 binding, uptake and activation of the JAK/STAT pathway in *Drosophila* tissue culture cells. I showed that ligand uptake is mediated by Clathrin and pathway activation is regulated by endocytosis not only quantitatively, but also qualitatively. I therefore tried to find the mechanism of how this qualitative signalling is achieved. My data shows that STAT92E phosphorylation was enhanced when ligand uptake was inhibited. Furthermore, the depletion of Clathrin or AP2 prevented JAK/STAT to signal, even though STAT92E phosphorylation still occurred at a conserved and for function crucial tyrosine residue.

Most studies investigating the interplay between signalling and endocytosis use artificial system by over expressing receptors, which was also marked as a potential concern of von Zastrow and Sorkin (2007). Even though Interferon endocytosis has been studied, the existence and importance of signalosomes within the JAK/STAT pathway still remains to be clarified. My research project allowed the evaluation of receptor signalling without ectopic expression of the receptor and points towards the existence of signalosomes. Investigating the modification of STAT92E closer I suggest a model to explain differential signalling by novel ways of JAK/STAT regulation. The data presented pave the way to a better understanding of JAK/STAT control. It also is the backbone of future investigations of finding the mechanism, which is responsible for the establishment of signalosomes and differential signalling.

CHAPTER 1. INTRODUCTION

More than 1 in 3 people will develop cancer during their lifetime. It is one of the most threatening diseases in Western society with a mortality rate of approximately 25% (Cancer Research UK, 2011). For a cell to become cancerous, it needs to undergo many alterations leading to a fast-growing and spreading disease.

There are eight common molecular features of cancer cells, which develop by analogy with Darwinian evolution: I) cells do not undergo apoptosis; II) cells have a limitless replicative potential; III) cells augment angiogenesis; IV) cells metastasise to invade other tissues; V) cells become self sufficient in growth signals; VI) cells become insensitive to growth inhibition signals; VII) cells reprogram their energy metabolism and VII) cells evade immune destruction (Hanahan and Weinberg, 2011). Naturally the body tries hard to avoid such an abnormal development of a normal cell. Cells contain a complex regulatory and maintenance network navigated by cell-cell signals to maintain cellular homeostasis. A balanced coordination, between a steady state condition and the possibility of the organism to react quickly and effectively to environmental changes is essential.

To achieve cell-cell communication one cell sends out a signal, a ligand, which will bind to a receptor on the receiving cell. The receptor cell transmits the signal through protein cascades, leading to an appropriate response, such as cellular proliferation or differentiation (Figure 1.1). Responses can be immediate and result in a direct effect on the cell or lead to changes in gene expression, which result in longer term responses to the initial signal. These signalling pathways control major aspects of organism development and homeostasis and are hence of great importance. In addition, relatively few signalling pathways are used repeatedly during development and in maintaining adult homeostasis, thus requiring very complex regulation. Cascades of protein modifications, including phosphorylation and ubiquitination, are one major regulatory mechanism (Alonso and Friedman, 2013; Doppler and Storz). Addressed in this study is another form of signal regulation. I analysed the control of signalling by spatial compartmentalisation of the endocytic pathway.

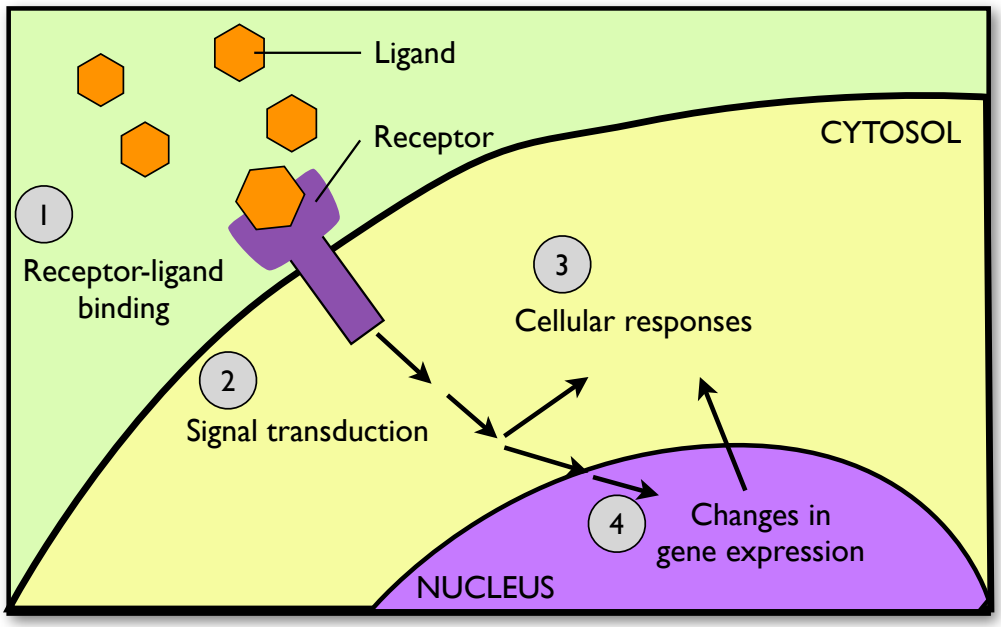

Figure 1.1: Cell signalling principle

A ligand sent from a donor cell binds to a receptor on the receiver cell (1), which leads to signal transduction (2) followed by cellular responses (3) and / or changes in gene expression (4), which leads ultimately as well to cellular response.

1.1 Overview of the endocytic pathway

Endocytosis is the process by which cells internalise molecules from the extra-cellular environment by actively engulfing them with their membrane. Nutrition, pathogen entry as well as receptor-regulation, which may modulate cellular signalling, including cell migration, neurotransmission and developmental processes, can be modulated by endocytosis (Palfy et al., 2012; Sorkin and von Zastrow, 2009). Therefore, the endocytic network is strictly structured, but highly plastic and, importantly, well regulated. Ingested material can be recycled, degraded, utilised or stored.

Cargo is internalised by small vesicles that bud from the cell surface. These vesicles may be coated or uncoated. Following uncoating, the vesicles fuse with the early endosome. This highly plastic compartment is the first point of cargo sorting and selection. Essentially, the decision is made whether cargo is either recycled back to the cell surface, via recycling endosomes (RE), or further travels though the endocytic pathway (Figure 1.3). Early endosomes mature into multi- vesicular bodies (MVB) or late endosomes by inward invagination of their membranes forming intraluminal vesicles (ILV). This is the second major selection point, since cargo can either be sorted into ILV, or once more recycled back to the surface (Hanson and Cashikar, 2012; Kelly

and Owen, 2011). Late endosomes fuse with primary lysosomes, which is the end-point of the endocytic pathway and degradation of internalised cargo occurs.

The protein composition of endocytic organelles is distinct and, in addition, the intravesicular pH drops along the trafficking pathway, from pH 6.5 (in early endosomes) to pH 5.5–4.5 in late endosomes and lysosomes. The reduction in pH is critical for sorting at each stage of the pathway (Kinouchi et al., 2011).

1.1.1 Portals of entry

1.1.1.1 Clathrin-dependent transport

One main route of endocytosis depends on Clathrin, which consist of a 190 kDa protein, the Clathrin heavy chain (CHC), and two 25 kD proteins, the Clathrin light chains (CLC) in vertebrates and one CLC in *Drosophila melanogaster*. These subunits self-polymerise to form three-legged trimers, which builds the main scaffold of the Clathrin coat. This structure allows for multiple interactions with the adaptor proteins (see section below). Clathrin is required for I) receptor-mediated and fluid-phase endocytosis from the plasma membrane to early endosomes (McMahon and Boucrot, 2011); II) the recycling of cargo back to the plasma membrane (Cardenas and Marengo, 2012); III) transport from the Trans Golgi Network (TGN) to endosomes (Kametaka and Waguri, 2012); IV) the efficient sorting of cargo into the degradative pathway (Raiborg et al., 2006) and V) Crosslinking of microtubules at the mitotic spindle (Royle, 2012).

At the plasma membrane, the Clathrin coat is assembled to form Clathrin-coated pits (CCPs) that incorporate cargo and then invaginate before pinching off (scission) to become Clathrin-coated vesicles (CCVs) (Faini et al., 2013).

1.1.1.2 Adaptor proteins and cargo selection

The Clathrin-coated pit captures its cargo concomitantly with Clathrin polymerisation and cargo load is dynamically monitored to prevent assembly and budding of empty vesicles (Aguet et al., 2013; Cocucci et al., 2012; Henry et al., 2012). The selection and capture of cargo depends on adaptor proteins, which recognise internalisation motifs in transmembrane cargo, linking it to the Clathrin lattice. Adaptors are able to bind Clathrin, cargo and phosphoinositides (PI) in the membrane. They represent the link of Clathrin to membranes. Classical heterotetrameric adaptor protein (AP) complexes are AP1 to AP5 (Hirst et al., 2013) and alternative adaptors include Arrestins, Epsin Disabled-2 and ARH (Reider and Wendland, 2011).

The recognition of the cargo can be mediated I) by protein modifications like ubiquitination via the Epsin adaptors (see also chapter 1.2.1 Huang et al., 2006; Mao et al., 2011) or II) by motifs, like the YXXØ or [DE]XXXL[LIM] (these motifs are recognised by different subunits of AP2), PxY (Arrestins) or [FY]XNPX[YF] (ARH). Interestingly, regulation by post translational modifications like phosphorylations at those sites is possible (Kittler et al., 2008). For example AP2, the most abundant sorting adaptor for CCPs, recognises the YXXØ motif on some cargo. AP2 is recruited to the plasma membrane by binding to phosphatidylinositide (4,5) P_2 (PI 4,5)P_2, which is enriched in the plasma membrane (Honing et al., 2005). AP2 binding is stabilised by cargo binding, enhanced by phosphorylation of the AP2 subunit μ2 (Semerdjieva et al., 2008). The final scission step to form a CCV is mediated by Dynamin, a large molecular weight GTPase, which constricts the neck of the invaginated CCP (Fabrowski et al., 2013).

In order for the vesicles to fuse with the early endosome they need to be uncoated. The un-coating of CCVs is mediated by the heat-shock cognate 70-kDa protein (Hsc70) and Auxillin/GAK (Brodsky, 2012), whereas the release of AP2 from CCVs is facilitated by dephosphorylation of μ2 and changes in the lipid composition, which results in the un-coating of the vesicle (Semerdjieva et al., 2008).

1.1.1.3 Clathrin-independent endocytosis

In addition to Clathrin-mediated endocytosis, there are other Clathrin-independent pathways. These include: the Caveolin-dependent pathway, macropinocytosis, GPI-AP-enriched early endosomal compartments (GEEC) pathway and Flotillin-dependent endocytosis. Caveolin is a cholesterol-binding protein and uptake takes place in a region enriched in cholesterol and glycolipids, via receptor recognition (Schroeder et al., 2010). Internalisation of large volumes is achieved by macropinocytosis (>1μm vesicles), which is mainly used for nutrition of the cell (Lim and Gleeson, 2011). The GEEC pathway is initiated by cholesterol–dependent recruitment and stabilisation of active Cdc42 on the plasma membrane (Chadda et al., 2007; Lakhan et al., 2009). A recently identified Clathrin-independent endocytosis mechanism is Flotillin–dependent endocytosis, which bears certain features of lipid rafts and seems to be involved in the uptake of the cholera toxin B, the basolateral uptake of GPI-anchored proteins and the trafficking of Wnt proteins in polarised cells (Ait-Slimane et al., 2009; Solis et al.,

2013). Data suggests, however, that it also plays a role as scaffold of signal transduction pathway components, aiding cellular signalling (Amaddii et al., 2012).

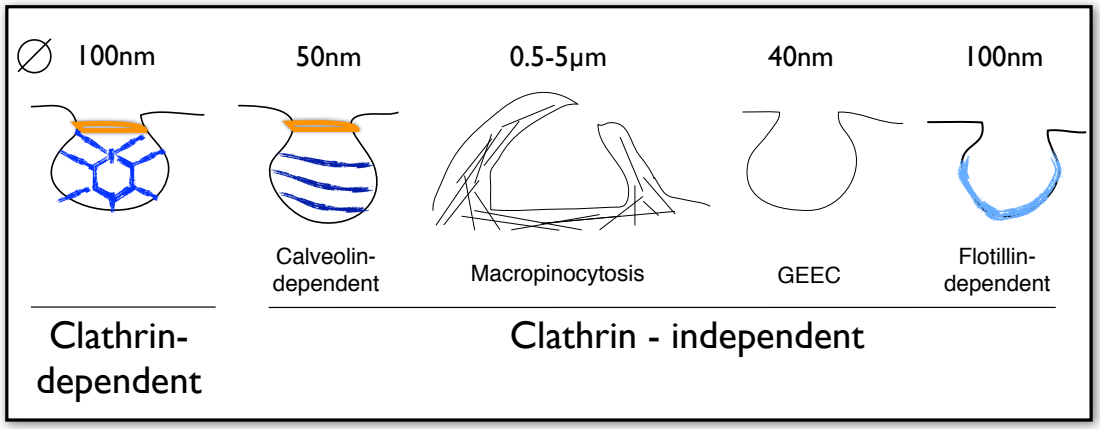

Figure 1.2 Endocytic internalisation pathways

The illustration shows major internalisation pathways: Clathrin dependent endocytosis; and Clathrin independent entry: Calveolin dependent, macropinocytosis, GEEC (GPI-AP-enriched early endosomal compartments) pathway and Flotillin dependent. Blue lines shall indicate the involvement of coat protein and orange GTPases.

1.1.2 Rab proteins regulate the endocytic pathway:

After vesicles bud from the plasma membrane by Clathrin-dependent or independent pathways, they fuse with the early endosome a process regulated by the small GTPase, Rab5.

Rab5 is a member of the family of Rab GTPases, which are major regulatory proteins of endocytic trafficking. There are greater than 60 family members in mammals, and 29 in *Drosophila melanogaster*, which belong due to their guanine nucleotide-dependent switch mechanism to the Ras superfamily (Jin et al., 2012; Pfeffer, 2013; Stenmark, 2009; Zerial and McBride, 2001). Rab GTPases are bound by GDP dissociation inhibitor (GDI), which stabilises their inactive form in the cytoplasm and more importantly chaperones their delivery to their cognate membranes, in which the specificity is probably facilitated by a Rab GDI displacement factor (Dirac-Svejstrup et al., 1997; Matsui et al., 1990; Sivars et al., 2003; Suh et al., 2010).

As a typical Rab GTPase, Rab5 cycles between a GTP bound (active) and a GDP bound (inactive) state. The activation of Rab5 is regulated by GTP exchange factors (GEFs: GDP→ GTP) and Rab5 returns into its inactive state (GDP-bound) through its own

GTPase activity, which is mediocre, but can be enhanced by the GTPase-activating proteins (GAPs: GTP→ GDP) (Pfeffer, 2013; Segev, 2001).

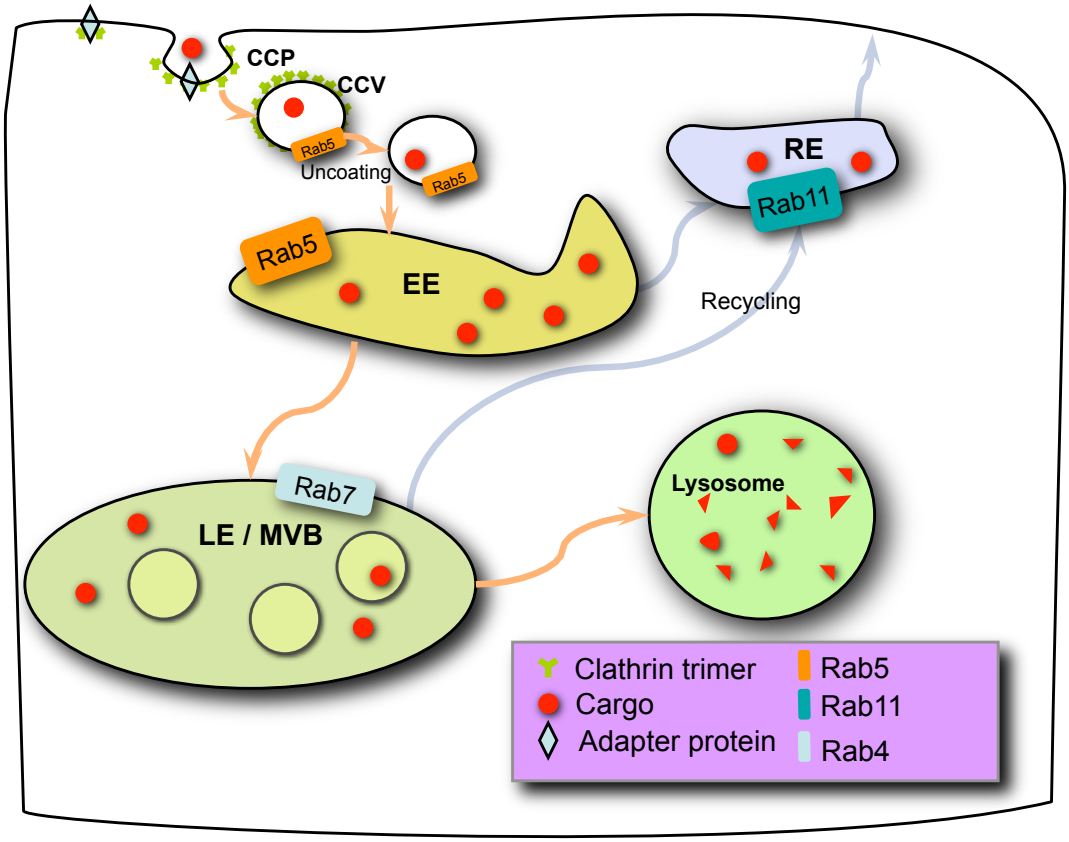

Figure 1.3: Endocytic trafficking

Clathrin-coated pits (CCP) are formed at the cell surface with the aid of adaptor proteins and cargo (red) is internalised when Clathrin-coated vesicles (CCV) are formed. After uncoating the vesicle fuses with the early endosome (EE) and the cargo can be sorted into the late endosome (LE) / multivesicular bodies (MVB) or to the recycling endosome (RE). The degradation of the cargo is then achieved in the lysosome if it is not recycled.

The endocytic machinery depends on Rabs in all its major functional steps (vesicle tethering, budding, motility and fusion). Hence, these GTPases function as coordinators of vesicle trafficking. Interestingly, the distinct endocytic compartments are characterised by specific Rabs: the late endosome is characterised by Rab7, Rab11 and / or Rab4 localise to the recycling endosome and the early endosome is typically enriched with Rab5 as illustrated in Figure 1.3 (Chavrier et al., 1990; Stenmark, 2009; Ullrich et al., 1996; van der Sluijs et al., 1992). The membrane specific recruitment of the various Rabs is mediated by their activating proteins, Rab5 GEFs {Blumer, 2013 #592;Semerdjieva, 2008 #238}

Rab5 was reported to localise to early endosomes, CCV and the plasma membrane. In addition to endosomal fusion, rab5 fulfils many essential functions in the early stages of trafficking including ligand selection into CCPs, un-coating, motility and signalling; consequently its regulation must be specifically tailored to each of its functions (Pfeffer, 2013; Stenmark, 2009). Rab5 in its active GTP conformation can interact with greater than 20 different cytosolic effectors (Christoforidis et al., 1999a; Christoforidis et al., 1999b; Christoforidis and Zerial, 2000).

1.1.3 Rab5 effectors determine the broad array of Rab5 functions

Rab proteins belong to one family of proteins and are highly homologous to each other. In contrast, Rab effectors are structurally highly divergent in order to fulfil a range of functions. Rab effectors are proteins, which are activated by the GTP-bound form of their specific Rabs. The effectors of Rab5 allow it to regulate many functions on the early endocytic pathway. Here I introduce some of the most important functions of Rab5 effectors.

1.1.3.1 Tethering and membrane fusion

The tethering of vesicles to endosomes is a crucial mechanism to ensure that the vesicle reaches securely its destination. EEA1 is a rab5 effector, which acts to tether endocytic vesicles to early endosomes. In addition to binding Rab5, it binds also to Phosphoinositide 3 P (PtdIns3P), which is enriched in early endosomes. This bivalent binding of Rab5 effectors ensures a high level of specificity of Rab5, since it recruits its effectors to the specific site they are needed. Tethering of endocytic vesicles primes them for subsequent fusion (McBride et al., 1999; Ramanathan et al., 2013).

In addition, another Rab5 effector, Rabenosyn-5 and another vesicle protein, the vacuolar protein sorting-associated protein 45 (VPS45), interact directly on vesicle membranes to enable their fusion (Morrison et al., 2008; Nielsen et al., 2000). Furthermore, Rabankrin-5 was identified as a Rab5 effector, which regulated the fusion of EE structures (Schnatwinkel et al., 2004; Zhang et al., 2012).

1.1.3.2 Cargo sorting

Highly conserved, Rabenosyn-5 is one of the best-characterized Rab5 effectors, (Nielsen et al., 2000). Its association with early endosomes is dependent on bivalent interactions with Rab5- and PtdIns3P and it interacts with multiple endosomal proteins, thereby acting as a molecular bridge within the endocytic machinery (Rahajeng et al.,

2010). Rabenosyn-5 is in addition to Rab5, also a Rab4 binding partner and enables cargo to be sorted into and transported by the recycling route (de Renzis et al., 2002; Naslavsky et al., 2004). Moreover, it also regulates sorting of cargo for lysosomal degradation (Nielsen et al., 2000) and into specialised early endocytic structures (Navaroli et al., 2012).

1.1.3.3 Dynamics and development of endosomes

Examples for the participation of Rab5 in membrane identity are its effectors phosphatidylinositol 3-kinase, phosphatidylinositol 4-phosphatase and phosphatidylinositol 5-phosphatase, which mediate PtdIns phosphorylation and de-phosphorylation (Christoforidis et al., 1999b; Murray et al., 2002; Shin et al., 2005). PtdIns contribute to membrane identity by recruiting proteins, including other Rab5 effectors (see above). Hence, Rab5 effectors contribute to the lipid composition of membranes and take an active part in the dynamics and development of vesicles and endosomes. In addition it was recently postulated that Rabenkyrin-5 also controls the remodelling of the apical plasma membrane during epithelial morphogenesis (Fabrowski et al., 2013).

1.1.3.4 Rab5 effectors can generate positive feedback loops

Rab5 effectors can recruit and enhance Rab5. For example; Rabaptin5 can recruit the Rab5 GEF Rabex5 and together they build a Rab5-Rabex5-Rababtin-5 complex, which stabilises and stimulates Rab5 within a positive feedback loop on the early endosome. This leads to additional binding of Rabex5 and hence further activation of Rab5. (Horiuchi et al., 1997; Stenmark et al., 1995). The increase in Rab5-GTP on endosomes stimulates phosphatidylinositol 3-kinase to generate more PtdIns3P, further enhancing the positive feedback effect (Christoforidis et al., 1999b).

1.1.4 Rab5 GEFs

The Vsp9 domain is a common feature of Rab5 GTP exchange factors, which contains their GEF activity (Figure 1.4). In *Drosophila* there are four Rab5 GEFs, Rabex5, Alsin, Sprint (hRin1) and RME-6. In mammals there are additional isoforms, which increases this number to 11. The proteins are likely to be responsible for specific functions, since they are associated with different parts of the early endocytic pathway controlling unique trafficking pathways (Barr and Lambright, 2010; Carney et al., 2006).

1.1.4.1 Rabex5

The Rab5 GEF, Rabex5 (CG9139) is tightly associated with Rabaptin-5 and their interaction builds a positive feedback loop leading in the activation of Rab5 (section above). However, Rabex5 recruitment to Rab5 can be either direct through an early endosomal targeting domain (EET), or indirect via the recruitment of Rabaptin-5 (Zhu et al., 2007) (Figure 1.4). Furthermore, data suggest a model of a Rabaptin-5 independent Rabex5 recruitment to the early endosome with its EET domain, located in; it is postulated that Rabex5 is mono-ubiquitinated when located in the cytoplasm, but has a higher affinity to ubiquitinated receptors on the early endosome and changes upon binding to ubiquitin on receptors, located on the early endosome to its active state, activating Rab5 (Mattera and Bonifacino, 2008).

Additionally, the Rabex5-Rabaptin-5 complex is considered to regulate the traffic from the trans-Golgi network to endosomes (Mattera et al., 2003; McBride et al., 1999). Importantly, the complex is essential for early endosome homotypic fusion (Horiuchi et al., 1997; Lippe et al., 2001) and the maturation of early endosomes depends on a Rab22–Rabex5–Rab5 cascade. Rab22, a member of the Rab5 GTPase family, requires Rabex5, which activates Rab5 on early endocytic membranes (Zhu et al., 2009).

Next to its role in Rab5 activation, Rabex5 also regulates Ras by marking it with ubiquitin and thus preparing Ras for degradation. This results in the repression of ERk phosphorylation, which acts downstream of Ras (1.2.1, Xu et al., 2010; Yan et al., 2010) Rabex5 acts together with Rabaptin-5 as neoplastic tumour suppressors also on other signalling pathways, since their loss results in tissue overgrowth and upregulating of JNK and JAK/STAT signalling (1.4 & Thomas and Strutt, 2013).

1.1.4.2 Rin (Drosophila: Sprint)

The Ras interferin1 (Rin) family has three members, Rin1, 2 and 3, which are multi-functional proteins, carrying a Vps9 domain. They regulate the trafficking of receptor tyrosine kinases (RTK) in response to external stimuli. This regulation is Rab5 dependent. Importantly, Rin1 regulates specifically signalling receptors and housekeeping cargo receptor internalisation is not influenced by Rin1 (Barbieri et al., 2003). As illustrated in Figure 1.4 next to its Vps9 domain, Rin1 also contains a Ras binding domain, which is likely to be responsible for its specific function modulating signalling pathways like EGF, insulin and IL3 receptor signalling (section 1.2.1, Balaji and Colicelli, 2012; Balaji et al., 2013; Hunker et al., 2006a; Hunker et al., 2006b).

However, Rin1 depletion leads to an inhibition of endosome fusion, dependent on Rab5 and EEA1 and thus suggesting a more central role for Rin1 in the regulation of signalling by endocytosis (section 1.1.3.1 and Galvis et al., 2009).

The *Drosophila* Rin1 homologue is called Sprint (CG34414) and regulates RTK trafficking to allow proper cellular migration (Jekely et al., 2005). Additionally it enhances a ligand induced tissue overgrowth within the fly compound eye (Mukherjee et al., 2006). Even though discussed separately here, Rab5 GEFs interact with each other within the cell. For instances Rin1 recruits the Rabex5-Rababtin-5 complex to Rab5 on early endosomes (Hu et al., 2008; Xu et al., 2010).

1.1.4.3 Alsin

Another Rab5 GEF is Alsin (CG7158). There are two gene products ALS1 and 2 (Amyotrophic lateral sclerosis 1 and 2) in mammals and one homologue in *Drosophila*. If ALS2 is mutated, it is linked to neurodegenerative disease and mainly associated with neuronal cells, for review (Cai et al., 2008; Hadano et al., 2001). Alsin controls Rab5 and its function in endosome fusion, coordinates the activation of Rac1 and Rab5 and also affects the retrograde transport of vesicles containing activated receptors (Otomo et al., 2003; Topp et al., 2004). To be able to undertake these multiple functions, it contains several distinct domains including: a regulator of chromosome condensation 1 like domain (termed RLD), a diffuse B-cell lymphoma homology /pleckstrin homology (DH/PH) domain, and a Vps9 domain (Figure 1.4).

1.1.4.4 RME-6

The receptor-mediated endocytosis protein 6 (RME-6, or also referred to as Gapex5 or GAPVD1) is a 130KDa boig protein with a highly conserved N-terminal Ras-GAP related domain as well as a C-terminal Vps9 domain (Figure 1.4). The GEF has homologues in *D. melanogaster* (CG1657, here stated as dRME-6) and *C. elegans* (cRME-6), where it was first described and where it was shown to localise and physically link to CCPs (Sato et al., 2005). Human RME-6 (hRME-6) participates in the regulation of early endocytosis, since it was discovered to play a role in the un-coating of Clathrin-coated vesicles (Semerdjieva et al., 2008). It is recruited to Rab5 positive compartments upon insulin stimulation, where it activates Rab5 leading to PtdIns3P production (Lodhi et al., 2008). In addition, RME-6 can also act as an exchange factor for Rab31, influencing thus the mobilisation of the insulin receptor Glut4 from intracellular compartments (Lodhi et al., 2007).

Interestingly, GEFs have overlapping as well as distinct functions e.g Sato et al. showed in *C. elegans* that a Rabex5 and RME-6 double mutant is lethal, whereas single knockouts / knockdowns did not affect viability (Sato et al., 2005). However GEFs have specific roles in the trafficking process, e.g. RME-6 is necessary for Rab5 dependent Clathrin-uncoating of CCVs, whereas the knockdown of Rabex5 does not show an effect (Semerdjieva et al., 2008). Furthermore, recent data in the Smythe laboratory suggested that RME-6 participates in the regulation of signalling pathways, organising signalosomes in human umbilical vascular endothelial cells (Ferreira, et al in prep).

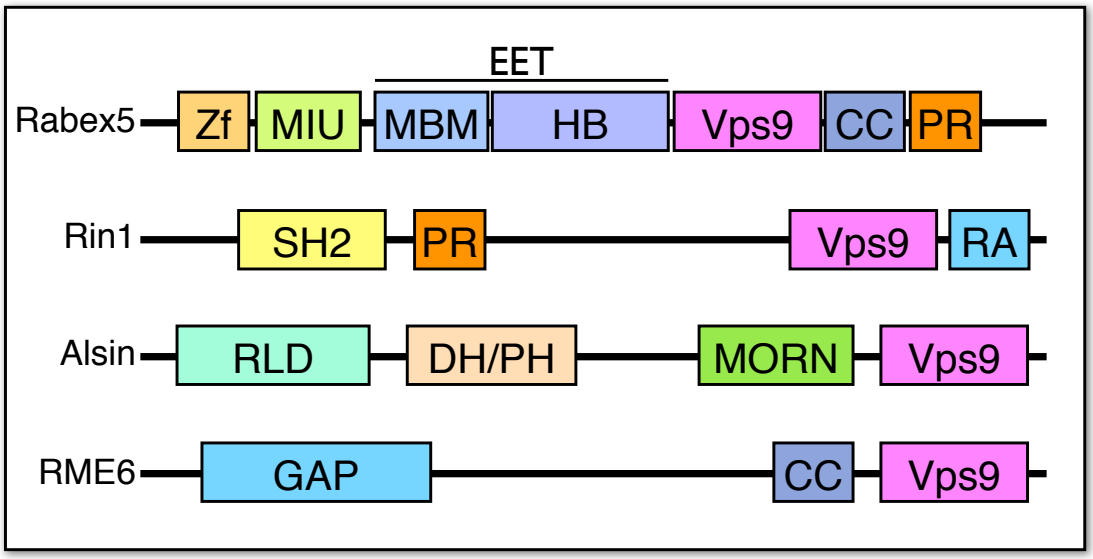

Figure 1.4: Overview of Rab5 GEFs structures

Schematic view of the four major Rab5 GEFs. Domain abbreviations as following: SH2: Src homology 2 domain, PR: proline rich domain, Vps9: Vps9 domain, RA: Ras binding domain; Zf: like zinc finger, MIU: Motif with ubiquitin, MBM: membrane binding motif, HB: Helical bundle EET: early endosome targeting domain, CC: Coiled coil domain, RLD: regulator of chromosome condensation like domain (3x), DH/PH: Diffuse B cell lymphoma homogoly/pleckstrin homology domain, MORN: membrane occupation and recognition nexus, GAP: Ras-GAP domain

1.1.5 Maturation of endosomes

Early endosomes mature into late endosomes by forming the MVBs containing structures with cisternal, tubular or multivesicular regions, forming a remarkably flexible trafficking compartment. The maturation process of MVB occurs gradually by losing early endosomes components and enrichment in their typical protein composition. and Yarden, 2011).

Typically the formation of MVBs is aided by the ESCRT machinery (Endosomal Sorting Complexes Required for Transport 0 to III). It regulates the movement of endocytic cargo from the early endosome to MVBs and facilitates further maturation.

The numbering of the complexes represents their order in which they act during endosomal maturation.

The first step in MVB formation is the recognition of ubiquitinated cargo by HRS, a PtdIns3P binding protein, which is recruited to early endosomes. Cargo destined for degradation is first sorted into flat Clathrin lattices on early endosomes and then moves into a HRS microdomain (Raiborg et al., 2006). HRS is a constituent of ESCRT-0. (Bache et al., 2003; Katzmann et al., 2003). It is clustered together with Clathrin establishing the docking point for the ESCRT-I complex by binding TSG101, a tumour suppressor protein that is a component ESCRT-I.

This second ESCRT complex consist of a number of proteins, including TSG101, VPS28, VPS37, and MVB12, whereby TSG101 plays a central role in ESCRT-I function and indeed its depletion leads to a coordinate loss of the entire complex (Bache et al., 2004). The ESCRT-I complex recruits ESCRT-II (Babst et al., 2002) and they are suggested to cooperate creating or stabilising the neck of the emerging ILV (Wollert and Hurley, 2010). Recruited by either ESCRT-I or –II, ESCRT-III is likely to be driving neck constriction and membrane scission as final complex of the ESCRT machinery (Hanson and Cashikar, 2012).

1.1.5.1 Late endocytic components

In general MVB develop further into late endosome, however invagination processes are not always necessary for late endosomal development. The exact temporal order of all involved proteins is still subject to further investigations. Nevertheless, it is commonly accepted that Rab7 is the main GTPase characterising late endosomes.

The maturation from early to late endosomes can be defined by the replacement of Rab5 by Rab7 and it is catalysed at least in part by SAND1/MON1–CCZ1 complex, which interrupts the Rab5 activating cycle, by replacing its activator and enables the recruitment of Rab7 to the site of endosomal maturation (Poteryaev et al., 2010; Rink et al., 2005).

Late endosomes lose tubular extensions and recycling capacity. They are enriched with triglycerides, cholesterol esters and selected phospholipids. In addition, membrane fusion specificity is changed by replacing the class C core vacuole/endosome tethering factor (CORVET) by the late endosomal/lysosomal homotypic fusion and vacuole protein sorting (HOPS) complex ((Solinger and Spang, 2013) for review). The interplay of CORVET and HOPS allows for specific tethering/fusion reaction and the late

endosome fuses subsequently with lysosomes and hybrid organelles, endolysosomes, are formed ((Huotari and Helenius, 2011) for review). The late endosome changes its pH from above 6 down to pH 4 as it becomes enriched in lysosomal hydrolases. Finally the compartment develops into the lysosome and cargo degradation occurs.

1.2 Signalling and endocytosis

During development a small number of signalling pathways are used repeatedly resulting in a fully functional organism. In addition there are many examples where a single growth factor can give rise to many different cellular behaviours depending on cell context (Igaki et al., 2009; Maurel-Zaffran et al., 2010). A key question is how cells manage to interpret a small number of signals to give so great a variety of cellular outputs. One emerging idea is that endocytosis provides a platform for regulation of signalling output (Miaczynska and Bar-Sagi, 2010; Palfy et al., 2012; von Zastrow and Sorkin, 2007)

1.2.1 EGF signalling pathway

The epidermal growth factor (EGF) signalling pathway is an example of a pathway that regulates several crucial processes, e.g. growth regulation, cellular survival, proliferation, and differentiation. In mammals the pathway is activated by ligands, like EGF, which binds the receptor and activates signalling. Ligand binding, followed by dimerisation and autophosphorylation is sufficient to activate several signal cascades e.g. the mitogen-activated protein kinase, ERK cascade, PtdIns-polyphosphate signalling or the cell cycle (Figure 1.5). This broad variety demands several positive and negative feedback loops, which are reviewed by Avraham and Yarden, 2011.

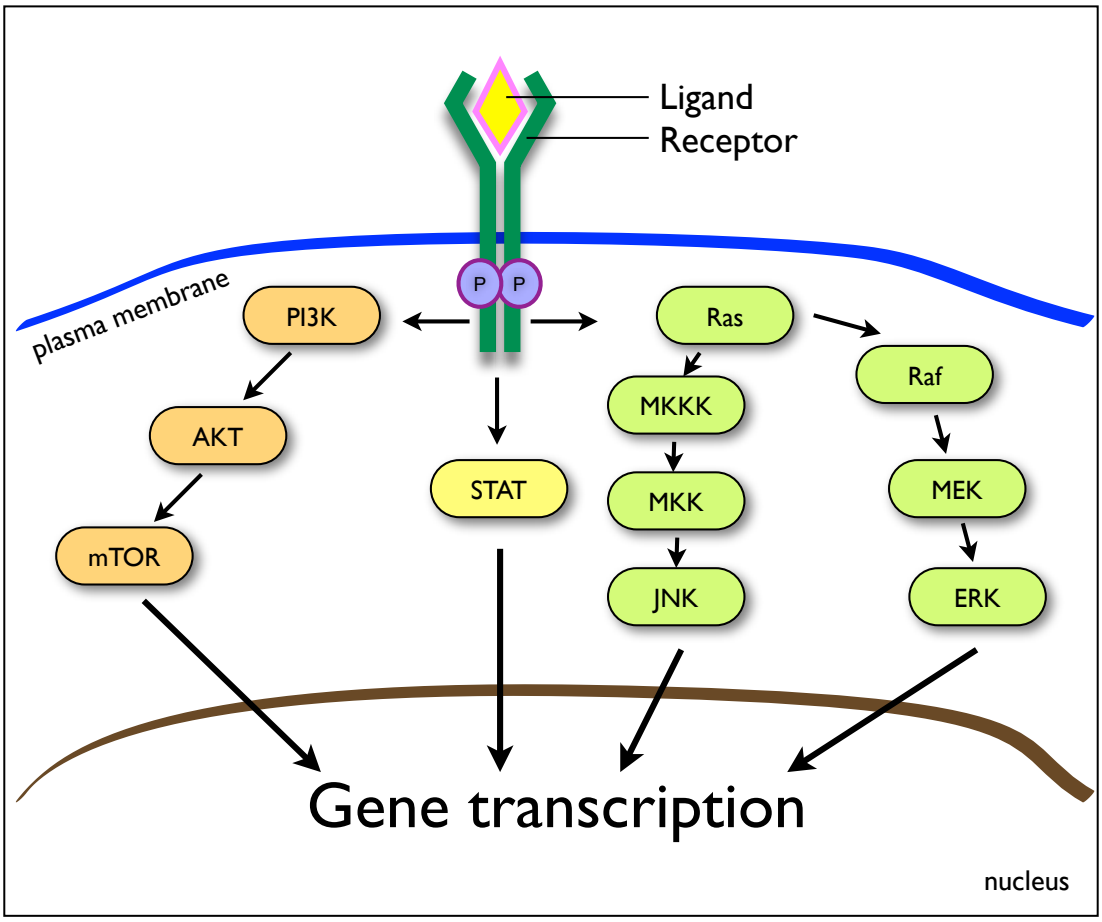

Figure 1.5: The EGFR signalling pathway

The EGFR receptor binds on the cell surface to its ligand (for instance EGF), is phosphorylated and ubiquitinated (not shown). The activation of EGFR can recruit several downstream pathways. Illustrated here is a simplified model of EGFR down stream pathways, including AKT signalling and STAT activation. Noticeably, the activation of Ras can lead to two distinct signalling cascades, which is the MAP kinase pathway, resulting this the activation of ERK and the JNK signalling pathway. Most activations steps are realised by phosphorylation of the signalling components.

1.2.1.1 EGFR endocytosis

It has been shown that a crucial way of regulation is the endocytosis of EGF receptor (EGFR), which can lead into its degradation or recycling (Sorkin and Goh, 2008). Hence EGF signals are either reduced or amplified, but the endocytic pathways can also lead to quantitatively different signalling (Vieira et al., 1996). The endocytic pathway enables EGF signalling to only activate a subset of its pluripotent outputs (Figure 1.5). The trafficking pathway contains pockets of discrete proteins and forms signalling domains, which are able to channel specific signals and result in distinct outputs. For instance by blocking Clathrin-mediated endocytosis the phosphorylation of ERK and PI3K was

downregulated, whereas PLCγ and SHC phosphorylation was enhanced (Vieira et al., 1996).

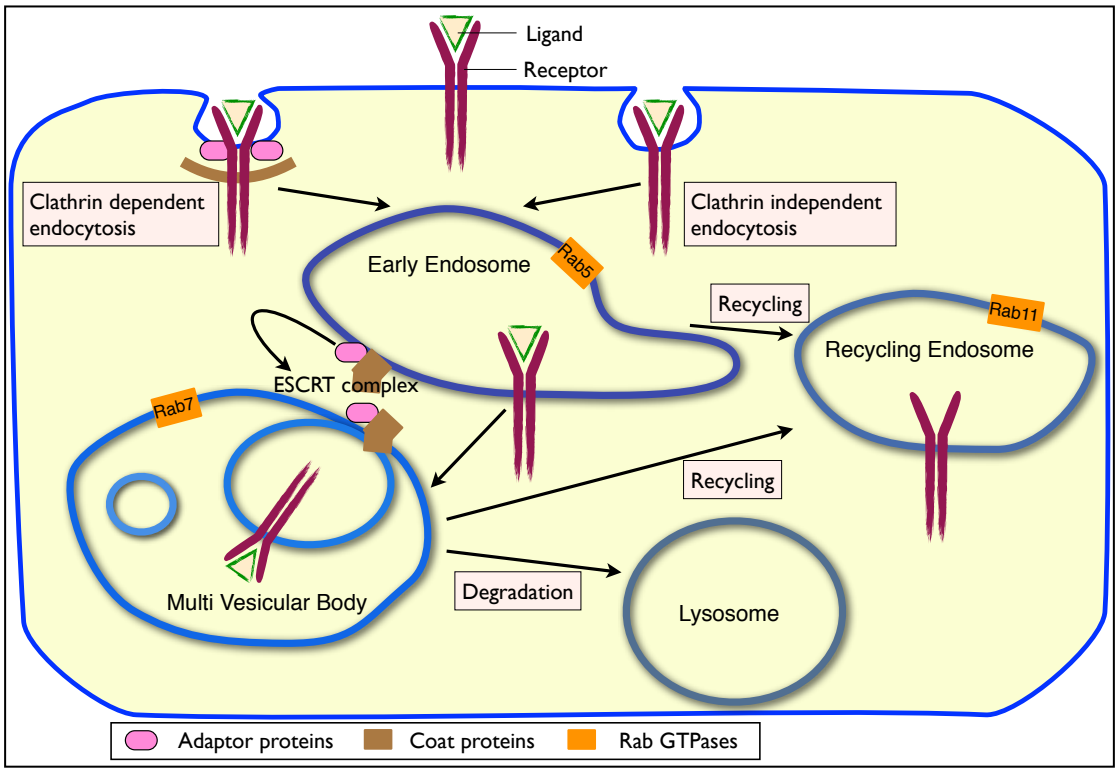

Figure 1.6: EGFR trafficking

Illustration of receptor mediated endocytosis and EGFR trafficking within the cell. The receptor (EGFR) is recognised by adaptor proteins (pink) and internalised either by Clathrin (brown)-dependent or independent endocytosis. After fusion of the vesicles with the early endosome this compartment works as a sorting station and EGFR is transported into the MVB and degraded via the lysosome or recycled. Note that each element is characterised by distinct Rab GTPases and signalling the EGFR can occur throughout the whole trafficking course.

The receptor is mainly internalised by CCV (approx. 85%), however Clathrin-independent mechanisms accelerate its uptake when ligand-saturation occurs (Arbouzova et al., 2006; Lanzetti et al., 2004; Puri et al., 2005; Sigismund et al., 2008, section 1.1.1 Figure 1.6), EGFR endocytosis is believed to be independent of its kinase activity, but requires the receptor to dimerise (Wang et al., 2005a).

The E3 ubiquitin ligase, Cbl is recruited by phosphorylated EGFR into CCPs and monoubiquitinates the receptor. Furthermore, the adaptor protein, Grb2 may regulate endocytosis by interacting directly with Cbl and subsequent EGFR polyubiquitination (Huang et al., 2004; Jiang and Sorkin, 2003; Stang et al., 2004). Structure function analyses of EGFR suggest that the ubiquitination of EGFR is not necessary for its

internalisation (Huang et al., 2007; Levkowitz et al., 1998). In contrast, more recent data suggest that EGFR ubiquitination contributes to receptor internalisation rates, however this post translational modification alone is not sufficient to allow cells to take up the receptor (Goh et al., 2010). The receptor is trafficked through the MVB, before it is degraded (Figure 1.6). Other post-translational modifications, e.g. acetylation, are believed to be important for the uptake of EGFR, which is in addition to Grb2 mediated by the adaptor AP2 (Goh et al., 2010).

1.2.1.2 EGFR signalosomes

One of the first indications of the existence of EGFR regulation by endocytosis was found by Vieira et al., 1996. They showed that when endocytosis was blocked there were different effects on downstream signalling, e.g. EGF- dependent proliferation was enhanced while, upon ligand stimulation, several proteins were either hyperphosphorylated or hypophosphorylated in endocytosis-deficient cells, suggesting that the EGFR endocytic trafficking was required to trigger distinct signalling pathways (Vieira et al., 1996). Although this became controversial with studies suggested that the endocytic pathway was merely a way for the cell to downregulate receptors (Clague and Urbe, 2001), other studies supported a role for endocytic regulation of signalling (Dubois et al., 2001; Incardona et al., 2002; Wu et al., 2001). Earlier controversies can be explained by the fact that the different studies used slightly different experimental settings, e.g. cell types, ligand concentration. These differences can be crucial in the analysis of the fine-tuned signalling by the endocytic pathway, since the particular microenvironments cells are in, play an important role in their signalling behaviour.

This also is likely to reflect cell and tissue specific differences *in vivo*. EGFR signalling in *D. melanogaster* is, for instance, positively and negatively regulated by endocytic trafficking depending on the developmental stage (Chanut-Delalande et al., 2010).

Evidence, furthermore, shows that even though EGFR signalling arises from the plasma membrane as well as internalised structures, signals from endosomes alone are sufficient to activate cellular EGFR functions (Pennock and Wang, 2003; Wang et al., 2002). In addition, only internalised receptors can activate AKT, whereas ERK activation already occurs from the cell surface and continues to signal from the early endosome (Goh et al., 2010), although the accumulation of phosphorylated ERK seems to be delayed when the pathway is activated from the plasma membrane (Wu et al., 2012).

In addition to the alterations of downstream signalling components like AKT and ERK phosphorylation EGFR activation was shown to phosphorylate the transcription factors c-jun and c-fos differently dependent on the location the activation occurred at. C-Fos was only phosphorylated when signals were triggered from the plasma membrane, whereas c-jun phosphorylation occurred independently on EFGR location (Wu et al., 2012). However, transcriptional profiling upon EGF stimulation indicated that EGFR signals occur robustly from the cell surface (Brankatschk et al., 2012). Within the same experiments it transpired, that although most EGFR signalling remained unchanged when endocytosis was blocked, this does not appear to be true for cytokine signalling. NF-kB and cytokine signalling seem to be down-regulated in HRS- or TSG101-depleted cells (Brankatschk et al., 2012). This suggests that the EGFR signalling tolerates changes in the location of the activation states of the kinases, whereas the NF-kB and cytokine signalling might be submitted to different regulation by the endocytic pathway (Brankatschk et al., 2012).

Dissecting the ESCRT machineries reveals that the termination of the signalling is independent of degradation (Bache et al., 2006). In addition to the establishment of signalling endosomes by early endocytic structures, components of the ESCRT III complex also participate in differential signal control. TSG101 depletion causes sustained pathway activation, whereas the depletion of hVps24 (ESCRT III component) does not have such an effect (Bache et al., 2006). EGFR signalling can be terminated, without the degradation of the receptor by the endocytic pathway. The ESCRT complexes fulfil thus distinct roles in EGFR trafficking, separating degradation from termination of signalling (Pons et al., 2008).

Not only traditional endocytic components regulate EGF signalling, but there is also evidence for a role for scaffolding proteins. For example, p14, builds a complex with the scaffold protein MP1, which is a MEK1 and ERK binding partner. P14 is an adaptor protein that facilitates the localisation of the MP1-p14 complex to late endosomes (Teis et al., 2006). *In vivo* analysis showed that next to p14 another adaptor protein, p18 is essential to anchor MEK1 to late endosomes, where ERK is activated from, by building the bridge to the MP1-p14 complex and MEK1 (Nada et al., 2009; Teis et al., 2006). In addition, recent computational models suggest that that differential regulation of ERK activation and EGFR endocytosis as a response to EGF concentrations both depend on scaffold proteins (Huang et al., 2011).

1.2.1.3 Ras

The small GTPase Ras is an essential protein that acts downstream of EGFR and other RTKs (Figure 1.5). It is involved in cell growth, differentiation and cell survival. A constitutive active mutation of Ras is the most common oncogene in human cancer, being mutated into a permanently active form in 20-25% of all human tumours. Ras regulation can also occur by the endocytic pathway ((Prior and Hancock, 2013 for review). This regulation appears to be isoform specific since H-Ras but not K-Ras signalling requires endocytosis and recycling (Roy et al., 2002). Importantly, Rab5 GEFs, RME-6 or Rin1, containing RasGAP, or Ras binding domains, respectively, can interact with Ras.

Ras directly influences the Rab5 GEF activity of Rin1 to facilitate the activation of Rab5 on early endosomes (Tall et al., 2001). In addition Rin1 promotes the Rab5-GTP-dependent recruitment of Rabex5-Rabaptin-5 complex to endosomal structures where Ras ubiquitination takes place. This ubiquitination is catalysed by Rabex5 itself and marks Ras for degradation. Hence further downstream signalling events, like the phosphorylation of ERK, are down regulated. This alternative way for attenuating Ras and RTK signalling suggest a fundamental role of Rabex5 mediated ubiquitination in pathway homeostasis *in vitro* and *in vivo* (Hu et al., 2008; Xu et al., 2010; Yan et al., 2010).

1.2.2 Subpopulations of endocytic structures enable discrete signalling

One way by which the fine nuances of differential signalling may be set up by the endocytic pathway is by channelling receptors through certain specific endocytic routes (Figure 1.6). It is already known that the uptake mechanism can influence the trafficking and signal output of receptors. For instance, specific G protein-coupled receptors (GPCRs) can internalise via different sub-populations of CCPs (Puthenveedu and von Zastrow, 2006); Phosphorylation of CLC is one way by which these different CCP populations are determined (Ferreira et al., 2012). Additionally, there are also sub-populations of endosomes.

1.2.2.1 APPL endosomes

EGFR, but not the house-keeping iron-uptake receptor transferrin, is internalised into a population of endosomes which is positive for the Rab5 effector, APPL. These endosomes are mostly localised close to the plasma membrane in contrast to EEA1 positive endosomes, which tend to be closer to the nucleus. In mammalian tissue culture

cells, most receptor tyrosine kinase (RTK) signalling occurs from APPL positive structures, including EGFR, which activation causes redistribution of these signalling compartments from peripheral locations to the cytoplasm and their components finally accumulate in the nucleus (Miaczynska et al., 2004; Varsano et al., 2006; Zoncu et al., 2009).

APPL positive structures were one of the first genuinely described signalosomes (Figure 1.7). I am here defining signalosomes as specialised domains and / or subsets of endosomes that are responsible for selective signalling. In an elegant series of experiments, Schenk et al. report that APPL1 regulates the activity of a subset of AKT and its downstream signalling specifically from an endosomal compartment in zebrafish, which is proposed to be a platform for the selective recruitment and activation of signalling components, since AKT signalling phosphorylates the downstream protein Gsk-3β (supports cell survival), but not Tsc2 (controls growth) (Schenck et al., 2008).

1.2.2.2 EEA1 endosomes

The second population of signalosomes are EEA1 positive early endosomes (Figure 1.7). The Rab5 effector, EEA1, serves as an obligate scaffold for ligand (specifically AngII) -induced Akt activation in early endosomes within the RTK signalling pathway. (Nazarewicz et al., 2010). Also the G-coupled α receptor (Gα) influences the maturation of EEA1, but not APPL endosomes. Importantly, Gαs determine the duration and strength of proliferative signalling from this compartment by prolonged EGFR signalling (Beas et al., 2012).

Additionally, the signalling endosome is able to enhance weak signals, as for C-Met, the receptor for hepatocyte growth factor signalling (Kermorgant and Parker, 2008). The strength of STAT3 phosphorylation can be modulated by the endocytic pathway. This is dependent on the ligand triggering activation. HGF, a c-Met ligand activates STAT3 is only weakly, but oncostatin M (OM), a JAK/STAT pathway ligand, strongly induces STAT3 phosphorylation and nuclear translocation. However, when the endocytic pathway is blocked, HGF cannot trigger STAT3 and ERK phosphorylation and anymore. Importantly, OM-induced STAT3 nuclear import still occurs, when endocytosis was blocked (Kermorgant and Parker, 2008). The authors of this study further suggest that both ERK and STAT3 signalling require the endocytosis of the HGF-bound c-Met receptor and that the signal strength differs between these two signalling events. Additionally they observed that the strong ERK signal can proceed via

cytosolic diffusion, whereas the weaker STAT3 signal required a microtubule-dependent perinuclear localization of c-Met (Kermorgant and Parker, 2008).

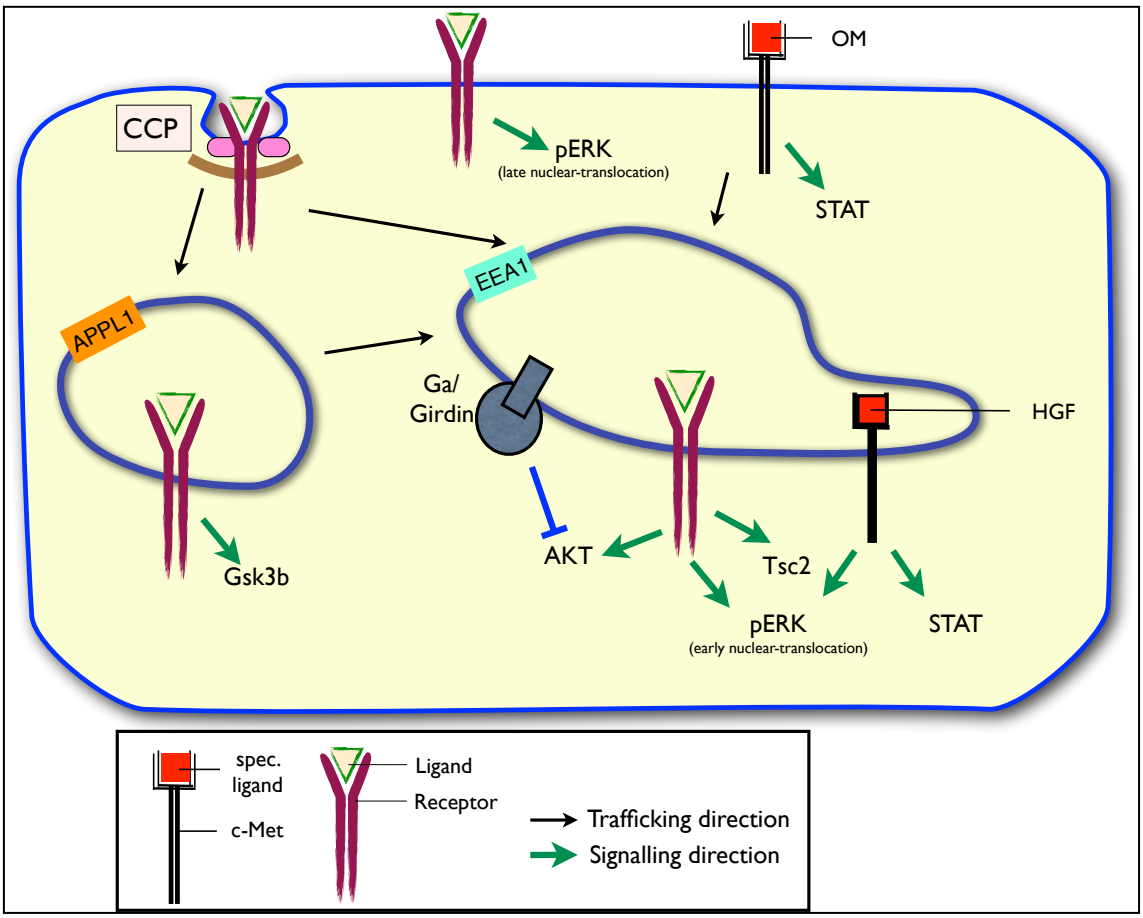

Figure 1.7: Examples of signalosomes

The illustration shows examples of signalling endosomes. Receptors are internalised by Clathrin-mediated endocytic and sorted into either EEA1 or APPL1 positive early endosomes. EGFR signalling causes early or late nuclear translocation of pERK depending on cellular compartment; AKT signalling either activates Gsk3b (from APPL1 positive early endosomes) or Tsc2 (from EEA1 positive early endosomes), Ga inhibits AKT signalling from EEA1 positive structures and c-Met activates STAT3 from the plasma membrane when activated with Om strongly, or from endosomes STAT3 weakly and ERK strongly when activated with HGF. For further details see section 1.2.2. Abbreviations as following: OM: Oncostatin M, Ga: Gα coupled receptor; HGF: Hepatocyte growth factor; pERK: phosphorylated ERK

1.2.3 Signalling affects the endocytic pathway

Even though most research focuses on how the endocytic pathway influences signalling, here I would like to point out that signalling pathways themselves are also able to modulate (their own) trafficking. They can affect trafficking, for example by enhancing virus entry via Clathrin-mediated endocytosis, increasing the number and internal

vesiculation of MBVs or modifying early endosome protein composition (Miaczynska et al., 2004; Pelkmans et al., 2005; White et al., 2006).

The ESCRT-0 component HRS, is phosphorylated, not only in a receptor-dependent manner, but also on receptor uptake into the cell (Urbe et al., 2000). Phosphorylation of HRS regulates its own degradation, which will thus impact on EGFR targeting to the degradative pathway (Stern et al., 2007).

In addition, not only the endocytic pathway influences signalling. Signalling molecules like H-Ras, Rac or Arf6 can stimulate Clathrin- independent endocytosis, inducing plasma membrane ruffling and macropinocytosis. (Donaldson et al., 2009 for review). This represent examples of the coupling of signalling pathways to endocytosis, establishing signalling compartments.

1.2.4 Signalosomes *in vivo*

Studies of signalosomes were long restricted to tissue culture. The growing interest and importance of these regulators propelled their studies *in vivo*.

HRS mutants show aberration of the endocytosis of several signal receptors, including EGFR in *Drosophila* (Jekely and Rorth, 2003). In addition, Schenk et al 2008 used zebrafish models to illustrate the differential signalling for APPL1 dependent Akt signalling, showing that microdomains on endosomes can influence the outcome of signals (Schenck et al., 2008).

1.3 Endocytosis in Drosophila

Many of the central organismal processes are conserved throughout the animal and plant kingdom. Endocytosis is such a fundamental requirement for all cells and *Drosophila melanogaster,* the common fruit fly, represents an excellent model to study this trafficking pathway. Some initial groundbreaking discoveries about endocytosis have been made in *Drosophila,* for instance due to the use of a temperature sensitive mutant of the *dynamin* gene (*shibire* in *Drosophila*). The role of Dynamin was identified in *D. melanogaster* and flies allowed the study of the impact of this protein on the developing nervous system (Kosaka and Ikeda, 1983; van der Bliek and Meyerowitz, 1991; Zhang et al., 2013;Vijayakrishnan et al., 2009a; Vijayakrishnan et al., 2009b)

Additionally, a component of the ESCRT-0 complex, HRS, was long suggested to play a role in vesicle trafficking and signal transduction (Komada et al., 1997), however investigating the protein in *Drosophila* revealed its role in the inward budding of

endosome membrane and MVB formation (Komada and Kitamura, 2001). More importantly, studies also could implement the role of HRS in the trafficking of several activating signalling pathways, including TGFR and EGFR (Jekely et al., 2005; Lloyd et al., 2002).

1.3.1 *Drosophila* as a model system

To study the mechanistic workings of endocytosis, *Drosophila* has the advantage of its extensive and well-developed genetic tools, but since endocytosis itself is a process to regulate other pathways, the use of a whole organism allows the assessment of the endocytic control of other cellular and organismal processes. One of these is planar cell polarity, which describes the orientation of cells evenly in one single plane (Strutt, 2009; Yu et al., 2007). Planar cell polarity complexes are controlled by the endocytic pathway. The Rab5 effector Rabenosyn-5 mediates the trafficking of the polarity components and thus controls the correct placement within each cell achieving correct orientation of all cells within a plane (Mottola et al., 2010).

Studies in *D. melanogaster* analysed so far at least 15 endocytic genes that are required for survival. These can be classified further into two groups, depending on the phenotypes they cause. The first group includes genes of the early endocytic pathway. For instance mutant clones lacking the Rab5 effector Rabenosyn5 become out-competed by the surrounding wild type cells (Lu and Bilder, 2005). The second group comprised late endocytic components like TSG101. Cells lacking TSG101 are able to proliferate autonomously and even promote growth in adjacent cells (Moberg et al., 2005). These different phenotypes occur due to the manipulation of different signalling pathways, within the endocytic pathway (Vaccari et al., 2009).

The use of the forward-genetic approaches within the fruit fly made it possible to draw the connections between tumour formation and endocytic regulation. The analysis of the influence of endocytic regulation within the full complexity of a developing organism represents a big advantage of using *Drosophila*.

The identification of novel endocytic genes using genetic screens influencing a big set of genes with either RNAi or mutagenesis and also modifier screens, can be used in *Drosophila* with ease to identify and study novel endocytic components.

1.4 JAK/STAT signalling

The JAK/STAT pathway, similar to the EGFR signalling pathway, is responsible for a considerable array of different signalling outputs. It plays a key role in development, immune response and homeostasis in mammals and *D. melanogaster* and it has been shown to be associated with cancer, myocardial hypertrophy and asthma (Agaisse and Perrimon, 2004; Arbouzova and Zeidler, 2006; Krzemien et al., 2007; Mukherjee et al., 2005). The JAK/STAT signalling pathway is highly conserved amongst mammals and has homologues in other model organisms. *D. melanogaster* represents one of the simplest models that still contains a complete set of canonical JAK/STAT pathway components (Figure 1.8). In vertebrates the JAK/STAT pathway is activated by a number of molecules, including interferons, hematopoietins and a subset of interleukins, growth factors and hormones. In the canonical model of JAK/STAT pathway activity, a dimerised trans-membrane receptor is bound by an extracellular ligand. The Janus kinases (JAKs) associated with the cytosolic portion of the receptors transphosphorylate each other resulting in their activation (Brown et al., 2003; Heldin, 1995; Ihle, 1995). Activated JAKs further phosphorylate the receptor on tyrosine residues, which serve in turn as docking sites for signal transducers and activators of transcription (STATs), which bind via their SH2 domains. After docking to the active phosphorylated receptor/JAK complex STATs are themselves tyrosine phosphorylated at a single highly conserved tyrosine residue by the JAKs (Zhong et al., 1994). Following their phosphorylation, STATs assume a dimerised '69' arrangement in which the phosphorylated tyrosine of one STAT is bound to the SH2 domain of the other and vice versa (Chen et al., 1998). The resulting phosphorylated STAT dimers translocate into the nucleus, where they bind with high specificity to palindromic DNA target sequences and induce the transcription of target genes (Figure 1.8 and Seidel et al., 1995).

Transcript profiling approaches have identified multiple JAK/STAT pathway target genes (Boudny and Kovarik, 2002). Targets include the negatively acting family of SOCS proteins, which form negative feedback loops to regulate pathway activity (Croker et al., 2008). In addition, pathway targets acting as effectors of haematopoietic tumour formation have been characterised (Bina et al., 2010). Furthermore, JAK/STAT targets are also able to repress other signalling pathways, like the Notch signalling (Flaherty et al., 2009).

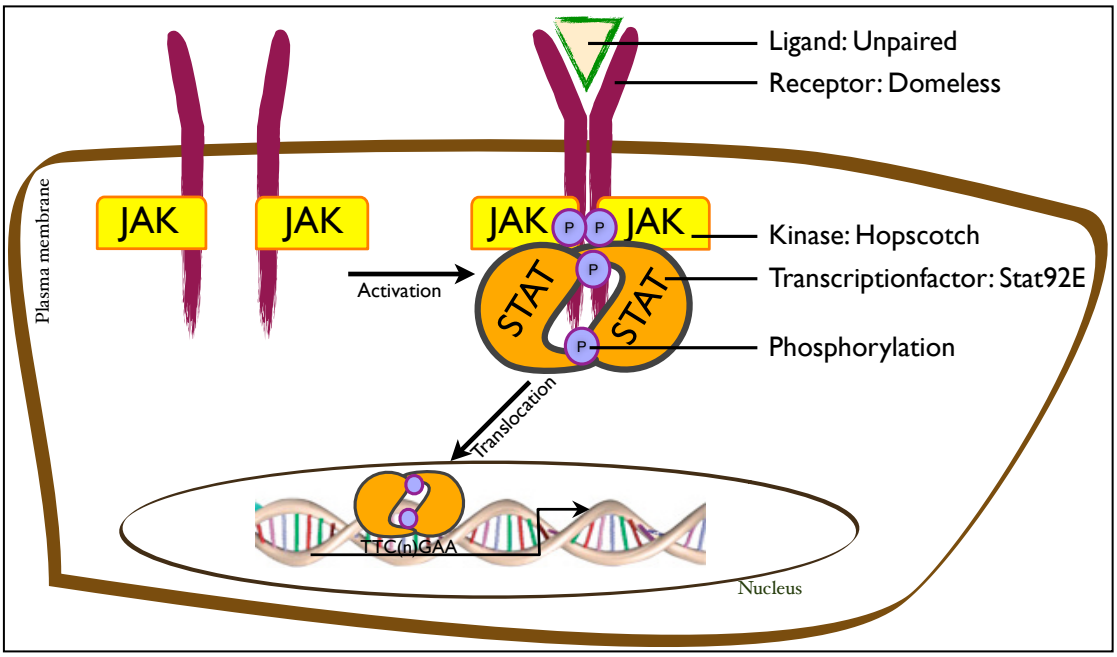

Figure 1.8: JAK/STAT signalling

After ligand binding the transcription-activator STAT is recruited to the receptor bound tyrosine kinase (JAK) and JAK as well as STAT phosphorylation events occur. STAT dimerises and translocates to the nucleus altering transcription. Indicated names of the components refer to the *Drososphila* JAK/STAT pathway.

1.4.1.1 The JAK/STAT receptor

Receptors activating the JAK/STAT pathway form a diverse family of transmembrane receptors, which include cytokine, receptors, growth factor and hormone receptors. There are over thirty JAK/STAT receptors as described to date. The majority of JAK/STAT pathway ligands share ⟨-helical structure, their receptors predominantly contain β–sheets at the sites of ligand interaction, often referred to as cytokine binding module. The module subdivides the cytokine receptor family into two subfamilies (type I and II) depending of the presence a semi-conserved WSxWS motif in the C-terminal portion (x represents any amino acid) (Bazan, 1990 and Thoreau et al., 1991).

Additionally, conserved disulfide-linked cysteins in the N-terminal portion of cytokine binding motive and an immunoglobulin-like domain present in several type I cytokine receptors has been reported to perform many functions, including stabilisation of protein trafficking in the case of IL-6R and contributes towards ligand/receptor complex assembly as reported for PDGF-PDGFR interactions (Miyazawa et al., 1998; Vollmer et al., 1999).

More membrane proximal are two to four fibronectin type-III domains (FNIII), characterised as mediators of interactions with heparins as well as other constituents of the cell surface environment. Position-specific residues in the FNIII domains have been implicated in receptor dimerization as reported for the shared gp130 receptor (Timmermann et al., 2002). Conversely, erythropoietin receptor (EpoR) has been shown to homodimerize in a transmembrane domain-dependent manner (Constantinescu et al., 2001). Interestingly, juxtamembrane domains of cytokine receptors have been deemed necessary for receptor activation following ligand binding via a conformational change (Couturier and Jockers, 2003; Seubert et al., 2003; Staerk et al., 2011).

The cytokine receptors exist as stable or transient preformed complexes on the cell surface. Composition of those complexes varies between cytokine receptors - EpoR and IFNαR form homodimers, while gp130 forms hetero-dimers/oligomers with OSMR, IL6R and LIFR (reviewed in Mohr et al., 2012). The transient heterodimers/oligomers of gp130 as well as homodimers of TpoR are stabilized by ligand binding which also triggers conformational change thought to alter the relative orientation of their cytoplasmic domains (Staerk et al., 2011; Dagil et al., 2012).

The intracellular domain of cytokine receptors generally contains classical Box domains common amongst JAK/STAT pathway receptors, which have been shown to mediate receptor/JAK and receptor/STAT interactions (reviewed by Grant and Begley, 1999).

1.4.2 JAK/STAT in *Drosophila*

The fruit fly displays a lower complexity system than the diverse mammalian network and therefore can be used as an excellent model to investigate the JAK/STAT pathway. Its simplicity is mirrored by the number of different ligands and receptors: mammals have over 80 different ligands and receptors, 4 JAKs and 7 STATS. In contrast *D. melanogaster* has only 3 ligands: Unpaired (Upd; Harrison et al., 1998), Unpaired2 (Upd2; Hombria et al., 2005 and Gilbert et al., 2005) and Unpaired3 (Upd3; Agaisse et al., 2003). All three ligands trigger JAK/STAT pathway activity by binding to one receptor, Domeless (Brown et al., 2001a).

The ligand-receptor complex activates one JAK (Hopscotch; Binari and Perrimon, 1994), which is the homologe of either human JAK1 or JAK2-depending on which domains are considered to determine similarities (Arbouzova and Zeidler, 2006).

There is only one STAT (STAT92E) in *Drosophila* and it most similar to the mammalian STAT5 (Hou et al., 1996; Yan et al., 1996).

In addition to the linearity of the JAK/STAT pathway, excellent genetic accessibility, screening methods and various analysis tools make *D. melanogaster* a powerful model system in which to study this signalling cascade.

1.4.2.1 Upd – like ligands

A loos-of-function mutant of Upd resulted in an embryonic segmentation phenotype similar to Hop and STAT92E. The Upd was the first identified JAK/STAT ligand as tyrosine phosphorylation could be observed upon ectopic Upd expression *in vitro* (Harrison et al., 1998). *In silico* searches identified the other two Upd-like homologues, Upd2 and Upd3 (Agaisse et al., 2003; Hombria et al., 2005).

All three proteins are similar in size ranging from 401 to 432 amino acids and encode a number of predicted post-translational N-linked glycosylation sites, which would suggest the potential secretion of all three molecules. Indeed, Upd has been shown to be glycosylated (Harrison et al., 1998).

Even though Upd2 was predicted to be anchored to membrane, all three ligands are capable of signalling non-autonomously and are able to activate the JAK/STAT pathway in neighbouring cells as well as condition media. (Baeg et al., 2005; Harrison et al., 1998; Hombria et al., 2005; Muller et al., 2005; Wright et al., 2011). Heparin has been shown to compete with the extra cellular matrix for the binding of proteins containing heparin binding domains (Hileman et al., 1998). The addition of heparin to cells expressing Upd and Upd2 revealed that Upd is likely to bind to the extra cellular matrix and consistent with the cell localisation data (Hombria et al., 2005).

Upd and Upd2 are semi-redundant (Hombria et al., 2005) and are expressed in multiple tissues throughout *Drosophila* development, for instance in the wing disc or in the adult ovary (Mukherjee, 2005; Muller et al., 2005; Silver and Montell, 2001). In addition, Upd2 was recently suggested to represent the functional homologue of Leptin, a human hormone regulating food intake and energy expenditure (Rajan and Perrimon, 2012). By contrast, Upd3 was reported to function as part of the immune response (Jiang et al., 2009). All three ligands have been shown to be able to signal at a distance *in vivo* (Tsai and Sun, 2004, Wright et al. 2010).

1.4.2.2 The Drosophila JAK/STAT receptor

In *Drosophila*, JAK/STAT signalling is activated by the binding of ligand to a receptor, Domeless (Brown et al., 2001a, Chen et al., 2002, Brown et al., 2003). Domeless (Dome) shows homology to both the vertebrate leukaemia inhibitory factor receptor and

the ciliary neutrophic factor receptor (Hombria and Brown, 2002). Similar to members of the vertebrate Class I cytokine receptor family, Dome also contains five fibronectin-type-III domains and two cytokine binding modules (Bravo et al., 1998; Wells and de Vos, 1996; Hombria and Brown, 2002).

A second potential receptor of JAK/STAT signalling in *Drosophila*, CG14225 (now referred to as Latran), was identified on the basis of homology to Dome (Hombria and Brown, 2002). Latran contains two cytokine binding motives and a long chain. This structure makes it most homologous to the vertebrate gp130 receptor and IL-6 receptor (Hombria and Brown, 2002, Kallio et al., 2010).

Latran was also thought to be a potential receptor of JAK/STAT signalling as upregulation of Latran was identified along with upregulation of Hop and Dome in response to parasitic wasp attack, suggesting a role in the *Drosophila* immune response (Wertheim et al., 2005). More recently, a role for Latran in the immune response has been confirmed. Surprisingly though, Latran has been determined as a negative regulator of JAK/STAT signalling forming heterodimers with Dome to antagonise its activity with effects observed in both the lymph gland (Makki et al., 2010) and the eye (Kallio et al., 2010).

1.4.3 JAK/STAT pathway regulation

The JAK/STAT pathway is used repeatedly during embryonic development and in adult homeostasis. In order to fulfil its differential functions it is tightly regulated.

The protein family of suppressors of cytokine signalling (SOCS) contain negative regulators of the JAK/STAT pathway, which act in a negative feedback loop, since STAT controls their expression (Stec and Zeidler, 2011). The multi-domained proteins can inhibit the pathway in distinct ways. They can bind to phosphorylated tyrosines on STATs acting via a competitive inhibition mechanism (Endo et al., 2003; Lavens et al., 2006). In addition, they can mediate the ubiquitination and subsequent degradation of their substrates (Linossi and Nicholson, 2012) while a subset of SOCS proteins also act by interfering with the interaction of JAK and STAT (Linossi et al., 2013).

As tyrosine phosphorylation plays a major role in JAK/STAT signalling, tyrosine phosphatases regulate pathway activation. There are five phosphatases belonging to three different protein families, which have been shown to regulate JAK/STAT signalling. The SH2-containing phosphatases, the transmembrane protein CD45 as well

as protein tyrosine phosphatase 1B and T cell protein tyrosine phosphatase are involved in the regulation of the JAK/STAT pathway (Xu and Qu, 2008).

1.4.4 The transcription factor, STAT

STAT activation by JAK is realised through phosphorylation on a highly conserved tyrosine at the C-terminus of the transcription factor (compare with Table 1.1). However, the N-terminal domain of STAT is also critical for its functions, since it is involved in nuclear import and export, receptor interaction, modulation of DNA binding and the formation of dimers (Decker and Kovarik, 1999).

Figure 1.9 illustrates the domain structure of STAT92E, which is a representative model also for mammalian STATs. STAT92E consisted of six main domains and the model shows their organisation and size in proportion to each other. The N-terminal region flanks a coiled-coil domain, which is responsible for protein dimerisation. The dimerised transcription factor binds with its DNA-binding pocket to DNA, this domain is connected to an SH2 domain, which allows for further protein-protein interaction, by a linker region. The transactivation domain is located at the C-terminus and contains a highly conserved tyrosine (at position 711 for STAT92E), whose phosphorylation is essential for STAT92E function (Ekas et al., 2010; Karsten et al., 2006; Yan et al., 1996).

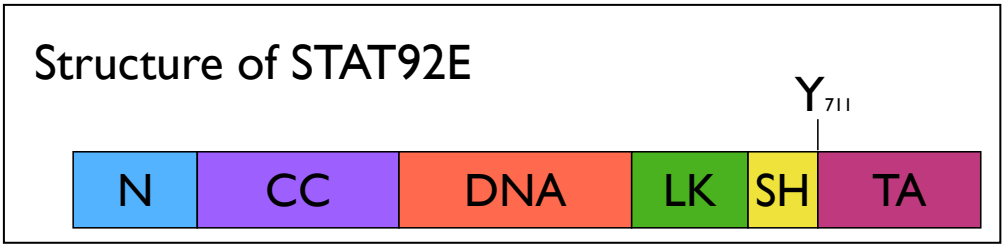

Figure 1.9: Model of STAT92E domains

N= N-terminal region, CC+ coiled coil domain, DNA= DNA binding pocket, LK= linker region, SH= SH2 domain, Y= tyrosine Y-711, crucial for biological function, TA= C-terminal trans-activation domain.

The dimerised protein binds to a palindromic DNA consensus motifes, TTC(n)GAA, where n represents a spacer of 2-4 nucleotides. Presumably each STAT prefers distinct binding sites, for instance, STAT6 shows a preference for 4n (TTC(nnnn)GAA), but can also bind to 4n or 2n sites (Ehret et al., 2001; Muller et al., 2012).

Apart from their roles as a transcription factor downstream of JAKs, STATs also play a part in additional 'non-canonical' processes. This rapidly expanding field of

investigations has revealed so far roles of STAT3, STAT5 and STAT92E in the regulation of migration, by binding to microtubules, of oxidative phosphorylation in mitochondria and modulation of the epigenetic landscape (Mohr et al., 2012). Interestingly, constitutively active STAT has been shown to associate with PI3K and activate the Akt signalling pathway, responsible for cellular growth (Harir et al., 2007). Furthermore, recent data suggests that STAT5b is serine phosphorylated through this pathway, resulting in its maximal activation (Mitra et al., 2012).

Table 1.1: Conserved tyrosine of STAT proteins

STAT	aminoacid								residues
STAT1	G	T	G	Y	I	K	T	E	698-705
STAT3	A	A	P	Y	L	K	T	L	702-709
STAT4	D	K	G	Y	V	P	S	V	690-697
STAT5	V	D	G	Y	V	K	P	Q	691-698
STAT6	G	R	G	Y	V	P	A	T	638-645
STAT92E	V	T	G	Y	V	K	S	T	708-715

1.4.4.1 Modifications

Additional to the phosphorylation on the single highly conserved tyrosine (Table 1.1), several mammalian STATs are serine phosphorylated by MAP kinases, for instance ERK. This serine phosphorylation occurs towards the C-terminal end of STAT. Its occurrence raised controversies in the scientific community as to whether it is enhancing or negatively influencing JAK/STAT signalling. However, this modification is not essential for DNA binding and transcriptional activation ((Lim and Cao, 2006) for review). Nevertheless, for instance STAT5 phosphorylation on a serine at position 193 results in a maximal transcriptional activity (Mitra et al., 2012). Furthermore, this residue has been reported to be constitutively phosphorylated in numerous malignant cells (Dephoure et al., 2008; Olsen et al., 2010). This suggests that serine 193 phosphorylation can cause over-activation of the JAK/STAT pathway and lead to cancerous cell growth if constitutively occurring.

Not only phosphorylation can affect STAT protein function, with other modifications including sumoylation or acetylation also shown to regulate the transcription factor. STAT92E was shown to be sumoylated on a non-conserved residue within the N-

terminal region of the protein, which inhibited signalling (Gronholm et al., 2010). A similar negative effect due to sumoylation was seen in mammalian STAT1 and 5 (Ungureanu et al., 2005).

In contrast, STAT acetylation enhances JAK/STAT signalling in general compare to Table 5.3 and reviewed in (Zhuang, 2013). The level of STAT acetylation depends on the balance between histone deacetylase and histone acetyltransferase activities. However, lysine residues shown to be the targets of acetylation are poorly conserved among STAT members and acetylation sites found in mammalian STATs are not represented in STAT92E.

Still discussed in the literature is the effect and existence of the modification by methylation on a highly conserved arginine in the N-terminus, mostly R-31 or R30 of STAT proteins. Even though STAT1 and STAT3 could be immunoprecipitated with anti-methylarginine antibodies, the direct detection of methylated STAT could not be shown by mass spectrometry (Komyod et al., 2005; Meissner et al., 2004; Mowen et al., 2001). Nevertheless, a point mutation in the arginine at position 31 of STAT1 destabilised its structure and impaired STAT function (Meissner et al., 2004).

Interestingly, post-translational modifications can act antagonistically to regulate STAT activity. STAT1 sumoylation and acetylation have opposing effects, since the sumoylation of a residue close to the activating tyrosine can negatively influence acetylation (Van Nguyen et al., 2011). Furthermore, the interchange of acetylation and phosphorylation of STAT1 takes place to act as a cycle limiting the duration of cytokine signalling (Kramer et al., 2009).

Table 1.2: Acetylation of STAT proteins

Protein	Function	Residues	Domain	Reference
STAT1	Interaction with NF-κB	K410, K413	DBD	(Kramer et al., 2006)
STAT2	Regulates interaction with STAT1	K390	DBD	(Tang et al., 2007)
STAT3	Increases DNA binding affinity Promotes protein-protein interaction Increases transcriptional activation Modulates dimerisation	K685	SH2	(Wang et al., 2005b; Yuan et al., 2005)
	Unknown	K49, K87	NH2-terminus	(Ray et al., 2005)
STAT5b	Modulates dimerisation	K694, K701	SH2	(Ma et al., 2010)
STAT6	Increases transcriptional activation		750–788 in the carboxyl terminus	(McDonald and Reich, 1999)

1.4.4.2 Nuclear import

Since there are differences between STAT proteins, naturally their nuclear import appears to be regulated in distinct ways. For instance, the translocation of STAT1 seems to be dependent of its tyrosine phosphorylation, with its following dimerisation and thus conformational change, which enables nuclear import by Importin5 (Meyer et al., 2002; Sekimoto et al., 1997). Most STATs lack a conserved nuclear localisation sequence (NLS). However, a leucine at position 407 is crucial for the STAT1-Importin5 interaction (McBride et al., 2002). Interestingly, STAT2 nuclear trafficking is regulated both prior to and subsequent to tyrosine phosphorylation. STAT2 constitutively binds to a non-STAT protein, IFN regulatory factor-9, containing an NLS in its un-phosphorylated form. In addition, the IFN regulatory factor-9 bound to STAT2 form a multimer complex with STAT1 upon phosphorylation, translocating thus into the nucleus (Banninger and Reich, 2004). Similar to STAT1, STAT5 translocates into the nucleus upon tyrosine phosphorylation (at position 694) (Gouilleux et al., 1994; Zeng et

al., 2002). It is associated with Importin3 and contains an unconventional NLS, which allows for nuclear import (Shin and Reich, 2013). STAT3 nuclear import on the other hand is independent on its tyrosine phosphorylation, but associates with several proteins to be shuttled into the nucleus, including Importin3 and 1 as well as Ran (Cimica et al., 2011; Liu et al., 2005). Additional to Importins, Rac1 and the MgcRacGAP have also been shown to facilitate STAT3 and STAT5 nuclear import. (Kawashima et al., 2009; Kawashima et al., 2006; Tonozuka et al., 2004).

Although the translocation of STAT92E to the nucleus in response to stimulation has been described (Karsten et al., 2006), the mechanism of STAT92E nuclear import has to my knowledge not yet been reported. However, STAT92E has been suggested to interact with HP1 and so to stabilize heterochromatin within the nucleus and, consistent with this, un-phosphorylated STAT92E can readily be detected in the nucleus (Shi et al., 2008). As such it seem likely that the regulation of STAT92E subcellular localisation is likely to be controlled at multiple levels.

1.4.5 JAK/STAT endocytosis and signalosome

JAK associated receptors are a diverse group of proteins and their cellular uptake and trafficking is likewise multifaceted, as reviewed in (Blouin and Lamaze, 2013; Claudinon et al., 2007). In general, receptors are endocytosed by Clathrin-dependent and -independent pathways, as described above.

Early electron microscopy studies from Sadir et al. 2001 showed that the interferon alpha receptor (IFNAR) and interferon gamma receptor (IFNGR) co-localise with Clathrin- and Calveolin- containing structures. Further studies revealed that IFNAR enriches in lipid raft structures after stimulation and its uptake is only partially blocked, when Clathrin-mediated endocytosis was inhibited. However, IFNAR signalling was suggested to occur from Clathrin and Dynamin dependent compartments. IFNGR on the other hand, does not occur in lipid rafts and its uptake is greatly inhibited in cell depleted of Clathrin. Interestingly, IFNGR signalling is suggested to be activated from the plasma membrane, whereas IFNAR signalling is strongly reduced when Clathrin- and Dynamin-dependent uptake mechanism are blocked (Marchetti et al., 2006).

Internalisation of cytokine receptors has been shown to require binding of a tertrameric AP-2 adaptor protein, which mediates interaction with Clathrin (Bonifacino and Traub, 2003). However, the process leading to AP-2 binding differs between cytokine receptors. As AP-2 requires non-phosphorylated tyrosine residues for binding, IFN⟨R

has to be dephosphorylated on Y466 by PTP1B to allow for interaction (Carbone et al., 2012). Intriguingly, the dileucine motif (an alternative AP-2 binding motif) of OSMR is masked by bound JAK1, which has to dissociate for internalisation to occur (Radtke et al., 2002). Similar process has been reported for internalization of IFN⟨R1 and Tyk2 (Ragimbeau et al., 2003). Finally, ubiquitination has been reported to be strongly associated with regulation of cytokine receptor stability, including receptor internalisation. Both, uptake and endocytic shuttling of G-CSFR and Prolactin receptor, among others, is regulated by site-specific ubiquitination (Swaminathan et al., 2008; Varghese et al., 2008; Wölfler et al., 2009). All of the aforementioned processes are not mutually exclusive and different combinations of these processes might be required for receptor endocytosis, as has been shown for EGFR (Goh et al., 2010).

The endocytic pathway is furthermore, suggested to be a platform, where STAT phosphorylation takes place. Next to constitutively phosphorylated site, Y-705 for STAT3, STAT3 is serine phosphorylated (S-727). Both phosphorylation sites are dependent on IL-6 uptake, but interestingly, S-727 phosphorylation seems to dependent on trafficking beyond the early endosome. Hence, it was suggested to take place at the late endosome, due to a cross-interaction with the MAPK pathway. Even though STAT3 accumulated in the nucleus, when trafficking beyond the early endosome was blocked, it could not activate a luciferase reporter measuring JAK/STAT activation (German et al., 2011).

The observations described above indicate that JAK/STAT signalling is qualitativly controlled by the endocytic pathway, however there is still the need to investigate whether signalosomes establish signalling platforms allowing qualitative differential signalling ((Blouin and Lamaze, 2013) for review). Being involved in many diverse, but essential processes within development and homeostasis, the endocytic pathway could allow for the fine tuning of distinct functions. The spatial compartmentalisation could enable the cell to allow distinct specific responses. Much research has been undertaken to uncover the importance of trafficking in the control of intracellular signalling. A large-scale simulation suggests the potential advantage for long distance STAT3 signalling to occur associated with trafficking components (Howe, 2005). This hypothetical model of signalling endosomes is partly supported by evidence showing that STAT3 is associated with late endosomes, where it is differentially phosphorylated and consequently maximal activated (German et al., 2011).

1.4.6 *Drosophila* JAK/STAT endocytosis

Investigating JAK/STAT signalling during the migration of border cells in the fly ovaries, Silver et al, 2005, showed that when receptor endocytosis in border cells was blocked by expression of a dominant negative form of Shibire (DN-Shibire), STAT92E is primarily localised in the cytoplasm rather than in the nucleus (Silver et al., 2005a). The ectopic expression of DN-Shibire, furthermore, resulted in a failure of border cells to migrate towards the oocyte as is required for the proper development of the egg (Silver et al., 2005a).

By contrast to the results from the ovary, the depletion of Rab5 or AP2 results in an enhanced activation of the *10xSTAT-GFP* reporter in border cells (Bach et al., 2007; Vidal et al., 2010). Within this study the endocytic pathway was suggested to act as a negative regulator of the JAK/STAT pathway. Using tissue culture cells and a *Draf*-based luciferase reporter they performed an RNAi screen identifying several components of the trafficking machinery, including Rab5, Clathrin, AP2 and TSG101, which enhanced signalling when depleted from cells (Vidal et al., 2010). Further analysis of JAK/STAT signalling showed that AP2 and TSG101 knockdown enhanced the *10xSTAT-GFP* reporter in imaginal wing disc and increased the size and numbers of melanotic tumours, in flies expressing a gain of function allele of the kinase (Hop^{Tum}) in the lymph gland, sensitising them thus for the haemocyte over proliferation due to the ectopic activation of JAK/STAT signalling (Luo et al., 1995).

In supporting cells in the *Drosophila* developing oocyte (for a more detailed discription of the oocyte development and border cell migration please see 3.2.2), the Dome receptor is localised in vesicular structures {Ghiglione, 2002 #415}, which was dependent on the presence of Upd in polar cells (Devergne et al., 2007). As previously shown for Upd2 in tissue culture cells, Dome positive structures within the cytosol of border cells in the developing oocyte co-localised with Rab5 and Rab7. Clonal mutant analysis in follicle cells within the same organ showed that Dome accumulates at the cell boundaries in *rab5,* or *clathrin* mutant cells, whereas cells missing components of the late endocytic pathway (Deep orange, VPS18) accumulated Dome intracellularly (Devergne et al., 2007).

The presence of STAT92E was greatly decreased in clones lacking Clathrin, Rab5 or HRS, indicating a lack of JAK/STAT signalling. The analysis of JAK/STAT signalling was realised using a *pointed-lacZ* reporter gene and Devergene et al, 2007 showed that JAK/STAT signalling is dependent on Clathrin in follicle cells. This finding is in

contrast with later published *in vitro* and *in vivo* data addressing JAK/STAT signalling with a 10xSTAT-reporter and suggesting endocytosis as a negative regulator (Vidal et al., 2010). However, the question remains as to the mechanism by which endocytosis regulates JAK/STAT in *Drosophila*.

1.5 Aim and objectives of the project

At the start of this PhD thesis I set out to investigate the role of Rab5 GEFs on *Drosophila* signalling pathways. I attempted to establish robust *in vivo* assays, measuring signalling pathways during developmental processes, since preliminary data, generated as part of the PhD Studentship grant proposal, suggested that individual Rab5 GEFs influence wing vein formation and JAK/STAT signalling within the wing disc. Even though I was able to reproduce previously obtained data, that Rab5 GEFs differentially influence developmental processes and signalling pathways, I could not dissect these phenomenon further because the phenotypes observed were not sufficiently strong and hence I focused my attention to setting up *in vitro* assays, investigating JAK/STAT signalling, with the ultimate goal to convert my findings into an appropriate *in vivo* system. The results of these *in vitro* assays led me into a detailed investigation of the transcription factor STAT92E.

The overall aim of the presented work was to understand how the endocytic pathway sets up JAK/STAT signalosomes.

1.6 Summary

Most studies investigating the interplay between signalling and endocytosis use artificial system with over-expressed receptors, which was also marked as a potential concern of von Zastrow and Sorkin (2007). Even though Interferon endocytosis has been studied, the existence and importance of signallosomes within the JAK/STAT pathway still remains to be clarified. My research project explored receptor signalling in a physiological system and points towards the existence of signalosomes. Furthermore, I have uncovered novel ways of JAK/STAT regulation. Investigating the modification of STAT92E closer I suggest a model to explain differential signalling and the data presented pave the way to a better understanding of JAK/STAT control. It also is the backbone of future investigations of finding the mechanism, which is responsible for the establishment of signalosomes and differential signalling.

CHAPTER 2. MATERIAL AND METHODS

2.1 General buffers, enzymes and chemicals

All buffers and solutions were prepared using dH_2O, sterilized by autoclaving unless otherwise stated, and stored at room temperature.

2.1.1 Phosphate buffered saline (PBS)

NaCl	137 mM
Na_2HPO_4	2.7 mM
KCl	10 mM
KH_2PO_4	2 mM

The pH was adjusted to 7.4 using NaOH.

2.1.2 Enzymes and chemicals

Restriction enzymes, RNase, T4 ligase polymerases and buffers for DNA modification were acquired from New England Biolabs (NEB). Concentrations and information about storage and solvents are stated in Table 2.1. All chemical reagents and other enzymes were of analytical grade and purchased from Sigma-Aldrich (St. Luis, USA) or MP Biomedicals (Irvine, USA), unless otherwise stated.

Table 2.1: Stock solutions

Stock solution	Solvent	Storage	Concentration
Isopropyl β-D-1-thiogalactopyranoside (IPTG)	dH_2O	-20 °C	20% (w/v)
Sodium Dodecyl Sulfate (SDS)	dH_2O	RT	10% (w/v)
Ammonium Persulphate (APS)	dH_2O	-20 °C	10% (w/v)
Formaldehyde	PBS	4°C dark	4% (w/v)

2.1.2.1 List of centrifuges

Various centrifuges, listed in Table 2.2, were used to harvest samples.

Table 2.2: Centrifuges used in this study

Centrifuge	Specific rotor	Max volume in ml	Max speed in g
Eppendorf centrifuge 5424		2	16,263
Sigma 4K15C		50	4,000
Avanti^{TM} J251 (Beckman)	JA-20	50	48,384

2.1.3 Microscopy

2.1.3.1 Tissue culture cells

Drosophila tissue culture cells were grown on round coverslips and mounted on microscopy slides using ProLong Antifade (Invitrogen) mounting solution. Slides were imaged using a DeltaVision RT system based on an Olympus 1X71 microscope of Applied Precision at 100x Plan Apo NA1.4 oil objective. De-convolution was carried out using a conservative ratio of the provided de-convolution algorithm on the DeltaVision system.

2.1.3.2 In vivo analysis

Drosophila tissues were observed using the microscopes stated in Table 2.3.

Table 2.3: Microscopes used in this study

Tissue	Microscope	Objective	Software
Adult wings	Leica DMR	HC PC 10x 0.3	Res C14
Imaginal wing discs Egg chambers	Zeiss LSM510 confocal	20x	
Egg chambers	Axioskop Z MOT Zeiss	20x	N/A for scoring border cell migration

2.2 Molecular biology techniques

2.2.1 Bacterial maintenance, strains and plasmids

Unless otherwise stated all media were prepared using distilled water (dH_2O) and were sterilised by autoclaving for 20 min at 121 °C (15psi)

2.2.1.1 Luria-Bertani (LB) (Miller, 1972)

Tryptone (Oxoid)	10 g l^{-1}
Yeast extract (Oxoid)	5 g l^{-1}
NaCl	10 g l^{-1}

The pH was adjusted to 7.4 before autoclaving using NaOH. Oxoid agar No.1 (1.5% (w/v)) was added for LB agar

2.2.1.2 Bacterial maintenance, culture and storage conditions

To obtain single colonies a sterile toothpick was used to streak out a sample from -80ºC bacterial strain collection on LB agar plates containing appropriate antibiotics. These plates were kept for up to two weeks at 4 °C. For long-term storage bacterial stocks were produced by transferring a single colony from a plate into a vial of Microbank™ (MP, Irvine, United states) beads and processed as per manufacturer's instructions.

Up to 4 ml liquid cultures were grown aerobically in sterile 25 ml polyethylene Universal tubes (Sarstedt, Nümbracht, Germany) or appropriate glass conical flasks. To ensure proper aeration the culture flask volume ratio was kept at 1:5 and incubation was carried out on an orbital shaker set at 250 rpm, 500 ml liquid cultures were grown in 2 l conical flasks on an orbital shaker set at 200 rpm. Bacterial strains used and/or created are listed in Table 2.3. *E. coli* strains Top10 were used for cloning and cultured in LB at 37ºC (unless otherwise stated).

Table 2.4: Bacterial strains used in this study

Strain	Use	Source
CDR 678	GFP overexpression	Rudener and Losdick 2002
Top10	Subcloning	Invitrogen
BL21	General protein overexpression	Smythe lab stock

2.2.1.3 Plasmids

All plasmids used and created in this study are listed and briefly described in Table 2.4. QIAGEN kits were used to purify plasmid DNA according to the manufacturer's protocol. Plasmid DNA was kept on ice and stored at -20 °C in dH_2O.

Table 2.5: Plasmids used in this study

Plasmid	Relevant genotype	Source
pQE-9-GFP	HIS-tagged GFP in pQE9	Rudener and Losdick (2002)
pAct-Upd2-GFP	GFP tagged Upd2 under control of actin expression	(Muller et al., 2005)
p10xSTATLuc	Fire-fly luciferase under control of10xSTAT binding sites	(Bach et al., 2003)
pAct-Renilla	Renilla luciferase under control of actin expression	(Muller et al., 2005)
pRK2	P element transformation vector pGX-attP	(Huang et al., 2008)
pKV13	pRK2 with each 3kb flanking regions of dRME-6	This study

2.2.1.4 Spectrophotometrically (OD600) Determination of bacterial cell density

The cell density of bacterial cultures was determent as a function of their spectrometric absorbance at 600nm. The spectrophotometer (Jenway 6100) was calibrated preceding use with fresh culture medium. To persevere the linear range of measurements with A600>0.8 cultures were diluted 10-fold before measurement.

2.2.1.5 Antibiotics

All antibiotics used in this study are listed in Table 2.2. The stock solutions were filter sterilised (0.2 µm pore size) and stored at -20 °C. For the use in Agar plates, the antibiotic stock solutions were added to the media once it had cooled below 60 °C. For use in liquid media, the antibiotic stock solutions were added just before use.

Table 2.6: Antibiotic stock solutions and concentrations

Antibiotic	Stock concentration (mg/ml)	Working concentration (µg/ml)	Dissolved in:
Ampicillin (Amp)	100	100- 25	dH_2O
Chloramphenicol (Chl)	10	10 - 30	100% (v/v) ethanol
Kanamycin (Kan)	50	50	dH_2O

2.2.1.6 General buffers

All buffers and solutions were prepared using dH_2O, sterilized by autoclaving unless otherwise stated, and stored at room temperature. All methods in this chapter are as indicated in (Sambrook and Russell, 2002) unless otherwise stated.

2.2.2 DNA extraction and detection

Qiagen is a trademark from Qiagen GmbH (Hilden, Germany)

2.2.2.1 TAE (50x)

Trizma base	242 g
Glacial acetic acid	57.1 ml
Na_2EDTA (0.5 M pH 8.0)	100 ml
dH_2O	to 1 l

Before use, the 50x stock was diluted 1:50 with dH_2O, to produce a working TAE 1x solution.

2.2.2.2 QIAGEN™ buffer P1

Tris-HCl, pH 8	50 mM
EDTA	10 mM
RNase A	100 µg ml^{-1}

After adding RNase A buffer was stored at 4 °C.

2.2.2.3 QIAGEN ™ buffer P2

NaOH	200mM
SDS	1% (w/v)

2.2.2.4 QIAGEN™ buffer P3

Potassium acetate, pH 5.5	3 M

2.2.2.5 QIAGEN™ buffer EB

Tris-HCl, pH 8.5	10mM

2.2.2.6 QIAGEN™ buffer QBT

NaCl	750 mM
MOPS	50 mM
Adjusted to pH 7.0 with NaOH.	
Isopropanol	15% (v/v)
Triton X-100	0.15% (v/v)

2.2.2.7 QIAGEN™ buffer QC

NaCl	750 mM
MOPS	50 mM
Adjusted to pH 7.0 with NaOH.	
Isopropanol	15% (v/v)

2.2.2.8 QIAGEN™ buffer QF

NaCl	1.25M
MOPS	50 mM
Adjusted to pH 8.5 with NaOH.	
Isopropanol	15% (v/v)

2.2.2.9 QIAGEN™ buffer AL, QG, PB and PE

Supplied by the QIAquick kit, details not provided.

2.2.2.10 Solution-A

Tris-HCl	0.1 M
EDTA	0.1 M
SDS	1% (w/v)
Diethylpyrocarbonate	1% (w/v)

2.2.2.11 Chromosomal DNA preparation

Drosophila melanogaster chromosomal DNA was extracted from a minimum of 5 up to 100 flies per sample. 10µl solution A per fly was used and the volumes of all solutions adapted according to the initial numbers of flies used.

Flies were collected in a microfuge tube and frozen down for at least 20 minutes. After thawing and covering the flies with Solution-A (100µl/5 flies) they were homogenised with a pestle and incubated for 30 minutes at 70ºC. 14µl 8M Potassium Actetate per 100µl Solution-A was added and the proteins were precipitated for 30 minutes at 4ºC. After centrifugation (Eppendorf centrifuge 5424; 13,523 x g, 15 min, 4ºC) the DNA was precipitated from the supernatant with ½ volume of iso-propanol for 3 to 5 minutes at RT. Centrifugation (Eppendorf centrifuge 5424; 13,523 x g, 15 min, 4ºC) resulted in a DNA pellet which was washed with 500µl 70% Ethanol, air dried and resuspended in sdH_2O (2µl/fly). Therefore the DNA was heated to 37ºC for 10 minutes. To further purify the DNA additional DNA precipitation as described in 2.2.2.14 was carried out.

2.2.2.12 Small scale plasmid preparation from E. coli

Plasmids were purified in a small scale using QIAprep (Mini), following the instruction of the manufacturer's. Overnight cultures (3 ml) were harvested and washed with sdH_2O using centrifugation (Eppendorf centrifuge 5424; 13,523 x g, 30 sec, RT). Cell pellets were resuspended in 250 µl buffer P1. To lyse *E coli* cells 250 µl of Buffer P2 were added and the solution mixed gently. For 5 min following the lyses 350 µl of neutralising buffer N3 were added. Centrifugation was applied (Eppendorf centrifuge 5424; 16,263 x g, 10 min, RT) and the supernatant transferred to QIAprep spin columns. Plasmid DNA was retrained on the column by centrifugation (Eppendorf centrifuge 5424; 13,523 x g, 30 sec, RT) and subsequently washed with 750 µl of buffer PE. To completely remove the washing buffer, the column was further centrifuged (Eppendorf centrifuge 5424; 13,523 x g, 60 sec, RT). The DNA was eluted with 30 to 50 µl dH_2O, (Eppendorf centrifuge 5424; 13,523 x g, 60 sec, RT).

2.2.2.13 Large scale plasmid preparation from E. coli

Plasmids were purified in a large scale using QIAprep (Maxi) following the manufacturer's instruction. 500 ml overnight cultures were harvested by centrifugation (Jouan, JAC50.10; 5500 rpm,10 min, 4ºC) and washed with PBS. The cell pellets were resuspended in 10 ml buffer P1. To lyse the cells 10 ml buffer P2 was added and the solution mixed gently. The lyses was stopped by adding 10 ml of buffer P3 and the sample mixed immediately but gently and incubated on ice for about 15min. Samples were centrifuged (Jouan, JAC50.10; 9500 rpm, 30 min, 4ºC) obtaining supernatants free of cell debris and chromosomal DNA. The supernatant was transferred to an equilibrated QIAGEN-tip 500 column. Plasmid DNA bound to the column and eluants went through by gravity flow. After washing three times with 30 ml buffer QC, the DNA was eluted in a clean 50 ml Falcon tube using 15 ml buffer QF. DNA was precipitated by the addition of 10.5 ml of isopropanol followed by centrifugation (Jouan, JAC50.10; 9500 rpm, 30 min, 4ºC). The pellet was washed with 2 ml 70% Ethanol (Jouan, JAC50.10; 9500 rpm, 30 min, 4ºC), air dried overnight and resuspended in 500 µl dH_2O. The sample was transferred into a clean microfuge tube and stored at -20ºC.

2.2.2.14 Ethanol / sodium acetate precipitation of DNA

To obtain pure DNA, free of ions and protein, The DNA was mixed with Na-Acetate (final concentration of 72.3 mM), Glycogen (final concentration of 2.2 % (v/v)) and Ethanol (final concentration of 70% (v/v)) and incubated at -20 °C for 15 to 60 min.

After centrifugation (16 263 xg, 10 min) the pellet was rinsed 5 times with 70% ethanol (16 263 xg, 3 min) and air-dried at room temperature.

2.2.2.15 Purification of DNA by gel extraction

DNA purification by gel extraction was performed with the QiagenQIAquick® gel extraction kit from Qiagen as per manufacturer's manual. DNA fragments were separated by agarose gel electroporesis in the presence of SYBR® Safe stain (Invitrogen) and the detected bands were manual excised under blue light using a sharp clean scalpel. Extracted gel fragments were dissolved in 3 volumes QF buffer at RT and one volume isopropanol was added. The mixture was applied to Qiagen spin columns and the DNA retrained by the columns while the debris was removed by centrifugation (Eppendorf centrifuge 5424; 13,523 x g, 30 sec). After discarding the flow through the columns were washed with 750µl PE buffer and any remaining buffer was removed by one additional centrifugation (Eppendorf centrifuge 5424; 13,523 x g, 60 sec). To elute the DNA 30 to 50µl dH2O were added to the column. After a 1 minute incubation at RT the DNA was eluted into a clean microfuge tube by centrifugation (Eppendorf centrifuge 5424; 13,523 x g, 60 sec).

2.2.2.16 Agarose gel electrophoresis

DNA fragments resulting from chromosomal or plasmid preparations, and from PCR amplifications were size separated by agarose gel electrophoresis. The samples were loaded into 0.8% to 1% agarose gels in 1x TAE buffer and were electrophoresed in the same buffer in Gibco BRL Horizontal Gel Electrophoresis tanks (Life technologies) at 15 volts/cm.

2.2.2.17 DNA detection in agarose gels

Bands separated by agarose gel electrophoresis were detected by Ethidium Bromide stain (2.5 µg/ml) of the gels for 15 to 30 min, followed by UV light detection by translumination (302 to 320nm wavelength) using the BioDoc-ATM Imaging system.

2.2.3 Polymerase chain reaction (PCR)

2.2.3.1 Primer design

Oligonucleotides (see table 2.6) were designed to amplify DNA fragments, which were uses as inserts in DNA cloning procedures and also to confirm generic constructs generated. When pertinent suitable restriction sides were engineered within the

oligonucleotide to enable cloning. Conventional rules of primer design were applied (like CG content, length, GC-clamp) and primer quality (hairpining, melting temperature, primer – dimmer) was further evaluated using NetPrimer (Premier Biosoft, Palo Alto, United States http://www.premierbiosoft.com/netprimer/index.html) to detect an optimal sequence.

Table 2.7: Primers

Marked in green are T7 binding sites, in red a palindromic sequence to enhance restrictions digest and in orange restriction enzyme binding sites.

Primer name	Sequence (5' to 3')
3'PhDKV24EGFP	taatacgactcactatagggACCCTCGTGACCACCCTGACCTAC
5'PhDKV24EGFP	taatacgactcactatagggGGACCATGTGATCGCGCTTCTCGT
3'PhDKV24LacZ	taatacgactcactatagggTAATACGACTCACTATAGGGAGAC AGTGGCGTCTGGCGGAAAA
5'PhDKV24LacZ	taatacgactcactatagggTAATACGACTCACTATAGGGAGATC CGAGCCAGTTTACCCGCT
3'PhDKV24TSG101a	taatacgactcactatagggTCCTATTTGTATTTGGTTGATGGA
3'PhDKV24TSG101b	taatacgactcactatagggATCCCTCAAATCCCAGTTCC
5'PhDKV24TSG101a	taatacgactcactatagggATATGGGGCTGCGATTTGT
5'PhDKV24TSG101b	taatacgactcactatagggAAAGTGGCGCTGTGGTG
3'PhDKV24CHCa	taatacgactcactatagggTTGCCACCAAGTATCACGAA
3'PhDKV24CHCb	taatacgactcactatagggCCCGAACGGGTGAAGAAC
5'PhDKV24CHCa	taatacgactcactatagggCCAGTTCGTCGGTTGAGAAT
5'PhDKV24CHCb	taatacgactcactatagggCACAATCCACGCTCGTAG
3'PhDKV24RME-6a	taatacgactcactatagggAGTGAGCACGAGATTTGGCT
3'PhDKV24RME-6b	taatacgactcactatagggCCAGAGATGTCTGCTGCAAG
5'PhDKV24RME-6a	taatacgactcactatagggCAGCATCAAGAGCTCCATCA
5'PhDKV24RME-6b	taatacgactcactatagggAAGCGCTGCAGTTTACCAAT
3'PhDKV24Rabex5	taatacgactcactatagggTACCCAACAGCGTGGTCAT
5'PhDKV24Rabex5	taatacgactcactatagggTTGTGGTTCTGCGTCATCA
3'PhDKV24Sprint	taatacgactcactatagggCAACAACAACGGCCAACC
5'PhDKV24Sprint	taatacgactcactatagggGTGGCAACCGCTGGACT
3'PhDKV34.5hs	ATAATAatgcatCGGAAACGAACTGCAAC
5'PhDKV34.5hs	ATAATActcgagGATCATCCACTCCACATTCG
3'PhDKV34.3hs	ATAATAgaattcCCTGCGACACATAGCTACAC
5'PhDKV34.3hs	ATAATAgcggccgcCGTTTGATGCTGTGGACAG

PhDKV45RpL32Rev	GACGCTTCAAGGGACAGTATCTG
PhDKV45RpL32For	AAACGCGGTTCTGCATGAG
PhDKV45DomeFor	ACTTTCGGTACTCCATCAGC
PhDKV45DomeRev	TGGACTCCACCTTGATGAG
PhDKV45Tsg101For	GAGGAGACACAAATAACAAAGTACC
PhDKV45Tsg101Rev	TGAGTGTCCATCAACCAAATAC
PhDKV45CHCFor	GTAGTAAAGATGACGCAACCAC
PhDKV45CHCRev	GTTCATGTCAATGATGACCACT
PhDKV45aAdpFor	ACCAGCGAAAATTAACAAGC
PhDKV45aAdpRev	GAGACGACTTCACACCCTTC
PhDKV45Rab5For	CACAGCTTAGCTCCCATGTA
PhDKV45Rab5Rev	TGTTTGACAAATCTGCCTTG
PhDKV45RME-6For	AGCGAGGCAACCAACTCCGATT
PhDKV45RME-6Rev	TTCACACAGCCAAAGACCACGC
PhDKV45Spr_a_for	GGCTCAATAGTGTCCTGTGCCGAG
PhDKV45Spr_a_rev	GTGCCACCTCGGCGTAGCG
PhDKV45Spr_b_for	ATTGGCGCGCCTGCGGTTCATCGCTAATCTGC
PhDKV45Spr_b_rev	CCTTCGAAGGCCTCAATGATGATGATGATGATGGCAGC TGGAGCGCCAGTCCAGG
PhDKV45Spr_c_for	ATTGGCGCGCCTGCGGTTCATCGCTAATCTGC
PhDKV45Spr_c_rev	CGCAATGATGCGGCACACTTCAC
PhDKV45baz_for	GGCACCTATCAGCGGAATAA
PhDKV45baz_rev	AAACTGGGCATTAGCACTGG
PhDKV45wnt4_for	GCAGCAAGGCCTTTACAACGAA
PhDKV45wnt4_rev	ATCTGCAGGGTCCACCCACT
PhDKV45CG3829_for	TTCTGATGAGCCGCAACGGG
PhDKV45CG3829_rev	TGCGATTGCACTCATCCCCC
PhDKV45CG10764_for	ACGATGCAGCCGAGCCAAAT
PhDKV45CG10764_rev	GCCCCCAACCTCACGTATAGAT
PhDKV45pxb_for	CGAAATTCGCAAGCAATACATTGGA
PhDKV45pxb_rev	CGGCCTTGTAGCCGCTTTTC
PhDKV45_SOCS36E_for	AAGTGCACACTGTCGAATGG
PhDKV45_SOCS36E_rev	TTCCCCGTTTTCACGTTATC

Table 2.8: Primer function

Primer	Function
PhDKV24	Amplify dsRNA
PhDKV34	Create pKV13
PhDKV45	Quantitative PCR

2.2.3.2 PCR conditions

Template DNA	1 to 100 ng
5' Primer	2 µM
3' Primer	2 µM
DNA Polymerase Buffer (provided by the manufacturer)	1 x concentrated
BSA	80 µg/ml
dNTPs	200 µM
DNA Polymerase	2.5 Units

DNA polymerases, template, primers, buffers and supplements were mixed to a final volume of 25 to 100 µl in thin wall 0.5 ml PCR tubes on ice. The reagents were added to the reaction in the order and final concentrations indicated below, unless otherwise stated.

The DNA reaction was performed in a TC-3000 (Techne) PCR machine with following conditions dependent of the needs of the DNA amplification.

Initial denaturation	94ºC	2 min	
Denaturation	94ºC	30 sec	30 cycles
Annealing	50ºC to 62ºC	30sec	
Extension	72ºC	1 – 6 min	
Final extension	72ºC	8 – 10 min	

2.2.3.3 DNA polymerases

Usually DNA fragments were PCR-amplified using the Extensor Hi-Fidelity ReddyMix™ PCR master mix, (Abgene) The reagents included a high fidelity mix of ThermoPrime Taq DNA Polymerase with a proprietary thermostable proofreading enzyme within the suitable buffer system including dNTPs.

To amplify DNA refractory to Reddy Mix amplification DNA polymerases, such as Pwo DNA polymerase (Roche), Deep Vent DNA polymerase (NEB), High Fidelity Extensor DNA polymerase (Roche) and Pfu DNA polymerase (Promega) were used.

2.2.3.4 Quantitative PCR (qPCR)

To analyse relative mRNA levels quantitative PCR was performed using the BioRad CFX96 Real time System, C100 Touch^{TM} thermal cycler. With a semiskirted 96 well plate 10 µl/ well total reaction volume containing:

Template cDNA	1 µl (from 2µg RNA, see 2.2.4.3)
5' Primer	2 µM
3' Primer	2 µM
Sybre Green Taq-DNA Polymerase	5 µl (Invitrogen)

Following protocol was applied:

Initial denaturation	94ºC	2 min	40 cycles with fluorescence measurement each cycle
Denaturation		94ºC	30 sec
Annealing/ extension	50ºC to 62ºC	30sec	40 cycles with fluorescence measurement each cycle raise up 0.5ºC

2.2.3.5 In vitro DNA manipulation techniques

During *in vitro* DNA manipulations the DNA, buffers, supplements and enzymes were kept on ice all the time handling and stored at -20ºC.

2.2.3.6 DNA restriction

Digestion of purified DNA (Small and large scale plasmid preparations, or purified PCR products) at specific restriction sites were carried out using New England Biolabs (NEB) enzymes in the provided NEB Buffers. Reactions were supplemented with BSA whenever pertinent as instructed by the manufacturer. Digestions were typically performed at 37 °C for three hours, or up to O/N occasionally.

2.2.3.7 DNA ligation

Linear DNA fragments resulting from restriction digests (see Sect. 2.18.1) were ligated using T4 Ligase (NEB) in the buffer provided by the manufacturer at 16°C O/N. Ligated

DNA was precipitated (see Sect. 2.2.2.14) and resuspended in sdH_2O prior to transformation into competent *E. coli*.

2.2.3.8 pENTR™ directional TOPO® PCR cloning

CACC-containing blunt end amplified and gel purified PCR products into pENTR™TOPO® Vector (Invitrogen) was carried out according to the manufacturer's instructions at a 1:1 (insert:vector) ratio in a final volume of 6 µl. Following incubation of the mixed reagents for 5 min at RT the sample was placed on ice for a few minutes, and 2 µl were immediately transformed (as described in Sect. 2.2.5.1) into competent *E. coli* , Top10 (Invitrogen, Cat. No.: C4040-50).

2.2.3.9 Gateway-cloning LR-Reaction

For the Gateway-cloning 25 ng of pENTR™ clone, containing attL1 and attL2 sites and the 50 ng of the destination vector, which includes attR1 and attR2 sites for recombination, were incubated with the LR-Clonase reaction buffer and enzyme in a total volume of 5 µl for 1h at RT, according to the manufacturer's instructions. Excess enzyme was removed by adding 0.5 µl proteinase K solution for 10 min at 37ºC and finally the whole reaction was transformed into competent bacteria (as described in 2.2.5.1).

2.2.4 In vitro RNA manipulation techniques

2.2.4.1 RNA extraction

For RNA extraction using Trizol from tissue culture cells, cells ($4x10^5$ to $3x10^6$ /well) were washed once with PBS and lysed with 1 ml of Tri-reagent. After transferring the lysates into a microfuge tube 200 µl of Chloroform was added and the samples mixed vigorously for 20sec, followed by 5 min incubation at RT and centrifugation (Eppendorf centrifuge 5424; 13,523 x g, 15 min). The upper layer was transferred to a fresh tube and RNA precipitated with 500 µl isopropanol for 10 min at RT. The pelleted (Eppendorf centrifuge 5424; 13,523 x g, 10 min) RNA was washed once with 70% ice-cold Ethanol, air-dried and resuspended in typically 20 µl of mqH_2O.

2.2.4.2 Amplification of dsRNA

Using the MEGAscript® RNAi Kit (Life Technologies) dsRNA was amplified from appropiate PCR products and the manufacturer's instructions were followed. The following reaction mix was prepared on ice:

PCR product	3µl
each dNTP	2µl
10x T7 Reaction Buffer	2µl
T7 Enzyme Mix	2µl
Nuclease-free Water	10µl

After an ON incubation at 37ºC 1µl of DNAseI was added to digest the remaining PCR product for 30min at 37ºC. dsRNA was ethanol precipitated and resuspended under sterile conditions in sterile, nuclease and RNase free water.

2.2.4.3 Reverse transcription RNA to cDNA

To write RNA into cDNA the High Capacity RNA-to-cDNA Kit (Applied Biosystems) was used, and according to the manufacturer's protocol, 2 µg of RNA was transcribed in 20 µl total reaction volume O/N at 37ºC, and after treatment with 1µl of DNase the cDNA was analysed by quantitative PCR as described in 2.2.3.4.

2.2.5 DNA transformation

2.2.5.1 Transformation of E. coli

Competent cells were thawed on ice and DNA was added and incubated for 30 min on ice. After a heatshock at 42ºC for 30 sec the cells were left to rest on ice for an additional 5 min before adding 200 µl of SOC media. The tubes were then incubated at 37ºC in an orbital shaker to allow expression of antibiotic resistance for about 1 hour. Cells were spread on LB plates containing the appropriate antibiotics and incubated O/N at 37ºC.

2.3 Protein Analysis Techniques

2.3.1 SDS-(PAGE) PolyAcryamide Gel Electrophoresis

Staining, destaining, incubation and washing steps were normally performed with mild rocking at RT. For recording purposes, SDS PAGE and PVDF membranes were scanned after development with an EPSON Perfection 3170 scanner, and the corresponding digital image stored.

2.3.1.1 SDS-PAGE sample buffer (2x)

Tris-HCL, pH 6.8	135 mM
Glycerol	11% (v/v)
SDS	2% (w/v)
Bromophenol Blue	0.1% (w/v)

5% (v/v) 2-mercaptoethanol added prior to use.

2.3.1.2 SDS-PAGE formulas and construction

Gels for SDS - PAGE were prepared as indicated below using BioRad Mini-PROTEAN Tetra system (0.75 mm thick chamber).

2.3.1.3 Separating gel

Bis-Acrylamide	8 to 12% (w/v)
Tris-HCl, pH 8.8	375 mM
SDS	0.1% (w/v)
Ammonim persulfate (APS)	0.05% (w/v)
Tetramethylethylenediamine (TEMED)	0.05% (v/v)

The contents were mixed gently to avoid air bubbles and approx. 4 ml were transferred into the gel casting apparatus. To seal the gel hermetically a layer of isopropanol was overlaid until the gel solidified.

2.3.1.4 Phos-tag™ gel

To cast a Phos-tag™ gel following solutions were added to a standard SDS-PAGE separating gel prior to casting the mixture.

Phos-tag™ Acrylamide	50 µmol/L
MnCL	100 µmol/L

2.3.1.5 Stacking gel

Bis-Acylamide	4% (w/v)
Tris-HCl, pH 6.8	125 mM
SDS	0.1% (w/v)
Ammonium persulfate (APS)	0.05% (w/v)
TEMED	0.05% (v/v)

The air exposed interface of the polymerised separating gel was washed with dH_2O. The stacking gel was applied on top and a plastic comb was placed within to create wells. Following polymerisation the comb was removed carefully and the wells were washed with dH_2O. The gel was transferred into the gel tank and submerged in 1x SDS-PAGE electrophoresis buffer.

2.3.1.6 SDS-PAGE electrophoresis buffer (10x)

Tris	250 mM
Glycine	1.9 M
SDS	1% (w/v)

The stock solution was diluted 1:10 with dH_2O to achieve the working concentration.

2.3.1.7 SDS-PAGE

SDS-PAGE electrophoresis was performed according to Laemmli (1970) Samples of protein extracts were heated in SDS sample buffer (1x final concentration) at 98°C for 10 min unless otherwise stated and centrifuged at 14,000 rpm for 10 min (Eppendorf centrifuge 5424). The supernatant was loaded onto a SDS mini gel prepared as described in 2.3.1.2. Electrophoresis was performed at 80 volts until the samples passed the stacking gel and subsequently the voltage was increased to 150V and the gel was allowed to run until the loading buffer reached the end of the gel.

2.3.2 SDS-PAGE staining

SDS PAGE gels were stained with SYPRO^R Ruby protein gel stain according to manufacturer's instructions. First, the gels were fixed for 30min at RT in the fixing solution with gentle agitation. The staining solution was allowed to incubate O/N at RT, before the gel was washed twice for 5 min in the wash solution to minimise background. Protein gels were consequently imaged using a UV light transluminator, connected to a CCV camera.

2.3.2.1 Fix solution

Methanol	50% (w/v)
Acetic acid	7% (v/v)

2.3.2.2 Wash solution

Methanol	10% (v/v)
Acetic acid	7% (v/v)

2.3.3 Western blotting

2.3.3.1 Blotting buffer

Tris	20 mM
Glycine	150 mM
Methanol	20% (v/v)

2.3.3.2 TBST

Tris-HCl, pH 7.4	20 mM
NaCl	137 mM
Tween 20	0.05% (v/v)

TBST (20x) was diluted 1:20 before using dH2O to obtain TBST (1x).

2.3.3.3 Blocking solution

TBST (1x)	50 ml
Dried Skimmed Milk Powder	5% (w/v)

Blocking solution was made fresh for each experiment and used without autoclaving.

2.3.3.4 Antibody solutions

Primary and secondary antibodies were diluted in blocking solution according to Table 2.9: prior to use.

Table 2.9: Table of antibodies used in this study

Name of antibody	antigen	Species	Source	Application and dilution
anti-α-Tubulin	chick brain tubulin	mouse monoclonal IgG1	Sigma-Aldrich	WB 1:2000
anti-Lamin (ADL67.10)	*Drosophila* lamin Dm1 and Dm2	mouse monoclonal IgG1	Developmantal Studies Hybridoma Bank	WB 1:500
anti-STAT92E	STAT92E peptide dN-17	goat polyclonal IgG	Santa Cruz Biotechnology	WB 1:1000
anti-Clathrin-heavy-chain (ab21679)	synthetic peptide (residue 1650 to C-term of human CHC)	rabbit polyclonal	Abcam	WB 1:500
anti-α-Adaptin	AP-2 adaptor polypeptides from bovine brain	mouse monoclonal IgG2a	Sigma-Aldrich	WB 1:500
p44/p42 MAPK (Erk1/2)	p44 MAP kinase	Rabbit monoclonal	Cell Signalling	WB 1:1000
Phospho-p44/p42 MAPK (Erk1/2) (Thr202/204)	synthetic phosphopeptide of human p44 MAP kinase	rabbit polyclonal	Cell Signaling	IF 1:1000
Phospho-Tyrosine (P-Tyr-100)	Phosphorylated tyrosines	mouse monoclonal IgG1	Cell Signaling	WB: 1:500
anti-GFP (KV)	His-tagged GFP	rabbit polyclonal	Garcia-Lara et al in prep.	ELISA 1:2000; IF 1:200; WB 1:2000
anti-GFP	GFP	goat polyclonal IgG	Abcam	ELISA 0.0625µg/ml
a21312	GFP	rabbit polyclonal	Invitrogen	IF 1:200, Alexa Fluor® 594 conjugated
a11122	GFP	rabbit polyclonal	Invitrogen	IF 1:200
a255	GFP	rabbit polyclonal	Cell Signaling	IF 1:200
a6556	GFP	rabbit polyclonal	Abcam	IF 1:200
a290	GFP	rabbit polyclonal	Abcam	IF 1:200
ab80968	SUMO 2+3	rabbit polyclonal	Abcam	WB 1:200
Ac-K2-100	Acetylated Lysin	Rabbin monoclonal	Cell Signalling	WB 1:200

2.3.3.5 Protein electrotransfer onto nitrocellulose membranes (blotting)

Proteins separated on SDS-PAGE gels were transferred onto 100% nitrocellulose membranes (pore size: 0.45 μm, Whatman Protean). The SDS-PAGE gel was laid on the membrane, which had been equilibrated with ice-cold blotting buffer and both were sandwiched in between 2 sheets of Whatman 3MM Chr blotting paper soaked in ice-cold blotting buffer. This construct was assembled onto a Transfer Apparatus (BioRad) and the transfer was carried out at 100 V for 75min at 4ºC.

2.3.3.6 Immunodetection of proteins on Nitrocellulose membranes

Membranes containing the blotted proteins were blocked at 4ºC O/N in blocking solution or for 30min at RT, and if applicable cut in appropriate sections to incubate O/N at 4ºC in blocking solution containing a dilution of an antibody specific for the desired protein (primary antibody). Table 2.9: summarises all antibodies used throughout this study. The membrane was washed 3 times for 10 min with TBS-T, and incubated for 30 min with a dilution of a secondary antibody raised against the Fc part of the primary antibody and conjugated to horse radish peroxidase (HRP), followed by 10 min washes (x3) with TSB-T.

Using the Amersham ECL Western blotting detection reagents manufacturer's instructions were followed and the chemiluminescence was achieved by performing the oxidation of luminol by the HRP in the presence of chemical enhancers. The Luminescence was detected using either autoradiography film (Amersham, Hyperfilm^{TM}) and a Protec Medical Systems x-ray developer Optimax 2010 or a CCV camera using UviPro Chemi and UviSoft UviBand softwares.

2.3.4 Protein over-expression

2.3.4.1 Buffer A – HIS-tag

Sodium Phosphate Buffer	100 mM
NaCl	500 mM

2.3.4.2 Buffer B – HIS-tag

Na_2PO_4	20 mM
NaCl	500 mM
Imidazole	500 mM

2.3.4.3 Wash Buffer

HEPES	10mM
DTT	1mM
NaCl	150mM

2.3.4.4 Elution Buffer

HEPES	10mM
DTT	1mM
NaCl	150mM
Glutathione (pH7.5)	5mM

2.3.4.5 Induction of recombinant proteins during growth

E. coli containing the over-expression plasmid was grown at 37ºC (25ºC for GFP) in 50 ml of LB containing ampicillin (100 µg/ml). When the culture reached an OD_{600} of 0.5-0.6, IPTG was added to the culture (1 mM final concentration) to induce the production of recombinant protein. The culture was further incubated at 37ºC for 3h (25ºC O/N for GFP). Induced samples were harvested by centrifugation (Avanti, Beckman, JA-20, 6000 x g, 15 min, 4ºC) and resuspended in 5 ml PBS (Buffer-A-HIS-tag for GFP).

2.3.4.6 Purification of O/E GFP by affinity chromatography

The harvested cells in Buffer A – HIS-tag (See Sect. 2.22.1) were broken through three times freeze/thaw cycles followed by sonication (3 x 10 second pulses (Sanyo)). The efficiency of the disruption was determined by light microscopy. When more ca. 95% of the cells were broken, the extract was centrifuged (Jouan centrifuge; JAC50.10; 10,000 rpm 4ºC) and the supernatant was filtered through a 0.45 µm filter. The resulting extract containing the HIS-tagged GFP protein was used for further purification by Ni-affinity chromatography.

A 5 ml Hi-Trap™ column (Amersham Biosciences) was washed with sdH2O, charged with 50 mM $NiSO_4.6H_2O$ and the excess of nickel salt flushed with sdH2O. The charged column was assembled onto a peristaltic pump (Econo Gradient, Bio-Rad) that had been flushed with Buffer A-HIS-tag. The protein solution was applied to the column and the attached recombinant protein was eluted using an increasing gradient of Buffer B-HIS-tag. Aliquots of 1 ml were collected. The Hi-Trap™ column was washed with 0.1 M EDTA and H_2O. For long-term storage the column was flushed with 20% v/v ethanol, sealed and placed at 4ºC.

The eluted fractions were analysed by SDS PAGE; those containing the majority of the protein of interest were pooled together and the purified protein was dialysed against PBS in 12-14 kDa cut off dialysis membranes (Medicell International Ltd.)

To determine the protein concentration a Bradford assay (2.3.4.8) was performed and aliquots were snap-frozen in liquid N_2 and stored at -80ºC.

2.3.4.7 Evaluation of protein over-expression yield

To evaluate the efficiency of over-expression (O/E) the amount of soluble protein (i.e., likely properly folded) was determined as follows. An aliquot of 1 ml of the cell sample in Buffer-A was incubated with 0.1 µg/ml lysozyme for 1 hour at RT, spun down at 16263 x g for 10 min (Eppendorf centrifuge 5424), and the pellet containing the insoluble fraction, was resuspended in 1 ml Buffer-A containing 8 M Urea. The soluble and insoluble fractions were separated in SDS-PAGE gels and detected by Coomassie stain.

2.3.4.8 Measurement of protein concentration via Bradford assay

The Bio-Rad Protein Assay was used to determine the concentration of soluble proteins. The assay is based on the method of Bradford and by following the instructor's manual, the 1x reagent was incubated with the sample or a standard, consisting of BSA with serial dilution ranging from 0.1 to 1 mg/ml, for 5 min at RT and the absorbance at 595 nm was measured. With the aid of a standard – curve the protein concentration was calculated.

2.3.5 Analysing proteins with mass spectrometry

To detect STAT92E by mass spectrometry (MS) an immunoprecipitation was performed according to section 2.3.8.3, eluted with 2x SDS Sample buffer and run on precast NuPAGE® NOVEX® Bis-Tris 4-12% gels in NuPAGE® MES buffer alongside with SeeBlue® Plus2Pre Stained Standard. After several washes with mqH_2O 5 bands were excised with a clean scalpel between 64 and 97 kDA and transferred into Eppendorf Protein LoBind S/L Tubes (1.5ml). The following described protocols and solution were executed according to instructions from Dr. R. Beniston.

2.3.5.1 Reduction Buffer

DTT	10mM
Ammonium Bicarbonate	50mM

2.3.5.2 Alkylation buffer

Iodoacetamide	55mM
Ammonium Bicarbonate	50mM

2.3.5.3 Solution 3

Acetonitrile	50% (v/v)
Ammonium Bicarbonate	50mM

2.3.5.4 Solution 4

Acetonitrile	9% (v/v)
Ammonium Bicarbonate	50mM

2.3.5.5 Solution 5

Acetonitrile	50% (v/v)
Formic acid	5% (v/v)

2.3.5.6 Switchoss Solution

Acetonitrile	3% (v/v)
Formic acid	0.1% (v/v)

2.3.5.7 Reduction and alkylation of proteins

To reduce the proteins 200µl of reduction buffer (prepared freshly) was added and incubated at 56ºC for 1hour. After pelleting the gel slice (13,000 x g for 10 sec) the supernatant was discarded and 200µl of the alkylation buffer was added and alkylation of the proteins was allowed for 30 min at RT in the dark. The slice was then washed twice with 200µl Solution 2 for 15 min at RT. After an additional wash step with Solution 3 at 37ºC for 15 min, the piece was centrifuged (13,000 x g for 10 sec) and all supernatant was removed carefully. Finally, the gel was dried in a vacuum concentrator for 30 min.

2.3.5.8 Enzymatic trypsin digestions

For the tryptic digest the dried gel slice was incubated with 0.4µg trypsin, typically in Solution 4 with 22.2 µM HCl in a volume that covered the slice (approximately 70 µl) at 37ºC for O/N.

2.3.5.9 Peptide extraction from gel slice

To extract peptides from the gel slice, the supernatant of the digestion was collected in a fresh siliconized microfuge tube, called from here onwards: SCT (supernatant collection tube). Three circles of extraction were undertaken. Therefore the gel slice was incubated with 20 µl of Solution 5 for 15 min at 37ºC, followed by a further 15 min incubation at 37ºC with 50 µl added Solution 6 and the supernatant was removed and added to the SCT. A final extraction step was achieved by incubating the gel piece with 50µl of Solution 7 at 37ºC for 30 min. All supernatants, collected in the same tube were vacuum dried and the dried peptides could be either stored at -20ºC or passed on for submission into the mass spectrometer.

2.3.6 LC-MS/MS Analysis

Dried down peptides were solubilized in 10µL of Switchoss Solution, sonicated for 5 min then centrifuged (20,000g for 5 min. 8.5µL of the supernatant was then taken and placed into an auto-sampler vial. For each sample analysis 10-40% of the material was injected onto the LC column/s for analysis. The uHPLC system was a Dionex Ultimate 3000 utilising a PepMap100 C18 2cm x75µm I.D. trap column and a 15cm PepMap100 C18 analytical column (2µM particle size, 100A pore size 75µM I.D). Peptides were loaded onto the column in 0.1% formic acid, 2% acetonitrile, and eluted with a gradient of increasing acetonitrile up to 72%, in 0.1% formic acid. Each uHPLC gradient, including column equilibration times, equated to 64 min. The mass spectrometer used was an electron transfer dissociation (EDT) enabled Thermo-Scientific Orbitrap Elite. Mass spectrometry (MS) spectra were acquired at a resolving power of 60,000 with an automatic gain control (AGC) target value of $1x10^6$ ions by the Orbitrap detector. Following MS analysis the top 10 most abundant precursors were selected for data dependent activation, using either collision induced dissociation, with a 100ms activation time, or ETD fragmentation, with a charge dependant reaction time, and an AGC setting of 5000 ions in the dual cell linear ion trap on normal scan rate. Precursor ions of single charge were rejected, and a 30 second dynamic exclusion setting was used.

2.3.6.1 Data Analysis

The resulting spectra in the .raw files from the Orbitrap Elite mass spectrometer were searched with Mascot (Matrix Science) against the NCBI nr database (with a taxonomy filter of *Drosophila melanogaster*), and decoy database, within the Proteome Discoverer

1.3 software package (ThermoScientific). Full trypsin enzymatic specificity was required with up to 2 missed cleavages permitted. Carbamidomethylation of cysteine was specified as a fixed modification. Oxidation of methionine and phosphorylation of serine, threonine and tyrosine were specified as variable modifications. A mass tolerance of 10ppm was used for precursors and 0.8Da for fragment ions. Following spectral searching, the resultant phosphopeptides were scored by the PhosphoRS algorithm. The false discovery rates were set at 1% and 5% by Peptide Validator (workflow node within Proteome Discoverer).

2.3.7 Enzyme Linked Immuno Sorbent Assay (ELISA)

2.3.7.1 ELISA – Lysis Buffer

Triton-X 100	0.5% (w/v)
$MgCL_2$	1mM
BSA	0.1% (w/v)

Protease inhibitor in PBS

2.3.7.2 ELSIA – Wash buffer

Triton-X 100	0.5% (w/v)
BSA	2% (w/v)

Protease inhibitor in PBS

2.3.7.3 HRP Developing Solution

H_2O_2	0.04% (v/v)
o-phenylenediamine	0.4mg/ml

in HRP assay buffer, prepared fresh for every assay

2.3.7.4 HRP assay buffer

Phosphate	51mM
Citrate	27mM

pH to 5.0 store filtered (0.2µm)

2.3.7.5 Anti-GFP ELSIA

The anti-GFP ELSIA was developed in this study (section 4.1.2) and this paragraph states the method for the assay used for all subsequent analysis.

A 96 well plate (EIA plate from Costar) was coated with a goat anti-GFP antibody (Abcam) 0.0625µg/ml in 100mM SodiumBiocarbonate ON at 4ºC. After three washes

with PBS (200µl/well) the plate was blocked in Wash Buffer for 1h at at RT or O/N at 4ºC. To bind the samples to the plate it was incubated for 3h at 37ºC. After three washes with PBS (200µl/well) the primary antibody (Rabbit GFP 1:2000) was incubated for 2h at RT or O/N at 4ºC. To enable development the plate was washed as before and incubated with the secondary HRP-linked anti-rabbit antibody (1:5000) for 1h at RT. After three washes the plate was incubated with 200µl/well freshly prepared HRP developing solution and the colour change as reaction observed. To stop the reaction 50µl/wll 2M H_2SO_4 was added and the absorbance read at 492nm.

2.3.8 Immunoprecipitation

2.3.8.1 IP-Lysis Buffer

Tris-HCl (pH 7.5)	20 mM
NaCl	150 mM
EDTA	1mM
EGTA	1mM
Triton-X 100	1% (w/v)
Glycerophosphate	1mM
Na-Pyrophosphate	2.5mM
Na_3VO_4	1mM
Protease inhibitor	

2.3.8.2 Acetylation-Lysis Buffer

Tris-HCl (pH 7.5)	50 mM
NaCl	150 mM
EDTA	1mM
SDS	0.1% (w/v)
NP-40	1% (w/v)
NaDesoxycholate	1% (w/v)
Melamine trisulfonic acid	200nM
NaFl	0.5mM
Na_3VO_4	1mM
Protease inhibitor	

2.3.8.3 STAT92E immunoprecipitation from cell lysates

To immunoprecipitate STAT92E from Drosophila $S2R^+$ cells, cells were chilled down with two washes of ice-cold PBS (on ice) and lysed with IP-lysis Buffer (approx. 5x 10^5 cells/100µl). Lysates were incubated with anti-STAT92E antibody (see Table 2.9 for details) or control IgG (raised in goat) in a ratio of 1µg antibody to 1µg protein for 1 h at RT. The mixture was then added to pre-washed, packed protein-G coupled beads (10 µl / 100 µg protein) and incubated for 1 h at RT on a spinning rotor. The beads were washed five times with 500 µl lysis Buffer. To settle the beads, they were centrifuged briefly (5,000xg, 30 sec) between washes and supernatants were kept for further analysis. Immuno-precipitated proteins were eluted with 2 x SDS sample buffer and incubation at 100ºC for 5 min.

2.4 Drosophila cell culture, maintenance, manipulation and analysis

2.4.1 Drosophila cell culture

2.4.1.1 Medium

Schneiders Insect Tissue Culture Medium (Sigma) supplemented with 10% heat inactivated Fetal Bovine Serum (FBS, Sigma) was used unless otherwise stated.

2.4.1.2 Drosophila cell culture maintenance

$S2R^+$ or KC^{167} cells were grown in T25 tissue culture flasks (Corning) to a density of between 5 x 10^5 and 1 x 10^7 cells/ml, as assessed by a haemocytometer. For long-term storage cells were kept in liquid nitrogen, in Schneiders medium, supplemented with 20% FBS and 10% DMSO. After reactivation cells were passaged up to 20 times.

2.4.2 DNA transfection into *Drosophila* cells

For the transfection high yield plasmid preparation (2.2.2.13) was used to ensure the highest quality of plasmid DNA. The Effectene Transfection Reagent (QIAGEN) was used and the manufacturer's instructions were followed.

Typically 5x10^6 cells were transfected with 2µg DNA. The DNA was preincubated in 200 µl EC Buffer and 16 µl Enhancer for 3min at RT and 20µl Effectene was added. After further 7 min incubation at RT the mix was diluted with 1ml media and carefully and evenly added drop-wise onto PBS washed cells. Cells were then returned into the 25ºC incubator and for 2-5 days.

2.4.2.1 Production of Upd2-GFP conditioned media

For the production of Upd2-GFP conditioned media $5x10^6$ cells Kc_{167} cells were transfected as described above with 2µg *pAct-Upd2-GFP* in one well on a 6-well plate (Costar). After 2 to 3 days the transfected cells were transferred to a T75 flask and further incubated for 5 days, before harvesting the medium by pelleting the cells (1,000 x g, 5min). The media was subsequently 0.2 µm filtered, aliquots were snap-frozen in liquid N_2 and stored at -80ºC.

2.4.3 RNA knockdown in *Drosophila* cells

$S2R^+$ *Drosophila* were counted and harvested by centrifugation (1,000xg, 5 min). Cells were resuspended in Schneiders medium without FBS and transferred into the appropriate cell culture plates, containing dsRNA in a ratio 10ng dsRNA / $1x10^6$ cells. After 1 h incubation at 25ºC equal amount of Schneiders media, containing 20% FBS, was added to each well and cells were further incubated for 4 days until subsequent assays were carried out.

2.4.4 Immuno-staining of *Drosophila* cells

Drosophila cells were grown on sterile, round glass cover-slips (∅ 13 mm) in 24 well plates. All handling steps were undertaken at RT. Cells were fixed with 4 % (w/v) Formaldehyde for 20 min. The fixing was quenched by incubation two times with 50mM Ammoniumcloride in PBS for 5 min. Cells were permabilised with 0.1% Triton in PBS for 5 min before blocking with 0.2% Gelatine in PBS for 30 min. The primary antibody was incubated for 2 h followed by three washes and the secondary antibody was incubated for 1 h in the dark. Cover-slips were washed and to stain the nucleus cells were incubated for 5 min with Dapi, before washed finally with mq-water and mounted onto microscope slides.

2.4.5 Luciferase Assay

2.4.5.1 BL Buffer

HEPES	50 mM
EDTA	0.5 mM
Phenylacetic acid	0.36mM
Oxalic acid	0.07mM

pH was adjusted with HCl to 7.8, and buffer stored at 4ºC.

2.4.5.2 Luciferase Buffers

Buffers were prepared freshly and based on the BL Buffer, as listed above, containing following:

DTT	41.5mM
ATP	3.3 mM
AMP	1.0 mM

D-Luc (13 µl/ml), for the firefly luciferase, or D-Coe (15 µl/ml), for renilla luciferase were added prior to use according to manufacturer's details (Invitrogen)

2.4.5.3 Measuring JAK/STAT activation with the Luciferase assay

$5x10^5$ cells were transfected with 5 µg p10xSTATDrafLuc, 15 µg pAct-Renilla and plated into a 96 well plate ($4x\ 10^4$ cells /well)

Cells were lysed with 40 µl BL Buffer containing 0.35% Triton per well. Lysates were split and 30 µl of the Luciferase buffer containing either D-Coe or D-Luc was added. Luminescence was measured using the Mitras LB 940 Luminometer, Berthold Technologies.

2.4.6 Endocytosis and Binding Assay

2.4.6.1 Endocytosis assay

Drosophila cells were seeded in 24 well plates ($5\ x10^5$cells/well) and allowed to settle down for at least 16h. After a PBS wash, media was replaced with Upd2-GFP conditioned media (unless otherwise stated), for various time-points. The plate was placed in a 25ºC water-bath until endocytosis was stopped by chilling the cells down with two ice-cold PBS washes. All subsequent steps were undertaken on ice with pre-chilled solutions. For acid stripping, cells were incubated twice (2min) with 0.2M glycine (pH 2.5) and washed again with PBS before lysing the cells with the ELSIA-lysis buffer. Cell lysates were then analysed by anti-GFP ELISA.

2.4.6.2 Upd2-GFP Binding Assay

Drosophila cells were seeded in 24 well plates ($5\ x10^5$cells/well) and allowed to settle down for at least 16h. Cells were chilled down with two ice-cold PBS washes and incubated with Upd2-GFP conditioned media (unless otherwise stated), for 30 min on ice. All subsequent steps were undertaken on ice with pre-chilled solutions. When appropriate cells were incubated twice for each 2 min with 0.2 M glycine (pH 2.5) and

washed again with PBS before lysing the cells with the ELSIA-lysis buffer. Cell lysates were then analysed by anti-GFP ELISA.

2.4.7 Fractionation assay

2.4.7.1 BA Buffer

HEPES	10mM
$MgCl_2$	1.5mM
KCl	10mM
DTT	0.5mM
Protease inhibitor	

2.4.7.2 S1 Buffer

Succrose	0.25 M
$MgCl_2$	10mM
Protease inhibitor	

2.4.7.3 S3 Buffer

Succrose	0.88 M
$MgCl_2$	0.5mM
Protease inhibitor	

2.4.7.4 $S2R^+$ fractionation

Cells were washed three tines with ice-cold PBS before adding BA buffer. All buffers and centrifuges were pre-chilled and the samples kept on ice at all time. Cells were disrupted by approx. 20 strokes if the Dounce Pestle. Nuclei were separated from the cyotosol by spinning them down at 250 x g for 5 min and the supernatant, containing the cytosolic fraction was further purified by a centrifugation (20,000 xg, 15 min). An equal volume of the S1 buffer was added to the pellet (nuclei) and layered over twice the volume of S3 buffer. After a centrifugation step (1,200 xg, 10 min) the pellet (nuclear fraction) was resuspended in 1 volume of the BA buffer.

2.5 Drosophila stock maintenance manipulation and analysis

2.5.1 *Drosophila* stock maintenance and crosses

All fly stocks used are listed in Table 2.10. Wild-type flies and embryos used were w^{1118} throughout. Flies were kept on standard yeast/dextrose medium (1% agar, 7.3%

dextrose, 5% yeast, 6.7% organic wholemeal flour, 0.25% nipagin, 0.3% propionic acid) in 30 ml vials or 250 ml bottles, plugged with cotton wool. Fly stocks and crosses were kept at 25ºC as standard, unless otherwise stated. All 'fly pushing' techniques were performed as described in (Greenspan, 2004).

All stocks were either available as lab stocks or ordered from Bloomington *Drosophila* Stock Centre, Vienna *Drosophila* RNAi Centre (VDRC) or Kyoto *Drosophila* Genetic Resource Centre (DGRC).

Table 2.10: *Drosophila* stocks used in this study

***Drosophila* stock**	**Type**	**Source**
w^{1118}	control	Zeidler lab stock
w^{1118}; Sco/CyO	balancer	Zeidler lab stock
FM7	balancer	Zeidler lab stock
w^{1118}; ;In(3L)D/TM3,Ser[1]	balancer	Zeidler lab stock
y,w,P{w1,GMR-updΔ3'}/FM7, ey-Gal4/ey-Gal4	Gal4	(Bach et al., 2003)
w^{1118}; P{w+,10xSTAT-GFP}, ptc-Gal4 / Cyo	Gal4	(Bach et al., 2007)
w^{1118}; P{w+,10xSTAT-GFP}, en-Gal4 / Cyo	Gal4	(Bach et al., 2007)
w^{1118}; Slbo-Gal4, UAS-GFP/cyo	Gal4	Zeidler Lab stock
w^{1118}; MS1096-Gal4	Gal4	Strutt Lab stock
w; Mj21a-Gal4	Gal4	Strutt Lab stock
stat92E^{397}/TM3, Sb, ry	mutant	(Silver et al., 2005a)
Spri^{6G1}	mutant	(Jekely et al., 2005)
Rabex^{ex45}	mutant	(Yan et al., 2010)
P{pKV13}/hs-FLP, hs-I-SceI*	targeting	This study
w;P{w$^+$, UAS-btl.lambda}1	UAS	Bloomington
w;P{w$^+$, UAS-Egfr.1 }11-7	UAS	Bloomington
y^1,w; P{w$^+$,UAS-htl.DN.M}33-B40; P{w$^+$,UAS-htl.DN.M}33-B61	UAS	Bloomington
y^1,w; P{w$^+$,UAS-Egfr.DN.B}29-77-1; P{w$^+$,UAS-Egfr.DN.B}29-8-1	UAS	Bloomington
y^1,w,P{w$^+$,UAS-argos.M}30-102-1; P{w$^+$,UAS-argos.M}30-85-1	UAS	Bloomington
y^1,w; P{w$^+$,UAS-htl.lambda\cI.M}40-22-2	UAS	Bloomington
y^1,w; P{w$^+$,UAS-Egfr.B}32-26-1	UAS	Bloomington
w^{1118}, P{w$^+$,UAS-Dl.J}TJ1	UAS	Bloomington
w; P{w$^+$,UAS-Dl::GFP}DA53	UAS	Bloomington
w; P{w$^+$,UAS-Dl.DN}TJ2/CyO	UAS	Bloomington
w;P{w$^+$,UAS-btl.lambda}1	UAS	Bloomington

CG10079 (#43267)	UAS-dsRNA	VDRC (Dietzl et al., 2007)
CG9375 (#106642)	UAS-dsRNA	VDRC (Dietzl et al., 2007)
CG13559 (#43123)	UAS-dsRNA	VDRC (Dietzl et al., 2007)
CG13559 (#53641)	UAS-dsRNA	VDRC (Dietzl et al., 2007)
CG9012 (#23666)	UAS-dsRNA	VDRC (Dietzl et al., 2007)
CG9012 (#22318)	UAS-dsRNA	VDRC (Dietzl et al., 2007)
CG4260 (#4267)	UAS-dsRNA	VDRC (Dietzl et al., 2007)
CG34414 (#106129)	UAS-dsRNA	VDRC (Dietzl et al., 2007)
CG34414 (#29623)	UAS-dsRNA	VDRC (Dietzl et al., 2007)
CG34414 (#38884)	UAS-dsRNA	VDRC (Dietzl et al., 2007)
CG34414 (#43501)	UAS-dsRNA	VDRC (Dietzl et al., 2007)
CG34414 (#47480)	UAS-dsRNA	VDRC (Dietzl et al., 2007)
CG34414 (#106127)	UAS-dsRNA	VDRC (Dietzl et al., 2007)
CG7138 (#104135)	UAS-dsRNA	VDRC (Dietzl et al., 2007)
CG7138 (#35279)	UAS-dsRNA	VDRC (Dietzl et al., 2007)
CG7138 (#35180)	UAS-dsRNA	VDRC (Dietzl et al., 2007)
CG9139 (#46329)	UAS-dsRNA	VDRC (Dietzl et al., 2007)
CG9139 (#105534)	UAS-dsRNA	VDRC (Dietzl et al., 2007)
CG1657 (#19649)	UAS-dsRNA	VDRC (Dietzl et al., 2007)

2.5.2 Embryo Immunohistochemistry

2.5.2.1 Fixing solution

EGTA	0.25 mM
Formaldehyde	4.625% (v/v)
Heptane	50% (v/v)

Prepared freshly on the basis of PBS.

2.5.2.2 Blocking solution

Horse serum	5% (w/v)
Triton X100	0.01% (v/v)

Prepared freshly on the basis of PBS.

To harvest embryos flies were incubated on apple juice plates, containing some bakers yeast. Embryos were harvested using a fine brush and water. Embryos were de-corinated for 3 to 5 min in 50% bleach, before fixing them in 8 ml fixing solution for 20-30 min slightly agitating. The fixing solution was removed (lower phase) and 4 ml methanol added. To remove residual membranes the embryos were vortexed hard for 10 sec and the floating membranes (top phase) were removed, before washing the embryos twice

with methanol. The embryos could be stored in methanol now at -20ºC before rehydrating gradually with PBS.

Before immuno-staining, the embryos were blocked with 5% horse serum in blocking solution at 4ºC for 1 h. The primary antibody was diluted in blocking solution and incubated O/N at 4ºC. Embryos were washed with PBS, containing 0.01% Triton X100 before incubation with the secondary antibody at 4ºC for 4 h. These steps were repeated as necessary for double stainings. To stain the nuclei embryos were incubated for 30 min at 4ºC with Dapi. To mount the embryos in 85% Glycerol containing N-Propalgalate, they were gradually shifted to solution containing a high percentage of glycerol.

2.5.3 Preparation of adult wings

Flies were anesthetised using CO_2 and wings dissected from as close to the hinge region as possible using blunt forceps. Wings were dehydrated using isopropanol and mounted on microscopy slides using GMM mounting solution. Dried slides were stored at RT.

2.5.3.1 GMM mounting solution

Canada Balsam	50% v/v
Methyl-salicylate	50% v/v

2.5.4 Dissection of wing discs

To dissect wing discs crawling third instar larvae were collected and washed in PBS. Larvae were parted and "turned inside out" before fixed for 20min in 4% Formaldehyde. After washing the fixative away, wing disc were carefully dissected and mounted onto microscopy slides using ProLong Antifade (Invitrogen).

2.5.5 Border cell migration analysis

Female flies were collected and their abdomen opened. Two ovaries from each fly were removed and washed in PBS before fixing them in 4% Formaldehyde in PBS for 20 min at RT. To examine structures better, F-actin was stained with Alexa-568- phalloidin (red) 1:5000 for 1h at RT. And ovaries were spread on Poly-L-lysine covered mircroscope slides, which separated the developing eggs. Egg chambers were examined using the microscope stated in Table 2.3.

CHAPTER 3. ROLE OF RAB5 GEFS IN SIGNALLING PATHWAYS *IN VIVO*

Many research studies showed that Rab5 regulates signalling using *in vitro* and *in vivo* systems. The understanding of the fine nuances of signalling especially its regulation by signalosomes only started in recent years (Schenck et al., 2008; Zheng et al., 2008). Additionally, novel data from the Smythe lab suggested that RME-6, as a Rab5 GEF, established differential signalling domains for the Tie2 signalling pathway (Ferreira, et. al. in preparation).

In the beginning of my PhD project I set out to address whether RME-6 and other Rab5 GEFs would be able to set up signalosomes *in vivo,* as they do in mammalian *in vitro* experiments (Ferreira, et. al. in preparation). By using *Drosophila melanogaster* as an *in vivo* model, I asked whether Rab5 GEFs regulate differentially signal transduction pathways, analysing in detail their influence not only on the direct outcome of signalling pathways, but also on developmental processes. I used the fruit fly, since it was a well-established, easily accessible, low complexity model organism with excellent genetic tools. These tools would allow me to gain insight into the role of Rab5 GEFs in various signalling pathways in a whole organism.

3.1 A RME-6 knockout mutant in flies

As previously described within this thesis (section 1.1.4), Rab5 GEFs are believed to fulfil specific functions within the cell. However, some redundancy has been demonstrated between the four major GEFs, Rabex5, Alsin, Rin1 and RME-6. For example, in *C.elegans*, null mutations in either RME-6 or Rabex5 are homozygous viable, however, RNAi targeting *rabex5* in a *rme-6 (b1014)* mutant background resulted in strong synthetic lethality (Sato et al., 2005).

RME-6 has, to my knowledge, not been characterised in flies as yet and no mutant allele is available from publically assessable sources. In addition, only one RNAi line targeting RME-6 is available. This line carries an inducible transgene, which expresses a transcript, which folds to generate a dsRNA hairpin. Upon expression, this hairpin is processed to generate siRNAs, which bind to the *RME-6* mRNA leading to its degradation by the cellular machinery.

To ensure that any phenotypes observed following expression of this dsRNA are truly due to the depletion of RME-6, and not the consequence of any off-target effects, a second non-overlapping RNAi construct would be required. In addition, whilst RNAi is a useful technique to generate conditional loss of function phenotypes, it cannot be relied upon to achieve a complete loss of protein activity.

In the light of this background I decided to make a *Drosophila* mutant in RME-6. Such a mutant would allow for the characterisation of RME-6's role in the trafficking pathway and the control of signalling by endocytosis. Furthermore, it would not only enable structure-function analysis of RME-6, by expression wild type and truncated forms of RME-6 in a mutant background, but also exploration of its level of redundancies with the other Rab5 GEFs, where null mutant lines are already available from the fly community.

A classic strategy for the generation of *Drosophila* mutants utilises the libraries of P-element insertions, which have been generated and mapped across the genome. In this method, imprecise excision of the transposon is used to make small deletions in the genomic locus of interest. However, there were no suitable P-elements in the genomic region of RME-6. Thus, I adopted the ends out homologous recombineering strategy (Huang et al., 2008). This method required the amplification of a ~3200bp long fragment from the RME-6 upstream genomic region and a ~2050bp long fragment downstream of RME-6 and cloning of these into the pRK2 vector, as described in section 2.2 and (Huang et al., 2008). The created vector (pKV13) was then transformed by a P-element into the fly genome.

In a typical ends out target procedure, as I undertook, there are three crosses (Figure 3.1 shows the first two). Firstly, in the targeting cross virgins homozygous for the transgenic line P{*KV13-RME-6*} was crossed to *y w/ Y hs-hid; hs-FLP, hs-I-SceI; / cyo, hs-hid* males. The flippase (FLP) and restriction enzyme (I-SceI) were expressed in the larval progeny by heat shocking them. The FLP then excises the contents of the *P{KV13-RME-6}* insert from the genome by homologues recombination of the FRT sites, flanking the construct. After excision, the restriction enzyme I-SceI linearises the fragment. As the males of this targeting cross carried a further transgene containing *hs-hid* on their Y chromosome all progeny was female, as expression of the cell-death-inducing Hid was activated in males during the heatshock.

During the heatshock it is anticipated that a small proportion of the linearised targeting DNAs were able to integrate by homologous recombination into the *RME-6* locus – in which case a *white*$^{+}$ gene should replace *RME-6*, creating mosaic tissues in the fly progeny at this stage. To eliminate false positives, the donor construct also carried a *UAS-Rpr*. Reaper (Rpr) is another cell-death-inducing gene and this *UAS-Rpr* construct is lost when *white* integrates into the *RME-6* locus, since it is located 3'prime of the homologous arm. In the second cross, female *P{KV13-RME-6}* / *hs-FLP, hs-I-SceI* flies are crossed to homozygous males expressing *GAL4* (Gal4^{477} (Huang et al., 2008)or *ubiquitin-Gal4[3xP3-GFP]* (Baena-Lopez et al., 2013)*)*. The *Rpr*$^{+}$*/GAL4* false positive progeny were thus directly eliminated due to the overexpression of Rpr.

Together with a Co-worker, we undertook three independent attempts for the ends out targeting, screening in each attempt over 20,000 flies (E. Smythe, unpublished data). Even though using an improved ubiquitous driven Gal4 line to eliminate unmobilised donor and false positives (*ubiquitin-Gal4[3xP3-GFP])* (Baena-Lopez et al., 2013) we were not able to create a mutant for RME-6. We obtained a number (approx. 10 per attempt) positive candidates, which all did not segregate on the correct chromosome (the X-chromosome for RME-6).

It is very unlikely that a heterozygote and even hemizygote (males) RME-6 mutant is embryonic lethal, since a) its ubiquitous knockdown by RNAi did not show any obvious phenotype affecting viability or fly-health (data not shown) and b) there is likely to be significant redundancy between the Rab5 GEFs. The failing of creating a RME-6 mutant is likely due to the donor construct. It may be that the homologous arms chosen, did not allow for a highly efficient homologues recombination, or the genomic region of RME-6 is densely packed with heterochromatin.

Since we were unable to create a genetic null mutant, we decided to carry out our analysis of RME-6 using the available RNAi line.

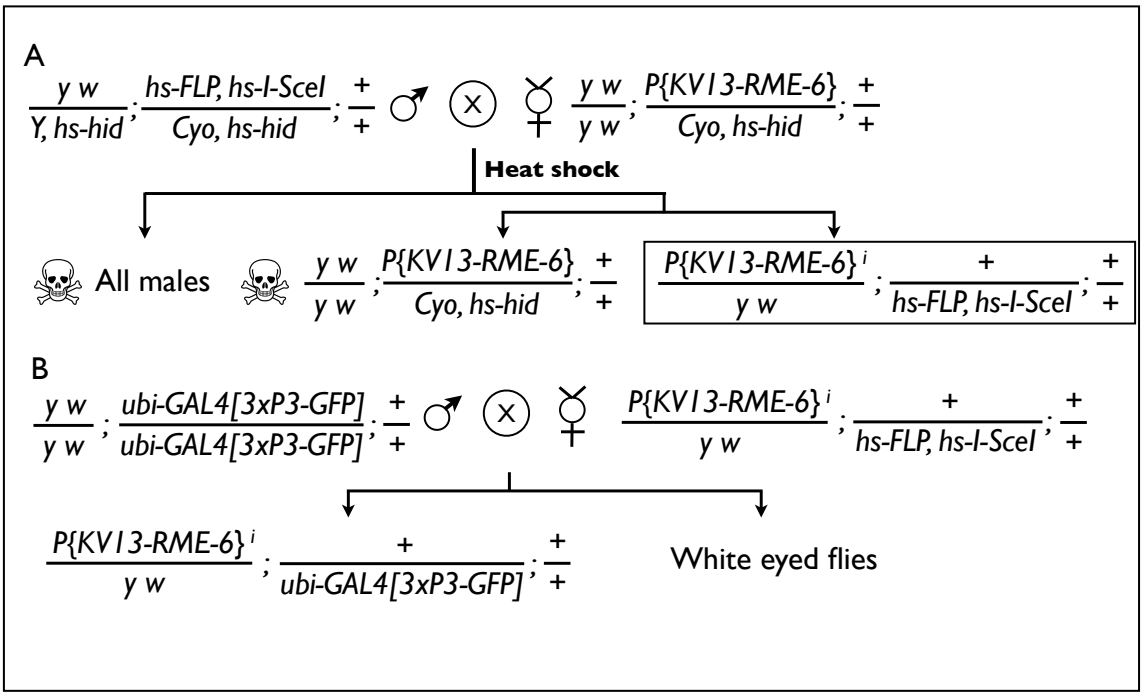

Figure 3.1: Crossing scheme to generate a RME-6 mutant fly

A: Virgins of transgenic donor DNA *P{KV13-RME-6}* on the second chromosome are crossed to males carrying *hs-FLP* and *hs-I-SceI* and their larvae progeny heat shocked (2h at 37ºC), thus expressing FLP and I-Sce and flipping out and linearising *P{KV13-RME-6},* which only exist transiently, since it is either lost permanently or inserted into a chromosome by targeted (on the *RME-6* location) or untargeted integration events *P{KV13-RME-6}*^{i}*.* Due to the expression of the heatshock induced *hid* gene, male progeny and not flipped out and lineraised *P{KV13-RME-6}* carrying progeny dye. B: Virgins carrying the *P{KV13-RME-6}*^{i} were crossed to males with a *ubi-Gal4[3xP3-GFP]* construct. Progeny with untargeted integration events *P{KV13-RME-6}*^{I} dye, since GAL4 activates the reaper gene on the full length *P{KV13-RME-6}* construct, or have white eyes, since they lack the marker for integrated *P{KV13-RME-6}*^{i}*.*

3.2 Influence of Rab5 GEFs on developmental processes

The failure to create a RME-6 mutant allele in flies forced me to use RNAi to study RME-6 effects of signalling events. First, I tested the general influence of Rab5 GEFs on developmental processes during wing development and border cell migration, before I went on to specifically look at their influence on JAK/STAT signalling and the MAP kinase pathway.

Developmental processes are extremely well described in *D. melanogaster,* since it was one of the founding organisms leading developmental studies. During development numerous spatially- and temporally- controlled signalling pathways are activated. For the correct development of the wing for instance several signalling pathways are

required, including JAK/STAT, EGF, Hedgehog, Notch, and Wnt signalling (Blair, 2007).

3.2.1 Knockdown of GEFs induces distinct wing vein patterns

Drosophila wing vein formation undergoes strict developmental regulation. All longitudinal- and cross- veins occur in a highly reproducible pattern (). There are five longitudinal veins L1 to L5, which originate from the hinge region. L3 and L4 are connected by an anterior and L4 and L5 by a posterior cross vein.

I wanted to investigate whether endocytosis by controlling distinct signalling pathways, plays a role in the formation of these wing veins.

I used the GAL4 / UAS system to drive the expression of dsRNA hairpins, which are processed to generate siRNAs, triggering the degradation of homologous mRNAs encoding for various proteins of interest (Table 3.1). Therefore, I crossed *MS1096-GAL4* or *MJ21-GAL4* flies with *UAS-dsRNA* lines to induce dsRNA within the wings only (Dietzl et al., 2007). The *MS1096-GAL4* and *MJ21-GAL4* lines express GAL4 in the dorsal compartment of the wing either during early pupal stages or late in the 3rd instar larvae, respectively (Lunde et al., 1998; Mukherjee, 2005). The dorsal compartment of the presumptive wing blade represents the origin of several wing veins, including the L3 and L5, proximal regions of L1 and distal regions of L4 (Blair, 2007).

The crosses were incubated at 25ºC and 29ºC. The higher temperature should give rise to a stronger expression of the dsRNA, due to increased GAL4 protein activity at increased temperatures, hence resulting in a stronger knockdown. Whereas reduced levels of knockdown is expected at 25°C (Tuan, 2000). The wings of the progeny were dissected, mounted onto microscope slides and observed by light microscopy.

Notably, when essential components of the endocytic machinery, such as Clathrin or Rab5, were knocked down progeny did not survive to adulthood. In addition, the knockdown of the adaptor protein, AP2, resulted in the death of the fly progeny. Hence, I was unable assess their wing vein formation, even though the used GAL4 driver ought to restrict dsRNA expression to the wing (Table 3.1 and data not shown). This indicates, that the used *GAL4* driver lines used express GAL4 in additional developmental stages. This is consistent with the low level expression observed in the ventral wing pouch and dorsal hinge region within the wings discs of 3rd instar larvae. Faint expression within the presumptive embryonic salvary gland (stage10 to 12) has also previously been described (Marquez et al., 2001; Neuman-Silberberg and Schupbach, 1996). Another

explanation could be that the *UAS-dsRNA* constructs were activated by proteins different to GAL4, resulting in the knockdown of Clathrin/Rab5 and hence the disruption of fundamental developmental processes. To control this I could use mutants or dominant active forms of the proteins, however this excided the scope of this work. Additionally, the use of the Gal80^{ts} system would have allowed me to restrict the dsRNA expression to a certain developmental time point stringently.

Figure 3.3 shows examples of wings, depleted of individually of the Rab5 GEFs: RME6, Rabex5 or Sprint (*Drosophila* Rin1). Their knockdown resulted in distinct alteration of the wing vein patterns. The decreased levels of Rabex5 or RME-6 resulted in a wide delta at the end of L4 and L5 at 25ºC. At 29ºC this phenotype was enhanced.

In the Rabex5 knockdown additional vein material developed anterior to L3 in approx. every third observed wing. Furthermore, the posterior cross vein (PCV) was shorter and did not fully connect L4 with L5, when Rabex5 was depleted from the developing wing. Depleting RME-6 resulted in more pronounced deltas at the ends of L4 and L5, also occasionally an additional vein anterior the L3 could be observed. Different to Rabex5, the knockdown of RME-6 resulted in an additional small vein originating in the middle of the PCV.

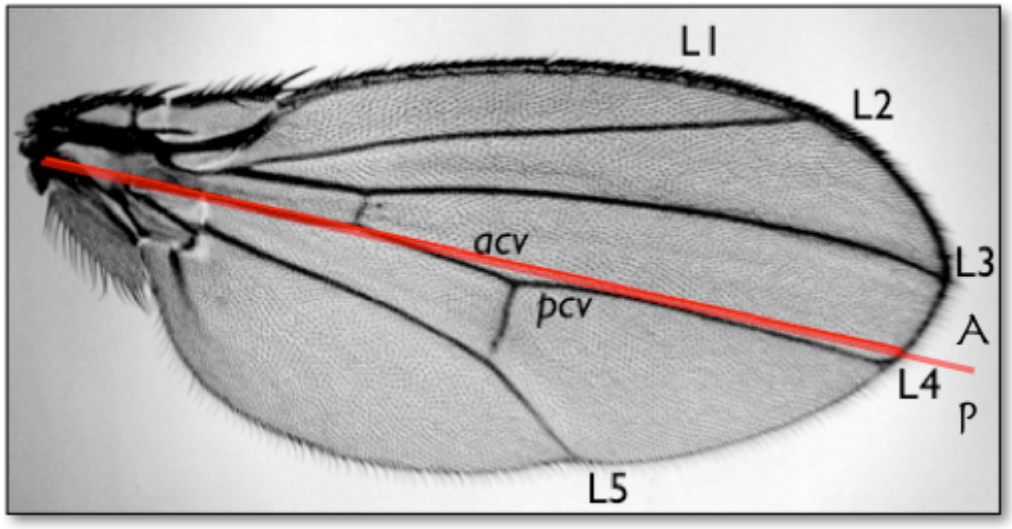

Figure 3.2: Nomenclature of wing veins in *Drosophila melanogaster*

Mounted wing demonstrated wing vein nomenclature: the five longitudinal veins labelled L1 through L5 and the anterior cross vein (acv) and posterior cross vein (pcv) formed a distinct and highly ordered pattern in every fly wing. A: anterior; P: posterior

The knockdown of Rabex5 using different dsRNA constructs, resulted similar vein patterns, which indicates that the described phenotype is likely due to the effect of Rab5

GEF depletion, rather than off-target effects of the RNA hairpins. On the contrary, I observed big differences in the phenotypes produced by the various lines used to knockdown Sprint. Three out of seven lines tested resulted in mild phenotypes including missing L4 and L5 vein ends and smaller wings (Figure 3.3 & Table 3.1). This was rather surprising, since the amorphic fly *sprint*^{6G1}, which was generated by a large deletion in the *sprint* locus following excision of an EP insertion (Jekely et al., 2005), did not show any abnormal wing development. Hence, it is likely that the observed phenotypes were the result of non-specific effects of the dsRNA, even though I compared all effects to the expression of control RNA hairpins (targeting GFP).

Similarly, I could observe an array of mild phenotypes, or no alteration on wing vein formation when Alsin was knocked down. Since Alsin is mainly associated with the nervous system and contributes to trafficking in neuronal cells (Cai et al., 2008), I suggest, that it does not play a role in the development of non-neuronal tissues, like the wing. I cannot exclude, however, that Alsin does not influence wing development, since I did not measure the levels of knockdown and a redundancy between the Rab5 GEFs could mask the effect of Alsin.

Considered together, I suggest that Sprint and Alsin do not influence wing vein development, but Rabex5 and RME-6 influenced the patterning of *Drosophila* wing veins, which could be a dose- dependent effect, since the observed phenotypes worsen when presumably more dsRNA is expressed, by incubating flies at higher temperatures. Importantly, the knockdown of Rabex5 and RME-6 each resulted in a distinct phenotype, suggesting them to fulfil separate roles.

Overall the wings and their veins could develop reasonably accurately in the presence of Rab5 GEF knockdown, suggesting that fundamental signalling processes were largely undisturbed. A high level of redundancy between the Rab5 GEFs could also explain the mild phenotypes observed.

One major pathway responsible for wing vein patterning is EGF signalling. Pathway activation occurs following ligand binding, which results in dimerisation of the receptor. Its trans-phosphorylation and the recruitment of downstream MAPK-cascade kinases result in their activation and culminate in the phosphorylation of ERK. I examined whether the failure to induce EGFR signalling phenocopies Rab5 GEF knockdown. Consequently, I knocked down EGFR, ERK and Ras and analysed the resulting wing vein distribution.

MS1096-GAL4 induced dsRNA within the dorsal wing, targeting the EGFR pathway components resulted in severe phenotypes. In most cases the wings were so impaired, that I was not able to mount them or the knockdown resulted in the death of the developing flies at various stages. Therefore, I also used an *MJ21a-GAL4* line, which induces a milder phenotype (H. Strutt personal communication), even though GAL4 is expressed in a similar pattern, the promoter driving GAL4 expression might not drive transgene expression as strongly as the *MS1096* driver. The knockdown of Clathrin or Rab5 using *MJ21a-GAL4* again resulted in the death of all progeny. Furthermore, wings depleted of components of the EGFR signalling pathways, did not appear smooth and plane, but showed strong morphological abnormalities, for instance they were curled up or folded numerous times, preventing me to be able to mount them. However, the knockdown of RME-6 did not have any discernable morphological phenotype using the *MJ21a-GAL4* driver Table 3.1. For an enhanced dsRNA expression I could also have used a dicer, which catalyses the production of siRNAs from long dsRNAs.

The experiments showed that Rabex5 and RME-6 influence *Drosophila* development in distinct ways and indicate that these two GEFs fulfil discrete functions. Nevertheless, the system used did not allow precise conclusions regarding which signalling pathway is influenced by components of the endocytic machinery to be drawn. I wanted now to address in more detail which signalling pathway they influence and the mechanisms underlying this.

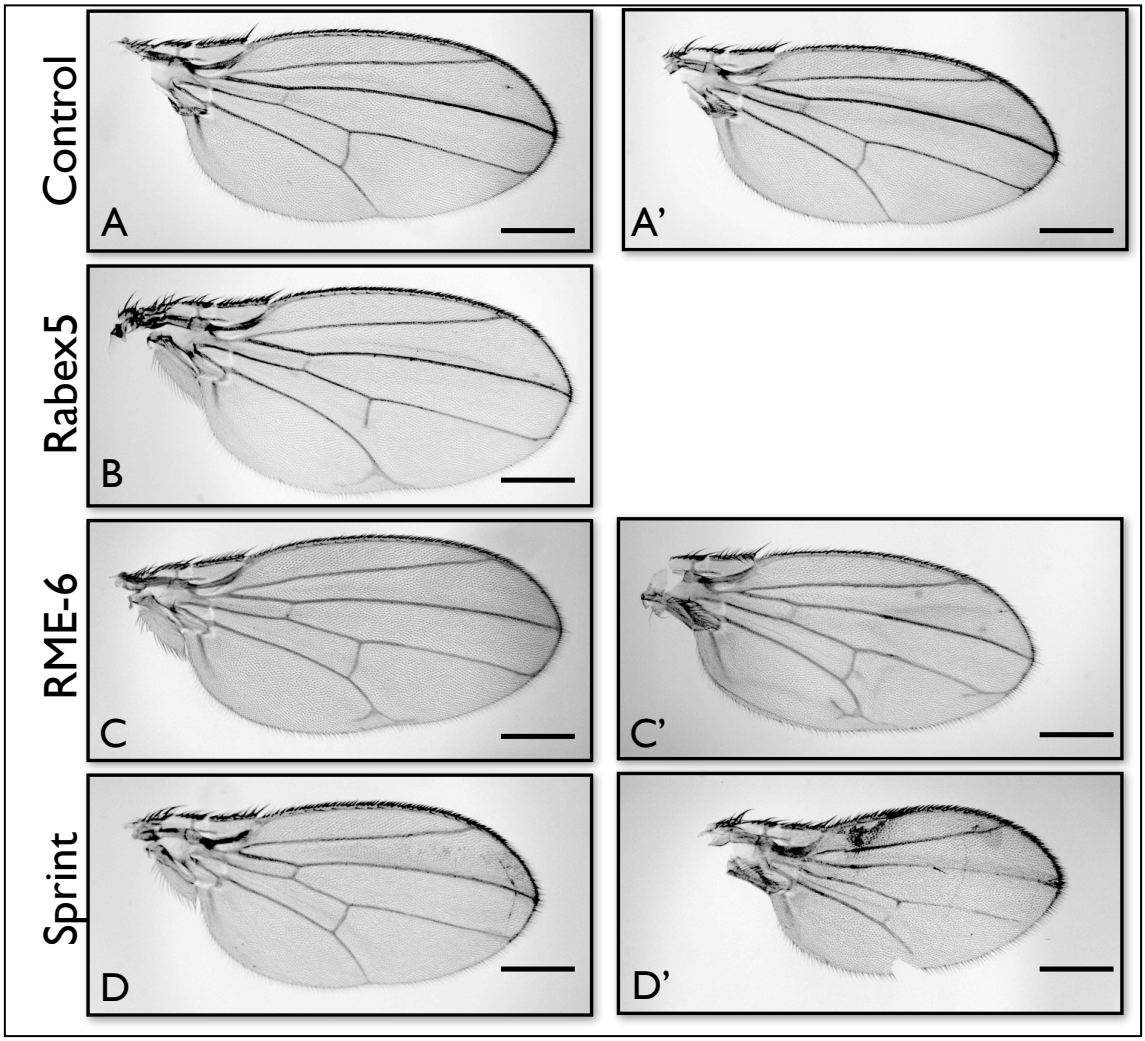

Figure 3.3: Occurrence of additional wing vein in the depletion of GEFs

The *MS1096-GAL4* line crossed to various *UAS-dsRNA* lines, inducing in: A&A': control dsRNA (GFP). B: 105534KK Rabex5 dsRNA, C&C': 106127KK Sprint, dsRNA and D&D': 19649GD RME-6 dsRNA Crosses were incubated at 25ºC (A to D) or 29ºC (A' to D'). One example for each cross of least 6 dissected and mounted wings, Scale bar represents 200µm.

Table 3.1:Summary of investigated genes for wing vein phenotypes

NM=not mounted; add: additional; A/P axis: anterior/posterior axis nomenclature according to Figure 3.2

Crossed with		*MJ21a-GAL4*		*MS1096-GAL4*	
RNAi target gene	Line ID	25ºC	29ºC	25ºC	29ºC
EGFR	43267GD	no phenotype	no phenotype	add veins	some curled around the A/P axis
Ras85DJ_1	106642GD	nothing some folded	add. veins (L1 and L2, thick veins) some curled around the A/P	folded, small, NM	very small, NM
Ras85DJ_2	9375R-3	curled around the A/P, NM	no progeny	delayed development, very small, NM	no progeny
ERK_1	35641GD	thick L2, curled around the A/P axis NM	curled around the A/P axis, NM	small folded, curled around the A/P axis NM	3rd instars
ERK_2	43123GD	curled around the A/P axis, NM	curled around the A/P axis, NM	small folded, curled around the A/P axis, NM	stubby, NM
Clathrin	23666GD	no progeny	no progeny	3rd instar	3rd instars
	22318GD			curled up, NM	no progeny
α *-Adaptin*	4267GD	no progeny	no progeny	no ACV	no ACV
Sprint	106129KK	no progeny	no progeny	thick L1	missing ends L4 and L5
	29623GD			no phenotype	no phenotype
	29624GD			no phenotype	no phenotype
	38884GD			no phenotype	no phenotype
	43501GD			no phenotype	no phenotype
	47480GD			delta on L5, add. veins at PVC	add. vein at PVC, delta on L4 and L5
	106127KK			no phenotype	small overall and L4 and L5 not complete

dAlsin	104135KK 35179GD 35180GD			no phenotype missing L5 delta on L5	no phenotype Missing L5 delta on L5 and L4
Rabex5	46329GD			delta on L5 and L4	strong delta on L5 delta on L4, add. vein dorsal L3
	105534KK			delta on L5 and L4	strong delta on L5 delta on L4, add. vein dorsal L3
RME-6	19649GD	no phenotype	no phenotype	delta on L5 and L4	add vein at PVC, PVC not full closed, delta on L4 and L5

3.2.2 The control of migrating cells

The development of eggs in the fly ovaries is a tightly regulated and complex procedure, involving multiple signalling pathways, which act at certain set developmental stages. One of these processes is the migration of border cells ((Montell et al., 2012) for review). Within the developing egg chamber initial asymmetric cell division gives rise to stem cells, either remaining in the niche, to support the follicle cells, or the cystoblast, which is the pioneer of germline cells. Germ-cells develop further, either into polyploid nurse cells and one oocyte, located in the posterior half of the chamber. Follicle cells, as specialised somatic cells, surround the egg chamber and a subset develops into polar cells, marking the anterior and posterior ends of the egg chamber. Later during stage 9 of oocyte development, 4-8 follicle cells are recruited by anterior polar cells to form the border cell cluster. The border cell cluster migrates from their anterior origin moving between the nurse cells towards the oocyte (Box1 in (Montell, 2003)).

This migration is tightly controlled by major signalling pathways including: JAK/STAT, RTKs and Notch signalling. The JAK/STAT pathway is responsible for initiating and required throughout the migration of border cells (Silver et al., 2005b; Silver and Montell, 2001). Whereas the RTKs, PDGF (platelet-derived growth factor) and VEGF (vascular endothelial growth factor) driven pathways, guide the cluster of cells to their destination (Duchek et al., 2001). The Notch pathway also plays an important role to specify particular follicle cell fates, it promotes the differentiation of all follicle cell types and thus border cell migration (Grammont and Irvine, 2001; Ruohola et al., 1991; Schober et al., 2005). Box1 in (Montell, 2003) illustrates the development of egg chambers until stage 10, after which the nurse cells continue to support the oocyte until they die and the follicle cells produce the eggshell (Montell et al., 2012).

I exploited this model to study the influence of Rab5 GEFs on signalling pathways. To follow the border cell cluster I used flies, carrying *UAS-GFP* and *slbo-GAL4* constructs. The promoter of *slbo* is only activated in migrating border cells, hence the induction of GFP by the UAS/GAL4 system is limited to the border cells, making it easier to identify the border cell cluster and restricts subsequent genetic manipulations to this cell type.

First, I defined the different border cell migration defects that can occur. Figure 3.4 shows examples of complete and defective border cell migration. Complete migration

occurred in wild type flies in both tested temperatures, as illustrated in Figure 3.4 A&A'. An example for defective migration is shown in Figure 3.4 B. Here the JAK/STAT receptor, Dome was overexpressed at 25ºC – this was previously shown to result in a dominant negative effect *in vivo* (Brown et al., 2001b). Even though the picture shows an egg later in its development than stage 10, the border cells were still visible spread out along the anterior-posterior axis, losing their cluster and inducing additional follicle cells to become invasive (Figure 3.4 B). Additionally, I observed a complete loss of follicle cell migration, when either the Dome levels were increased further (by incubating flies at 29ºC, Figure 3.4 B') or inducing strong overexpression of the dominant negative DomeΔCyt (Figure 3.4 C') (Silver et al., 2005b).

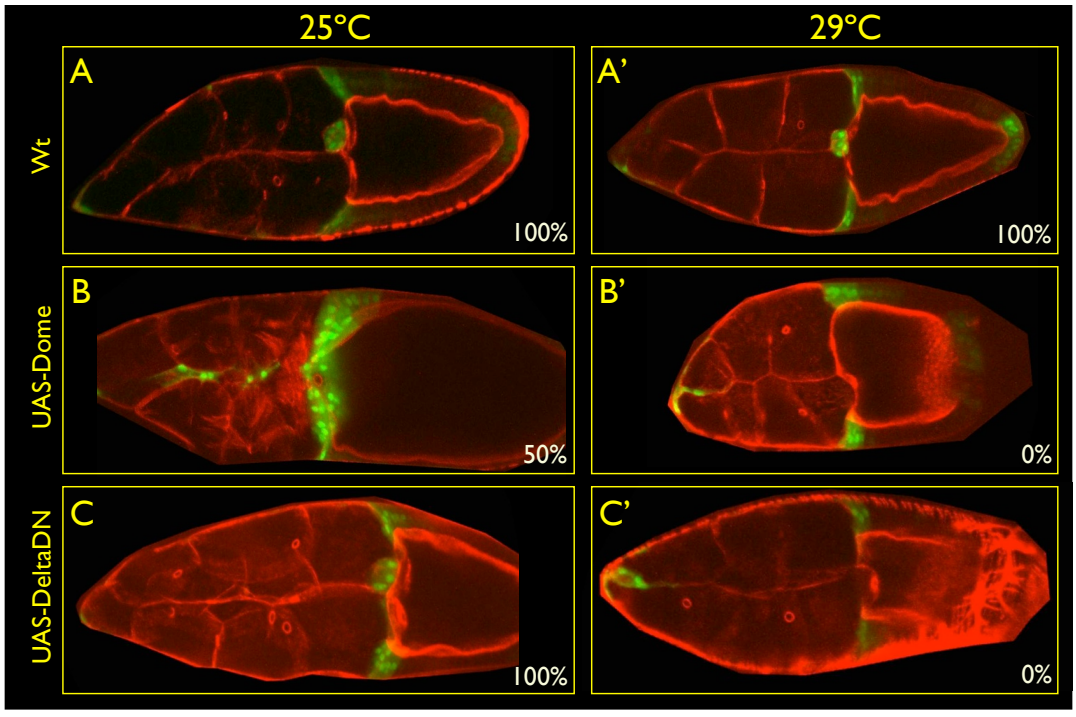

Figure 3.4: Examples of complete and defective border cell migration

Oocytes of female flies expressing GFP under the control of *slbo* (green) with indicated genotypes were dissected and stained with Phylloidin (red). Flies were kept at 25ºC (A to C) or 29ºC (A' to C') to increase expression levels of GAL4-UAS induced genes. Pictures showed approx. developmental stage 10 with 100% successful border cell migration (A, A' & C) 50% migration (later stage-see text for details) (B) and no migration of the border cell cluster (B' & C')

I used these phenotypes as references and examples to designate the rating of migration. I defined cells as 100% migrated when the border cells reached the oocyte at the end of stage 10 and for instance border cells, which were found half-way between oocyte and anterior tip of the egg chamber were scored as 50% migrated. Accordingly, I rated the

migration of border cells in the developing egg chambers from 100%, 75%, 50%, 25% to not migrated. I blindly scored at least about 50 oocytes at stage 10 per genotype and temperature and plotted the results in Figure 3.5 & Figure 3.6.

To determine the contribution of individual signalling pathways, I decided to overexpress individual signalling pathway components, using overexpression of both wildtype (wt) receptors and their dominant negative mutant forms. I set out to find signalling pathways, which influenced border cell migration when their dominant negative forms were overexpressed, but the ectopic expression of the wt receptors would not impair the migrating cells. This would allow me to study the influence of specific signalling pathways, which play a role in border cell migration, by singling one receptor I could study its influence on the migration process rather than looking at the collection of signalling pathways occurring in the developing egg.

Figure 3.5 summarises receptors and ligands tested. The overexpression of the RKTs, EGFR, Htl and Btl did not influence border cell migration, only dominant negative EGFR impaired migration at 25ºC. Furthermore, the overexpression of Argos, an EGFR signalling antagonist, altered border cell migration at 29ºC. This suggested the EGFR pathway as a good candidate to study the influence potential regulators, like the Rab5 GEFs, since EGFR (wt) overexpression did not alter border cell migration, but a dominant negative form delayed migration, as did the high-level expression of an antagonist, suggesting repressing the pathway leads to migration delays.

In addition, the slight delay in migration when Htl was overexpressed at 25ºC, suggests that the pathway is involved in egg chamber development, but the overexpression of the dominant negative Htl did not affect this process, which suggests that Htl does not play a role in border cell migration. Even though the overexpression of Htl wt at 25ºC reduced almost half of the clusters to migrate only 50%. The ectopic expressed receptor at certain levels could impair migration by influencing other pathways. The lack of influence of the ectopic expressed dominant negative form of Htl and the low to very low expression levels of Htl and its ligands in the ovary suggests that this RTK does not play a role in border cell migration (Gelbart and Emmert, 2013). However, a more detailed analysis of for instance the expression levels and effectiveness of the used constructs would be necessary to draw concrete conclusions.

I also examined the role of JAK/STAT and Notch signalling in border cell migration. Figure 3.5 shows the effect of overexpressing the receptor Dome, wild-type and truncated forms, as well as the Notch ligand, Delta, wt and dominant negative form.

As discussed earlier, I expected the overexpression of Dome with its mutant forms to delay border cell migration (Ghiglione et al., 2002). The overexpression of full-length Dome and Dome without its cytosolic domain (ΔCYT), strongly impaired the migration of border cells. However, overexpressing a construct, missing also the transmembrane domain of the receptor (Dome ΔTMCYT) did not influence migration (consistent with (Ghiglione et al., 2002)), suggesting that the intracellar domain of Dome is not able to influence JAK/STAT signalling to impair border cell migration. The overexpression of the ligand Upd and Upd3 has previously been shown to also stall border cell migration (Silver et al., 2005a; Wright et al., 2011).

Together this indicates that a de-regulation of the JAK/STAT pathway impairs migration. Since, the overexpression of the wt form of Dome impaired the migration of border cells, I decided not to study the influence of Rab5 GEFs on JAK/STAT regulation during this process, even though I could conceive to perform rescue experiments by the knockdown of Rab5 GEFs when Dome is over expressed.

The activation of Notch signalling is required for border cell migration and also the overexpression of the dominant negative form of the ligand, Delta results in a delay of border cell migration (Wang et al., 2007). I wanted to know whether the ectopic expression of Delta impairs border cells to migrate, with the objective to find a signalling pathway to study the influence of Rab5 GEFs. Hence, I overexpressed the ligand, in its wt and dominant negative form. Increased amount of ligand, delta, did not impair border cell migration, whereas the expression of its dominant negative form caused over 80% of border cells to remain at the anterior pole, when I incubated the female flies at 29ºC (Figure 3.5 B &B', consistent with (Wang et al., 2007)).

Consequently, I could use either Delta or EGFR overexpression to investigate their regulation by Rab5 GEFs. I decided to start looking at EGFR signalling, since Jekely et al 2005 suggested Sprint as a novel regulator for RTK signalling in border cell migration (Jekely et al., 2005).

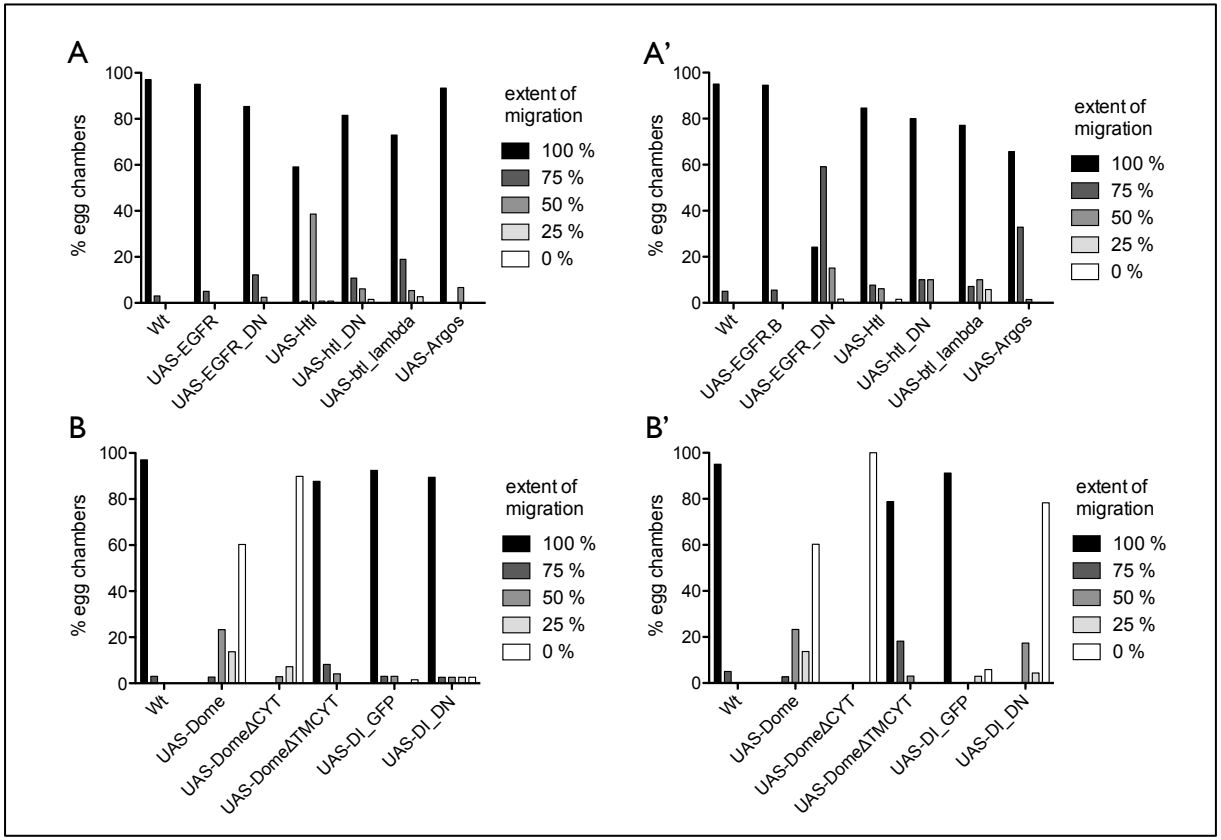

Figure 3.5: Influence of receptor overexpression on border cell migration

Graphs showed quantification of border cell migration in egg chambers at stage 10. Oocytes of female flies expressing GFP under the control of *slbo* with indicated genotypes were dissected and stained with Phylloidin for better staging, (for examples note Figure 3.4). Flies were kept at 25ºC (A & B) or 29ºC (A' & B') to increase expression levels of GAL4-UAS induced receptors. At least 50 egg chambers were used for quantifycation.

3.2.3 Sprint did not influence Border cell migration

One of the four known Rab5 GEFs, Sprint, the *Drosophila* homologue of Rin1, has previously been shown to regulate border cell migration (Jekely et al., 2005). Jekely reported 2005, that a Sprint null mutation delayed border cell migration, when EGFR or PVR was overexpressed. Whereas the overexpression of EGFR or PVR alone did not influence the migration of border cells. They suggested that Sprint acts together with Cbl, an E3 ubiqutin ligase acting early on the endocytic pathway and regulating the trafficking of EGFR and PVR. In this publication they used a *UAS-EGFR* construct, driving receptor overexpression with a *slbo-GAL4* construct and showed that border cell migration was impaired, in the absence of Sprint.

I intended of using a similar approach to perform structure-function analysis of Sprint or other Rab5 GEFs, by rescuing the described phenotype of border cell migration delay (Jekely et al., 2005) and by re-expressing the wt proteins and/or mutant forms. That would allow me to gain a more detailed understanding of the mechanism of RKT pathway regulation by Sprint. For instance, I would like to address whether Sprint influences RKT signalling with its Rab5-GEF domain or its Ras-binding site. Furthermore, I could use this system to investigate the role of RME-6 and other Rab5 GEFs within border cell migration.

Figure 3.6 shows the effect of Sprint null mutations, $sprint^{6G1}$, on border cell migration. I examined stage 10 egg chambers in Sprint hetero- and homozygote mutants with and without the induction of EGFR expression. The absence of Sprint did not influence the ability of border cells to migrate across the egg chamber, even when EGFR was overexpressed over 90% of border cell cluster migrated fully towards the oocyte. To increase GAL4 activity, I incubated flies at 29ºC, but could observe similar effects (data not shown). This stood in contrast to the results presented in Jekely et al 2005.

One possible reason for this inconsistency could be the saturation of GAL4 proteins in the system. In contrast to the work of Jekely et al, I also used an *UAS-GFP* construct within the flies to follow border cells. This additional UAS could have depleted the pool of available GAL4 necessary for the overexpression of EGFR. The receptor overexpression might not have been sufficient to induce the delay of border cell migration in a $sprint^{6G1}$ background, as seen in the Rorth laboratory. Further experiments including the analysis of EGFR expression levels would be necessary to elicit this effect.

As I would need to introduce another UAS controlled protein (e.g. Sprint with its mutant forms), to carry out structure-function experiments, I decided not to pursue this line of research, since this additional UAS would quite likley compete with the GAL4 protein pool, similarly to the UAS-GFP.

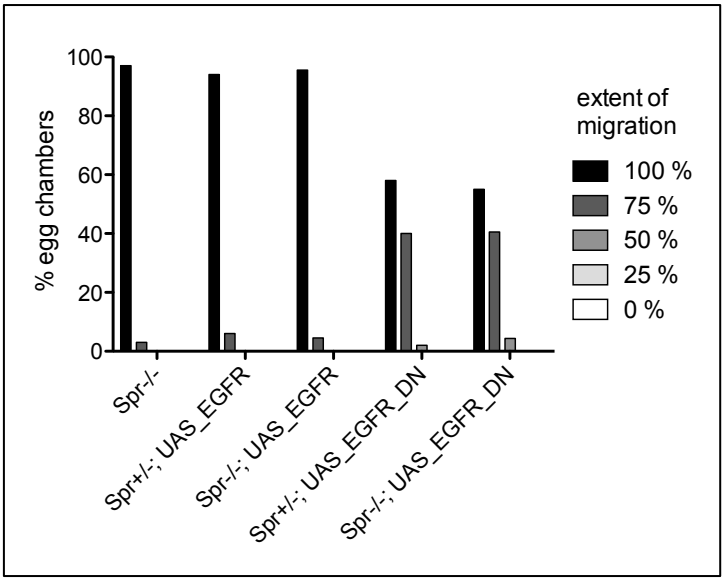

Figure 3.6: Sprint did not affect Border cell migration

Graph showed quantification of border cell migration in egg chambers at stage 10. Oocytes of female flies expressing GFP under the control of *slbo* with indicated genotypes were dissected and stained with Phalloidin for better staging, (for examples see Figure 3.4) Flies were kept at 25ºC and at least 50 egg chambers were used for quantification.

3.3 Influence of Rab5 GEFs on JAK/STAT signalling

The alteration of wing vein formation due to Rabex5 and RME-6 knockdown could have many reasons. One was the regulation of JAK/STAT signalling by these Rab5 GEFs. As this signalling pathway has previously been shown to be influenced by endocytosis, I decided to investigate the influence on Rab5 GEFs further (Devergne et al., 2007; Vidal et al., 2010).

3.3.1 *10xSTAT92E-GFP* reporter in wing disks

The development of *Drosophila* organs starts early during its development. The wing development is set up in very early larvae stages and at the last larvae stage – the third instar wandering larvae, the precursor organ for the wing – the imaginal wing disc is a well established organ in which multiple developmental processes and signalling pathways can be studied.

I used *patched-GAL4 (ptc-GAL4)* and *engrailed-GAL4 (en-GAL4)* lines to express RNA hairpins targeting Rab5 GEFs in discrete regions, which are demonstrated in Figure 3.7 A. The knockdown of the targeted proteins occurred in either half of the wing disc, when driven by *ptc-GAL4* (green in Figure 3.7 A) or in a stripe along the anterior-posterior axis of the imaginal disc, when dsRNA was induced by *en-GAL4* (red in Figure 3.7 A). In addition, the activation of JAK/STAT signalling was assessed by the expression of GFP in third instar discs derived from a [*10xSTAT-GFP*] larva. Wing imaginal disc cells activated the reporter in four regions: two patches in the hinge region anterior and posterior of the anterior-posterior axis, one region on the anterior-posterior axis dorsal of the hinge region and anterior of the margin as illustrated in blue in Figure 3.7. Upd expression was suggested to coincide with the *10xSTAT-GFP* reporter activation. (Johnstone et al., 2013; Vidal et al., 2010).

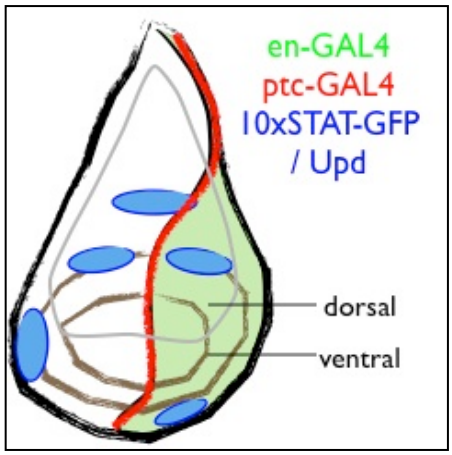

Figure 3.7: 10xSTAT-GFP reporter in wing disc

Drawing of third instar imaginal disc showed the expression of the JAK/STAT pathway activation and ligand, Upd expression (blue) and the transcripton activator protein GAL4, driven by engrailed (*en*-GAL4 in green) and patched (*ptc*-GAL4 in red). The grey line indicate the dorsal/ventral compartments, regline also separates the anterior/posterior compartments

Importantly, when RME-6 or Sprint was knocked down by *ptc-GAL4*, the 1*0xSTAT-GFP* reporter was activated in a stripe through the middle of the wing disc pouch (indicated by arrows in Figure 3.8 B). Additionally, using *en-GAL4* STAT-controlled GFP expression occurred in the posterior half of the wing disk, which was depleted of RME-6 (Figure 3.8 C). Hence, the knockdown of Sprint and RME-6 resulted in an activation of the JAK/STAT pathway presumably due to a ligand-independent mechanism. Naturally, further experiments including the overexpression and depletion of the ligand would enhance these evidences.

This seemingly ligand-independent induction of the *10xSTAT-GFP* reporter was overwritten by the presence of the JAK/STAT ligand. The expression of GFP was not altered in regions of ligand-dependent pathway activation when the Rab5 GEFs were

knocked down. I analysed all wing disc using constant confocal microscope settings. No difference could be detected in the strength of *10xSTAT* controlled GFP expression within the ligand-dependent regions of pathway activation as indicated in blue in Figure 3.7.

Interestingly, Rabex5 did not influence the *10xSTAT-GFP* expression, neither ligand-dependent nor ligand-independent. This again points towards a differential regulation of signalling pathways by Rab5 GEFs.

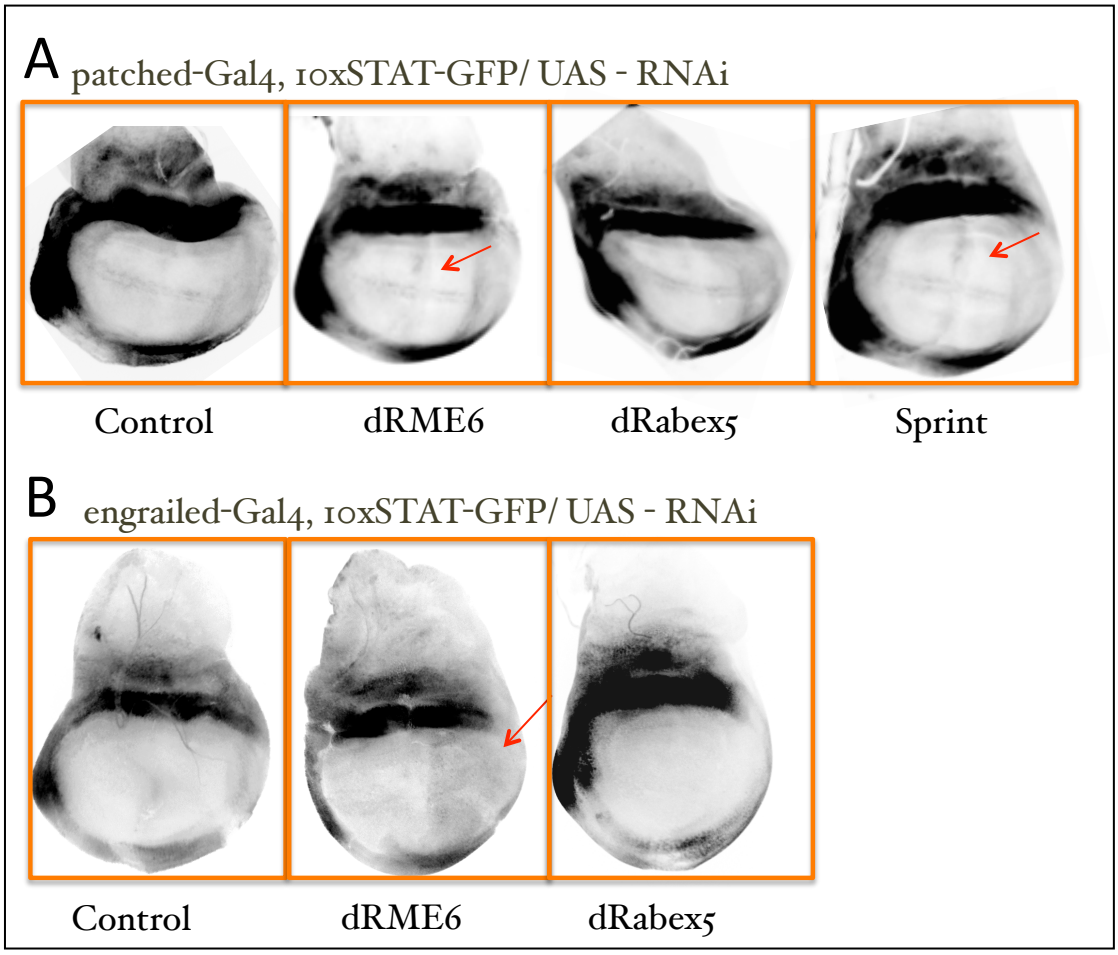

Figure 3.8: Knockdown of Sprint and RME-6 induced 10xSTAT92E-GFP reporter ligand independent

Imaginal wing discs were dissected from third instar larvae with indicated genotypes and at least 10 discs per cross were analysed. The expression of GFP driven by a 10xSTAT92E binding site was captured and shown was each one representative example. red arrows indicated the expression of GFP in the absence of ligand Upd A: indicated dsRNA was driven by patched and B: dsRNA was induced in half of the disc under the control of *engrailed*; used UAS-dsRNA lines: Sprint: 106127KK, RME-6: 19649GD, Rabex5: 105534KK

3.3.2 GMR-Upd overexpression in eye

Another system to investigate genetic interactions with the JAK/STAT pathway was to examine the development of the *Drosophila* eye.

The ectopic miss-expression of Upd in the developing fly eye leads to an overgrowth of the eye disc, resulting in an abnormally large eye. This dosage-sensitive dominant eye overgrowth phenotype was caused by ectopic activation of the JAK/STAT pathway, induced by Upd under the control of *GMR*, an eye specific promoter. This system was used in several screens, looking for finding novel genetic interactions within the JAK/STAT pathway (Bach et al., 2003; Mukherjee et al., 2006). I wanted to use it to investigate whether Rab5 GEFs influenced Upd-induced eye overgrowth and hence address if they are modifiers of the JAK/STAT signalling pathway.

In Figure 3.9 A to C examples of *Drosophila* eyes overexpressing Upd are illustrated. The compound eye increased in size when the JAK/STAT ligand was ectopically controlled by *GMR* (Figure 3.9 A). I quantified observed phenotypes using a simple scoring scheme from one to five, in which one accounted for a normal grown eye and five for an over-large eye. Scores of investigated genotypes were plotted in Figure 3.10 A.

Upd-induced overgrowth could be reduced when one copy of the transcription factor STAT92E was lost. This applied for two independent mutant alleles. The eye overgrowth was not influenced when one copy of Sprint ($sprint^{6G1}$) or Rabex5 ($rabex^{ex42}$) was missing in examined flies. This could be due to the remaining Sprint proteins left within the flies. Since *sprint* and the *GMR-Upd* overexpression construct was both on the X-chromosome, I would have to recombine the P[*GMR-UpdΔ3'*] insertion with the $sprint^{6G1}$on the same chromosome, to investigate the effect of the homozytote $sprint^{6G1}$. A different and faster approach to reduce protein levels was to knockdown Sprint and Rabex5.

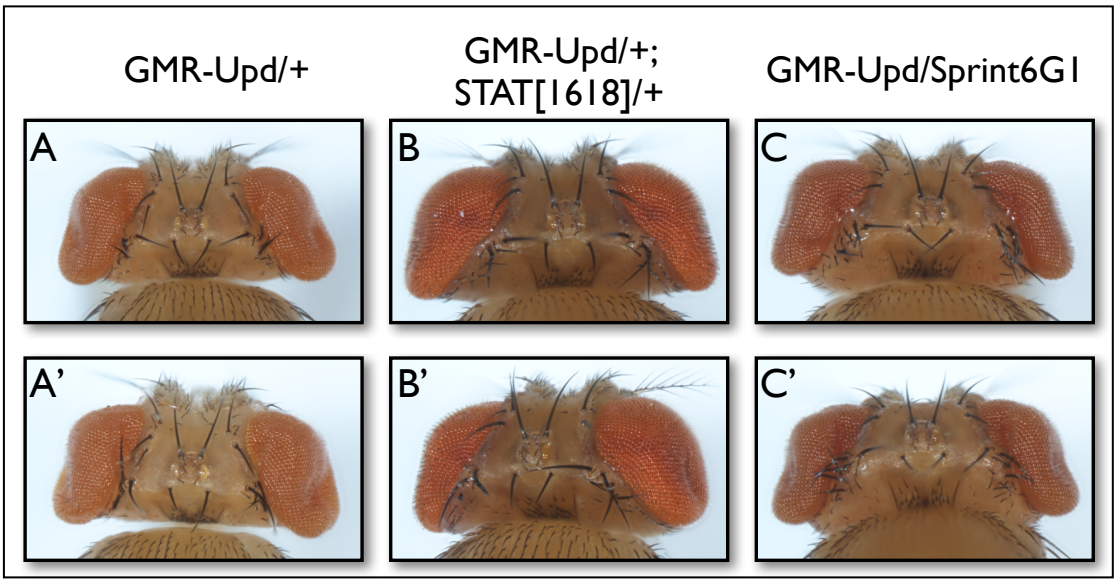

Figure 3.9: Examples of Upd induced eye-overgrowth

Eye-overgrowth was induced by placing Upd expression under the control of GMR. Genes were analysed by either taking away one copy, heads of flies with indicated genotypes as each two examples of the eye overgrowth for A and A': GMR-Upd control background, B and B': GMR-Upd and STAT[1618] mutant, and C and C': GMR-Upd in a Sprint6G1 background..

For this I could use a fly line not only carrying the *GMR-Upd,* but also a *ey-GAL4* construct, enabling me to drive *UAS-dsRNA* constructs in the eye only. This also allowed me to investigate the role of RME-6 and Alsin, which did not have any available mutants in *D. melanogaster*. Hence, I decided to knockdown these Rab5 activators (Figure 3.10 B).

Since endocytosis was suggested to regulate the JAK/STAT pathway, I also knocked down Clathrin, Rab5 and AP2. Unfortunately, the knockdown of Clathrin and Rab5 resulted in the failure of flies to develop to adulthood. However, the depletion of AP2 resulted in an increase of eye overgrowth when Upd was overexpressed (Bach et al., 2003). The fly eyes were not only larger, it also seemed that the AP2 knockdown caused a slightly rough phenotype. Since such a phenotype was to my knowledge so far not reported, even when Upd was driven at different eye-specific developmental stages or using known regulators of the JAK/STAT pathway, I would suggest that this effect might be due to an interference with an additional signalling pathway, but more experimental evidence, including the effect of AP2 knockdown without the ectopic expression of Upd, would be necessary to draw any conclusions.

Like the lack of one copy of Rabex5 or Sprint, the knockdown of all tested Rab5 GEFs did not influence eye overgrowth, when the JAK/STAT pathway was hyper-activated within the eye.

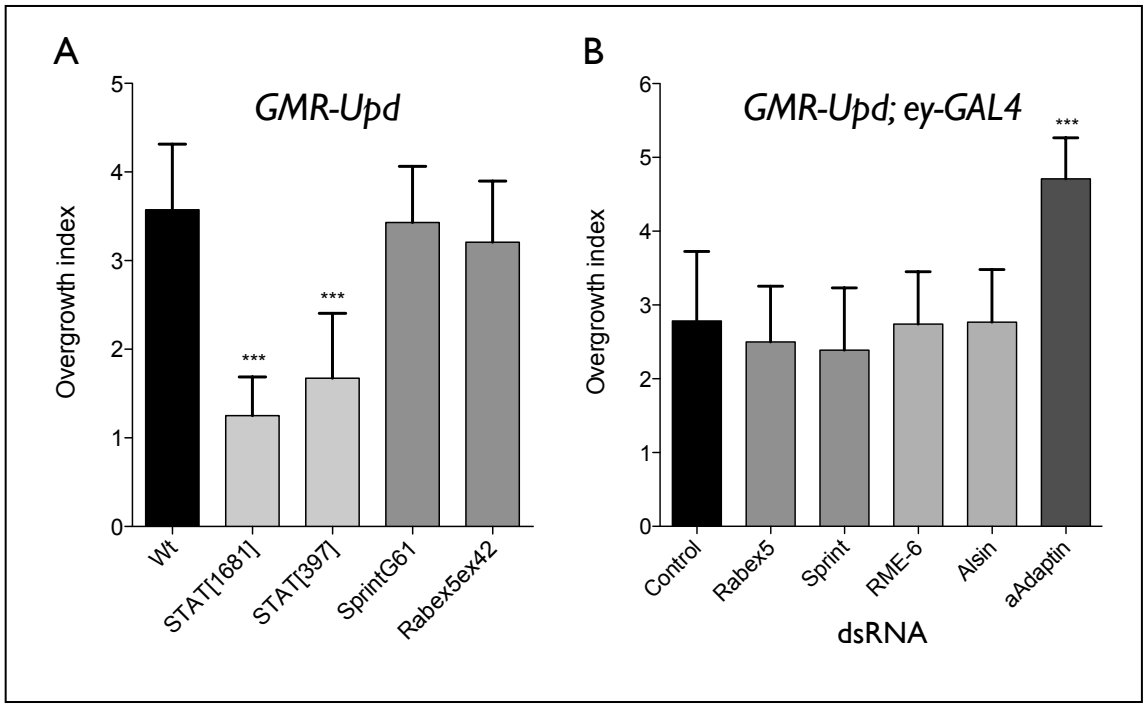

Figure 3.10: Upd induced eye-overgrowth is not influenced by GEF knockdown

Eye-overgrowth was induced by placing Upd expression under the control of GMR Genes were analysed by either taking away one copy (A) or inducing dsRNA within the eye against them (B), Graphs showed overgrowth index with 1=normal eye and 5=very strong overgrowth, at least 50 flies each cross were used for quantification. A: overgrowth index when the loss of one copy of indicated genes occurred and B: overgrowth index for eyes of flies carrying an *ey-GAL4* driver and indicated indicated UAS-dsRNA constructs; used UAS-dsRNA lines: Sprint:106127KK, RME-6 19649GD, Rabex5 105534KK, Alsin:104135KK, α-Adaptin: 15565GD error bars represent standard deviation, students t-test was performed by comparing the different genotypes (A) or knockdowns (B) with the control (wt in A, or dsRNA targeting GFP in B*p>0.05, **p>0.01,***p>0.001

3.4 Influence of Rab5 GEFs in RTK signalling pathways

RTK pathways are crucial signalling pathways involved in many developmental processes within the fly. In RTK signalling the receptor itself has a kinase activity, resulting after a cascade of signal transduction in the phosphorylation of ERK. ERK as an endpoint of various RTK signalling pathways can be activated, ergo phosphorylated by a number of ligands and receptors. Analysing this endpoint of RTK signalling would enable me to work backwards in order to pinpoint exactly where regulation took place

and which pathway(s) were involved. However, first I needed to examine whether the phosphorylation ERK was altered when Rab5 GEFs were absent.

3.4.1 The activation of ERK

3.4.1.1 dpERK Immunohistochemistry of embryos

I investigated whether the phosphorylation of ERK occurred during embryogenesis, in *sprint*^{6G1} embryos. *Drosophila* embryo development is a tightly regulated process occurring in approximately 15 stages within 12 hours (at 25ºC). Luckily, a well-established anti-phospho-ERK antibody was available, which could be used staining embryos at various stages. Additionally, I co-stained fixed embryos also with Crumbs, which allowed me to judge their developmental stage better, by visualising the morphology of the embryo. This approach enabled me to examine signalling at various developmental phases, including many different RTK receptor and ligand activities, as illustrated in Figure 5 in Gabay et al., 1997. The earliest described RTK leading to dp-ERK staining at the anterior and posterior poles of the embryo is Torso after approx. 2 hours post-fertilisation (Figure 5 in Gabay et al., 1997). And for instance the closest homologue to EGFR, DER, is active at stage 5 to 10 in the ventral ectoderm and in several other organs, for instance the cephalic furrow (stage 7) or tracheal placodes (stage 10) (Figure 5 in Gabay et al., 1997).

Figure 3.11 shows a few examples of different staged embryos. Depending on the developmental stage of the embryo, phosphorylated ERK was due to a variety of RTK pathways. For instance the anti-phospho-ERK signal within the tracheal pits, in Figure 3.11 A, is likely to be caused by Btl signalling (Figure 5 in (Gabay et al., 1997), where as the dorsal segmental pattern in stage 12 embryos (Figure 3.11 B'), were due to DER signalling, according to (Figure 5 in Gabay et al., 1997).

I examined around 50 embryos, for each wild type flies and *sprint*^{6G1} at different stages and I could not detect any obvious change in phosphorylation pattern or intensity, using consistent confocal microscopy settings and antibody staining procedure (for example pictures see Figure 3.11)

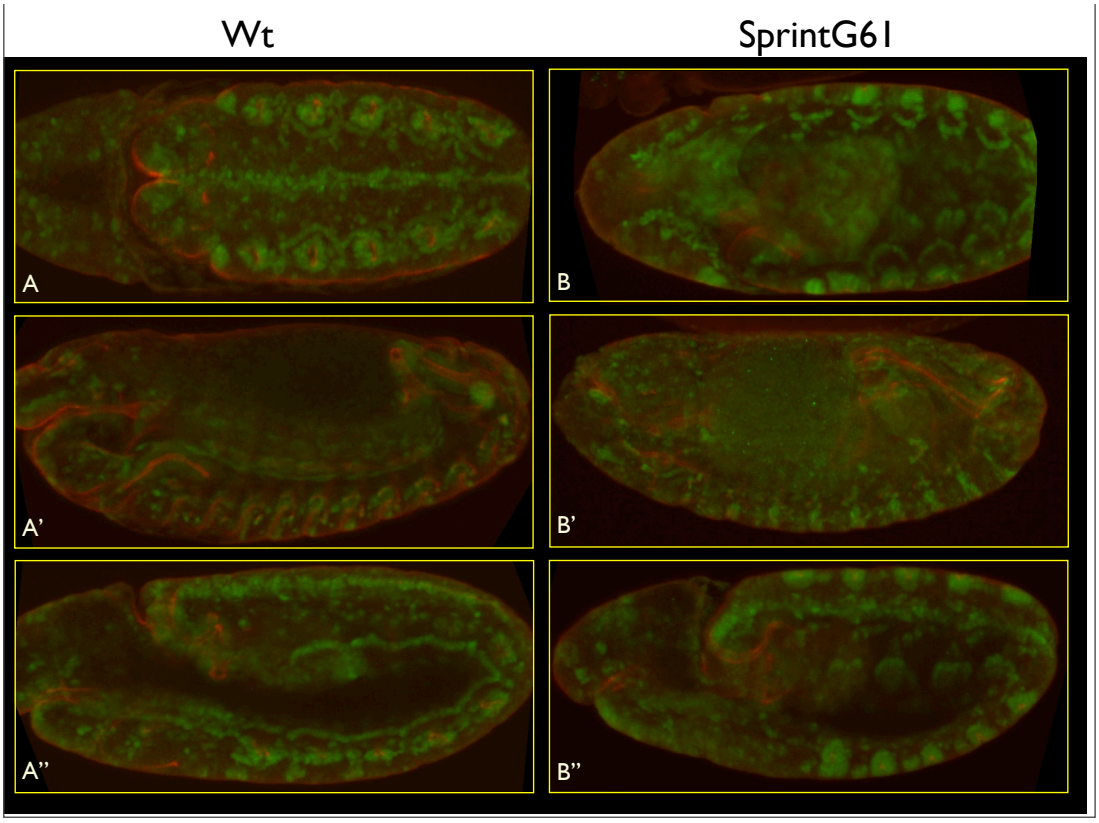

Figure 3.11: Phosphorylation of ERK in embryos independent of *sprint*^{6G1}

Example pictures of anti-pdERK (green) and Crumbs (red) immuno-stained embryos in different developmental stages A&B: 10 to 11 A'&B': 12 to 13 A''&B'': 14 to 15 A to A'': wt embryos and B to B'': *sprint*^{6G1} embryos examples of approx. total 30 embryos at various stages for each genotype.

3.4.1.2 The phosphorylation of ERK in adult flies

This microscopic approach is subjected to restrictions quantifying straightforwardly the occurrence of dp-ERK. Therefore, I explored the use of immunoblotting. Additionally, I wanted to investigate the role of RME-6 and Rabex5 in phosphorylation of ERK. Unfortunately, the knockdown of genes within embryos was an obstacle, since maternal proteins were often still present and knockdowns become thus very inefficient and due to the lack of suitable antibodies, I would be unable to confirm levels of knockdown. Hence, I decided to knockdown Rab5 GEFs within the entire adult fly, using an *actin-GAL4* driver and examined whole fly lysates by western blot.

I crossed flies containing UAS controlled dsRNA to target the mRNA transcripts of RME-6, Sprint, Rabex5 and AP2 to an *actin-GAL4* driver fly line. I evaluated the levels of phosphorylated ERK within the offspring (Figure 3.12). Therefore, I probed the western blots, containing whole fly-lysates with anti-ERK (bottom panel Figure 3.12 A)

and anti-dp-ERK (top panel Figure 3.12 A) to normalise phosphorylated proteins to the total levels of ERK (Figure 3.12 B). Additionally, I also examined *sprint*^{6G1} flies by blotting their lysates with anti-dp-ERK antibodies, as illustrated in Figure 3.12 C. Unsurprisingly, the levels of phospho-ERK were similar in *sprint*^{6G1} flies to the wt controls.

As suggested by the immunostaining of embryos, neither Sprint knockdown, nor its mutation had an effect of ERK phosphorylation. In addition, RME-6 depletion showed no effect of phospho-ERK levels. Never the less this experiment indicated a decrease on the phosphorylation of ERK, when AP2 was depleted. Surprisingly, the global knockdown of AP2 allowed fly survival, whereas AP2 depletion within the wing (using *MS1096*) resulted in the death of the fly progeny (Table 3.1). This also indicates that the used *Actin-GAL4* line might not express GAL4 in high levels and the knockdown of AP2 was inefficient. Further repeats would need to be undertaken to show a reduction of phospho-ERK levels, when AP2 was knocked down, also assessing the extent of the AP2 knockdown. Nevertheless, this experiment indicated a decrease in the phosphorylation of ERK.

The knockdown of Rabex5, increased phospho-ERK over 8 fold. This was consistent with published data (Xu et al., 2010; Yan et al., 2010). Ras activates phosphorylation of ERK and Rabex5 was shown to suppress the effect of Ras, by marking Ras with ubiquitin and leading thus to its degradation. Hence, the loss of Rabex5 lead to accumulation of phosphorylated ERK. This process was likely to be caused by the ubiquitin ligase activity of Rabex5 rather than its Rab5 GEF activity (Xu et al., 2010; Yan et al., 2010).

As RME-6 and Rabex5 had a ligand-independent effect on JAK/STAT signalling within the wing disc, I also tried to examine their effect within this larvae tissue on phosphorylated ERK. Unfortunately, in preliminary experiments I undertook, I could not immuno-stain the phosphorylated ERK in the wing discs (data not shown). Due to time restrictions I could not further improve the immuno-staining protocol for dp-ERK in the wing disc to further examine the influence of Rab5 GEFs on RKT signalling in the developing wing.

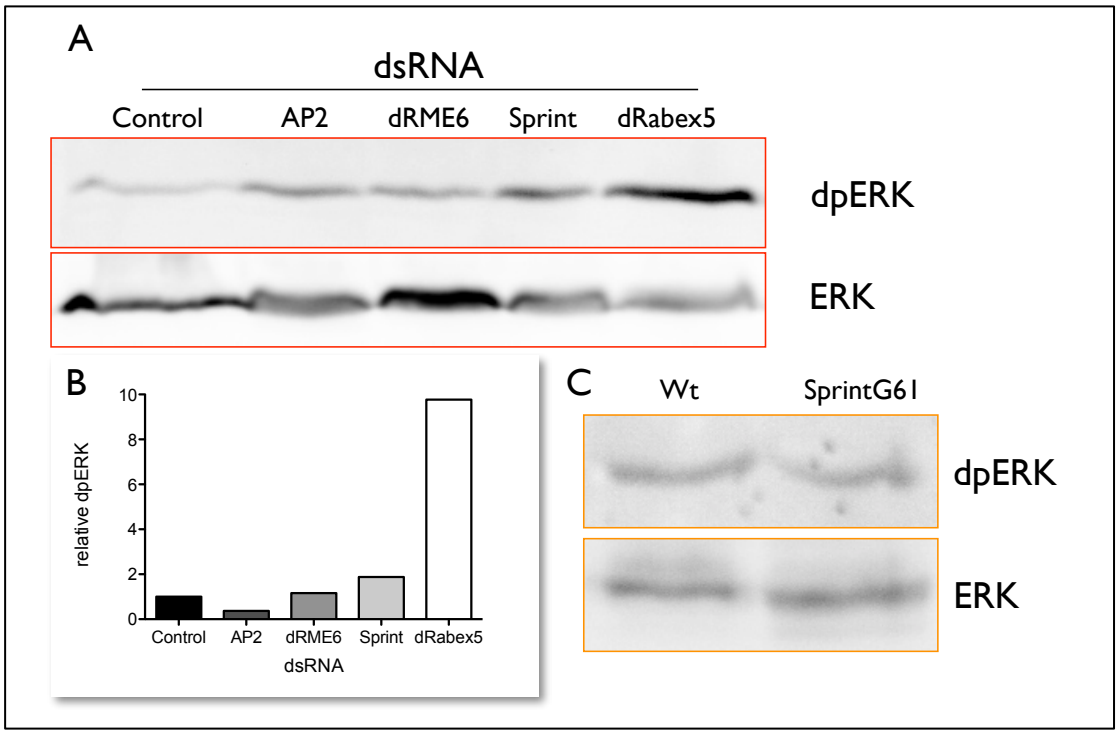

Figure 3.12: Influence of Rab5 GEFs on phospho-ERK in adult flies

A and C Immunoblots against dpERK and ERK of whole fly extracts segregated by SDS-PAGE of A: flies with *actin*-GAL4 driven dsRNA against indicated genes and C: wt or *sprint*^{6G1} flies. B: Quantification of A, whereby the ratio of pdERK to ERK was plotted as relative pdERK; used UAS-dsRNA lines: Sprint: 106127KK, RME-6 19649GD, Rabex5 105534KK, AP2: 15565GD

3.5 Summary

This chapter highlighted some evidence that Rab5 GEFs influence *Drosophila* signalling *in vivo*. Wing vein patterns were altered, when RME-6 or Rabex5 were knocked down, however, Alsin and Sprint knockdown did not influence wing vein formation. By trying to reveal which signalling pathway was responsible for those alterations, I showed that the JAK/STAT pathway was activated independently of ligand when RME-6 or Rabex5 were knocked down within the developing wing disc. Furthermore, I could not alter JAK/STAT ligand-induced overgrowth of the eye, by depleting the different Rab5 GEFs. However, due to the severity of the Upd induced eye overgrowth, this assay might be unsuitable to detect negative regulators of JAK/STAT signalling.

Therefore, I moved on and further examined the effect of Rab5 GEFs on ERK phosphorylation. Rabex5 depletion caused an increase in phospho-ERK, which was

likely due to its ubiquitin ligase activity rather than its GEF function (Xu et al., 2010; Yan et al., 2010).

Unfortunately, I could not reproduce published effects of Sprint, regulating border cell migration, which I would have used as the foundations for structure function analysis of Sprint.

Investigating the effect of Rab5 GEFs *in vivo* I did not account for their possible redundancies, by performing either double knockdown experiments or knockdowns of the Rab5 GEFs in mutant backgrounds (as possible for $sprint^{6G1}$ and $rabex5^{ex42}$).

Even though I did not address the levels of knockdown by qPCR to measure mRNA or western blot to measure proteins, I could observe a Rab5 GEF specific effect in either the wing vein development for RME-6 and Rabex5 or wing disc for RME-6 and Sprint, hence I conclude that the dsRNA constructs depleted proteins from the organism to which extend this occurred, still needs to be determined.

Overall this chapter represents an insight on Rab5 GEFs and the notion that they have an distinct effect on developmental processes. It marked in addition the versatility of using *Drosophila* as a model organism, by showing various possibilities to study signalling pathways. I simultaneously performed *in vitro* experiments to investigate their role further within the JAK/STAT pathway.

CHAPTER 4. CHARACTERISATION OF JAK/STAT (ENDOCYTOSIS) *IN VITRO*

The challenges encountered in establishing *in vivo* assays to study endocytic regulation of intracellular signalling urged me to focus more on establishing *in vitro* assays. Specifically I aimed to investigate whether JAK/STAT is quantitatively and qualitatively controlled by endocytosis.

Studies suggested that JAK/STAT signalling was controlled by endocytosis (Devergne et al., 2007; Vidal et al., 2010). Interestingly, the studies were contradictory as to whether endocytosis was a negative or positive regulator of the JAK/STAT pathway. I wanted to address further how its signalling is regulated by endocytosis and most importantly, I set out to investigate whether JAK/STAT signalosomes exist.

Firstly, I needed to quantitatively measure endocytosis to be able to study ligand uptake. The in depth knowledge of the bio-chemical properties of Upd2 uptake would allow me to study its regulation by endocytic components and other regulators, suggested to play a role in JAK/STAT control.

Furthermore, I wanted to directly measure JAK/STAT signalling in order to evaluate the influence of endocytosis quantitatively and qualitatively. The use of well-established luciferase assays would enable me to get a general insight into signalling regulation (Baeg et al., 2005). Additionally, to investigate differential signalling I wanted to adapt an endogenous JAK/STAT target assay (Bina et al., 2010). With these approaches I ought to be able to study the effect of the depletion of endocytic components and other potential regulators.

4.1 Endocytosis assays

To measure the uptake of JAK/STAT ligand by *Drosophila* cells, I used immunofluorescence to visualise the uptake of Upd2-GFP in the first instance. This would allow me to visualise the ligand within different compartments of the cell.

In addition to the immunofluorescence approach, I wanted to measure endocytosis of Upd2-GFP biochemically. This would enable me to analyse the ligand binding, endocytic rates and also the amount of Upd2-GFP within conditioned medium. Together these two methods would allow me to show by two independent techniques the uptake mechanism and regulation of JAK/STAT signalling.

4.1.1 Endocytosis-assays using Immuno- fluorescence

Immunofluorescence is a widely used approach to follow ligand uptake and trafficking through the cell. In the first series of experiments, I used this approach to investigate the uptake of Upd2-GFP, which was able to activate JAK/STAT signalling (Section 4.2). Technical reasons (higher expression, no use of heparin to collect in conditioned media ect.) lead me into using Upd2, rather than Upd or Upd3 (compare to Wright, et at. 2011). Since *Drosophila* cells in culture have a high background, I optimised the detection of) the ligand Upd2 fused to GFP (expressed by the same reading frame) by using a variety of staining protocols and antibodies (see 2.1.3.1 and Table 2.9 for further details). I incubated cells grown on cover slips with Upd2-GFP conditioned media (CM) before washing them and staining with a variety of antibodies against GFP. Figure 4.1 shows that out of five different antibodies tested, none could detect Upd2-GFP above background levels. Fortunately, an anti-GFP antibody, generated in-house, was able to detect Upd2-GFP in a convincing manner (Figure 4.2).

4.1.1.1 Heterogeneous uptake of Upd2-GFP in KC_{167} cells

In order to establish whether ligand uptake was time-dependent, I treated KC_{167} cells for 0, 15 and 30 minutes with Upd2-GFP CM. After 15 minutes incubation, Upd2-GFP was visible in distinct vesicular structures and, after 30 minutes incubation, the staining for the ligand is brighter and still in punctae although these appear to be deeper within the cell (Figure 4.2). Consequently, I could conclude that KC_{167} cells take up the ligand Upd2-GFP in a time-dependent manner.

Unfortunately, this uptake was heterogeneous and only some cells stained for GFP when treated with Upd2-GFP as highlighted with arrows in Figure 4.2. This phenomenon was consistent with data shown in (Vidal et al., 2010). In order to show that endocytosis regulated Upd2 uptake one could use such a heterogeneous system, but to study the fine nuances of endocytic regulation and to facilitate the quest of finding novel modulators of JAK/STAT signalling and the visualisation of the ligand uptake by all cells would be desired.

One possible explanation for the heterogeneous uptake could be a heterogeneous expression of the receptor, which could be proven by for instance immunostaining of the cells with an anti-Dome antibody.

However, I examined the uptake of Upd2-GFP in $S2R^+$ cells, since I used this cell line in subsequent experiments, but unfortunately the optimised staining protocol for KC_{167}

cells did not work well on these cells and time restrictions confined additional optimisation efforts to a minimum.

To study the regulatory effect of endocytosis on the JAK/STAT signalling pathway I wanted to use one cell line only in order avoid misinterpretation of the data due to variations between *Drosophila* cell lines. Since the immunofluorescent signals of Upd2-GFP uptake in KC_{167} cells was variable and the cell line was unsuitable for the enzyme-linked immunosorbent assay (ELISA) analysis of internal Upd2 (section 4.1.4.1), I used $S2R^{+}$ cells in all subsequent experiments.

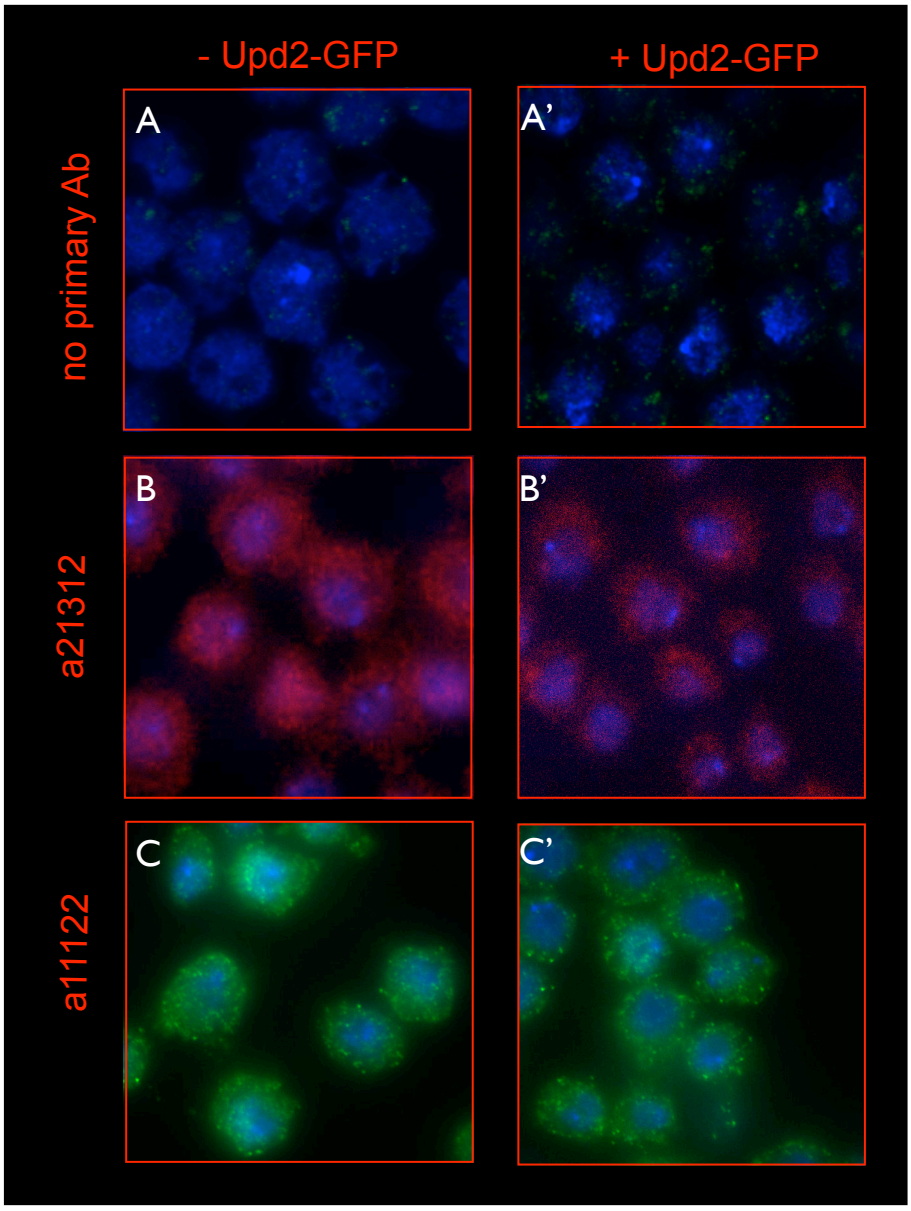

Figure continues on next page

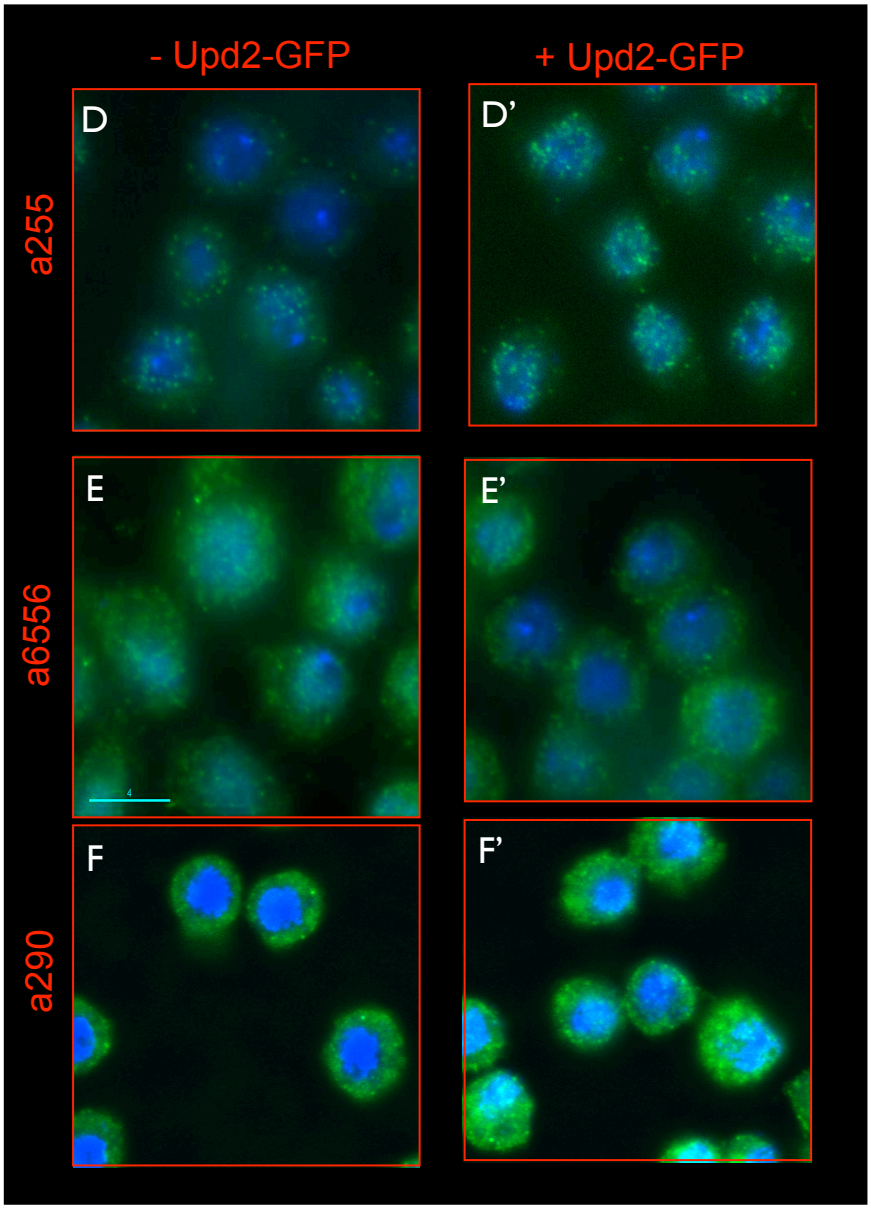

Figure 4.1: Evaluation by Immunofluorescence of anti-GFP antibodies in KC_{167} cells incubated with Upd2-GFP

Cells were incubated with 20nM Upd2-GFP (A' to F') or Control media (A to F) for 15min at 25ºC and then stained with the indicated antibodies (B to F) and appropriate secondary antibodies, for details of the antibodies Table 2.9. Fluorescent signals were detected using the Delta Vision microscope

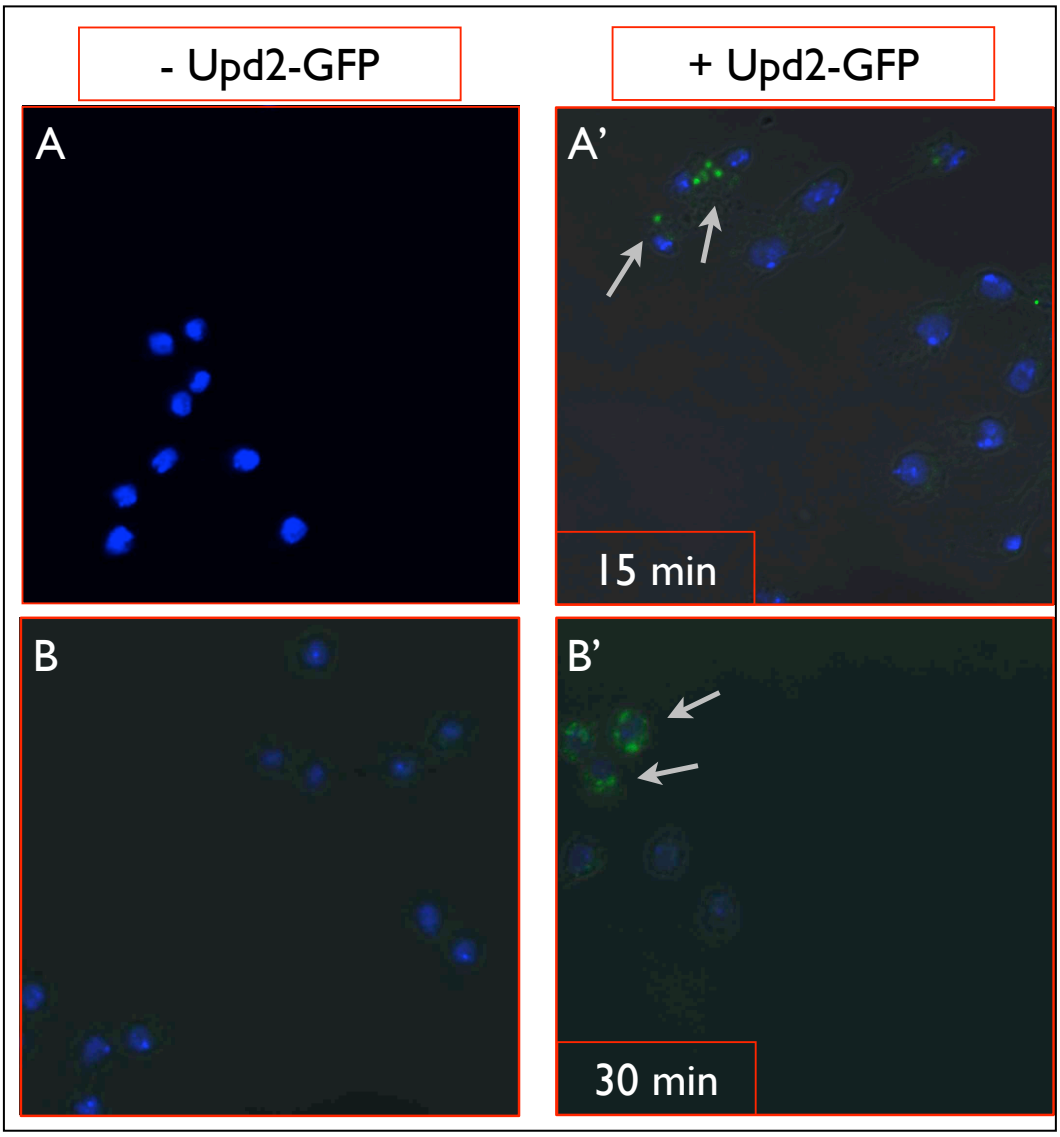

Figure 4.2: Immunofluorescent images of Upd2-GFP detection in KC_{167} cells

Cells were incubated with 20nM Upd2-GFP for 15(A') or 30min(B') and Control media (A and B) for 15min (A) or 30min (B) at 25ºC, Upd2-GFP uptake was stopped by chilling the cells down to 4ºC and bound Upd2-GFP was removed by an acid wash. Cells were fixed and stained with pre-cleared anti-GFP (KV) antibodies. Fluorescent signals were obtained by using Confocal microscopy and internal staining is indicated by the white arrows.

4.1.2 Establishment of an ELISA assay to measure GFP

Parallel to the microscopic investigations of Upd2-GFP uptake, I established an *in vitro* assay to measure endocytosis. I decided to measure Upd2-GFP by the detection of the fused GFP via an anti-GFP ELISA. This tool allowed not only the quantification of ligand in the CM, but also quantitative measurement of Upd2 uptake in cells and binding to cells.

Figure 4.4 showed the main scheme of the composition of the GFP ELISA. To capture the antigen, GFP, plates were coated with a goat anti-GFP antibody (purple). GFP was then detected using a primary rabbit anti-GFP (red) and secondary anti-rabbit antibody (brown) (for details see Table 2.9).

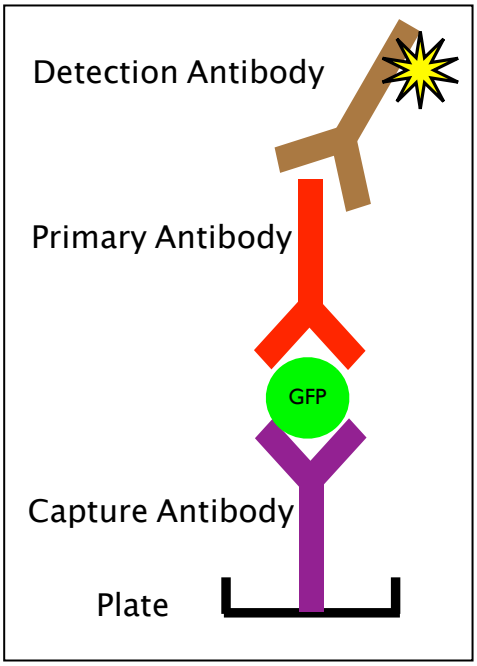

Figure 4.3: Schematic illustrating the basis of the ELISA assay

The antigen GFP was sandwiched between the capture antibody (goat anti-GFP) in purple and primary antibody (rabbit KV anti-GFP) in red. The detection antibody (brown), raised against rabbit and coupled to HRP (yellow star), allowed for signal detection by absorbance at 492nm

In order to avoid cross-reactivity and reduce background levels, I tried to use the smallest amount of antibody possible. Hence, I titred primary and capture antibodies individually using GFP recombinant protein up to 4ng/ml as an antigen (Figure 4.4). All tested concentrations of the primary antibody resulted in a linear range of absorbance when plotted against the GFP concentration. The most diluted concentration of capture antibody was suitable for the ELISA. Absorbance was directly proportional to concentration using 0.0625µg/ml of the capture antibody and 0.0625ng/ml of the primary antibody, over a range of 0.5 to 2ng/ml GFP. Those conditions were subsequently used for all ELISA assays.

Having developed an anti-GFP ELISA I could now not only assess the amount of Upd2-GFP bound to the surface or internalised into cells, but also the concentration of Upd2-GFP in the CM. During the production of CM, Upd2-GFP concentration varied from batch to batch. By measuring and thus adjusting it I was able to ensure that equal concentrations of CM were used in all experiments. Most importantly the exact quantification of ligand allowed me to precisely characterise ligand binding and uptake properties, which was described in following sections.

Using the ELSIA, I could measure endocytosis and distinguished three different aspects: I) bound ligand only, II) internalised material only and III) external and internal ligands.

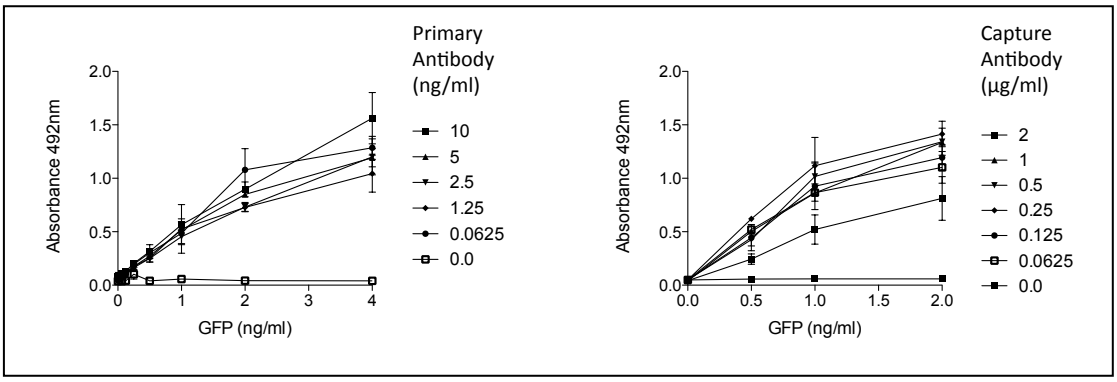

Figure 4.4: Development of an ELISA to detect GFP

Graphs show the relationship between a known concentration of GFP and absorbance at 492nm To establishing the working range of the ELISA in A: 2µg/ml of capture antibody (goat anti-GFP) was used and the primary antibody (KV anti-GFP) titred over the indicated range and in B: 0.0625ng/ml of the primary antibody (KV anti-GFP) was used and the capture antibody (goat anti-GFP) was titred accordingly.

4.1.3 Binding of Upd2-GFP to S2R$^+$ cells

The binding of the ligand to the receptor is the initial step of receptor-mediated endocytosis, and hence it is crucial to describe the characteristics of the JAK/STAT ligand, when studying endocytic regulation. I therefore examined the specificity and concentration dependence of Upd2 binding to S2R$^+$ cells.

To measure binding I incubated S2R$^+$ cells with the Upd2-GFP CM at 4ºC, preventing endocytosis of any material, followed directly by lysis of the cells. This method was used to estimate Upd2 binding saturation and specificity.

4.1.3.1 Upd2-GFP binding to S2R$^+$ cells is saturable

I wanted to determine the concentration at which Upd2-GFP saturates Domeless in S2R$^+$ cells. I wished to avoid using a concentration of Upd2-GFP, which oversaturated the system, since receptor-independent endocytosis could occur under these circumstances and complicate analysis of the data. Consequently, I wanted to use the lowest possible ligand concentration required to saturate the receptor while investigating JAK/STAT signalling.

Media conditioned with Upd2-GFP was prepared by transfecting cells with an Upd2-GFP expression vector (Hombria et al., 2005) section 2.4.2.1 details). Individual batches of Upd2-GFP were titred for each experiment.

I used CM containing Upd2-GFP at a minimum concentration of 40nM to investigate the linear range and saturation point of Upd2 binding. Figure 4.5 A shows binding of Upd2-GFP to $S2R^+$ cells following incubation of cells with increasing concentrations of ligand at 4ºC. Upd2 binding behaves as predicted for a ligand-receptor interaction. At low concentrations of Upd2-GFP, there is a linear increase of the binding, leading into a plateau, which is due to saturation. Upd2 binding starts to be saturated at around 25nM. Consequently I used 20nM Upd2-GFP in all subsequent experiments, unless otherwise stated.

4.1.3.2 Binding of Upd2-GFP to Drosophila cells is Upd2 specific

As mentioned above it is crucial for the evaluation of endocytosis to be able to distinguish between internalised and cell surface ligand. To remove the ligand from the cell surface I decided to acid wash the cells. This allowed the measurement of internalised material only (Hopkins, 1983). To test the effectiveness of the acid wash, I incubated cells with two different concentrations of Upd2-GFP (10 and 40nM) at 4ºC. Subsequently, the cells were washed either with a pH neutral solution or with a buffer with a pH of 2.5 (Figure 4.5 B). For both concentrations of Upd2-GFP tested, the binding of Upd2-GFP to $S2R^+$ cells could be reduced significantly by exposing the cells to the acid.

Furthermore, in subsequent endocytosis experiments, in order to measure total Upd2-GFP, I incubated one sample with Upd2-GFP CM (for the longest time point), and then I washed the cells with PBS, which gave a measure of the total amount of Upd2-GFP available for internalisation (internal and external). Acid washed cell lysates (all remaining samples) always contained less Upd2-GFP, than lysates of PBS washed samples (data not shown), confirming that internal Upd2-GFP concentrations are lower than the total amount of ligand (external and internal Upd2-GFP). Together with the binding experiment, I could conclude that the used acid wash removes effectively bound Upd2-GFP. Importantly, I could use this acid sensitivity to distinguish between internalised and bound ligand in following endocytosis assays and thus expressed internalised Upd2-GFP as percentage of the total ligand. (Figure 4.6 for an example)

Furthermore, ligand-receptor interaction requires a pH neutral environment. Mild acids can interrupt receptor-ligand binding. Since Upd2 binding to the JAK/STAT receptor, Dome, was disrupted due to an acid wash (Figure 4.5 B) it might be an added indicator that Upd2 but biochemically interacted with its receptor and it does not bind non-specificly to the cells. If Upd2 bound to the cell surface in a receptor-independent manner, this binding might be weaker than the ligand/receptor binding and a much weaker acid wash might be sufficient. An acid wash occurring with a pH of 5.2 did only mildly reduce Upd2 binding (data not shown). However, this decrease was not comparable with the loss of ligand binding when cells were washed with the strong acid (pH 2.5 used in Figure 4.5 B).

To eliminate the possibility that the observed binding of Upd2-GFP to $S2R^+$ cells resulted from non-specific binding of GFP, I measured the binding of CM containing GFP to $S2R^+$ cells (Figure 4.5 C). Even though the concentration of GFP was 3-fold greater than the concentration of Upd2-GFP there was significantly less GFP bound (0.2nM) compared to Upd2-GFP (approx. 1nM bound). These data lead me to conclude that the binding of Upd2-GFP to the cells was due to the ligand and not due to the fused GFP.

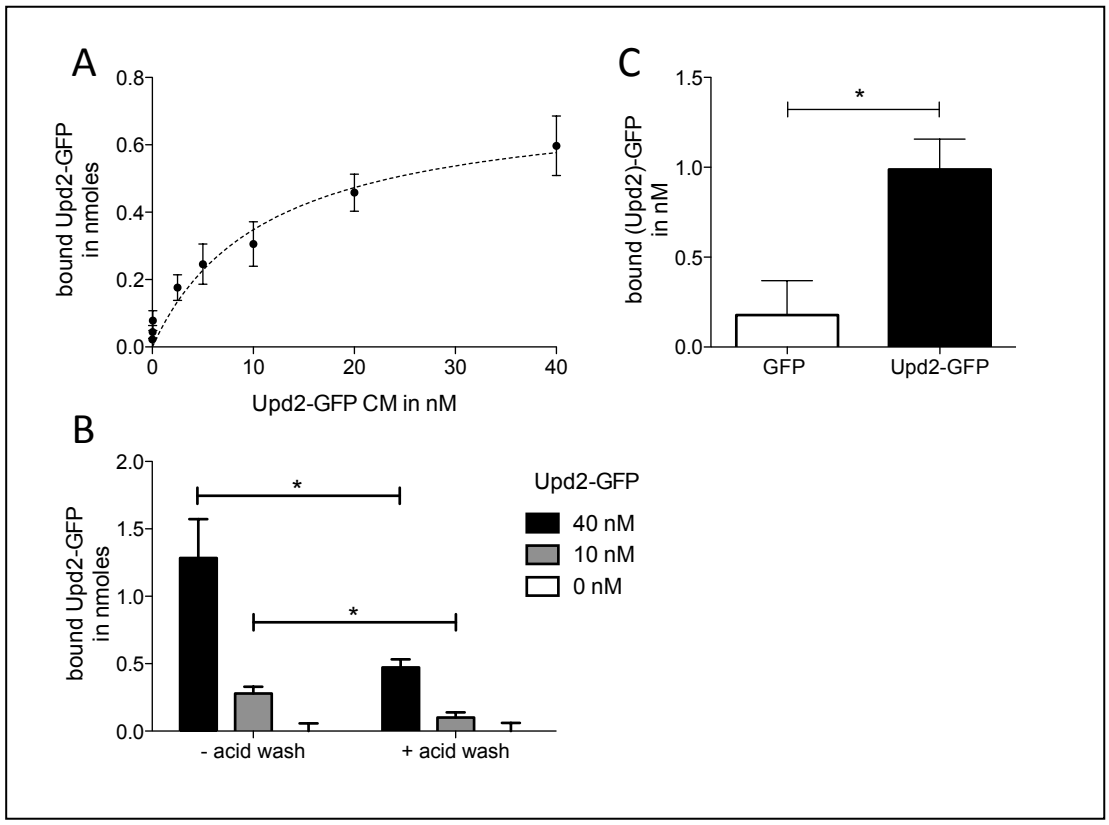

Figure 4.5: Binding of Upd2-GFP to S2R$^+$ cells is specific

S2R$^+$ cells were incubated with GFP or Upd2-GFP at 4ºC for 30min and cell lysates were analysed with the anti-GFP ELISA. A & B: Cells were treated with indicated concentrations of Upd2-GFP; and in B subsequently PBS or acid washed as indicated. In C: S2R$^+$ cells were treated with approx. 90nM GFP and 30nM Upd2-GFP. Data is expressed as total bound Upd2-GFP/GFP (A &B). Error bars represent standard deviation (C) and standard of the mean (A &B); students t-test was performed with *p>0.05, **p>0.01,***p>0.001

4.1.4 Endocytosis of Upd2-GFP

Using the anti-GFP ELISA, I characterised Upd2 internalisation biochemically and wanted to confirm that its uptake is due to Clathrin-mediated endocytosis.

To measure internalised Upd2-GFP, I allowed cells to take up Upd2-GFP from CM for various time points, before I stopped endocytosis by chilling the cells quickly down to 4ºC. Subsequently, I acid washed the cells, removing all bound ligand. The acid was replaced by PBS when I measured the total amount of Upd2-GFP (internal and external Upd2-GFP). The measurements were carried out by ELISA analysis of the lysates and I was able to express internalised Upd2 as a ratio to the total.

4.1.4.1 Uptake of Upd2-GFP in S2R$^+$ cells is receptor dependent

Having eliminated the possibility that the signal observed in the ELISA assay was due to GFP rather than Upd2, I next evaluated the endocytosis of Upd2-GFP when the JAK/STAT receptor, Dome, was knocked down by dsRNA.

In Figure 4.6 A I incubated S2R$^+$ cells with either Upd2-GFP or GFP CM (as in sections above) for up to 30 minutes. Endocytosis was stopped by chilling the cells on ice and surface-bound material was stripped away with an acid wash. The internalisation of GFP alone remained at background levels, whereas Upd2-GFP uptake increased over time (Figure 4.6 A green vs. black line). The graph demonstrates thus that Upd2-GFP was specifically endocytosed.

To confirm that Upd2-GFP uptake was dependent on Dome, I used dsRNA to knock down the receptor prior to exposing the cells to Upd2-GFP and allowing endocytosis to occur. After incubating for various times, internal Upd2-GFP was measured using the anti-GFP ELSIA and a significantly lower level of uptake of Upd2-GFP could be detected when Dome was knocked down, compared to control treated samples (Figure 4.6 B, blue vs. black line, 2 way anova test). Therefore I could conclude that endocytosis of JAK/STAT ligand Upd2 is receptor-dependent.

The observed background levels of GFP uptake (Figure 4.6A, green line) and residual Upd2-GFP in Dome depleted cells (Figure 4.6B, blue line) were likely to be due to non-specific uptake of GFP / Upd2-GFP probably caused by fluid-phase uptake and in case of the knockdown possibly a result of incomplete Dome depletion, as assessed by measuring *Domeless* mRNA in control and knockdown samples (Figure 4.7)

When I measured the uptake of Upd2-GFP in KC_{167} cells, I observed considerable variability between experiments and a high background, which actually masked the Upd2-GFP uptake (data not shown). This, together with the heterogenous uptake as shown by immunofluorescence (Figure 4.2) promoted the use of S2R$^+$ instead of KC_{167} cells.

4.1.4.2 Upd2-GFP uptake is mediated by Clathrin dependent endocytosis

After evaluating the *in vitro* assays and showing that the Upd2 uptake was ligand- and receptor-specific, I went on to investigate the role of Clathrin-mediated endocytosis in Upd2 uptake. Using dsRNA, I knocked down Clathrin heavy chain (CHC) and AP2 individually and measured their Upd2-GFP uptake rates by incubating the cells with Upd2-GFP CM and analysing endocytosed ligand via the established anti-GFP ELISA.

Figure 4.6 B shows that there was decreased Upd2-GFP uptake when AP2 (orange) or Clathrin (red) was knocked down. This suggests that the JAK/STAT signalling pathway ligand uptake is mediated by Clathrin-dependent endocytosis.

The decrease of ligand uptake was not reduced to background levels, when compared to the receptor knockdown (blue line). This could be down to residual protein left after the knockdown. *Clathrin* mRNA levels were knocked down to about 20% (Figure 4.7) and approximately 25% of AP2 proteins remained after a knockdown for five days (Figure 4.8). The remaining, presumably quite stable proteins could explain why endocytosis still occurred at higher than background levels even after knocking down the major components of Clathrin-mediated uptake. A Clathrin-independent receptor-specific uptake mechanism like Caveolin-mediated endocytosis, might be another cause for the residual internalisation (Sadir et al., 2001). Both considerations are not mutually exclusive, however it seems that Upd2 is predominantly taken up via Clathrin coated pits.

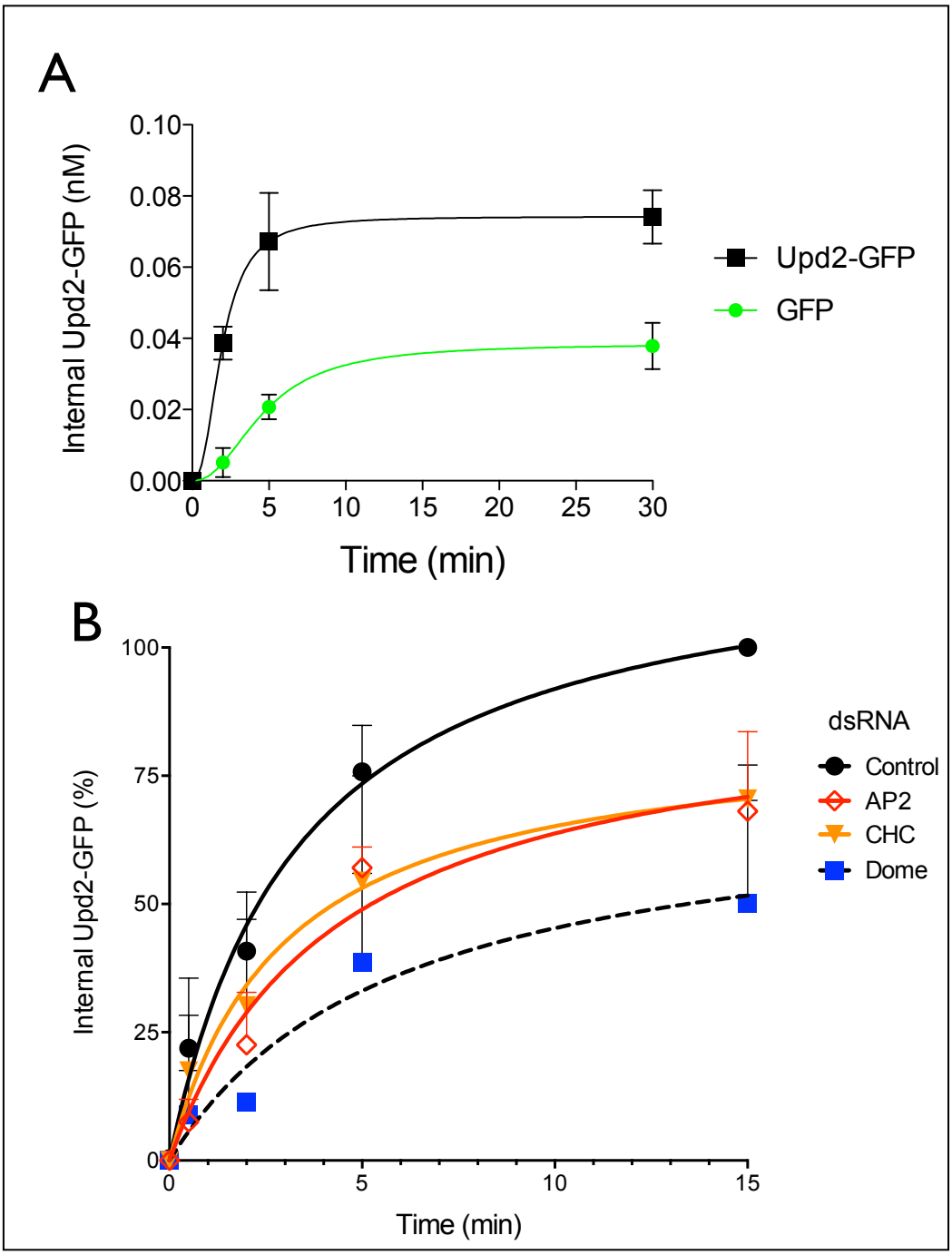

Figure 4.6: Uptake of Upd2-GFP is due to Clathrin-mediated endocytosis

S2R$^+$ cells were incubated with GFP or Upd2-GFP (20nM) for indicated time points at 25ºC, after acid washes cell-lysates were analysed with the anti-GFP ELISA. In A: S2R$^+$ cells were treated with either Upd2-GFP or GFP and the internal Upd2-GFP /GFP amount was plotted. Error bars show standard deviation of two individual experiments; B: After cells were treated for 5 days with dsRNA as indicated, the uptake of Upd2-GFP was measured. The internal Upd2-GFP amount is represented as %, whereby the longest time point (15min) of the control was set to 100% in each individual experiment, to allow comparison. Graph represents at least 3 independent experiments and error bars show standard error of the mean. In a two-way ANOVA statistical test, the Dome dsRNA has an effect on the uptake rate into cells, which is considered significant with a P value of 0.0216.

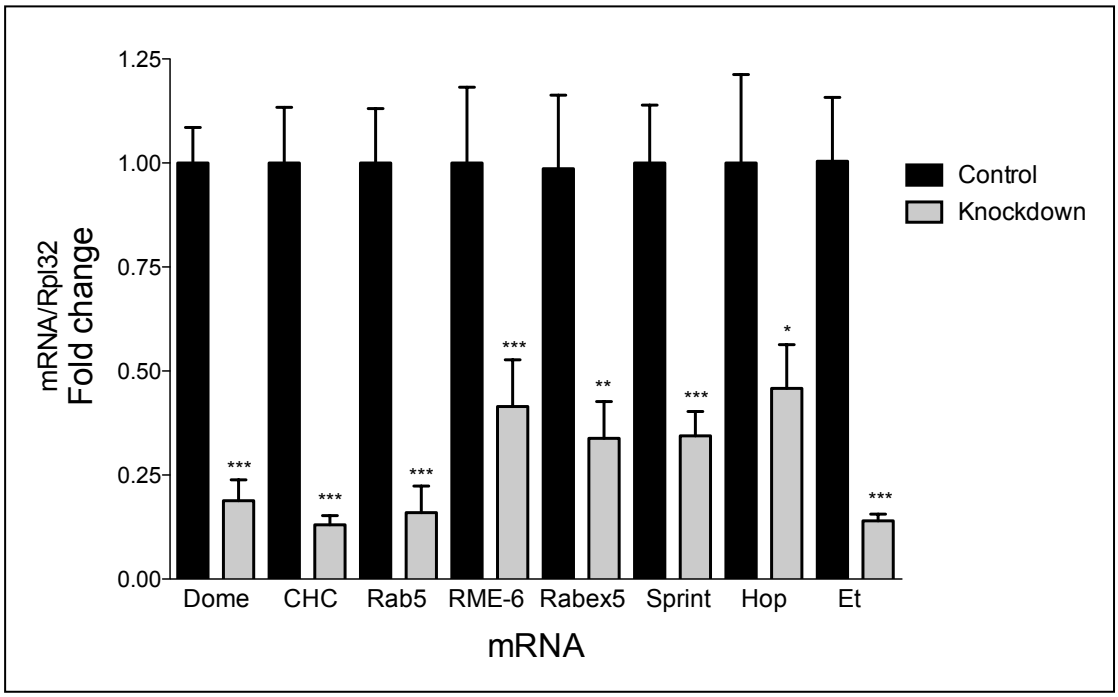

Figure 4.7: mRNA levels after knockdown of selected genes

S2R^{+} cells were treated with dsRNA as indicated for five days. RNA was harvested and mRNA analysed by qPCR. The levels of the target mRNA were normalised to the housekeeping mRNA *Rpl32* and their ratios were plotted as fold change to control treated samples for each gene. Graphs represent the mean of at least 3 independent experiments and error bars show standard error of the mean. The students t-test was performed comparing control knockdown vs. indicated gene knockdown for each individual gene, with *p>0.05, **p>0.01,***p>0.001, ns= not significant.

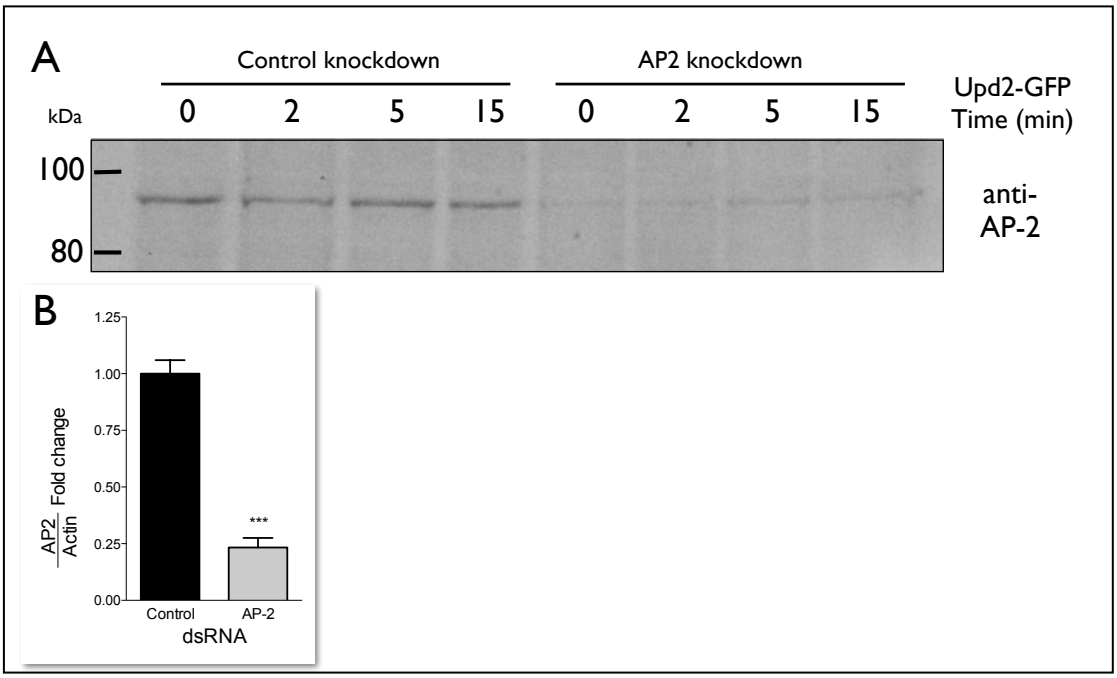

Figure 4.8: AP2 knockdown levels

S2R$^+$ cells were treated with dsRNA as indicated, five days prior to incubation with 20nM Upd2-GFP for indicated time points at 25ºC. Total protein extracts were analysed by SDS-PAGE and immuno-blotted with anti-AP2. B: One example blot showing depletion of AP2 in knockdown cells. B: Quantification of AP2 depletion, whereby the ratio of AP2 to Actin was plotted and it was normalised to control samples, error bars show standard error of the mean, representing at least 2 independent experiments, with *p>0.05, **p>0.01,***p>0.001, ns= not significant students t-test.

4.2 JAK/STAT activation assays

In the previous section I showed the dependence of JAK/STAT ligand uptake on Clathrin-mediated endocytosis. I next addressed the role of endocytosis in quantitative and qualitative JAK/STAT pathway activation. To measure pathway activation I used a STAT driven reporter system and I also applied an endogenous target assay, which I adapted from Bina et al, 2010 (Bina et al., 2010)

4.2.1 Luciferase reporter assay

I first measured JAK/STAT activation with a well-characterised luciferase reporter assay (Baeg et al., 2005), which consisted of a firefly luciferase under the control of STAT92E binding sites (*10xSTATLuc*) and an actin-promoter controlled renilla luciferase, which controlled for cell numbers and transfection efficiency, transfected into S2R$^+$ cells. After ligand stimulation and further incubation allowing the expression of the 10xSTAT luciferase reporter, I analysed cell lysates with chemiluminescense. Data was presented as the ratio between the firefly and renilla luciferase.

I characterised this assay further using S2R$^+$ cells in order to ask the question of whether it would be applicable to use for studies of the quantitative regulation of the JAK/STAT pathway by endocytosis.

First, I wanted to establish when the expression of the JAK/STAT controlled luciferase reaches its peak after stimulation with ligand-CM to be able to investigate activation as early as possible without losing the strength of the signal. Therefore, I measured Upd2 induced expression of the firefly luciferase for different time points (Figure 4.9). Ligand induced luciferase expression and thus JAK/STAT pathway activation increased after 8 hours and peaked at 13h after pathway stimulation. Consequently, I allowed expression for around 13 hours in all following experiments (unless otherwise stated).

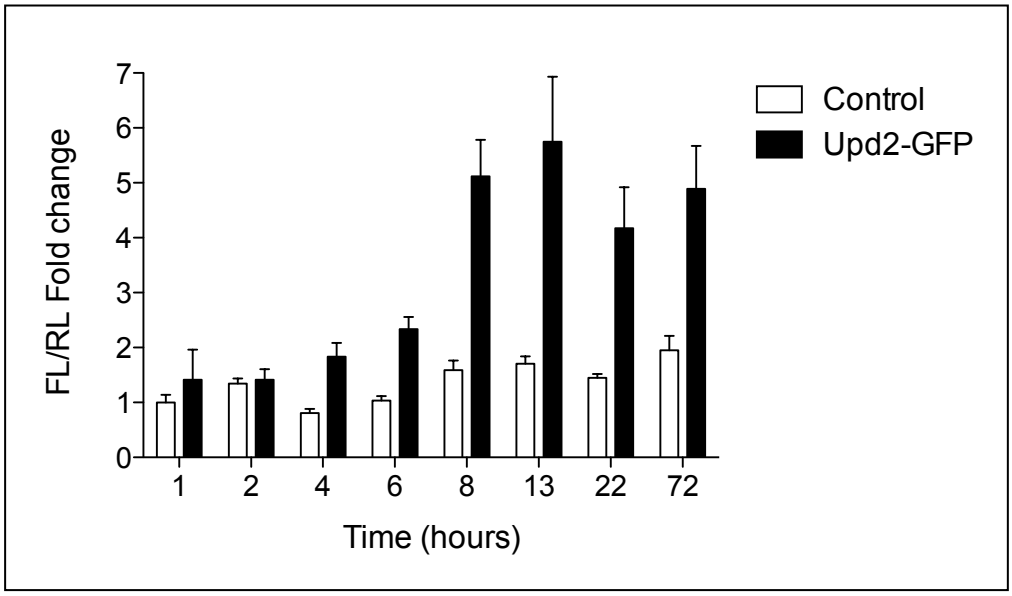

Figure 4.9: Time dependence of JAK/STAT controlled luciferase expression

Two days after transfection of S2R$^+$ cells with an *Actin* driven Renilla Luciferase (RL) and a *10xSTATLuc* (FL) reporter construct, cells were incubated with control or Upd2-GFP conditioned medium (20nM Upd2-GFP) for 30min at 25ºC, followed by an acid wash. The bioluminescence of the cell lysates was measured after incubation for indicated time points at 25ºC. The ratio of FL to RL was plotted as fold change to control treated cells. A representative experiment (one of 3 independent experiments) is shown, error bars represent the standard deviation of triplicates within one experiment

4.2.1.1 Upd2 specifically activates the JAK/STAT pathway

Section 4.1.3.2 and 4.1.4.1 showed that ligand binding and uptake was Upd2 specific and not due to the fused GFP. Next, I wanted to test if the same specificity also applies to pathway activation, to be certain that observed effects are JAK/STAT dependent. To

confirm that the activation of luciferase was due to the ligand Upd2, I incubated luciferase-transfected cells with Upd2-GFP and recombinant GFP alone.

Figure 4.10 A shows that cells did not respond to GFP (in mock-CM) with JAK/STAT pathway activity. Even when treated for two days with the recombinant GFP the activity was significantly lower than cells treated with Upd2-GFP for only 30min. Additionally, if cells were exposed to half the amount of Upd2-GFP for 2 days the JAK/STAT activation was higher that when incubated with GFP alone. Hence, I concluded that Upd2 specifically activates the JAK/STAT pathway.

In order to evaluate if this activation was concentration dependent, cells were incubated with a wide range of Upd2-GFP concentrations for 30 min at 4ºC, before I measured JAK/STAT activation. The amount of ligand plotted against JAK/STAT activation, is shown in Figure 4.10 C. The graph portrays a typical saturation curve, which rose first linearly before it plateaus at around 15 to 20nM. This suggests that activation of JAK/STAT signalling by Upd2 is saturated at 20nM ligand concentration. Importantly, this curve looked very similar to the binding-curve of the Upd2-GFP to the cell surface of $S2R^+$ cells (compare with Figure 4.5 C) and saturation levels equal each other. In comparison to Figure 4.5 A the graph in Figure 4.10 C does not represent binding alone, since cells had to be warmed up, while binding to the ligand, to allow luciferase expression to occur. This resulted naturally in the uptake of Upd2-GFP, so could not be classed as purely ligand binding.

4.2.1.2 Upd2-GFP uptake activates the JAK/STAT pathway

The measurement of pathway activation required the cells to be physiologically active (to express luciferase), hence binding alone could only be measured when uptake mechanisms were blocked genetically or with inhibitory drugs. The main disadvantage of the latter was, that I would not be able to distinguish between pathway modification caused by the drug and its inhibition of endocytosis. The genetic approach is described in section 4.2.1.3.

Nevertheless, I could address the effects of acid wash to the pathway activation. Therefore, I incubated cells with Upd2-GFP (at 4ºC), acid or PBS washed them and shifted them back to 25ºC. Subsequently, I measured JAK/STAT activation. As expected, pathway activation of acid washed cells did not occur (Figure 4.10 B). This demonstrates that binding alone of Upd2-GFP at 4ºC is insufficient to activate the pathway (when removing Upd2 after binding) and suggests that JAK/STAT activation is

ligand-dependent. Additional to the ligand binding experiments in section 4.1.3.2 the experiment also confirmed the effectiveness of the acid wash.

I also addressed the question of how long I needed to incubate the cells to achieve saturated activation levels. The graph in Figure 4.10 D shows a typical experiment in which cells were incubated for various time-points with Upd2-GFP CM and the 10xSTAT luciferase reporter was measured. Ligand incubation of approximately 10 minutes was sufficient to elicit luciferase expression, nevertheless, I used a 30 minutes incubation period in all subsequent experiments, since JAK/STAT activation seemed to be more stable and reproducible with this longer incubation (data not shown).

In contrast to the *in vitro* endocytic assays (as described in section 4.1.4) an acid wash succeeding the incubation with ligand was technically not possible, since cells detached from their plate shortly after returning them from 4ºC to 25ºC and the observed signals were extremely low, so that the experimental error increased too much (data not shown). The experiments described above (Figure 4.10 B) included an acid wash, using a larger number of cells (6 well plates instead of 96 well plates) to overcome those technical problems. Luckily, this increased effort was not necessary to undertake for all the luciferase assays, since it was not crucial to distinguish between internalised and total amount of Upd2-GFP.

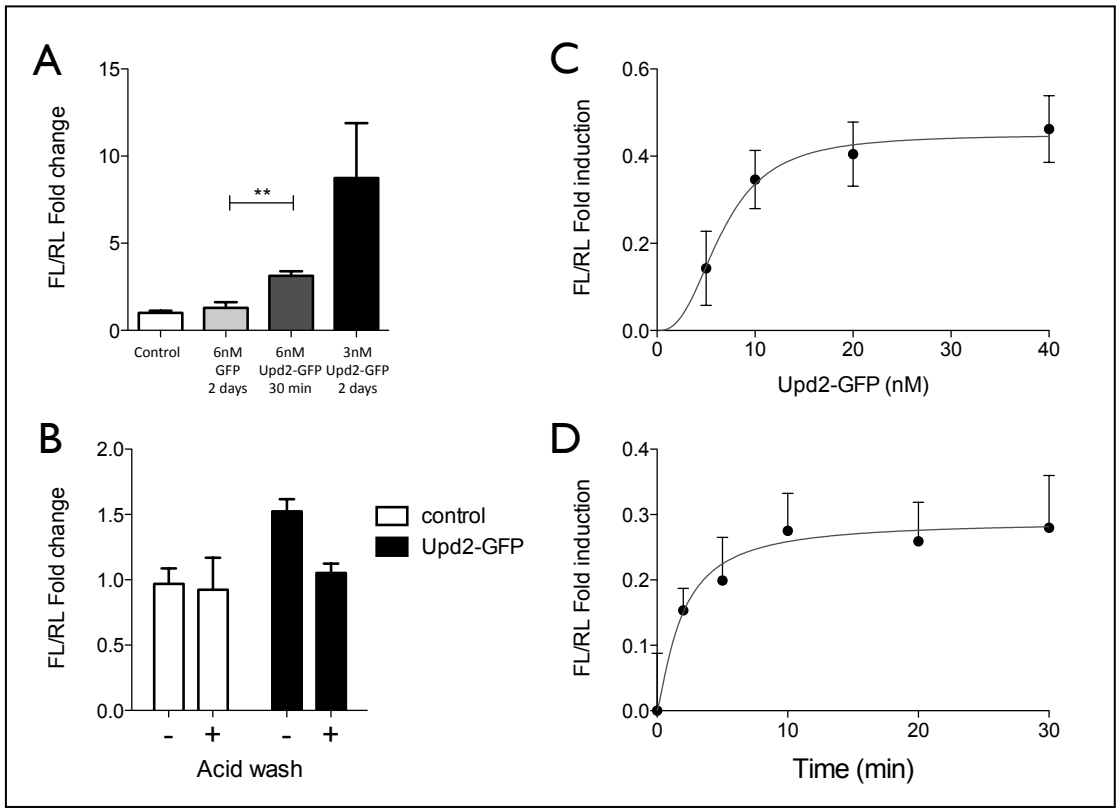

Figure 4.10: Characterising the JAK/STAT controlled luciferase reporter assay

Two days after transfection of S2R$^+$ cells with an *Actin* driven Renilla Luciferase (RL) and a *10xSTATLuc* (FL) reporter construct, cells were incubated with control, GFP or Upd2-GFP conditioned medium and bioluminescence of the cell lysates was measured 8h later.

A: **Upd2 activates the JAK/STAT pathway specifically:** Cell treatment occurred at 25ºC as for indicated time points, control cells were treated for 2 days with mock CM alone.

B: **JAK/STAT pathway activation is Upd2 dependent:** The treatment for 30min with CM (20nM Upd2-GFP) at 4ºC was followed either by an acid or PBS wash.

C: **JAK/STAT pathway activation is Upd2 concentration dependent:** The treatment for 30min at 4ºC with indicated concentrations of Upd2-GFP indicates that the binding of Upd2-GFP to S2R$^+$ cells activates the JAK/STAT pathway in a concentration dependent manner and saturates at around 20nM.

D: **JAK/STAT activation is time dependent:** Treatment of 20nM Upd2-GFP at 25ºC for indicted time points,

The ratio of FL to RL was plotted in A and B as fold change, whereas the control was set to 1 and in C and D as fold induction where the control was set to 0.

A to D: Shown are each one representative experiment out of 3 independent ones and error bars represent error of the mean. *p>0.05, **p>0.01,***p>0.001.

4.2.1.3 JAK/STAT pathway activation is dependent on receptor- and Clathrin-mediated endocytosis

Having established in section 4.1.4 that Upd2 uptake is receptor-dependent and largely controlled by Clathrin-mediated endocytosis, I wanted to analyse whether signalling is also controlled thus. Addressing this, I decided to deplete endocytic pathway components and use first the 10xSTAT luciferase (*10xSTATLuc*) reporter assay.

First, I needed to assess if the pathway activation is receptor-dependent. Therefore, I knocked down the receptor and induced signalling with Upd2-GFP CM, which was measured with the *10xSTATLuc* reporter assay. One representative experiment is shown in

Figure 4.11. Importantly, depleting cells of the receptor resulted in a failure to activate signalling. This confirmed that the reporter assay that was being used as a read-out for JAK/STAT signalling is receptor-dependent and the system used was in keeping with the accepted literature (Bach et al., 2007; Brown et al., 2001a).

Within the same experiment I investigated whether Clathrin-mediated endocytosis had an effect on the JAK/STAT signalling, by knocking down major endocytic components, including Clathrin and TSG101, a component of the ESCRT complexes that function at late endosomes. I wanted not only investigate if Upd2 uptake is necessary for pathway activation, but also the stage where signalling took place, dissecting from which endocytic compartment signalling occurs.

The *10xSTATLuc* reporter was not activated by Upd2-GFP CM, when AP2 and Clathrin were knocked down (

Figure 4.11). Loss of these crucial early endocytic components retained the ligand-receptor complex on the cell surface and signalling, as measured by expression of *10xSTATLuc*, no longer occurred. This suggests that endocytosis has a positive effect on signalling.

By contrast, inhibiting later stages of the endocytic pathway, by the knockdown of TSG101, did not alter the transcription of *10xSTATLuc*, which suggests that signalling occurs somewhere before the receptor reaches the late endosome. Following arrival at the late endosome, the receptor is likely to be targeted for degradation (Stec et al., 2013). These data suggested that JAK/STAT operates from signalling endosomes.

Surprisingly, cells where Rab5 was depleted showed similar 10xSTAT driven luciferase expression as the control samples in response to ligand stimulation (

Figure 4.11). Hence, the knockdown of Rab5 did not have any effect on JAK/STAT signalling within this assay. This contradicted previous studies of JAK/STAT signalling,

which were not consistent with each other (Devergne et al., 2007; Vidal et al., 2010) and suggested that signalling occurred from structures independent of Rab5.

The lack of an apparent effect on 10xSTATLuc expression in cells treated with Rab5 dsRNA could result from an inefficient knockdown. Unfortunately, I could not measure Rab5 protein levels after its depletion caused by dsRNA exposure, due to the lack of a suitable anti-Rab5 antibody. The mRNA levels however decreased significantly to less than 25%, when cells were treated with dsRNA (Figure 4.7).

In conclusion, I showed that JAK/STAT endocytosis, specifically Clathrin-mediated endocytosis, controls JAK/STAT pathway activation.

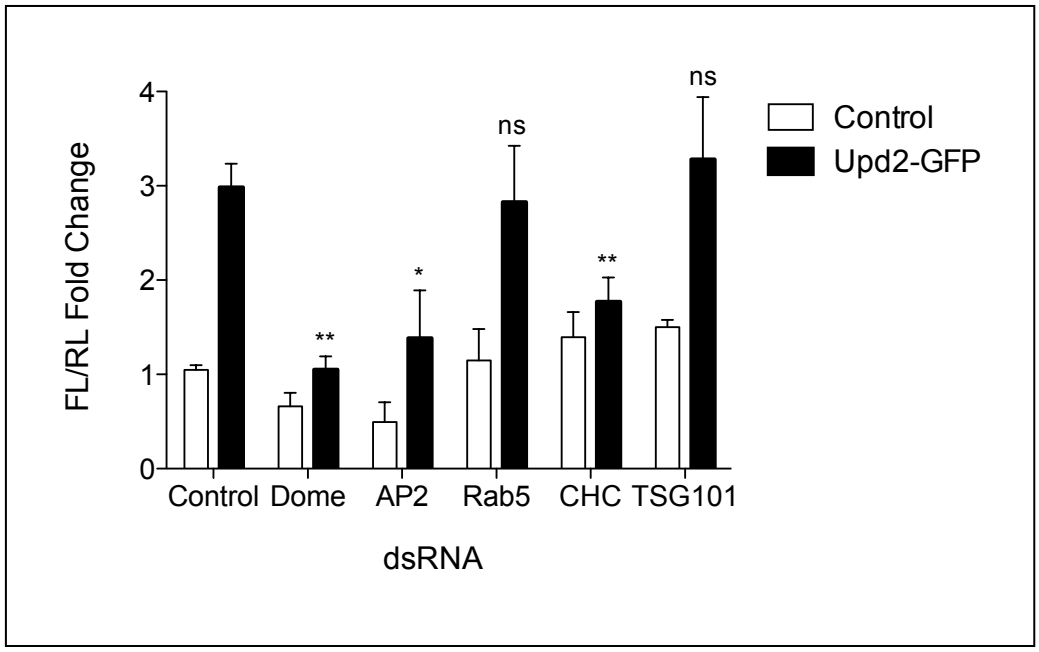

Figure 4.11: Receptor and Clathrin-mediated endocytosis regulates JAK/STAT signalling

S2R$^+$ cells were treated with dsRNA as indicated, three days prior to transfection with an *Actin* driven Renilla Luciferase (RL) and a *10xSTATLuc* (FL) reporter construct, cells were incubated with 20nM Upd2-GFP for 30min at 25ºC, and the bioluminescence of the cell lysates were measured 8h afterwards. The ratio of FL to RL was plotted as fold change to control treated cells, with control dsRNA, which was set to 1. Shown is a representative experiment out of 3 independent ones and error bars represent error of the mean. Students t-test was performed comparing control dsRNA and Upd2-GFP treated samples with targeted dsRNA and Upd2-GFP treated samples *p>0.05, **p>0.01,***p>0.001, ns= not significant

4.2.1.4 Ras but not Rab5 GEFs decrease JAK/STAT pathway activation

The effect of Rab5 knockdown was minimal on the pathway activation as measured by luciferase expression. Since its involvement in JAK/STAT control was seen before (Devergne et al., 2007; Vidal et al., 2010) and the lack of an effect could result from

inefficient knockdown, I wanted to investigate if Rab5 activators, GEFs, could act as novel regulators of this signalling pathway.

I tested whether the knockdown of three Rab5 GEFs: Rabex5, RME-6 and Sprint, have an effect on the *10xSTATLuc* reporter. The knockdown of three proteins singly and in combination did not affect JAK/STAT signalling upon ligand stimulation for 30 minutes (Figure 4.12 A). Conversely a slight increase of the pathway was observed when the GEFs were knocked down in mock-CM treated cells, compared to mock-CM incubated cells treated with control dsRNA.

Since RME-6 contained a Ras-GAP and Sprint a Ras binding domain, it was feasible that these domains might influence JAK/STAT signalling via the ERK/Ras/MAPK pathway, which ought to enhance JAK/STAT signalling (Callus and Mathey-Prevot, 2002). I wanted to investigate the role of Ras on JAK/STAT signalling using the 10xSTAT luciferase assay and address further whether ligand-independent JAK/STAT signalling activation caused by Rab5 GEFs depletion, is due to an indirect effect via Ras.

Therefore I knocked down Ras singly and in combination with the GEFs and measured signalling by the 10xSTAT luciferase assay. Figure 4.12 B shows the inability of cells to induce JAK/STAT signalling with Upd2-GFP, when Ras was knocked down. This effect was not altered when either of the GEF was additionally knocked down. Moreover, the slight increase of Upd2 independent pathway activation by GEF knockdown did not occur when Ras was knocked down, either on its own or in combination with the Rab5 GEFs.

The failure to activate JAK/STAT signalling might be due to crosstalk with the ERK/Ras/MAPK pathway. This receptor tyrosine kinase (RTK) pathway stimulates JAK/STAT signalling (Callus and Mathey-Prevot, 2002). Importantly, since Ras knockdown influenced only ligand dependent signalling, it was unlikely that the ligand-independent effect was due to the function of the RasGAP / Ras-binding domains. This indicates that Ras apparently acts upstream of the JAK/STAT signalling pathway. Furthermore, the double knockdown of the Rab5 GEF with Ras mirrored the effect of Ras single knockdown, suggesting that there was no rescue of any residual Ras by the GEFs.

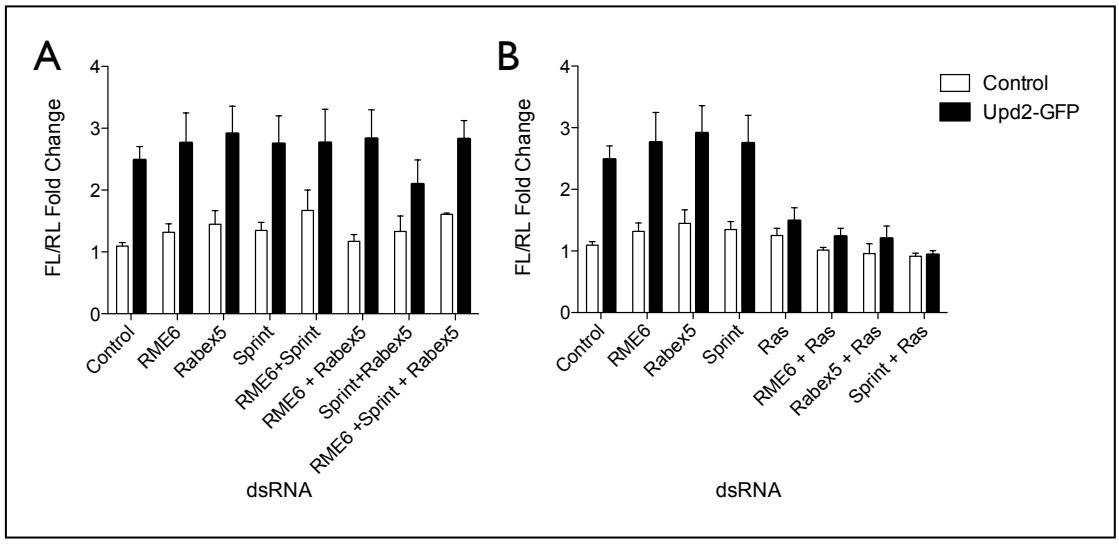

Figure 4.12: Ras decreases JAK/STAT pathway signalling

S2R$^+$ cells were treated with dsRNA as indicated, three days prior to transfection with a Renilla Luciferase (RL) and a *10xSTATLuc* (FL) reporter construct, cells were incubated with 20nM Upd2-GFP for 30min at 25ºC, followed by an acid wash, and the bioluminescence of the cell lysates were measured 8h afterwards. The ratio of FL to RL was plotted as fold change to control treated cells, with control dsRNA. In A: Knockdown of Rab5 GEFs singly and in combination B: Knockdown of Rab5 GEFs and Ras singly and in combination. The ratio of FL to RL was plotted as Fold change, whereas the control was set to 1. A representative experiment is shown, one of at least 2 independent ones and error bars represent the standard deviation.

4.2.2 JAK/STAT transcription targets

The luciferase reporter assay is an excellent tool for high throughput screens and (simple) yes/no questions (Baeg et al., 2005; Muller et al., 2005). However, I found it was difficult to compare experiments with each other. The extent of activation varied greatly, even though I used constant concentrations of Upd2 and equal incubation times.

One of the objectives of my thesis was to evaluate whether endocytosis regulates JAK/STAT signalling in a qualitative manner. Consequently, I decided to measure endogenous JAK/STAT targets. This enabled me to measure established STAT92E-regulated genes. As well as novel targets, I could also measure endogenous target activation in the absence of potential effects due to transfection and/or ectopic protein production. This also meant that the incubation times after stimulation with the ligand could be decreased. Extracting mRNA and analysing it by qPCR involved a considerable increase in the manual workload, compared to the luciferase assay, where fewer handling steps could be easily automated (especially using the RNAi facility at

Sheffield University) but its advantages compensated greatly for this increased technical effort.

First, I characterised JAK/STAT target activation in $S2R^+$ cells, optimising timing and finding robust transcriptional targets, which are both ligand- and receptor-dependent.

To analyse the time course of activation of endogenous targets, I chose to measure *SOCS36E* mRNA levels. SOCS36E is a negative regulator and a known target of the JAK/STAT pathway (Bina et al., 2010; Flaherty et al., 2009; Kwon et al., 2008; Terry et al., 2006; Wang et al., 2013). Cells stimulated with Upd2-GFP up-regulated *SOCS36E* levels quickly. A 30 minutes stimulation was followed by an incubation with fresh media to allow transcription to occur. *SOCS36E* mRNA levels increased after only one-hour (Figure 4.13). Even though, *SOCS36E* mRNA levels continued to rise for three hours following induction, I decided to incubate for two hours after induction, trying to minimise possible feedback-loops and also after three hours the data were less robust, yet still significant, due to the extent of the activation.

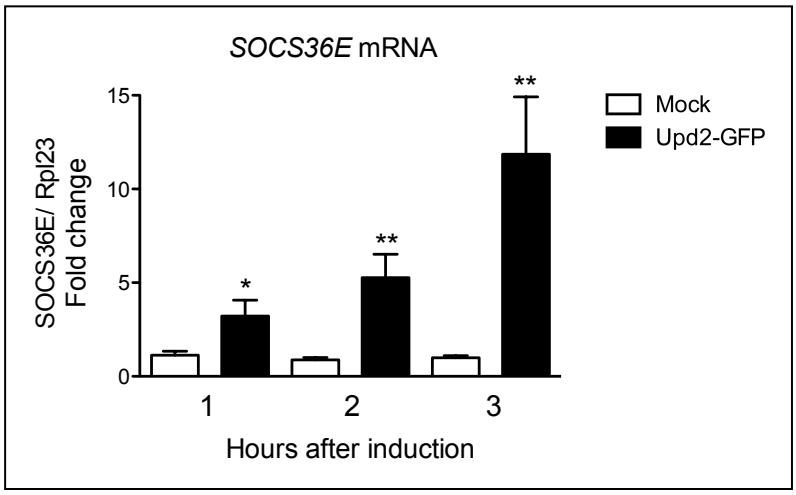

Figure 4.13: JAK/STAT activated *SOSC36E* mRNA expression is time dependent

$S2R^+$ cells were treated with 20nM Upd2-GFP for 30min at 25ºC (induction), followed by incubation in media for indicated time points. RNA was harvested and mRNA analysed by qPCR. The levels of *SOCS36E* mRNA were normalised to the housekeeping mRNA *Rpl32* and their ratios were plotted as fold change to control treated samples. Error bars represent standard error of the mean, with *p>0.05, **p>0.01,***p>0.001 students t-test

4.2.2.1 Gene expression upon Upd2-GFP stimulation of selected targets

A previous study (Bina et al., 2010) had identified a number of JAK/STAT targets. I selected from the published material 12 targets, which all changed in an early (2h) response to Upd stimulation, and additionally, I also tested the receptor Dome (which

was not identified in this screen), but is a well known *in vivo* JAK/STAT target (Brown et al., 2001a). I aimed to select those targets that would fulfil two main requirements: their mRNA expression needed to depend A) on the ligand Upd2 and B) on the presence of Dome. These dependencies were investigated by A) stimulating with Upd2-GFP CM and B) depleting cells of the receptor using dsRNA, consequently comparing un-stimulated to stimulated cells.

The genes selected could be placed into four distinct groups based on their mRNA expression: First, there was a group of genes that were transcribed in an Upd2-independent manner: These included *CG3829*, *Pbx* and *Hopscotch* (Figure 4.14). Even though identified as early JAK/STAT targets in (Bina et al., 2010), their mRNA levels did not increase after stimulation with Upd2-GFP CM within the system I used. Using a different cell line, ligand and also slightly different experimental set up might explain these discrepancies.

The mRNA of endocytic components like *clathrin*, *rab5* and *rab5 GEFs* also did not increase upon ligand stimulation (data not shown), which was consistent with the transcript profiling data from (Bina et al., 2010).

The second category contained mRNAs, which were only weakly induced by Upd2-GFP: *STAT92E*, *Bazooka*, *GC10764*, *Wnt4* and *CG4804* (Figure 4.15). Their induction could be considered non-significant for most target genes. Even though these targets were moderately induced upon Upd2-GFP stimulation, their mRNA levels remained at the same levels when the receptor, Dome was knocked down, as samples from mock-treated cells, indicating that they were receptor-dependent. It was possible that their expression would increase further if incubated for a longer time period, but since I wanted to avoid possible feedback loops and indirect effects, I decided to take other targets forward. Furthermore, the absolute levels of some target mRNA, especially *Wnt4* and *CG4804*, were relatively low, so that the qPCR operated at its limits of detection, becoming thus more unreliable (data not shown).

Those genes whose expression of mRNAs was Upd2-GFP dependent, but Dome-independent constituted the third in category. *CG13559*, *gAlpha73B* and *Net* mRNA levels rose slightly when cells were induced with Upd2-GFP. However Dome-depleted cells also responded to Upd2-GFP in a similar way, thus suggesting these targets were receptor-independent (Figure 4.16). Interestingly the expression of *gAlpha73B* and *net* mRNA was increased when the receptor was depleted, even in the mock-treated

samples. Their increased expression might be due to a stress response, caused by Dome knockdown and / or ligand treatment.

Since the aim was to analyse only those transcriptional targets that were both ligand- and receptor-dependent in order to study Clathrin-mediated endocytosis of JAK/STAT signalling, none of the genes in the first three categories fulfilled both conditions. However the fourth category of tested targets contained *Domeless* and *SOCS36E*, whose mRNA expression was both ligand- and receptor-dependent (for details see next section).

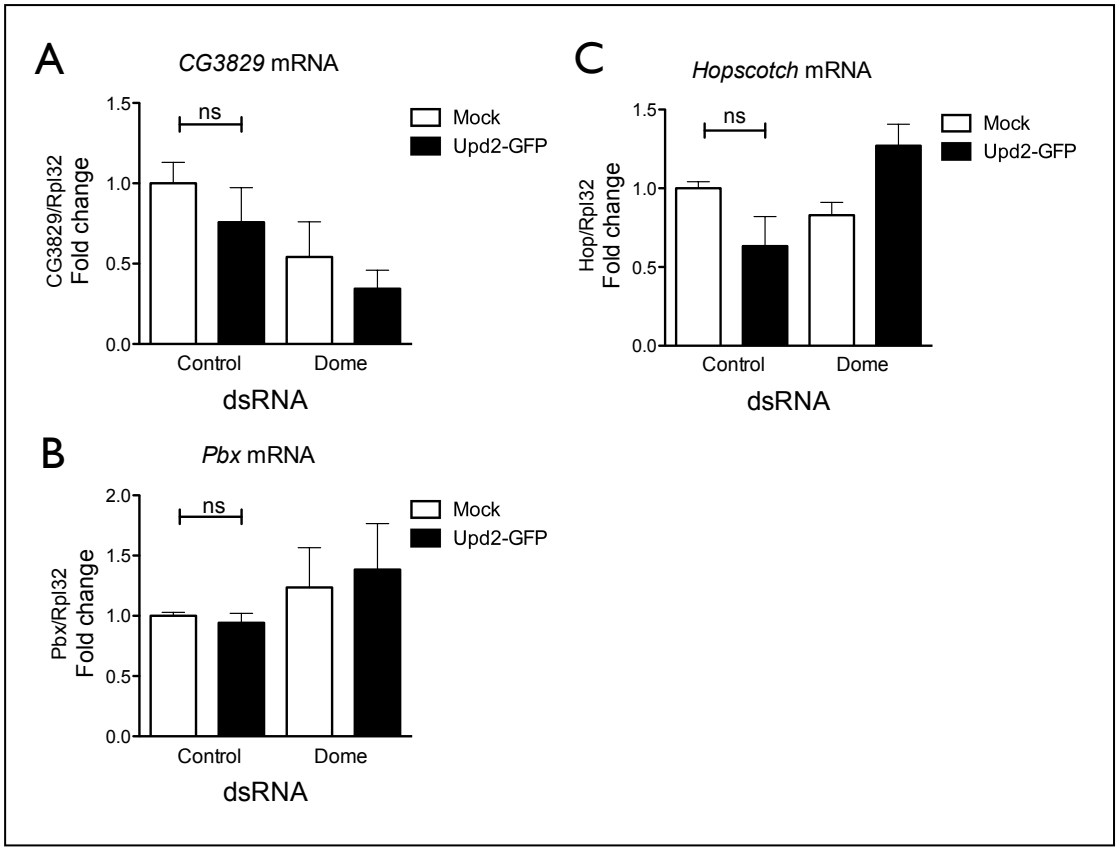

Figure 4.14: *CG3829*, *Pbx* and *Hopscotch* mRNA expression is independent of Upd2

S2R$^+$ cells were treated with dsRNA as indicated, five days prior induction. Cells were induced with 20nM Upd2-GFP for 30min at 25ºC, followed by 2h incubation in media. RNA was harvested and mRNA analysed by qPCR. The levels of the target mRNA A: *CG3829*; B: *Pbx* and C: *Hopscotch* were normalised to the housekeeping mRNA *Rpl32* and their ratios were plotted as fold change to control treated samples. Graphs represent 3 independent experiments and error bars show standard error of the mean, with *p>0.05, **p>0.01,***p>0.001, ns= not significant students t-test

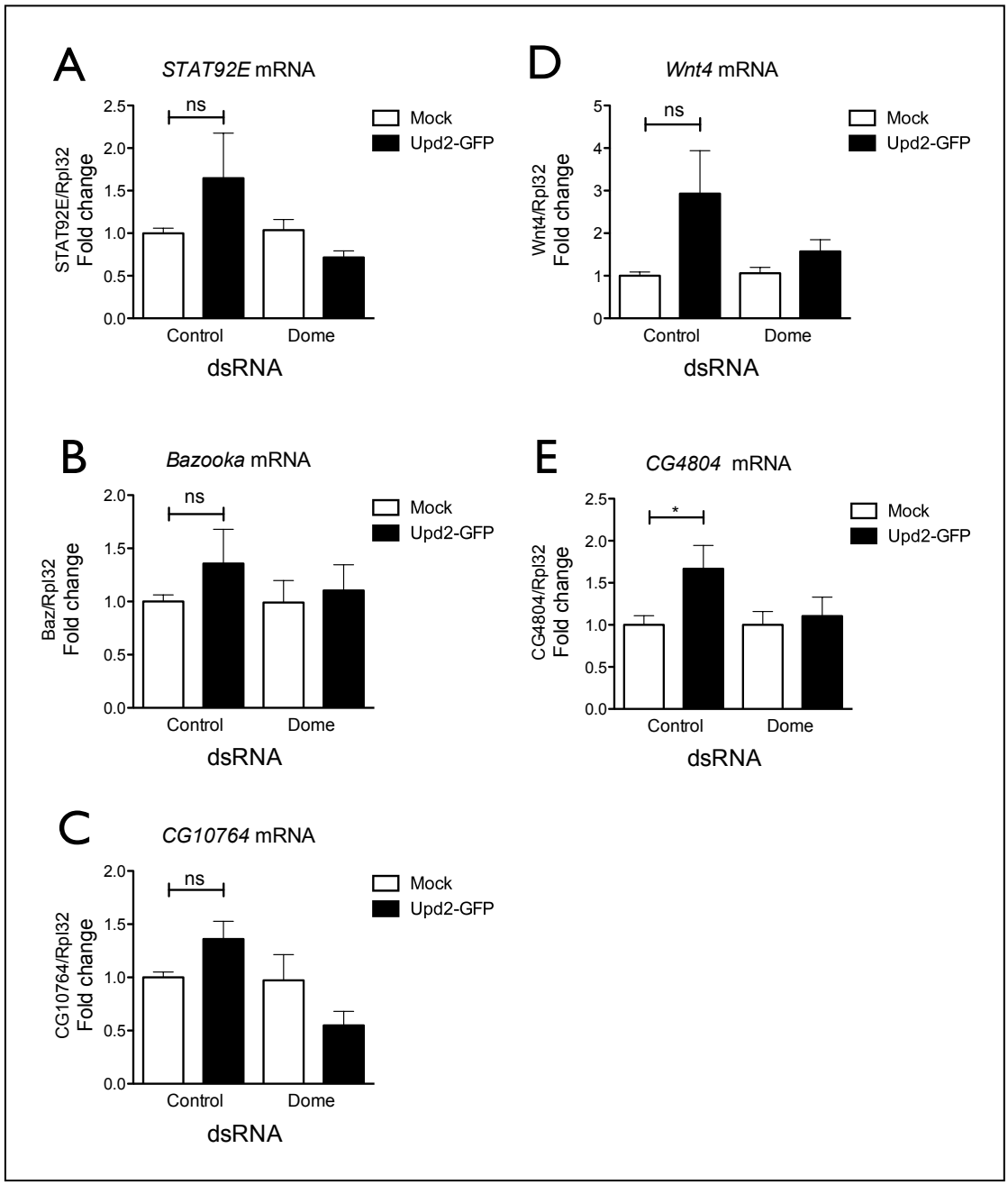

Figure 4.15: mRNA expression of *STAT92E*, *Bazooka*, *CG10764*, *Wnt4* and *CG4804* are weakly activated by Upd2

S2R^{+} cells were treated with dsRNA as indicated, five days prior induction. Cells were induced with 20nM Upd2-GFP for 30min at 25ºC, followed by 2h incubation in media. RNA was harvested and mRNA analysed by qPCR. The levels of the target mRNA A: *STAT92E*; B: *Bazooka*; C: *CG10764*; D: *Wnt4* and E: *CG4804* were normalised to the housekeeping mRNA *Rpl32* and their ratios were plotted as fold change to control treated samples. Graphs represent 3 independent experiments and error bars show standard error of the mean, with *p>0.05, **p>0.01,***p>0.001, ns= not significant students t-test

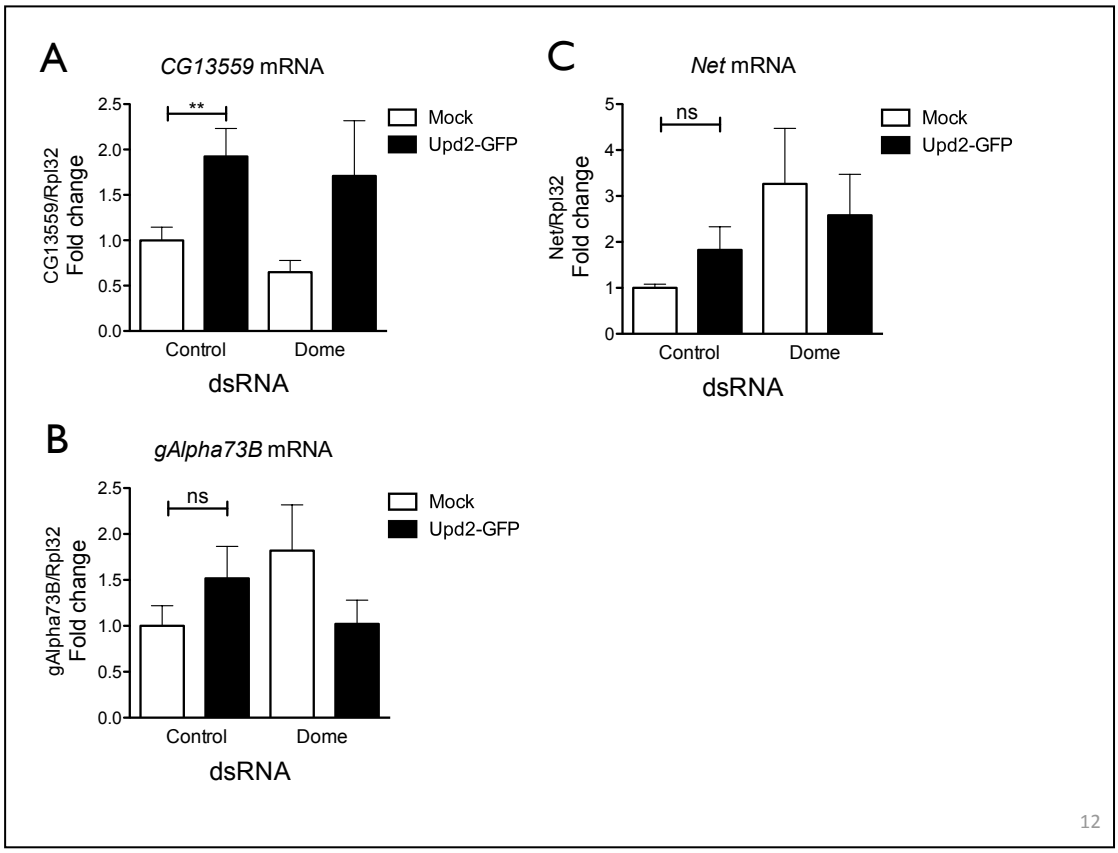

Figure 4.16: *CG13559*, *gAlpha73B* and *Net* mRNA expression is weakly activated by Upd2, but it is receptor independent

$S2R^+$ cells were treated with dsRNA as indicated, five days prior induction. Cells were induced with 20nM Upd2-GFP for 30min at 25ºC, followed by 2h incubation in media. RNA was harvested and mRNA analysed by qPCR. The levels of the target mRNA A: *CG13559*; B: *gAlpha73B* and C: *Net* were normalised to the housekeeping mRNA *Rpl32* and their ratios were plotted as fold change to control treated samples. Graphs represent 3 independent experiments and error bars show standard error of the mean, with *p>0.05, **p>0.01,***p>0.001, ns= not significant students t-test.

4.2.2.2 Dome and SOCS36E are receptor and Upd2-GFP dependent targets

Although *Domeless* was not an identified target in Bina et al it is known as a well-established JAK/STAT *in vivo* target (Brown et al., 2001a). Another JAK/STAT pathway component, SOCS36E, was not only shown to be a negative regulator, but also a JAK/STAT target, acting thus in a positive feedback loop (Stec and Zeidler, 2011). To test whether these transcriptional targets were Upd2- and receptor-dependent in the system I used, I induced signalling by Upd2-GFP CM in control and Dome depleted cells and measured the mRNA levels of *Domeless* and *SOCS36E* via qPCR.

The mRNA levels for both, *Domeless* and *SOCS36E*, increased significantly upon induction with Upd2-GFP and failed to be induced when the receptor was knocked

down (Figure 4.17). Naturally the levels of *Domeless* were decreased in the Dome-knockdown samples, but importantly *Domeless* mRNA levels were not induced by Upd2-GFP stimulation. This induced mRNA should not be influenced by the use of dsRNA, since the exposure to dsRNA occurred 5 days prior induction and it was highly likely it would have been degraded by the time the assay was performed.

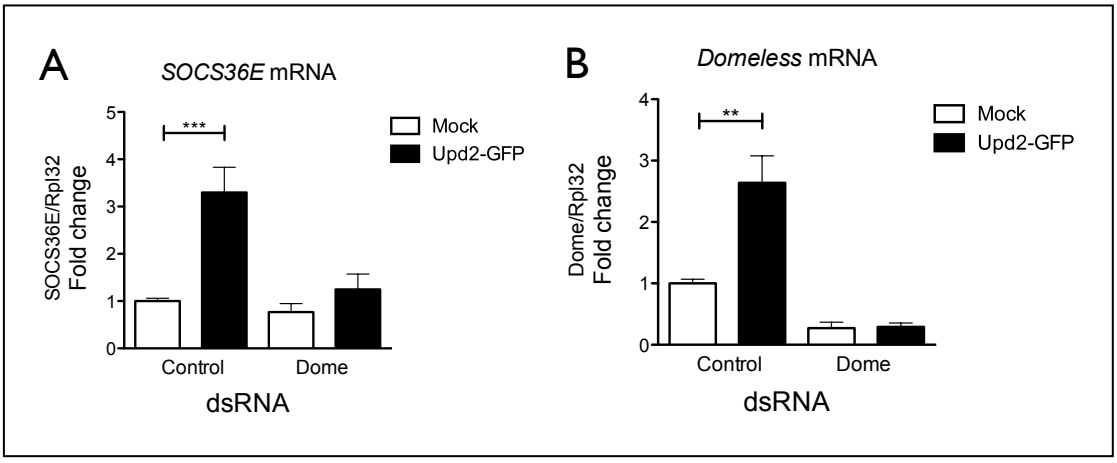

Figure 4.17: mRNA expression of *SOCS36E* and *Domeless* is Upd2 and Receptor dependent

S2R$^+$ cells were treated with dsRNA as indicated, five days prior induction. Cells were induced with 20nM Upd2-GFP for 30min at 25ºC, followed by 2h incubation in media. RNA was harvested and mRNA analysed by qPCR. The levels of the target mRNA A: *SOCS36E* and B: *Domeless* were normalised to the housekeeping mRNA *Rpl32* and their ratios were plotted as fold change to control treated samples. Graphs represent 3 independent experiments and error bars show standard error of the mean, with *p>0.05, **p>0.01,***p>0.001, ns= not significant students t-test.

4.2.2.3 JAK/STAT target activation occurs during early endocytosis

Having established that *Domeless* and *SOCS36E* were Upd2- and receptor- dependent targets, I asked the questions: Was JAK/STAT signalling qualitatively and quantitatively influenced by the endocytic pathway and / or other regulatory proteins? And was this alteration to a similar extent for both targets or was only one and not the other influenced? Hence, I knocked down endocytic components, to address whether endogenous JAK/STAT targets were influenced by intracellular trafficking. Figure 4.18 shows target activation when the early endocytic components: Clathrin and AP2, or the later acting proteins: Myopic and HRS were knocked down and cells stimulated with mock-CM or Upd2-GFP CM.

Both Clathrin and AP2 depletion resulted in the inability of the cells to react to Upd2-GFP stimulation for both target genes, suggesting that the receptor needed to be able to

enter the cell to generate a signal. Signalling was thus controlled quantitatively at this stage in the endocytic pathway. This was consistent with the 10xSTAT luciferase reporter assay.

Notably, cells depleted of HRS, an ESCRT0 component, were not able to induce *SOCS36E* or *Domeless* mRNA as a response to Upd2-GFP (Figure 4.18). JAK/STAT target mRNA levels stayed at the same level in induced samples, when compared to Upd2-GFP treated cells in the absence of the HRS. This suggests that the pathway signals downstream of HRS. Within the endocytic pathway, HRS acts after the Rab5-dependent formation of early endosomes and ensures the sorting of cargo into MVB. My results indicate that Upd2 induced JAK/STAT target expression occurs from a compartment beyond the early endosome. However, this compartment has not reached the maturation level of the MVB, since the TSG101 knockdown did not influence target mRNA expression.

In addition it is unlikely that cells were able to signal from the late endosome, since the transcription factor would have to travel not only through one membrane layer, but also escape from the internal vesicle a MVB typically creates. Consistently, the knockdown of an essential late endosomal protein, TSG101, did not impair signalling, suggesting it occurred before the receptor reached the late compartments (Figure 4.19).

A slightly later role than HRS has been suggested for Myopic. It was shown to regulate EGFR signalling from the MVB (Miura et al., 2008). Here its knockdown only blocked the activation of *Domeless* as a target, whereas *SOCS36E* expression was induced as normal. However, further investigations and repeats would be necessary to conclude a qualitative differential signalling. Furthermore, the remaining Myopic protein concentration may have been still high enough to trigger only *SOCS36E*, but not *Domeless* mRNA induction upon Upd2-GFP incubation, since the *SOCS36E* mRNA response in general was more sensitive to Upd2 induction (data not shown).

Figure 4.18 and Figure 4.19 show that JAK/STAT target expression was dependent on Clathrin-mediated endocytosis and did not occur from late endocytic structures, since the knockdown of Clarthin or AP2 blocked mRNA induction and TSG101 depletion did not influence the *SOCS36E* and *Domeless* expression. The *10xSTATLuc* reporter could not be induced by Upd2-GFP, when these endocytic components were depleted (Figure 4.6).

Strikingly the knockdown of Rab5 did not influence activation upon Upd2-GFP treatment, however *SOCS36E* and *Domeless* expression were dependent on HRS, which

acts in a compartment past the Rab5 positive early endosomes. My data demonstrates that different JAK/STAT signalling occurs is dependent on distinct endocytic components, suggesting the occurrence of signalosomes. It indicates that the endocytic pathway creates niches for differential JAK/STAT signalling.

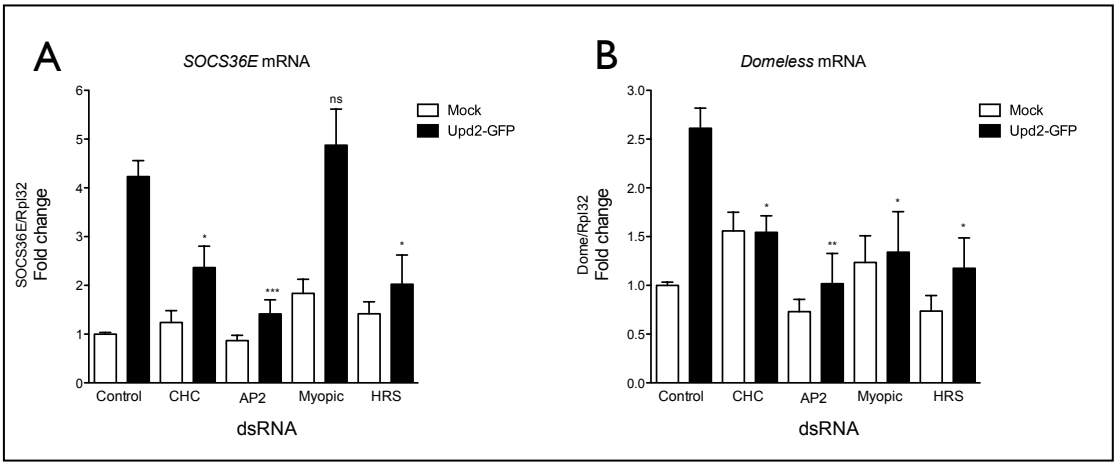

Figure 4.18: Upd2 induced *SOCS36E* and *Domeless* mRNA expression is dependent on Clathrin-mediated receptor uptake

S2R$^+$ cells were treated with dsRNA as indicated, five days prior induction. Cells were induced with 20nM Upd2-GFP for 30min at 25ºC, followed by 2h incubation in media. RNA was harvested and mRNA analysed by qPCR. The levels of the target mRNA A: *SOCS36E* and B: *Domeless* were normalised to the housekeeping mRNA *Rpl32* and their ratios were plotted as fold change to control treated samples. Graphs represent at least 3 independent experiments and error bars show standard error of the mean. The students t-test was performed comparing induced samples of control knockdown vs. indicated gene knockdown, with *p>0.05, **p>0.01,***p>0.001, ns= not significant.

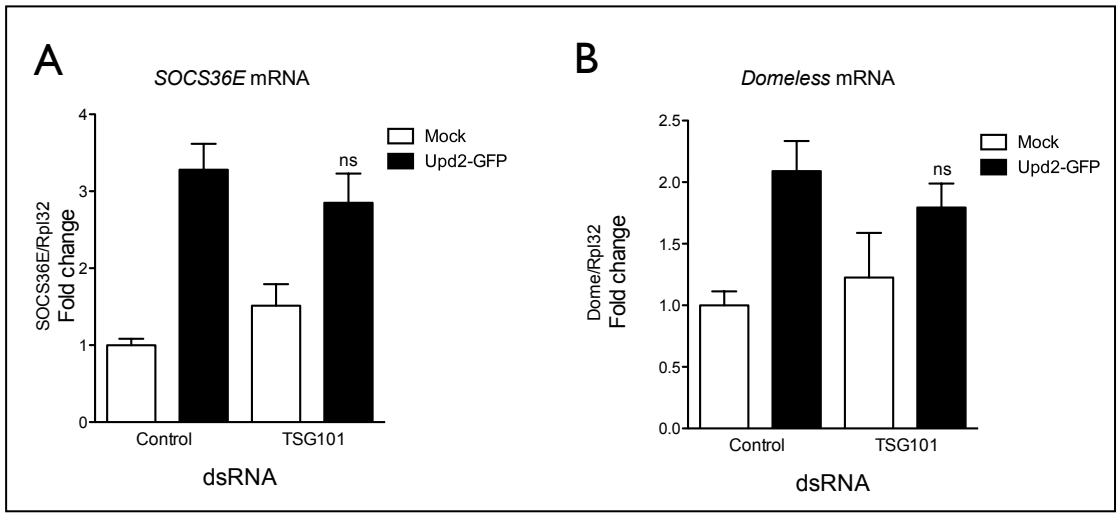

Figure 4.19: Upd2 induced mRNA expression of *SOCS36E* and *Domeless* occurs upstream of TSG101

S2R$^+$ cells were treated with dsRNA as indicated, five days prior induction. Cells were induced with 20nM Upd2-GFP for 30min at 25ºC, followed by 2h incubation in media. RNA was harvested and mRNA analysed by qPCR. The levels of the target mRNA A: *SOCS36E* and B: *Domeless* were normalised to the housekeeping mRNA *Rpl32* and their ratios were plotted as fold change to control treated samples. Graphs represent 3 independent experiments and error bars show standard error of the mean. The students t-test was performed comparing induced samples of control knockdown vs. TSG101 knockdown, with *p>0.05, **p>0.01,***p>0.001, ns= not significant.

4.2.2.4 Rab5, TSG101 PtpF61, Hop knockdown induces Upd2-GFP independent target activation

As mentioned earlier, I also investigated the effect of Rab5, alongside with known STAT modulators, the kinase, Hopscotch (Hop), and the phosphatase, PtpF61 on JAK/STAT target activation.

In Figure 4.20 the effect of these known JAK/STAT regulators is illustrated, surprisingly all of them had elevated levels of *SOCS36E* and *Domeless*. This increase occurred already in mock treated cells and the mRNA levels in most cases did not rise further after ligand treatment. It was moreover astonishing that especially the negative regulator, Hop elevated the targets to such a considerable extent. Rab5 also increased ligand-independent weaker targets, like *CG10764* or *Bazooka* (data not shown). This suggests that the knockdown of these crucial cell components triggers stress-responses within the cell and thus this assay might be too sensitive having picked up these stress related mRNA changes.

To confirm the degree of the knockdown I analysed *Rab5* and *Hop* mRNA levels by qPCR. Figure 4.7 showed that *Hop* mRNA levels remained at approximately 50% upon dsRNA treatment and *Rab5* mRNA was decreased below 25%.

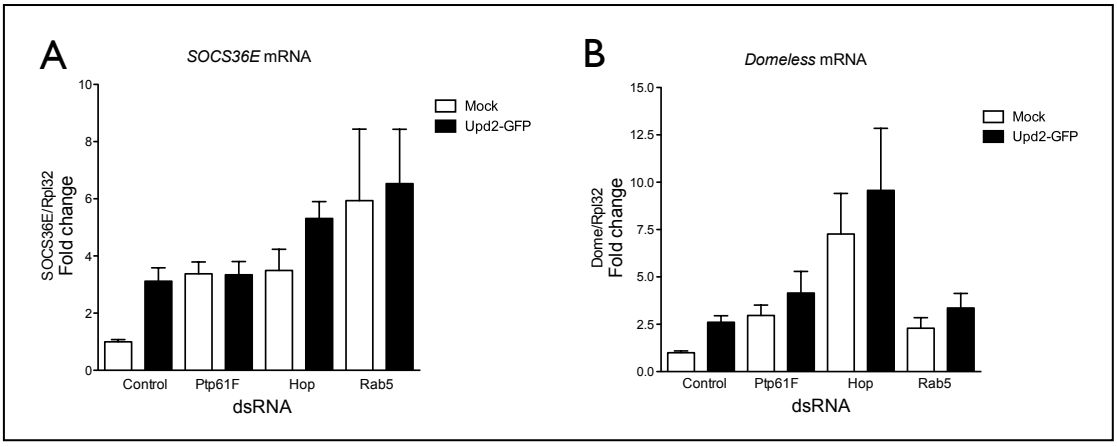

Figure 4.20: JAK/STAT target activation due to stress

S2R$^+$ cells were treated with dsRNA as indicated, five days prior induction. Cells were induced with 20nM Upd2-GFP for 30min at 25ºC, followed by 2h incubation in media. RNA was harvested and mRNA analysed by qPCR. The levels of the target mRNA A: *SOCS36E* and B: *Domeless* were normalised to the housekeeping mRNA *Rpl32* and their ratios were plotted as fold change to control treated samples. Graphs represent 3 independent experiments and error bars show standard error of the mean.

4.2.2.5 Normal JAK/STAT target-activation in Rab5 GEF knockdowns

Within this assay the knockdown of Rab5 resulted in high up-regulation of both *SOCS36E* and *Domeless*, in un-stimulated and stimulated cells, hence I suggested that this increase of target mRNA might be a stress response (Figure 4.20 & section 4.2.2.4). As described above Rab5 knockdown was shown to control the JAK/STAT pathway (Baeg et al., 2005; Vidal et al., 2010), yet, I again wanted to examine if Rab5 GEFs regulate JAK/STAT target activation.

Consistent with Figure 4.12 B, the knockdown of Rab5 GEFs did not alter JAK/STAT target activation (Figure 4.21 A&B). Interestingly, there was a significant enhancement of target mRNA (*Domeless*) in un-induced cells, when Rabex5 or Sprint was knocked down (Figure 4.21 C) (compared to mock-treated control cells). A similar effect occurred when measuring JAK/STAT activation with the 10xSTAT luciferase assay (section 4.2.1.4). Additionally, *in vivo* experiments indicated ligand-independent JAK/STAT pathway activation in the developing wing disc (section 3.3.1). This increased expression was not additive with ligand-dependent signalling, since Upd2 induced samples showed the same extent of target activation than the control cells

(Figure 4.21 C). This suggests that the Upd2-dependent pathway activation overwrites ligand-dependent signalling. Since, I primarily wanted to study receptor-dependent endocytosis, this ligand-independent behaviour was not my main interest and unfortunately the investigation of this mechanism was beyond the scope of my work.

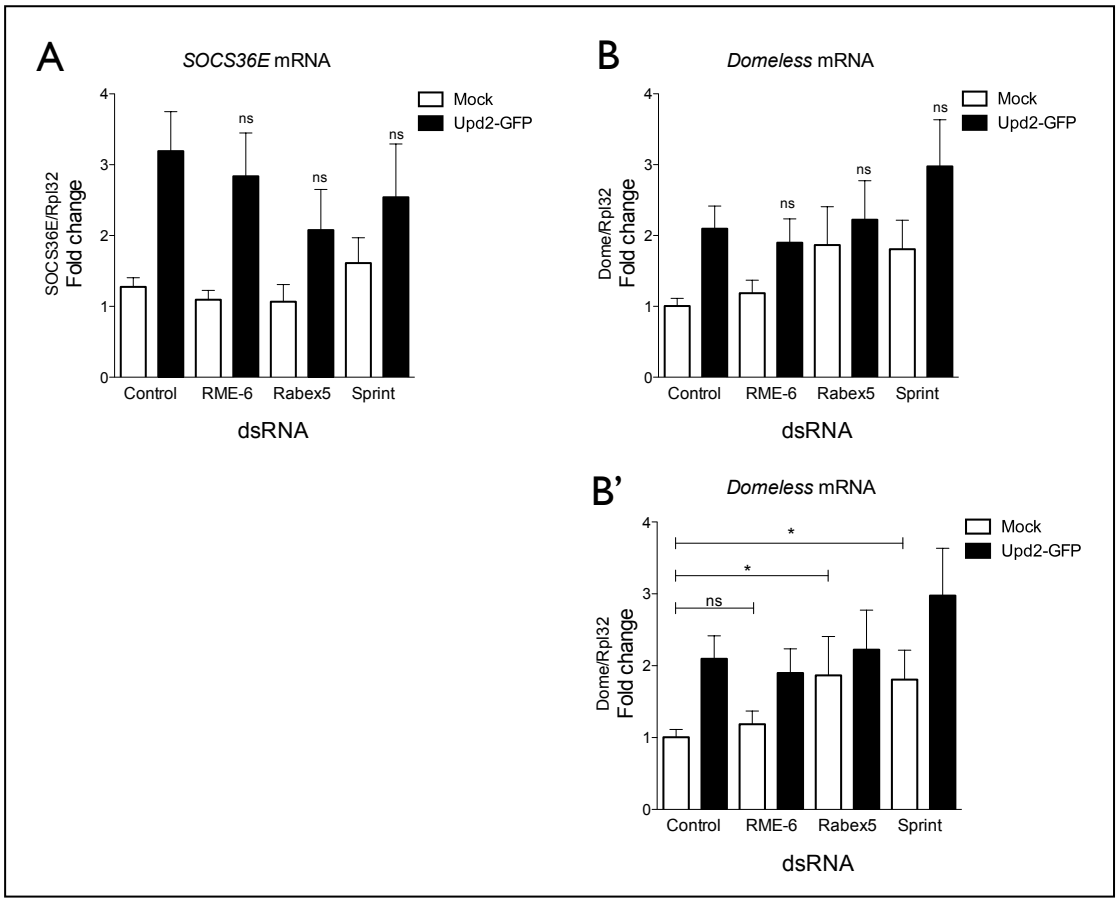

Figure 4.21: Rab5-GEFs do not influence Upd2 induced *SOCS36E* and *Domeless* mRNA expression

S2R^{+} cells were treated with dsRNA as indicated, five days prior induction. Cells were induced with 20nM Upd2-GFP for 30min at 25ºC, followed by 2h incubation in media. RNA was harvested and mRNA analysed by qPCR. The levels of the target mRNA A: *SOCS36E* and B & B': *Domeless* were normalised to the housekeeping mRNA *Rpl32* and their ratios were plotted as fold change to control treated samples. Graphs represent 3 independent experiments and error bars show standard error of the mean. A and B: The students t-test revealed no significant differences between induced samples of control knockdown vs. indicated Rab5 GEF knockdown. B': Same data as in B, but the students t-test was performed comparing mock treated samples of control knockdown vs. Rab5 GEF knockdowns with *p>0.05, **p>0.01,***p>0.001, ns= not significant.

4.2.2.6 RacGAP as novel regulator of JAK/STAT signalling

Studying the fine nuances of JAK/STAT regulation, my interest was raised by another potential novel regulator. Recent literature suggested the RacGAP MgcRacGAP as a

novel regulator of JAK/STAT signalling. To evaluate if the *Drosophila* homologues (Tumbleweed and Rotund) also played a role in JAK/STAT target regulation I knocked them down and investigated *Domeless* and *SOCS36E* target activation. The main role of RacGAP50C/Tumbleweed was thought to be its regulation in cytokinesis, by allowing cells to form furrows and localise cytokinetic components during anaphase (Zavortink et al., 2005). But, it was also implemented in non-cytokenetic functions such as the control of Wnt signalling (Jones et al., 2010), The mammalian homolog, MgcRacGAP was reported to be necessary for phospho-STAT import in nucleus via its nuclear localisation sequence (NLS), acting as a molecular chaperone (Kawashima et al., 2009; Kawashima et al., 2006). However, the *Drosophila* Tumbleweed actually did not contain the NLS, but another RacGAP, Rotund, contained a NLS..I blasted with the MgcRacGAP NLS for similar proteins and interestingly Rotund showed highest resemblance and thus was the first hit. Hence, I investigated the influence of both RacGAPs on JAK/STAT signalling.

Figure 4.22 shows the effect on JAK/STAT signalling of both RacGAPs. Although neither of the RacGAPs knockdowns significantly affected JAK/STAT target activation a decrease in *Domeless* induction was observed when the RacGAPs were depleted. This just escaped statistical significance with $p=0.0533$ (t-students test comparing induced control, with knockdown samples) when Rotund was knocked down. Also *SOCS36E* mRNA was less induced when Tumbleweed was knocked down ($p=0.0898$). Further experiments, including additional repeats and double knockdowns would be necessary to determine if these RacGAPs regulate JAK/STAT signalling and if they are redundant. Furthermore, it would be very interesting to investigate whether there is a qualitative signal regulation as the initial data suggests (Figure 4.22).

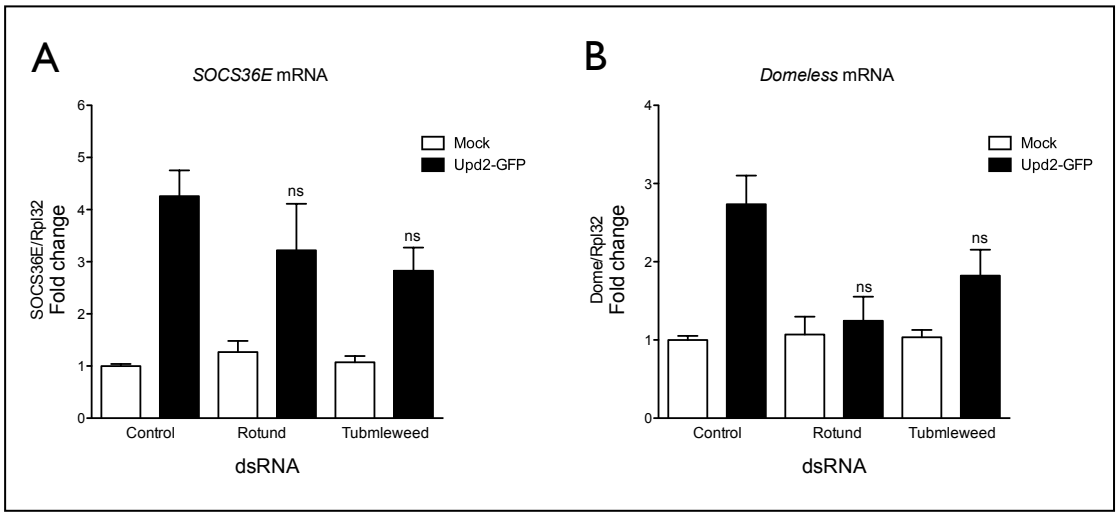

Figure 4.22: Upd2 induced *SOCS36E* and *Domeless* mRNA expression is independent of RacGAP

S2R$^+$ cells were treated with dsRNA as indicated, five days prior induction. Cells were induced with 20nM Upd2-GFP for 30min at 25ºC, followed by 2h incubation in media. RNA was harvested and mRNA analysed by qPCR. The levels of the target mRNA A: *SOCS36E* and B: *Domeless* were normalised to the housekeeping mRNA *Rpl32* and their ratios were plotted as fold change to control treated samples. Graphs represent 3 independent experiments and error bars show standard error of the mean. The students t-test was performed comparing induced samples of control knockdown vs. RacGAP knockdown, with *p>0.05, **p>0.01,***p>0.001, ns= not significant.

4.3 Summary

This chapter shows first an in-depth bio-chemical analysis of JAK/STAT ligand uptake (section 4.1). I attempted to study the JAK/STAT endocytosis by immuno-fluorescence, but I could observe only heterogenous staining of the ligand. The inconsistency of staining behaviours of *Drosophila* cells led me additional to other advantages, into developing an anti-GFP ELSIA assay to measure Upd2-GFP uptake. I showed that Upd2 was taken up by Clathrin-mediated endocytosis. In the analysis of the trafficking of JAK/STAT signalling I focused on measuring three different properties: A) the binding potential of Upd2 to its receptor Dome, which was saturated at around 25nM (Figure 4 A) the internalisation rates of Upd2, which peaked after already 5 min ligand exposure (Figure 4.6) the main mechanism for Upd2 uptake, which was AP2, Clathrin and receptor dependent as shown in Figure 4.6.

The analysis of uptake mechanism was followed by the functional investigation of JAK/STAT signalling, using a 10xSTAT luciferase assay (Section 4.2.1) and an endogenous JAK/STAT target assay, which I described within section 4.2.2. The activation *Domeless* mRNA, encoding the JAK/STAT receptor, and *SOCS36E*,

translating into a negative regulator of the pathway, were excellent endogenous pathway targets. Their induction was both receptor- and ligand-dependent

Both functional readouts showed that JAK/STAT signalling was controlled by or dependent on Clathrin-mediated endocytosis. I also demonstrated with both assays that only the early stages of endocytosis were required for Upd2 induced signalling, since blocking late endosomes (TSG101 knockdown) did not affect signalling. The luciferase assay suggests the existence of signalosomes, as signalling was activated from Clathrin and AP2 dependent, but Rab5 independent structures.

Adding both signalling assays together my data suggests further, that the JAK/STAT signalosome is responsible for the differential signal outputs. Since the generic signalling measured by the 10xSTATluc was Rab5 independent, wereas endogenous targets SOCS36E and Dome were at least dependent on HRS, which acts beyond a Rab5 positive compartment. This suggested the occurrence of distinct signalling for generic of specific transcriptional activation.

Furthermore, the analysis of additional endocytic components suggested that HRS and Myopic establish specialised endocytic compartments- signalosomes where differential signalling could occur.

I also addressed and excluded the influence of Rab5 activators, GEFs, since no Upd2 dependent effect of any of the Rab5 GEFs in both functional assays was confirmed.

Conversely, RacGAP proteins might have an effect on qualitative signalling, by blocking one, but not the other transcriptional target to be induced by Upd2. However, these effects still remained to be verified.

Together the analysis of ligand uptake and functional signalling induced the concept of JAK/STAT regulation by Clathrin-mediated endocytosis. Especially the target assay revealed interesting novel regulators, which were further investigated in the next chapter. Chapter Chapter 5 will focus on the modification of STAT92E. I will describe methods of detecting phosphorylated STAT92E, which I used to investigate the influence of Clathrin-mediated endocytosis and other suggested regulators of JAK/STAT.

CHAPTER 5. STAT92E MODIFICATIONS DURING THE ENDOCYTIC PATHWAY

In the previous chapter, My data allowed me to suggest the novel model that endocytosis qualitatively regulated JAK/STAT signalling. In this chapter, I asked whether this resulted from novel post-translational modifications of STAT92E.

5.1 Analysis of STAT92E phosphorylation

Phosphorylation of proteins is a widely used modification method by nature to regulate signalling pathways (Friedbichler et al., 2011). In the case of *Drosophila* JAK/STAT signalling the transcription factor STAT92E must be phosphorylated by a Janus kinase (JAK) on Y-711 in order to function properly (Ekas et al., 2010; Karsten et al., 2006; Yan et al., 1996). This phosphorylation event is highly conserved through evolution (Yan et al., 1996).

The analysis of phosphorylated proteins is often achieved by using phospho- specific antibodies. However, the visualisation of phosphorylated STAT92E has become difficult, since the only commercially anti-phospho STAT92E antibody became un-available. Phosphorylation of proteins can for some cases be visualised with their standard (non-phospho-specific) antibodies due to a charge- and molecular mass change. Many proteins, when phosphorylated, run slightly slower on an SDS-PAGE gels and result this in a bandshift. This characteristic was applied by Shi et al 2008 to visualise STAT92E phosphorylation in S2 cells and embryos.

To test whether I could detect a phosphorylated form of STAT92E after stimulating cells with Upd2, I treated cells with Upd2-GFP CM for various time points and analysed cell lysates by immunoblotting with anti-STAT92E antibodies. Whereas, I detected a single band for STAT92E in cells incubated with mock-CM, an additional second band was present in cells treated with Upd2-GFP (Figure 5.1). These bands are pointed out by arrows in Figure 5.1. This suggests that STAT92E is phosphorylated upon ligand stimulation.

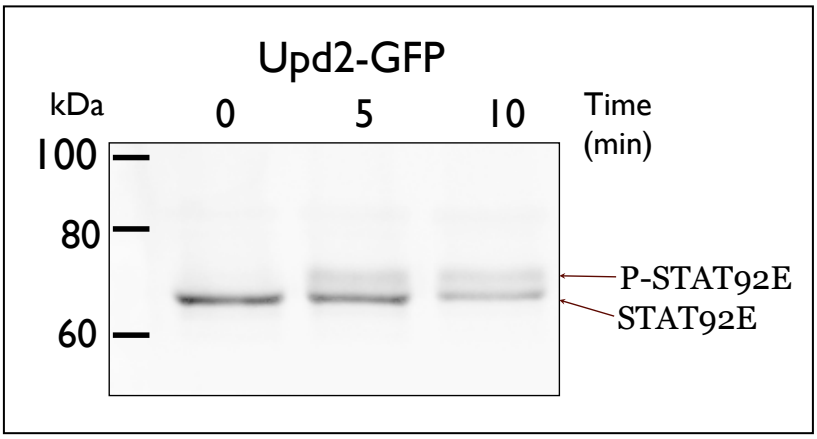

Figure 5.1: STAT92E bandshifts upon Upd2-GFP stimulation

S2R$^+$ cells were treated with 20nM Upd2-GFP for indicated time points at 25ºC. Total protein extracts were analysed by SDS-PAGE and immuno-blotted with anti-STAT92E. STAT92E is expected to migrate at approximately 75 kDa and its phosphorylated form migrates more slowly. STAT92E and phosphorylated (P-) STAT92E are indicated by arrows.

In order to show that the bandshift was due to STAT92E phosphorylation, I used calf intestinal alkaline phosphatase (CIP) to dephosphorylate the protein. I immunoprecipitated the transcription factor from cells incubated with Upd2-GFP CM and subsequently treated the immunoprecipitate (IP) with CIP. An example of this procedure is shown in Figure 5.2. Following incubation of the IP with CIP, no bandshift occurred. Furthermore, when I inhibited CIP itself by treating the IPs with EDTA (a magnesium chelator, hence depleting the buffer of Mg^{2+}, which is crucial for the phosphatase to function, there was a bandshift similar to control samples. Together these data allowed me to conclude that the phosphorylation of STAT92E caused the bandshift.

In addition, the right hand panels of Figure 5.2 shows also the efficiency of the IP. Lanes 10&11 contained the lysates after immunodepletion with anti-STAT92E antibody where much less STAT92E was observed compared to control IgG treated lysates (lanes 12&13), whereas the amount of a loading control, Actin, was comparable (data not shown).

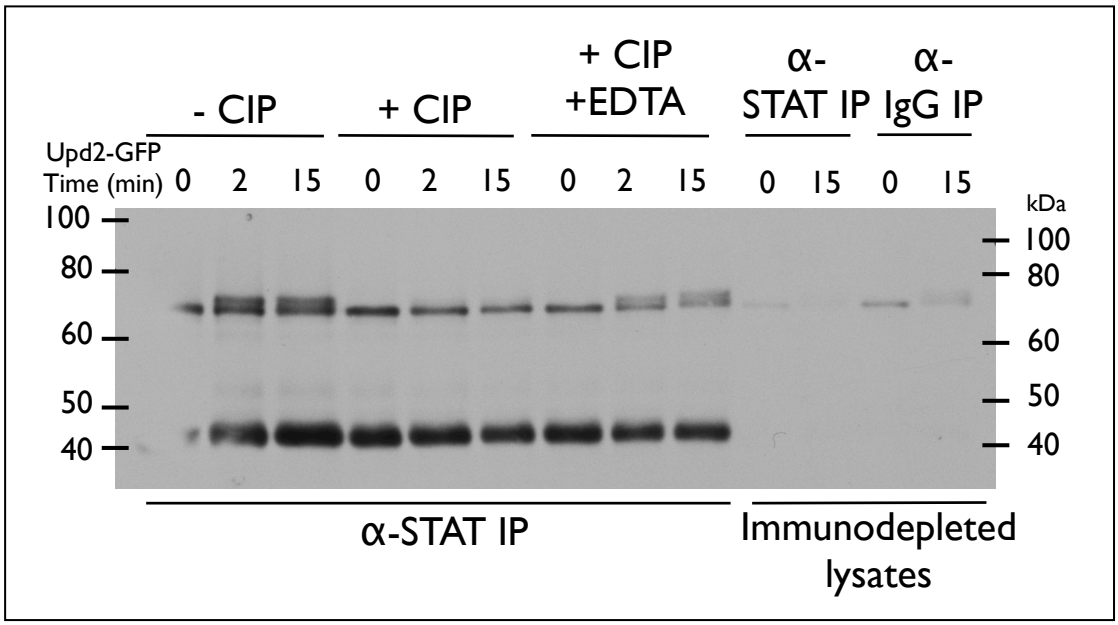

Figure 5.2: STAT92E bandshift is due to phosphorylation

S2R^{+} cells were treated with 20nM Upd2-GFP for indicated time points at 25ºC. After immunoprecipitating STAT92E with anti-STAT92E antibodies, IPs were either with mock-treated or incubated with phosphatase (CIP) or prior to phosphatase treatment, EDTA was added. IPs and immunodepleted total protein extracts were analysed by SDS-PAGE and immunoblotted with anti-STAT92E antibody. Representative example (one of two repeats).

As I described earlier, the main phosphorylation site on of STAT92E that has been reported to be functionally important is tyrosine 711. Even though I was not able to detect the specific phosphorylation sites, I used a generic anti-phospho-tyrosine antibody to show that STAT92E is tyrosine phosphorylated, without being able to pinpoint the specific site.

First, I tested whether I could detect phosphorylated STAT92E from whole cell lysates using the anti-phospho-tyrosine antibody. Therefore, I stimulated cells with either mock CM or Upd2-GFP CM and analysed cell lysates with the anti-phospho-tyrosine antibody on a western blot. Unsurprisingly, I was unable to detect an Upd2-GFP induced band in whole cell lysates. The generic antibody detected many tyrosine-phosphorylated proteins within the lysates and amongst the bands detected, no additional phospho-protein occurred after ligand stimulation (data not shown). Either the amount of STAT92E proteins within cells was too low to be able to detect specifically phospho-STAT92E with the anti-phospho-tyrosine antibody, or another tyrosine phosphorylated protein separated at the same height as phospho-STAT92E and thus masked the detection of the phosphorylated transcription factor.

Consequently, I enriched for STAT92E by IP with anti-STAT92E antibody, from cells that had been stimulated with ligand for various times. The IPs were electrophoresed on a SDS-PAGE gel and immunoblotted with an anti-phospho-tyrosine antibody. The asterisk in Figure 5.3B marks a faint band at around 75 kDa, visible 2 minutes after ligand stimulation, corresponding to the bandshifted phosphorylated STAT92E (phospho-STAT92E), described above. This suggested that STAT92E was tyrosine-phosphorylated. In addition, the detected band appeared stronger when cells were transfected with the kinase, Hop, or depleted of the phosphatase, Ptp61F or the negative regulator SOCS36E (W. Stec personal communication).

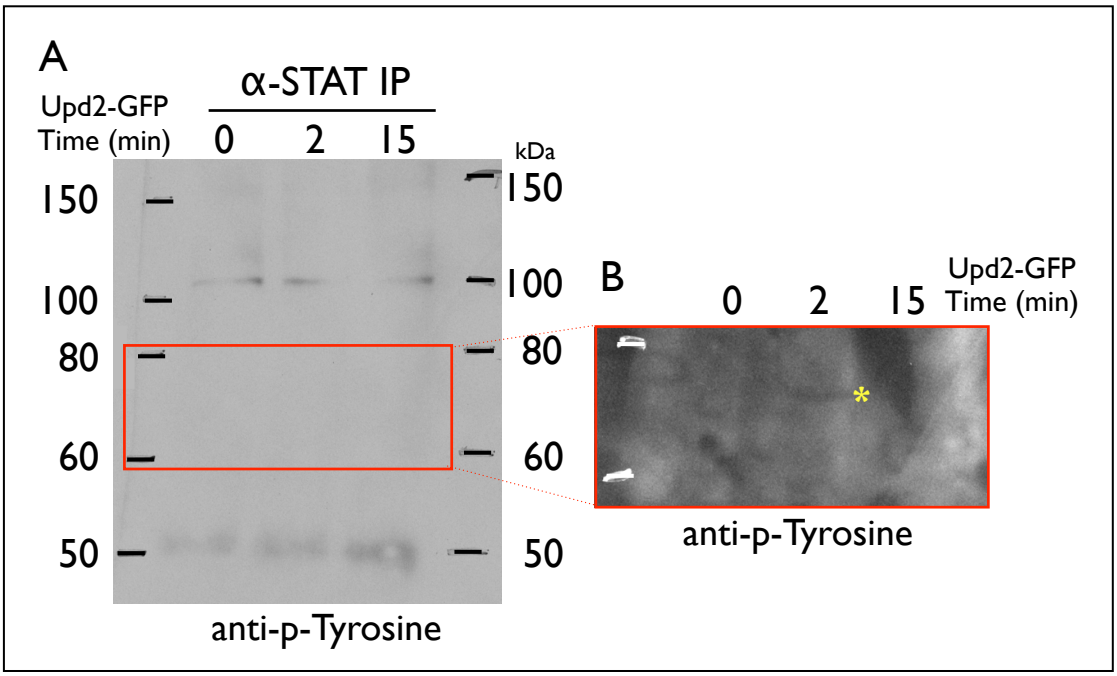

Figure 5.3: Tyrosine phosphorylation of STAT92E

S2R^{+} cells were treated with 20nM Upd2-GFP for indicated time points at 25ºC. After immunoprecipitating STAT92E with anti-STAT92E antibodies, IPs were analysed by SDS-PAGE and immunoblotted with anti-p-Tyrosine. A: normal exposure, B: high exposure and magnified red boxed area. Yellow asterisk indicates presence of a faint band corresponding to tyrosine phosphorylated STAT92E. Representative example (one of two repeats).

One of the main advantages of using the bandshift assay to address the phosphorylation of STAT92E is its straight-forward quantification. I could calculate the proportion of phospho-STAT92E by quantifying the signal in the upper band and expressing it as a percentage of the signal in both STAT92E specific bands. Using this method no loading control was needed, since I considered total STAT92E protein and controlled internally

for the amount of cell lysate analysed. Nevertheless, a fairly equal amount of cell lysates was loaded in each case.

Since, I wanted to investigate the influence of the endocytic pathways on STAT92E phosphorylation, it was crucial to use an assay, which is quantitative, precise and reproducible. Immunoprecipitating STAT92E and then probing for phospho-tyrosine, which was barely detectable, made this possibility of phospho-protein detection unsuitable for the questions I was attempting to address. Consequently, I used the quantification of STAT92E bandshift upon ligand stimulation in all subsequent experiments (for example see Figure 5.4C).

5.1.1 Phosphorylation of STAT92E is Upd2-, time-, and receptor-dependent

Having shown that treatment with Upd2-GFP CM resulted in a bandshift of STAT92E, which was due to the phosphorylation of the transcription factor, I then asked whether STAT92E phosphorylation was ligand-, time- and receptor-dependent.

In Figure 5.4 A, I compared the phosphorylation of STAT92E upon mock and Upd2-GFP stimulation. Cells were treated with CM with or without the ligand and analysed for STAT92E by western blot. A bandshift and thus phosphorylated STAT92E only occurred in Upd2-GFP treated samples. I showed in Chapter 4 that JAK/STAT signalling was activated by Upd2 and not by its fused protein GFP. Consequently, I conclude that the bandshift observed is an Upd2 specific response and thus the phosphorylation of STAT92E is ligand dependent.

To address the kinetics of STAT92E phosphorylation, I incubated cells for various times with Upd2-GFP CM. Figure 5.4 B shows one example blot and Figure 5.4 C the quantification of phospho-STAT92E. STAT92E phosphorylation occurred rapidly following stimulation and could be detected as early as 2 minutes (compare Figure 5.5 and subsequent experiments). The extended time course in Figure 5.4 B&C shows that phosphorylation increased with time, peaked around 30 minutes followed by a subsequent decrease in phosphorylation. After 30 minutes the rate of de-phosphorylation was higher than the activating phosphorylation. This points towards a regulatory mechanism, in which STAT92E is slowly dephosphorylated, after constant stimulation.

Given that the phosphorylation of STAT92E occurred rapidly following ligand stimulation. I decided to investigate this phosphorylation by stimulating cells only up to 15 minutes in subsequent experiments.

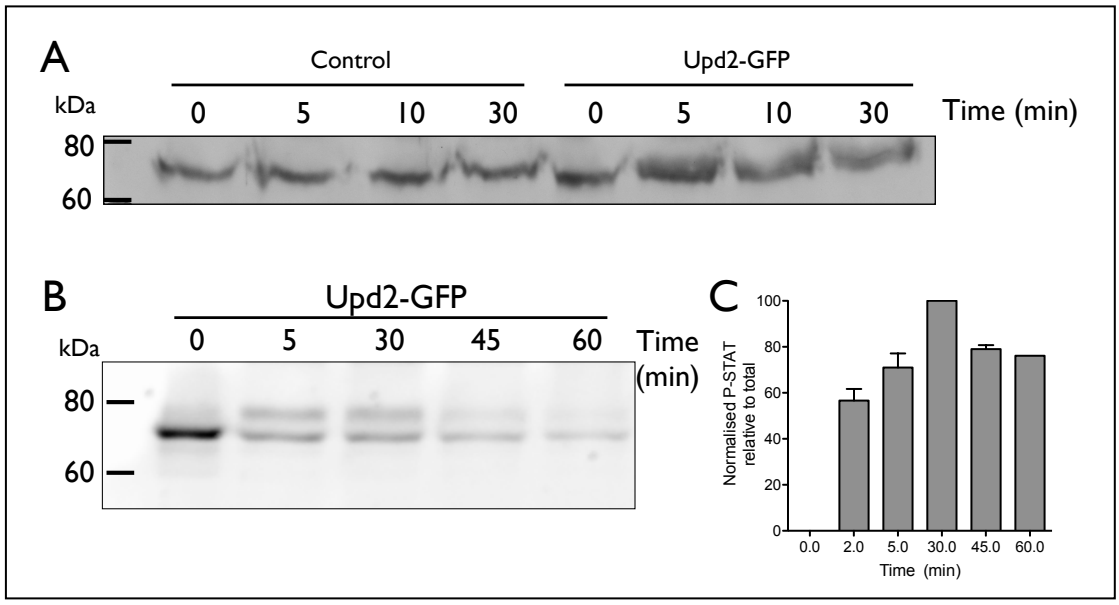

Figure 5.4: STAT92E is phosphorylated upon Upd2-GFP stimulation

S2R$^+$ cells were treated with control (GFP) or ligand (Upd2-GFP) CM each 20nM for indicated time points at 25ºC. Total protein extracts were analysed by SDS-PAGE and immunoblotted with anti-STAT92E. A: example of control samples vs. Upd2-GFP treated samples, B: Time course of Upd2-GFP treatment. C: Quantification of time-dependent phosphorylated STAT92E (P-STAT), whereby the ratio of P-STAT92E to total STAT92E, normalised to 30 min (as highest value set to 100) was plotted against time of activation with Upd2-GFP, error bars show standard error of the mean. Representative examples (one of two repeats, except for 60min Upd2-GFP treatment (C)).

In order to show that STAT92E phosphorylation is receptor dependent, Dome-depleted and control-treated cells were stimulated with ligand for various times. The anti-STAT92E immuno-blot shows a significantly reduced STAT92E phosphorylation for early time points, when Dome was depleted from cells ($p=0.0399$ at 2 minutes and $p=0.0003$ at 5 minutes, unpaired students t-test, Figure 5.5). STAT92E phosphorylation of about 50% at 15 minutes was still evident, but this was quite likely due to an incomplete removal of Dome during the knockdown. However, it also indicates that the phosphorylation of STAT92E is particularly sensitive to pathway activation since even with residual levels of receptor, STAT92E became phosphorylated albeit at reduced levels.

I was unable to perform a students t-test for the last time-point, since I set the control samples in each individual experiment to 100% (relative phosphorylation), which resulted in a missing standard deviation for this sample. However, a reduction in STAT92E phosphorylation was clearly visuable.

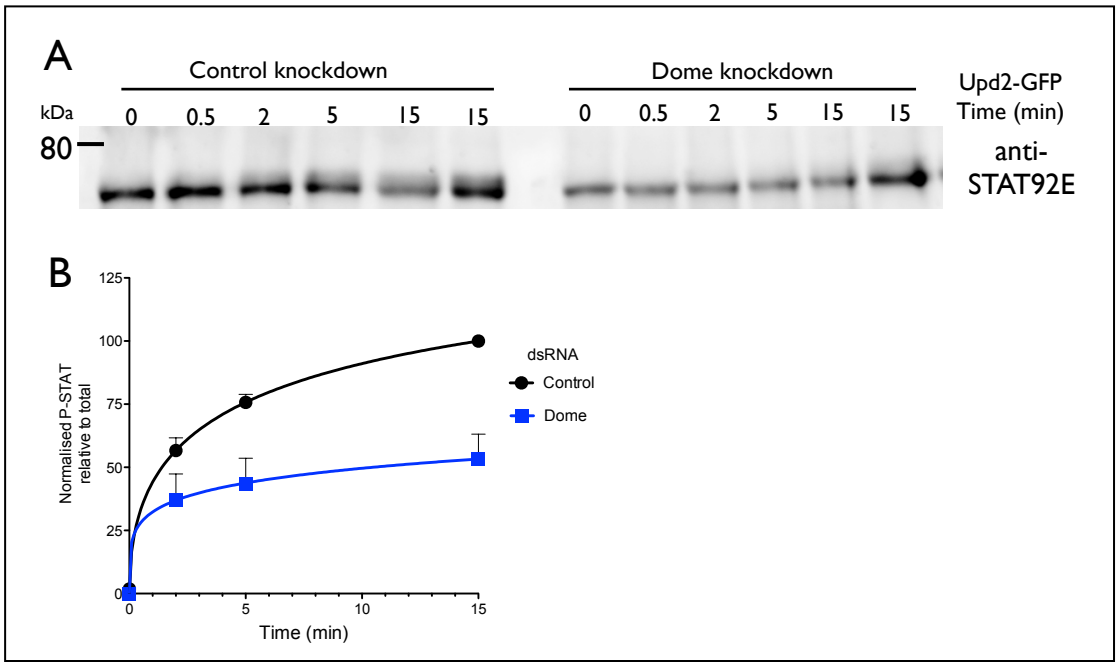

Figure 5.5: STAT92E phosphorylation is receptor dependent

$S2R^+$ cells were treated with dsRNA as indicated, five days prior to exposing them to 20nM Upd2-GFP for indicated time points at 25ºC. Total protein extracts were analysed by SDS-PAGE and immuno-blotted with anti-STAT92E. A: One example blot showing the lack of bandshift in Dome knockdown upon ligand stimulation. B: Quantification of time dependent phosphorylated STAT92E (P-STAT), whereby the ratio of P-STAT92E to total STAT92E, normalised to the latest time point of control samples, was plotted against time of activation with Upd2-GFP, error bars show standard error of the mean, representing at least 4 independent experiments.

5.2 Endocytic regulation of STAT92E phosphorylation

Having established that STAT92E phosphorylation is ligand-, time- and receptor-dependent, I went on to investigate whether endocytosis affected STAT92E phosphorylation.

5.2.1 Clathrin and AP2 knockdown increases phosphorylation of STAT92E

Early components of Clathrin-mediated endocytosis were required for Upd2-GFP uptake (see section 4.1.4). In addition, I showed within the previous chapter, that endogenous and exogenous pathway target activation was dependent on AP2 and Clathrin. I hypothesised that the inhibition of transcription of these targets could result from an impairment of STAT92E activity, which could be due, for example, to a post-translational modification such as phosphorylation.

To test whether Clathrin and AP2 influenced the phosphorylation of the transcription-factor, I depleted cells of Clathrin or AP2 and analysed cell lysates after Upd2-GFP

stimulation for phosphorylation of STAT92E. Unexpectedly, the knockdown of Clathrin and AP2 resulted in an enhanced phosphorylation of STAT92E.

Figure 5.6 shows example blots of STAT92E with its phosphorylated form when Clathrin (A) or AP2 (B) was knocked down. The upper band for STAT92E (phospho-STAT92E) increased strongly over time in the knockdown samples. After only 2 minutes ligand exposure, there was a significant enhancement of STAT92E phosphorylation in cells depleted of Clathrin or AP2, without increasing background levels (0 minutes). Quantifications are shown in Figure 5.7. This enhanced phosphorylation was significant at 2 minutes post ligand stimulation and there was still a significant enhancement at 5 minutes, which increased with time. I was unable to perform a students t-test for the last time-point, since I set the control samples in each individual experiment to 100% (relative phosphorylation), which resulted in a missing standard deviation for this sample.

This effect was surprising since signalling is blocked when AP2 or Clathrin was knocked down, even though phosphorylation has been shown to be crucial for the function of the transcription factor. The decreased internalisation of the receptor could result in its accumulation at the cell membrane and hence in an enhanced phosphorylation. However, the same circumstance also results in the inability to signal, which could be due to an additional phosphorylation site, inhibiting signalling.

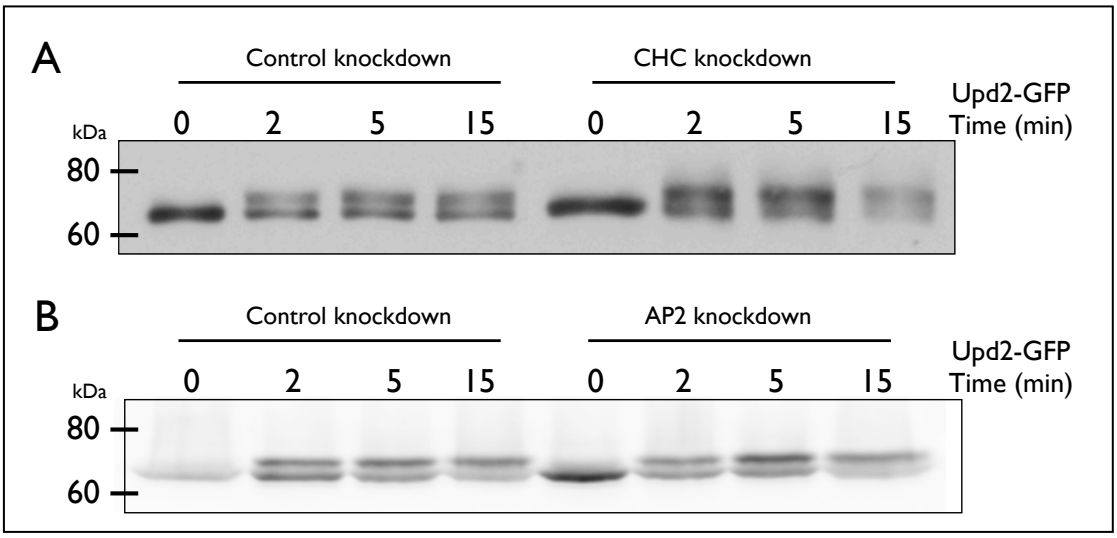

Figure 5.6: Examples of STAT92E phosphorylation upon Clathrin and AP2 knockdown

S2R$^+$ cells were treated with dsRNA as indicated (A: Clathrin heavy chain (CHC) and B: AP2), five days prior exposing them to 20nM Upd2-GFP for indicated time points at 25ºC. Total protein extracts were analysed by SDS-PAGE and immunoblotted with anti-STAT92E. Blots are representative of at least 4 experiments.

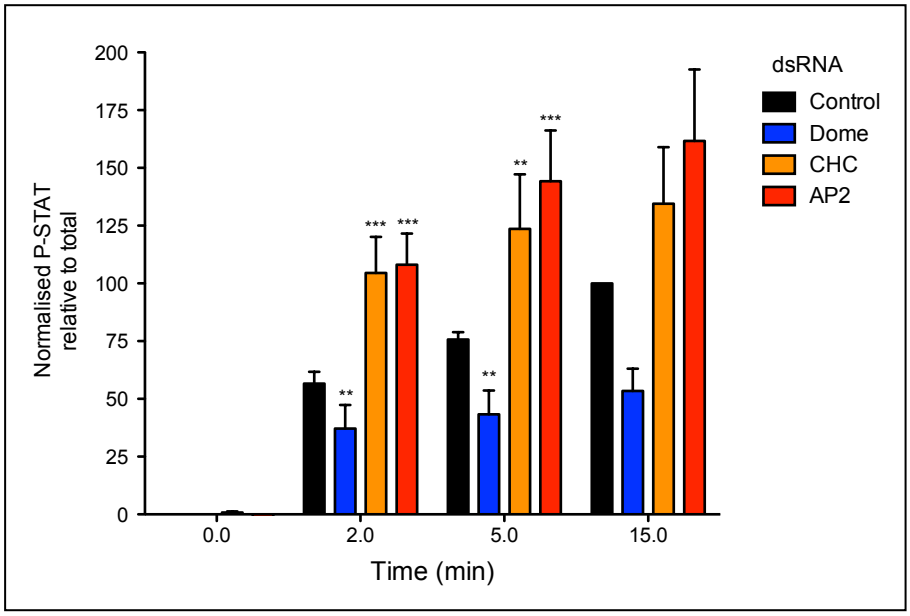

Figure 5.7: Clathrin-mediated endocytosis increases STAT92E phosphorylation

S2R$^+$ cells were treated with dsRNA as indicated, five days prior to exposing them to 20nM Upd2-GFP for indicated time points at 25ºC. Total protein extracts were analysed by SDS-PAGE and immunoblotted with anti-STAT92E. Quantification of phosphorylated STAT92E: ratio of P-STAT92E to total STAT92E was normalised to the latest time point of control dsRNA samples. Ratios were plotted against time of incubation with Upd2-GFP, error bars show standard error of the mean, representing at least 4 independent experiments. Students t-test was performed comparing control knockdown vs. the indicated knockdowns within the same time point, with *p>0.05, **p>0.01,***p>0.001, ns= not significant.

5.2.2 Knockdown of RME-6, HRS, Myopic and RacGAPs does not increase STAT92E phosphorylation

Given the surprising result that Clathrin and AP2 knockdown enhanced STAT92E phosphorylation and simultaneously blocked pathway activation, I wanted to test the effect of the knockdown of other endocytic components on STAT92E phosphorylation. This could shed more light on the correlation between enhanced phosphorylation and pathway signalling.

Using the same approach as described for Clathrin and AP2, I incubated cells, depleted of the protein in question, for various time points with Upd2-GFP CM and analysed their lysates with anti-STAT92E antibody. The effect of the knockdown of RME-6, Myopic, and HRS is exemplified in Figure 5.8 and the quantification of STAT92E phosphorylation is illustrated in Figure 5.9. The phosphorylation of STAT92E appeared

to be comparable to the one in control samples, when cells were depleted of these endocytic components.

Although depleting RME-6 might have resulted in a slight decrease in STAT92E-phosphorylation, no significant difference could be detected. RME-6 is a relatively early acting endocytic component, aiding the un-coating of CCV (Semerdjieva et al., 2008). Since its knockdown does not seem to influence STAT92E phosphorylation, I suggest that a normal STAT92E phosphorylation occurs once the receptor enters in a Clathrin-dependent manner the cell. Consistently, the knockdown of the later components, HRS or Myopic also did not affect STAT92E phosphorylation.

I also analysed the influence of other potential regulators, the RacGAPs (Chapter 4.2.2.6 and Figure 4.22). Their knockdown had no apparent effect on phosphorylation, when compared to control treated cells (Figure 5.8 B). However, these results represent quite preliminary data and I more experimental repeats are needed before conclusions can be made.

To test whether the lack of effect on STAT92E phosphorylation was due to an ineffective depletion of the investigated protein, qPCR analysis was performed and the remaining mRNA levels were tested. This method did not allow me to be conclusive about the remaining protein levels, but would indicate that the dsRNA used did target their specific mRNAs.

Although, knockdown of all investigated genes was significant, the mRNA of *Rab5 GEFs*, including *RME-6* was only decreased down to approx. 50% (Figure 4.7). Together with potential redundancies between the Rab5 GEFs this high level of remaining mRNA could explain the lack of effect. However, the mRNA levels of *Clathrin* and other endocytic components were decreased to below 25%. This depletion was sufficient to have an effect of STAT92E phosphorylation, when *Clathrin* was targeted. Additionally, I was able to evaluate AP2 protein levels after its knockdown (Figure 4.8), which decreased down to 20%. This indicates that the residual AP2 proteins were not able to prevent the enhanced STAT92E phosphorylation or its failure to activate signalling.

The question remained open whether the after the levels of Myopic or HRS that remained following knockdown, were sufficient to prevent any effect of STAT92E phosphorylation or if these proteins did not influence the post-transcriptional modification. For an answer, further qPCR and western blot, if possible, analysis would

be needed. However, the knockdown of these endocytic components influence JAK/STAT signalling, suggesting their protein levels change after dsRNA treatment.

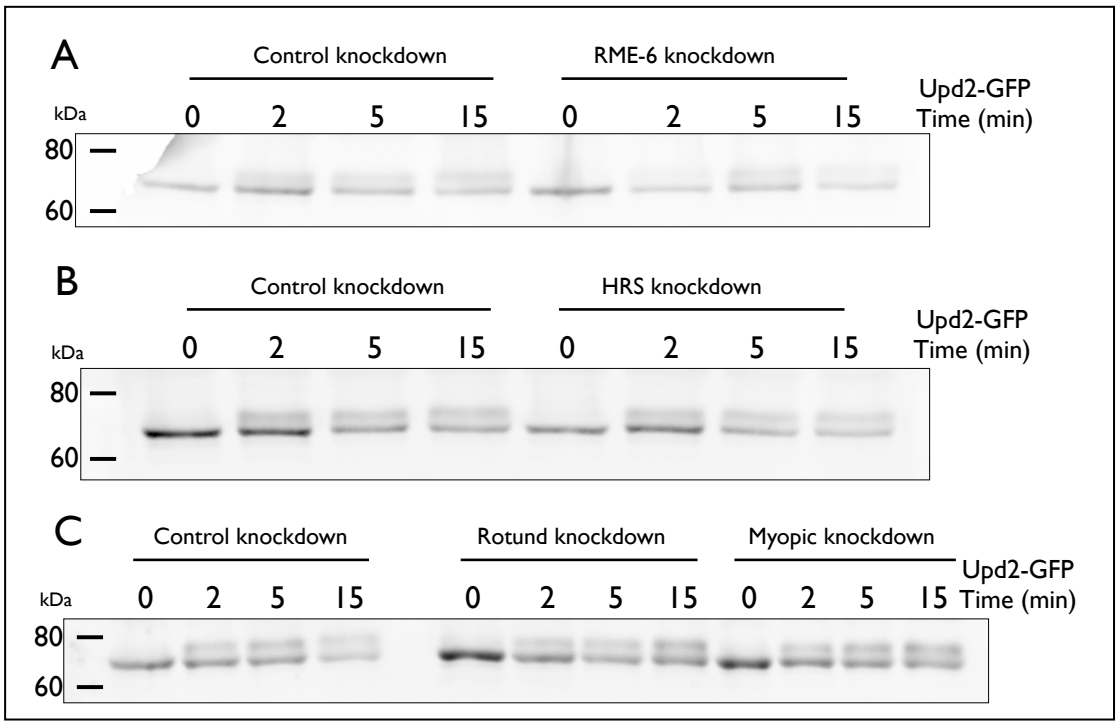

Figure 5.8: Examples of STAT92E phosphorylation in various knockdowns

S2R$^+$ cells were treated with dsRNA as indicated (A: RME-6; B:HRS; C: Myopic & Rotund) five days prior exposing them to 20nM Upd2-GFP for indicated times at 25ºC. Total protein extracts were analysed by SDS-PAGE and immunoblotted with anti-STAT92E antibodies. Blots are representative of at least 2 experiments

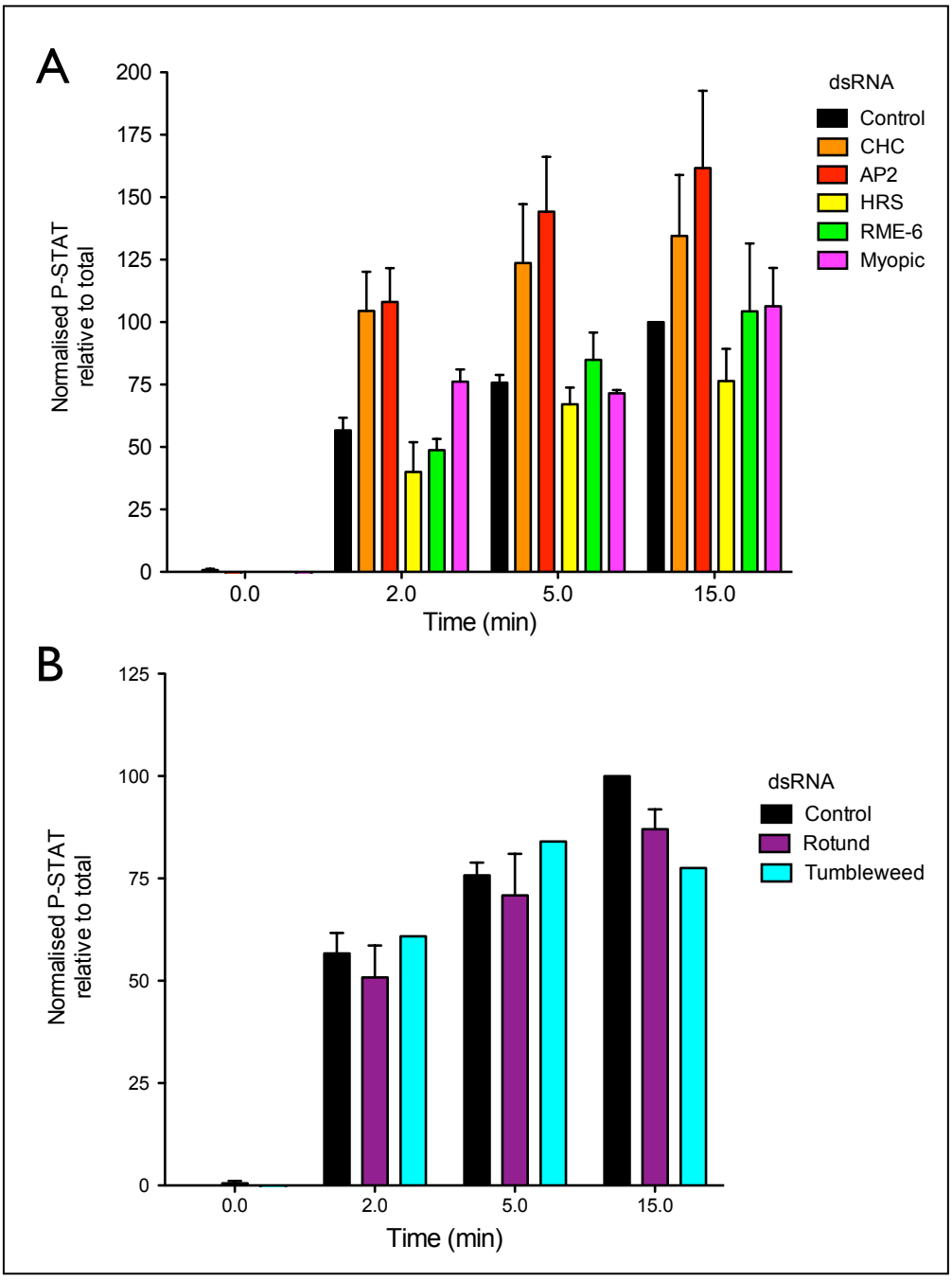

Figure 5.9: Effect of the endocytic pathway and RacGAPs on STAT92E phosphorylation

S2R^{+} cells were treated with dsRNA as indicated, five days prior exposing them to 20nM Upd2-GFP for indicated time points at 25ºC. Total protein extracts were analysed by SDS-PAGE and immunoblotted with anti-STAT92E. Quantification of time dependent phospho-STAT92E (P-STAT), whereby the ratio of P-STAT92E to total STAT92E, normalised to the latest time point of control samples, was plotted against time of activation with Upd2-GFP, error bars show standard error of the mean if applicable, A: Influence of endocytic components, representing at least 2 independent experiments, and B: Analysis of RacGAP effects, representing 2 independent for Rotund and 1 experiment for Tumbleweed.

5.2.3 Phos-tag™ reveals different phosphorylated forms of STAT92E

Next to the conserved and functionally crucial phosporylation of STAT92E on a tyrosine at position 711, numerous other STAT phosphorylation sites have been reported – especially in mammalian cancer cells (Olsen et al., 2010; Yan et al., 1996). There were also indications that STAT92E was phosphorylated on other sites in addition to tyrosine 711, since some phosphorylated STAT92E could be detected even in a Y-711 phospho-mutant (Ekas et al., 2010).

I next investigated whether the enhanced phosphorylation of STAT92E in cells depleted of Clathrin and AP2 resulted from the modification of the same or different sites on the transcription factor. I decided to use a system named Phos-tag™. This was an indirect way of revealing differentially phosphoryated proteins. The Phos-tag™ compound binds strongly to anionic substituents, and will thus bind with a high affinity to phosphates on proteins in SDS-PAGE gels. The tag causes a mobility shift of the bound protein, making it easier to visualise phosphorylated species.

I added Phos-tag™ to SDS-PAGE gels and probed immunoblots with anti-STAT92E. Analysing lysates of cells stimulated with Upd2-GFP, two distinct forms of phospho-STAT92E could be detected (Figure 5.10). I referred to these forms as P-STAT92E (a band occurring above un-phosphorylated STAT92E) and PP-STAT92E (a band of even lower mobility). P-STAT92E appeared clearly after 2 minutes ligand treatment and PP-STAT92E was most pronounced after 15 minutes Upd2-GFP exposure.

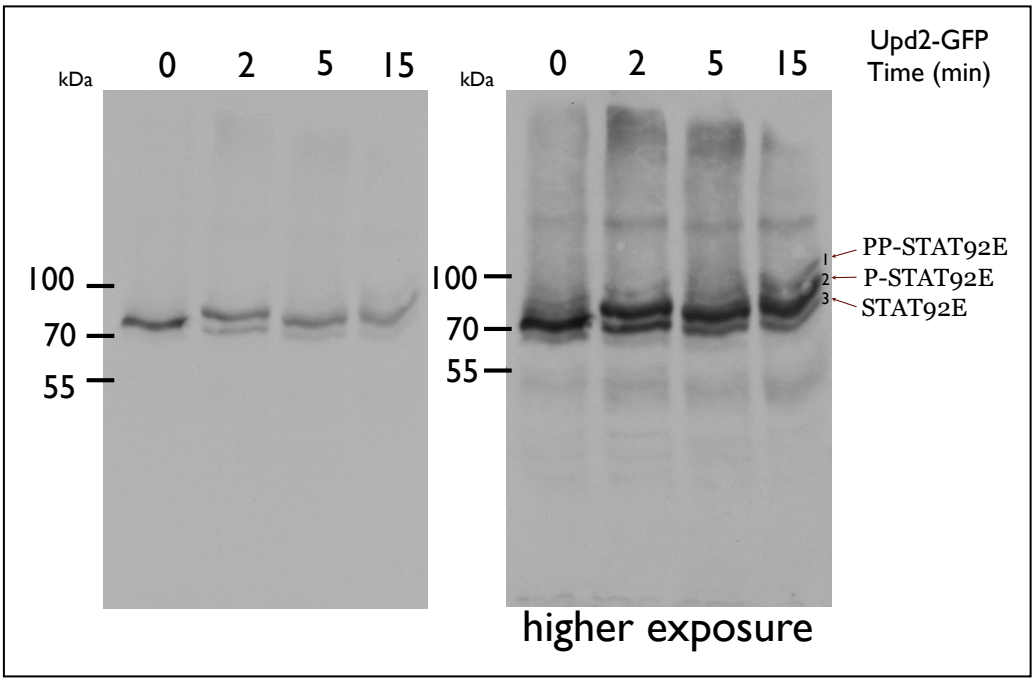

Figure 5.10: Phos-tag SDS-PAGE reveals two species of phosphorylated STAT92E

S2R$^+$ cells were treated with 20nM Upd2-GFP for the indicated time points at 25ºC. Total protein extracts were analysed by SDS-PAGE with the addition of Phos-tag^{TM} reagent and immunoblotted with anti-STAT92E. A: usual exposure of western blot, and B: higher exposure of the same blot to better demonstrate the appearance of now three bands for STAT92E. 1=PP-STAT92E, 2=P-STAT92E and 3=STAT92E

Next, I wanted to confirm that both mobility-shifted bands of STAT92E were due to phosphorylation. Therefore, I pulled down STAT92E from S2R$^+$ cells incubated for various times with ligand and treated the IPs with CIP, as described in section 5.1.1. The enzyme treatment reduced the occurrence of those top bands (band 1 & 2 in Figure 5.11) and slightly increased the strength of the lower band, which represented un-phosphorylated STAT92E. Hence, I can conclude that P-STAT92E and PP-STAT92E are due to phosphorylation.

The detection of two distinct phosphorylated forms of STAT92E was promising, indicating that STAT92E was differentially phosphorylated. However, it still remains to be determined whether P-STAT92E and PP-STAT92E reflect different forms of phosphorylated STAT92E. There is a possibility that the two species could also be an artefact of the system: it might be that both bands corresponded to STAT92E phosphorylated on the same residue and the two distinct forms occurred due to differential binding to the Phos-tag^{TM} add-on, or that the P-STAT92E band was due to

the bandshift also seen on standard gels and the PP-STAT92E related to phosphorylated STAT92E bound to Phos-tag™.

One possibility to show there was phosphorylation additional to the Y-711 of STAT92E, would be to transfect the cells with a tagged STAT92E Y-711-phospho-mutant and analyse the phosphorylated forms. This methodology would also allow for structure-function analysis of STAT92E modifications. The transfected STAT92E would have to be tagged, since I would have to distinguish the artificial expressed protein from the endogenous form. This is crucial to determine a.) the transfection efficiency and b.) the knockdown efficiency of the endogenous STAT92E to evaluate the effect of expression mutant forms of the protein. Unfortunately, transfected wt STAT92E (Myc or GFP tagged) did not bandshift upon ligand stimulation, thus preventing this experiment from being feasible. A more direct way of investigating novel and known phosphorylation sites was the use of mass spectrometry, as discussed in section 5.3.

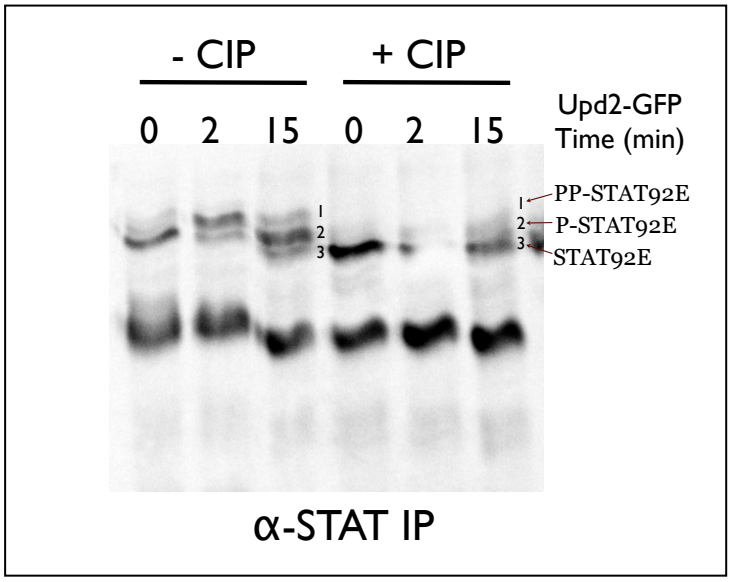

Figure 5.11: The slower migrating forms of STAT92E are due to phosphorylation

$SR2^+$ cells were incubated with 20nM Upd2-GFP for indicated time points at 25ºC. After immunoprecipitating STAT92E with anti-STAT92E antibodies, IPs were treated either with control or phosphatase (CIP). IPs protein extracts were analysed by Phos-tag™-SDS-PAGE and immuno-blotted with anti-STAT92E. Both STAT92E modifications (band 1=PP-STAT92E and 2=P-STAT92E) are decreased in the CIP treated samples

5.2.4 The effect of AP2 and Clathrin depletion on differentially phosphorylated STAT92E forms

The increase of STAT92E phosphorylation by depleting cells of Clathrin or AP2 was a novel and yet unexplained phenomenon. In this section, I asked whether the knockdown of AP2/Clathrin has an effect on P-STAT92E or PP-STAT92E or both by using Phos-tag™ gels analysing STA92E phosphorylation. The method is an indirect way of showing differential phosphorylation. However, if the block of early Clathrin-mediated endocytosis were to influence one phospho-form over the other, it would further strengthen the suggestion that STAT92E is phosphorylated on distinct sites.

Cells were depleted of early endocytic components before inducing STAT92E phosphorylation with Upd2-GFP. Analysis of lysates from control cells with Phos-tag™ gels revealed an increase in both P-STAT92E and PP-STAT92E (Figure 5.12). A similar increase of both STAT92E phosphorylated species was observed in the knockdown samples (Figure 5.12 B). However, PP-STAT92E increased to a slightly higher extent than P-STAT92E, when AP2 or Clathrin was knocked down (Figure 5.12 C), indicating that the effect of enhanced phosphorylation in Clathrin/AP2 depleted cells might be due to PP-STAT92E. Additional experiments are, nevertheless, essential to dissect these differences and to allow their statistical significance.

Interestingly, the knockdown of AP2 resulted in a slight higher extent of STAT92E phosphorylation (Figure 5.7) than the effect of Clathrin on standard SDS-PAGE gels. This could be due to a more effective knockdown of AP2 or to a differential regulation of STAT92E phosphorylation by AP2 and Clathrin. Interstingly, the analysis of the Phostag gels shows that the knockdown of AP2 enhanced P-STAT92E more than the Clathrin knockdown (Figure 5.12 B), whereas the PP-STAT92E form did nt differ between the Clathrin and AP2 knockdown (Figure 5.12 C). This suggests a differential phosphorylation. Again, more data is needed to confirm these preliminary suggestions.

In general the enhanced phosphorylation did not appear to be as pronounced when visualised on Phos-tag™ gels as when using standard SDS-PAGE gels (compare with Figure 5.7). This could be due to the poorer quality of the Phos-tag™ gels and hence increased variability of the quantification. The Phos-tag™ system is, nevertheless, an excellent method to gain first insights into differential phosphorylation of proteins.

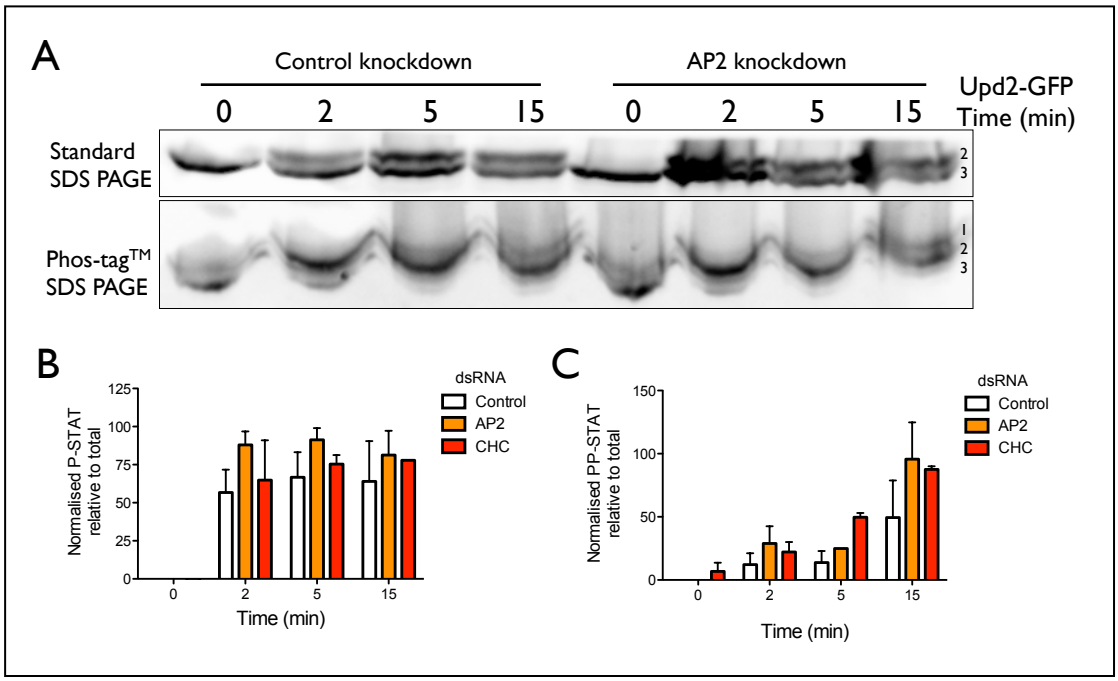

Figure 5.12: Clathrin-mediated endocytosis influences both species of STAT92E phosphorylation

S2R^{+} cells were treated with dsRNA as indicated, five days prior exposing them to 20nM Upd2-GFP for indicated time points at 25ºC. Total protein extracts were analysed by Phos-tag™ SDS-PAGE and immunoblotted with anti-STAT92E. A: Example of Standard SDS-PAGE blot (top) and Phos-tag™ SDS-PAGE blot (bottom) for an AP2 knockdown, 1=PP-STAT92E, 2=P-STAT92E, 3=STAT92E. B and C: Quantification of time dependent phosphorylated forms of STAT92E as shown/analysed with the Phos-tag™ SDS-PAGE, whereby the ratio of P-STAT92E or PP-STAT92E to total STAT92E, normalised to the latest time point of control samples, was plotted against time of activation with Upd2-GFP, error bars show standard error of the mean, representing at least 2 independent experiments. B: normalised P-STAT92E (band 2) C: Normalised PP-STAT92E (band1)

5.3 Identifying STAT92E modifications

An excellent way to analyse protein modifications, especially novel modifications is the use of mass spectrometry (MS). Proteins are identified by the flight behaviour of their peptides, due to ionisation and trapping the ionised peptides on an ion?? trap. With this method I could directly detect STAT92E modifications, since they would alter the flight behaviour of their peptides. Additionally I could examine whether STAT92E was phosphorylated on additional sites, other that the Y-711, as suggested by the use of Phos-tag™ SDS-PAGE gels. Most importantly, I could study the role of Clathrin-mediated endocytosis on the modulation of STAT92E.

5.3.1 STAT92E putative modification sites

STAT92E consisted of various domains (Figure 1.9), which are responsible for canonical functions including, protein dimerisation and DNA binding. The transactivation domain is located at the C-terminus and contains a highly conserved tyrosine (at position 711 for STAT92E), whose phosphorylation enables STAT92E function as a transcription factor (Ekas et al., 2010; Karsten et al., 2006; Yan et al., 1996).

In order to fully exploit MS analysis of novel STAT92E modifications, I wanted to know, which potential modifications of STAT92E might be expected. Therefore, I looked at the mammalian STAT literature and gathered information about all reported STAT modifications. Next, I examined in detail if the region, where the modification was described, is conserved in *Drosophila* STAT92E. Numerous modifications occurred on conserved amino acids.

Table 5.1 lists reported mammalian STAT phosphorylation and methylation sites with their *Drosophila* counterparts. In addition to listing all potential modifications, I marked them on the amino acid sequence of STAT92E (Figure 5.13). I could match nine phosphorylation sites, including Y-711. Other conserved phosphorylation sites that have been described are serine or tyrosine phosphorylation, but also one threonine and one histidine was reported to be phosphorylated (Dephoure et al., 2008; Imami et al., 2008; Mayya et al., 2009; Okutani et al., 2001; Olsen et al., 2010).

In addition to STAT phosphorylation, methylation, acetylation and sumoylation sites have also been reported (Gronholm et al., 2010; Komyod et al., 2005; Kramer and Moriggl, 2012; Mowen et al., 2001; Shankaranarayanan et al., 2001; Wieczorek et al., 2012).

Figure 5.13 and Table 5.1 highlight an arginine at the very N-terminus of STAT92E. It was discussed to be methylated in STAT1 and STAT3 (Komyod et al., 2005; Meissner et al., 2004; Mowen et al., 2001), this site is conserved and point mutation of arginine 31 of STAT1 destabilised its structure and impaired STAT function (Meissner et al., 2004).

Table 5.1: Putative and known STAT modifications

The table demonstrates how STAT92E could be modified; by comparing mammalian STAT modifications (left column) to STAT92E (middle column). The references on the right acknowledge the publication, where the mammalian STAT modification was described in. Cell Signaling Technology (CST) curation use PhosphoSitePlus®, which is an open, dynamic, continuously curated, and highly interactive systems biology resource for studying experimentally observed posttranslational modifications. mam.: mammalian

Mammalian STAT with modification	*Drosophila* homologue	Reference
STAT1-Met-R31 (all mam STAT)	STAT92E-R30	(Komyod et al., 2005; Meissner et al., 2004; Mowen et al., 2001)
STAT1-Y701 (all mam .STAT)	STAT92E-Y-711	(Lim and Cao, 2006; Yan et al., 1996)
STAT1-S727 (also in STAT4,5)	STAT92E-S728	(Kloth et al., 2002; Weaver et al.,2006)
STAT3-Y539	STAT92E-Y557	(CST curation 2012)
STAT3-S727	not conserved	(Hazan-Halevy et al., 2010)
STAT5-K71	STAT92E-K68	(CST Curation, 2008)
STAT5-S193	STAT92E-S200	(Dephoure et al., 2008) (Mitra et al., 2012; Olsen et al., 2010)
STAT5b-S128	STAT92E-S118	(Daub et al., 2008; Mayya et al., 2009; Weber et al., 2011)
STAT5-S372	STAT92E-S385	(CST Curation, 2010)
STAT5-T647	STAT92E-T652	(CST Curation, 2010)
STAT5 Y683 or Y682	STAT92E-Y694	(CST Curations from 2005 to 2011)

5.3.2 Detection of STAT92E by Mass Spectrometry

To facilitate the detection of STAT92E by MS, I decided to enrich samples by immunoprecipitating STAT92E from cell lysates. In addition I cross-linked the anti-STAT92E antibody to agarose beads prior to the IP. This resulted in a cleaner IP with negligible antibody contamination (data not shown). Unfortunately, following this approach STAT92E could not detected by MS. Antigen release from the cross-linked antibodies was achieved by a harsh acid incubation (~pH 1), which could have precipitated STAT92E. Since precipitated proteins were difficult to separate from the

beads used in the IP and STAT92E might not have been in the soluble solution analysed by MS. Hence this method, of cross-linking the antibodies was not suitable for the detailed study of STAT92E.

Consequently, I decided to separate STAT92E from other proteins (for instance the antibodies used) after a standard IP using SDS-PAGE before the MS analysis. Therefore, I ran IP samples on SDS-PAGE gels and cut out gel-slices corresponding to the molecular weight of STAT92E.

To be able to identify and visualise STAT92E without an immunoblot, I separated anti-STAT92E- and control IgG IPs on an SDS-PAGE gel and stained it with SYPRO® Ruby Protein Gel Stain. This staining method is as sensitive as silver-staining and, more importantly, it is compatible with MS analysis. The fluorescent stain was detected with a standard blue-light transilluminator. Unfortunately, I could not detect any additional band that could be attributed to STAT92E in the anti-STAT IP, when I compared it with an IgG control IP (data not shown).

The detection of STAT92E via any stain would be an advantage because I would be able to cut out this specific band from a SDS-PAGE gel. Fortunately, this is not a necessity. Consequently, I cut out 5 slices between approximately 65 and 85kDa of a 4 to 12% SDS-PAGE gel separating an anti-STAT92E IP, in order to analyse STAT92E by MS. Those gel pieces should contain STAT92E protein and they were further processed for an in-gel digest with protein degradation enzymes, for instance trypsin. (see 2.3.5 for details). After enzyme digestion I extracted the peptides and samples were further separated by high pressure liquid chromatography (HPLC). The ionised peptides were collected by the Orbitrap system and data analysed using the Mascot search algorithm.

STAT92E could usually be detected in two or three of the five analysed gel slices with a certainty of over 99%, while it was absent in IgG control IPs.

5.3.3 Peptide coverage of STAT92E

After I established that I was able to detect STAT92E, I tried different digestion enzymes to maximise peptide coverage. In addition to the standard tryptic digest I used chemotrypsin and GluC. Trypsin cleaves amino acids on the carboxyl side of arginine and lysine residues while GluC cuts on the carboxyl side of glutamate and chemotrypsin cuts on the carboxyl side of tyrosine, phenylalanine, tryptophan and leucine residues. These different cleavage sites result in distinct peptides after protein digest. Using the

ExPASy PetideMass calculator as published by (Gasteiger et al., 2003; Wilkins et al., 1997) I ran theoretical digests evaluating the coverage possibilities. The theoretical peptides covered about 66.9% for trypsin, 50.7% for GluC and 50.2% for chemotrypsin of STAT92E sequence, while allowing peptides from 650 to 4000 Dalton to be detected. I highlighted all theoretical peptides in Figure 5.14.

Even though the overall coverage of the additional enzymes were lower than the coverage of the trypsin digest, many additional peptides could theoretically be detected when using chemotrypsin and GluC, so that a theoretical coverage of 92.5% could be achieved. Importantly, I covered most putative phosphorylation sites (as illustrated in Figure 5.14)

Next, I analysed the anti-STAT92E IP several times with MS and could identify 431 amino acids using either trypsin, chemotrypsin or GluC to digest the protein. Identified peptides are listed in Table 5.2 and illustrated in Figure 5.15. Over 50% of STAT92E sequence was detected by peptides, which were typically around 15 amino acids long. Figure 5.15 highlights the identified regions, which on some cases were composed of several overlapping peptides. Therefore the figure demonstrates the range of coverage of STAT92E by MS.

Importantly, several putative phosphorylation sites were covered by the MS analysis, including the crucial Y-711 as well as the methylation site, R30. Overall since the use of chemotrypsin and GluC did not add significantly to the peptide coverage, I decided to use the standard trypsin digest for subsequent experiments, especially since it covered reproducibly the crucial Y-711.

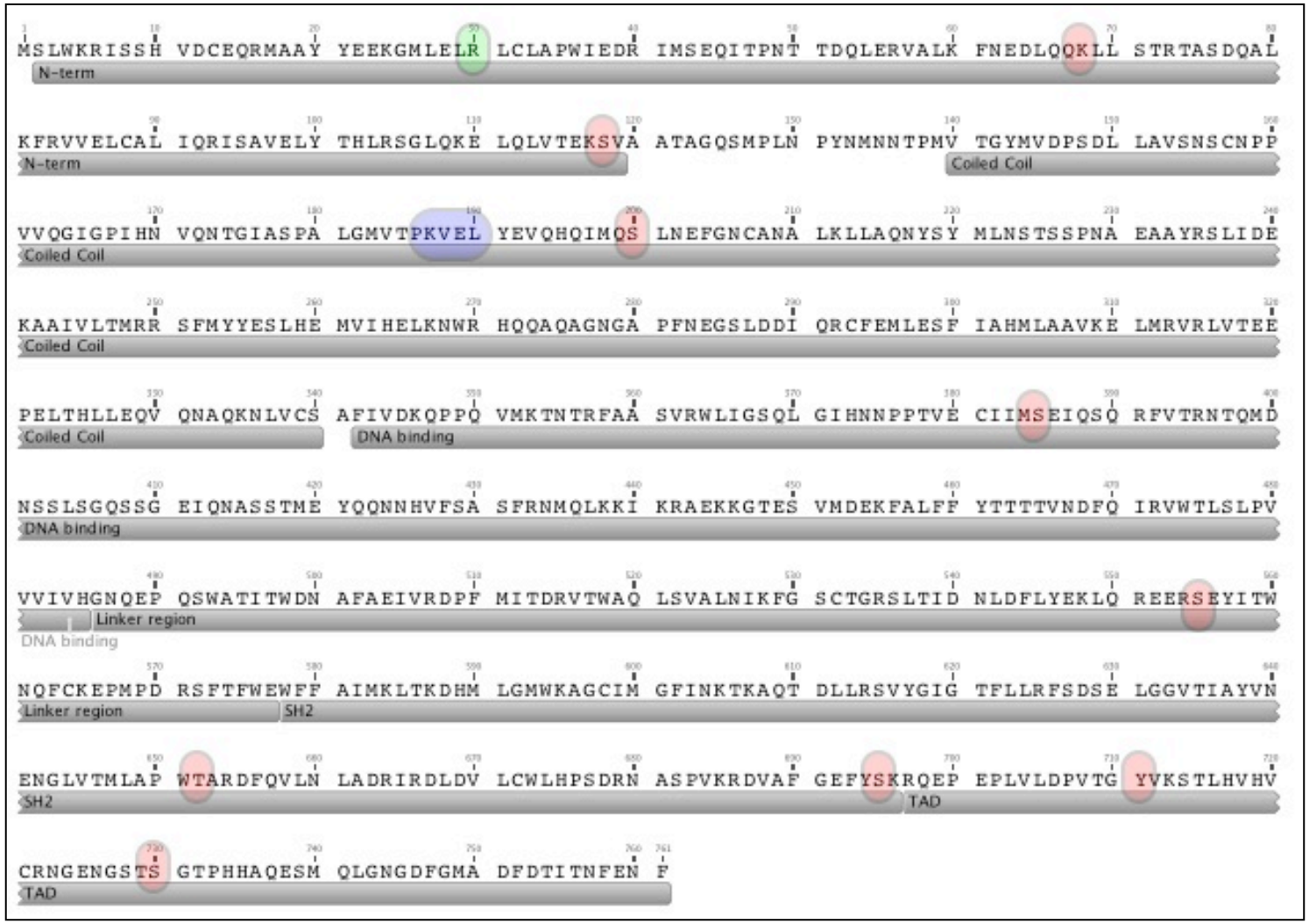

Figure 5.13: Sequence of STAT92E with its putative modifications and known domains

Amino acids of STAT92E with indicated known domains. Circled are amino-acids which could be potentially modified (see text and Table 5.1 for details) with following colour-coding: green: Acetylation, blue: sumoylation, red: phosphorylation. Regions, either from the FASTA file of STAT92E or Linker region predicted by InterPro. TAD: transactivation domain

and can be composed of several overlapping peptides.

Figure 5.14: Theoretical peptide coverage of STAT92E with trypsin, chemotrypsin or GluC digestion

Amino acids of STAT92E demonstrated putative modifications sites and theoretical peptide coverage. Circled are amino-acids which could be potentially modified with following colour-coding: green: acetylation, blue: sumoylation, red: phosphorylation. For theoretical digest ExPASy PetideMass calculator was used and petides between 750 and 4000 Dalton were illustrated by underling the sequence: in green for the trypsin digest; red when used GluC and blue for chemotrypsin. Regions corresponding to peptides did not necessary correspond to one peptide

Figure 5.15: Sequence of STAT92E with its putative modifications and identified peptides via MS

Amino acids of STAT92E with indicated known domains. Circled are amino acids which could be potentially modified with following colour-coding: green: acetylation, blue: sumoylation, red: phosphorylation, Underlined are all identified peptides found by MS, which can be in detailed found in Table 5.2 were illustrated by underling the sequence: in green for the trypsin digest; red when used GluC and blue for chemotrypsin.

5.3.4 Identification of STAT92E phosphorylation sites

MS experiments provided coverage of over 55% of the STAT92E sequence, including approximately half of its putative modification sites. In order to identify STAT92E phosphorylation sites, I analysed STAT92E IPs by MS after inducing signalling with Upd2. Hence, I incubated cells with mock CM, or Upd2-GFP CM and performed an anti-STAT92E IP. Proteins were then separated by SDS-PAGE and gel slices at around 70 kDa were cut out and trypsin digested. I extracted the resulting peptides and submitted them for MS analysis.

Satisfyingly, the MS detected phosphorylation of Y-711 in Upd2-GFP stimulated samples, whereas control treated samples did not induce a mass change due to phosphorylation of the peptide covering to Y-711. This showed that endogenous STAT92E was phosphorylated at its conserved Y-711. This result was not surprising, but it was to my knowledge the first data, which directly showed STAT92E phosphorylation upon Upd2 stimulation in an endogenous system.

Other novel modification could not be detected, but the successful identification of Y-711 as phosphorylation proved the principle of using MS. At least this phosphorylation was stable to withstand all executed manipulations and the MS was sufficiently sensitive to identify possible phosphorylation sites.

Time restrictions meant that it was not feasible to improve the protocol further for the detection of novel modifications, but these first positive experiments paved the way for further experiments, in which phospho-peptides could be enriched and/or the use of Phostag^{TM} could be implemented to be able to confirm putative modifications and / or find novel phosphorylation sites.

Table 5.2: STAT92E peptide coverage

To define confidences false discovery rates were set at 1% and 5% by Peptide Validator. If a match passed the strict filter they were assigned a high confidence, a medium confidence if they passed the 5% filter and a low confidence if they fail to pass either filter.

Enzyme	Confi-dence	Sequence	Modi-fication	Trypsin-overlap
Trypsin	High	AAIVLTMR		
Trypsin	High	AEIVRDPF		
Trypsin	High	AGCIMGFINK		
Trypsin	Medium	AQTDLLR		
Trypsin	High	DFQVLNLADR		
Trypsin	Medium	DHMLGMWK		
Trypsin	High	DLDVLCWLHPSDR		
Trypsin	Medium	DPFMITDR		
Trypsin	High	DVAFGEFYSK		
Trypsin	Low	ELQLVTEK		
Trypsin	High	FALFFYTTTTVNDFQIR		
Trypsin	High	FNEDLQQK		
Trypsin	Medium	GMLELR		
Trypsin	High	HQQAQAGNGAPFNEGSLDDIQR		
Trypsin	High	IMSEQITPNTTDQLER		
Trypsin	High	INKTKAQTDLL		
Trypsin	Medium	IRDLDVLCWLHPSDR		
Trypsin	High	ISAVELYTHLR		
Trypsin	High	LCALIQRISAVE		
Trypsin	Medium	LCLAPWIEDR		
Trypsin	High	LLAQNYSYMLNSTSSPNAEAAYR		
Trypsin	High	LRLCLAPWIE		
Trypsin	High	LTHLLE		
Trypsin	High	NLVCSAFIVDK		
Trypsin	High	NSTSSPNAEAAY		
Trypsin	High	RFSDSELGGVTIAY		
Trypsin	High	RQEPEPLVLDPVTGYVK	Y15 (Phospho)	
Trypsin	High	RSLIDEKAAIVL		
Trypsin	High	RVALKFNE		
Trypsin	High	SEYITWNQFCK		
Trypsin	High	SFIAHMLAAVKE		
Trypsin	High	SFTFWEWFFAIMKL		
Trypsin	High	SLPVVVIVHGNQEPQSW		
Trypsin	High	SLTIDNLDFLYEK		
Trypsin	High	STLHVHVCR		
Trypsin	High	SVYGIGTFLLR		
Trypsin	High	VELYEVQHQIMQSLNEFGNCANALK		
Trypsin	High	VQHQIMQSLNE		
Trypsin	High	VTEEPELTHL		
Trypsin	High	VTRNTQMDNSSL		
Trypsin	High	VTWAQLSVALNIK		
Trypsin	High	VVELCALIQR		
Trypsin	High	YEEKGMLEL		

Chemotrypsin	Medium	AEIVRDPF		partly
Chemotrypsin	High	INKTKAQTDLL		fully
Chemotrypsin	High	MITDRVTW		fully
Chemotrypsin	High	MLNSTSSPNAEAAY		fully
Chemotrypsin	High	NEGSLDDIQRCF		partly
Chemotrypsin	High	NLADRIRDL		fully
Chemotrypsin	High	NSTSSPNAEAAY		fully
Chemotrypsin	High	RFSDSELGGVTIAY		
Chemotrypsin	High	RSLIDEKAAIVL		partly
Chemotrypsin	High	SLPVVVIVHGNQEPQSW		
Chemotrypsin	High	VTEEPELTHLL		partly
Chemotrypsin	High	VTRNTQMDNSSL		
Chemotrypsin	High	YEEKGMLEL		fully
Chemotrypsin	High	YEEKGMLEL		fully
GluC	High	LCALIQRISAVE		fully
GluC	High	LRLCLAPWIE		fully
GluC	High	LTHLLE		
GluC	High	RVALKFNE		partly
GluC	High	SFIAHMLAAVKE		
GluC	High	VQHQIMQSLNE		

5.3.5 Phosphorylation of STAT92E in AP2 knockdown

My earlier results had demonstrated that the block of early endocytosis by AP2 and Clathrin knockdown resulted in the failure to induce Upd2 dependent JAK/STAT signalling while enhancing STAT92E phosphorylation. This suggested that this form of STAT92E was not able to activate signalling. The question remained open whether STAT92E was phosphorylated on a different amino acid, when AP2 was knocked down or the enhanced phosphorylation occurred on the same site as within control treated cells. To address this I performed MS analysis of STAT92E immuno-precipitated from Upd2-GFP induced cells and analysed both control and AP2 depleted cells.

Interestingly, STAT92E was phosphorylated on Y-711, when AP2 was depleted and cells stimulated with Upd2-GFP. This tyrosine was also phosphorylated in control cells as expected and highlighted above. The fact that AP2 knockdown inhibited pathway activation and STAT92E was still phosphorylated on the Y-711, suggest that there is an additional modification of STAT92E. This novel level of modification could be due to phosphorylation, since I observed enhanced phosphorylated STAT92E, when AP2 was knocked down. Importantly, this shows that the phosphorylation on Y-711 is necessary, but not sufficient for JAK/STAT regulation.

5.3.6 Analysis of other STAT92E modifications

Having established that the knockdown of Clathrin and AP2 led to an increased phosphorylation of the transcription factor, I wanted to investigate whether this phosphorylation is the only modification of STAT92E and ultimately I wanted to address whether the endocytic pathway could influence other post-translational modifications as well as phosphorylation, and how these then correlate to the ability to activate signalling.

Apart from phosphorylation there are several additional ways of protein modification. A second major post-translational modification is ubiquitination, one function of which is to prepare proteins for their degradation. Ubiquitination of proteins can induce them to migrate more slowly, due to their change in molecular mass and thus induce a bandshift on SDS-PAGE gels. For STAT92E I could not detect any other bands other that those caused by phosphorylation. In addition, I did not have any evidence that STAT92E was regulated by degradation. Hence, I did not investigate ubiquitination further. However, other modifications can post-translationally alter STAT92E without changing its mobility on SDS-PAGE gels.

One of these modification is the attachment of a Small Ubiquitin-like Modifier (SUMO) protein, which is involved in various cellular processes, such as nuclear-cytosolic transport, transcriptional regulation, apoptosis, protein stability, response to stress, and progression through the cell cycle (Yang and Chiang, 2013). Indeed nuclear import of STAT has been reported to be regulated by sumoylation and STAT92E has been shown to be sumoylated (Gronholm et al., 2010; Van Nguyen et al., 2011).

Additionally, acetylation is another protein modification, controlled by acetylases and de-acetylases and its cycles of acetylation and de-acetylation could be fairly well compared to the phosphorylation-cycles of proteins. The best characterised examples of regulation by acetylation are histone and tubulin regulation. However, STAT proteins have also been shown to be regulated by acetylation (Wieczorek et al., 2012) for review. However the sites are largely not conserved and there has been to my knowledge no report of acetylation of the *Drosophila* STAT92E.

In addition to MS analysis of STAT92E I could resort to modification specific antibodies. A generic anti-SUMO2/3 and an anti-acetylation antibody promised the detection of these post-translational modifications by western blot.

Table 5.3: Acetylation of STAT proteins

Protein	Function	Residues	Domain	Reference
STAT1	Interaction with NF-κB	K410, K413	DBD	(Kramer et al., 2006)
STAT2	Regulates interaction with STAT1	K390	DBD	(Tang et al., 2007)
STAT3	Increases DNA binding affinity Promotes protein-protein interaction Increases transcriptional activation Modulates dimerisation	K685	SH2	(Wang et al., 2005b; Yuan et al., 2005)
	Unknown	K49, K87	NH2-terminus	(Ray et al., 2005)
STAT5b	Modulates dimerisation	K694, K701	SH2	(Ma et al., 2010)
STAT6	Increases transcriptional activation		750–788 in the carboxyl terminus	(McDonald and Reich, 1999)

5.3.6.1 Sumoylation of STAT92E

SUMO protein-tags are similar to ubiquitin, but in contrast to ubiquitinylation, sumoylation is not used to mark proteins for degradation (Yang and Chiang, 2013). The SUMO-tag is a negative regulator of STAT. It inhibited STAT's transcriptional activation, by acting upon nuclear import (Lim and Cao, 2006). Gronholm et al 2010 showed that STAT92E could be sumoylated by the human enzymes (Gronholm et al., 2010). In that report a mammalian culture-system was used to show sumoylation while over-expressing *Drosophila* proteins. Furthermore, an interaction of STAT92E with Smt3 (the *Drosophila* sumoylase) was shown. The knockdown of Smt3 in the two major JAK/STAT signalling dsRNA screens did not alter the signal activation (Baeg et al., 2005; Muller et al., 2005). However, they (Gronholm et al., 2010) showed that a mutation of the suggested sumoylation-site increased JAK/STAT signalling.

To detect sumoylation a SUMO-specific antibody I used to blot IPs from $S2R^+$ cells stimulated with Upd2-GFP. The generic anti-SUMO antibody could not detect an additional protein in the anti-STAT92E IP in the presence or absence of ligand

stimulation (Figure 5.16 A). Unfortunately, I could not confirm the specificity of the used anti-SUMO antibody, since I did not use a positive control, containing known sumoylated proteins. However, in the literature STAT92E sumoylation was only shown to occur when transfecting STAT92E into a mammalian cell line while simultaneously overexpressing sumoylases (Gronholm et al., 2010).

5.3.6.2 Acetylation of STAT92E

To test whether endogenous STAT92E was acetylated, I induced JAK/STAT signalling with Upd2-GFP and immunoprecipitated STAT92E from cell lysates. Following a method suggested by Kramer 2013 I used a special acetyl group- conserving lysis buffer as described in 2.3.8.2 (Kramer, 2013). Unfortunately, an anti-acetyl antibody could not detect any specific band for STAT92E, even not after pathway stimulation (Figure 5.16 B). This does not imply that STAT92E is not acetylated, it merely suggested that if an acetylation exists, if might be relatively weak. Similar to the detection of sumoylation, I did not have a positive control, which contained known acetylated proteins. Therefore, I cannot exclude that the antibody (or immunoblot procedure) was unable to detect acetylation.

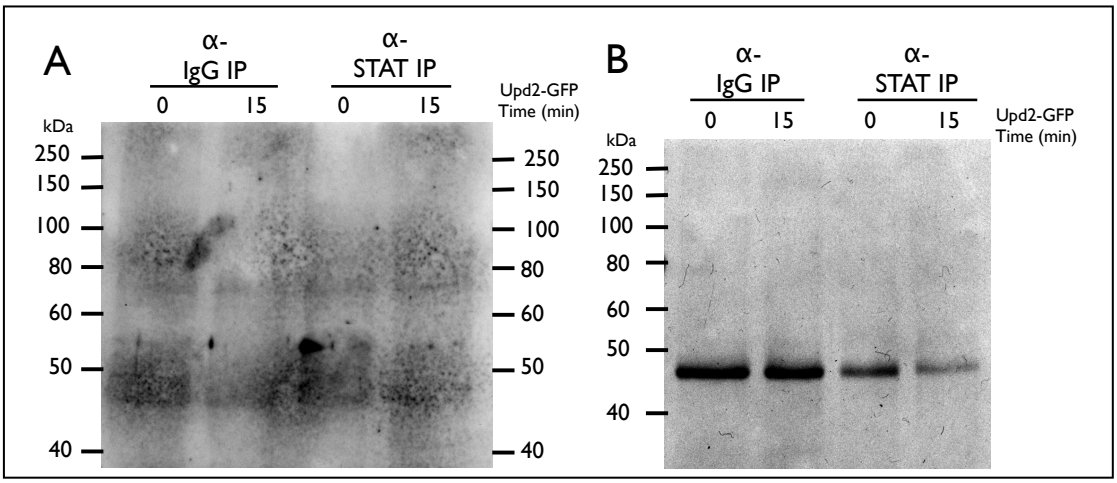

Figure 5.16: Sumoylation or acetylation of STAT92E cannot be detected

S2R$^+$ cells were treated with 20nM Upd2-GFP for indicated time points at 25ºC. After immunoprecipitating STAT92E with anti-STAT92E antibodies, IPs were analysed by SDS-PAGE and immunoblotted with A: anti-SUMO antibody and B: anti-acetylation antibody

To investigate if the STAT92E phosphorylation resulted in an aberrant nuclear import of the transcription factor, I analysed the distribution of STAT92E within the cell.

5.4 Nuclear import of STAT92E

As the transcription factor for the JAK/STAT pathway, STAT has to travel into the nucleus to be able to activate its signalling. This import is dependent on Importins, which are specific to the nuclear import sequence of the different STATs. I wanted to investigate whether this import is altered in cells depleted from AP2. I chose an assay, where I also could address whether the phosphorylated forms of STAT92E translocated as usual into the nucleus, when I inhibited Clathrin-mediated endocytosis.

5.4.1 Fractionation assays reveal role of nuclear import

To study the nuclear import of STAT92E I decided to use a biochemical fractionation approach. I isolated the cell components, by gently lysing the cells and separating them into their cytosolic and nuclear components by various centrifugation steps. This enabled me to analyse STAT92E by western blotting. Importantly, I could not only follow the translocation of STAT92E into the nucleus, but also specifically investigate how phosphorylated STAT92E is imported into the nucleus.

First, I fractionated cells using a detergent- and sucrose-containing buffer. This buffer was shown to open cells gently without disturbing the nucleus (Mendez and Stillman, 2000). Subsequent slow centrifugation steps ensured the separation of nucleus and cytoplasm (for full protocol see 2.4.7). Nuclear and cytosolic fractions were then analysed by western blot. To control the purity of the fractionation I probed the membranes for α-tubulin, as a cytosolic marker and Lamin, which is only found in the nucleus. Unfortunately, the nuclear fraction showed a signal for α-tubulin almost as strong as in the cytosolic fraction (data not shown). Consequently, I could not ensure a suitable pure fractionation with this method.

In order to improve cell lysis, without disrupting the nuclei, I used a Dounce pestle. Following this physical cell-disruption I performed, gentle separation steps over a sucrose gradient, which could enable a more stringent fractionation. Again, I analysed the total cell lysates, nuclear and cytosolic fraction.

Figure 5.17 A shows one example of the distribution of α-tubulin, Lamin and STAT92E using this fractionation protocol. Even though I detected some α-tubulin in the nuclear fraction, this trace of contamination of cytosolic protein was acceptable. More importantly, the fraction of the cytosol was not contaminated with nuclear protein, since the anti-Lamin immunoblot did not show any band in the cytosolic fraction, but I could detect a strong signal for Lamin in the nuclear fraction (Figure 5.17).

This separation of cytosolic fractions and enrichment of nuclear proteins was appropriate to analyse the import of STAT92E into the nucleus. Hence, I quantified phosphorylated STAT92E in total lysates and the cellular fractions (Figure 5.17 B&C). Both graphs illustrate that ligand exposure up to 45 minutes did not influence nuclear import of phosphorylated STAT92E. Only after 60 constant ligand treatment phospho-STAT92E accumulated in the nucleus.

This suggests that a continuous ligand stimulation of the JAK/STAT pathway is necessary to enrich phospho-STAT92E in the nucleus. Additionally it could reveal a more efficient nuclear import after 30 minutes of ligand stimulation. These preliminary data sets, however, need further repeats to allow to drawing concrete conclusions. Further analysis and even further extended time courses would be necessary to confirm this late accumulation of phospho-STAT92E in the nucleus.

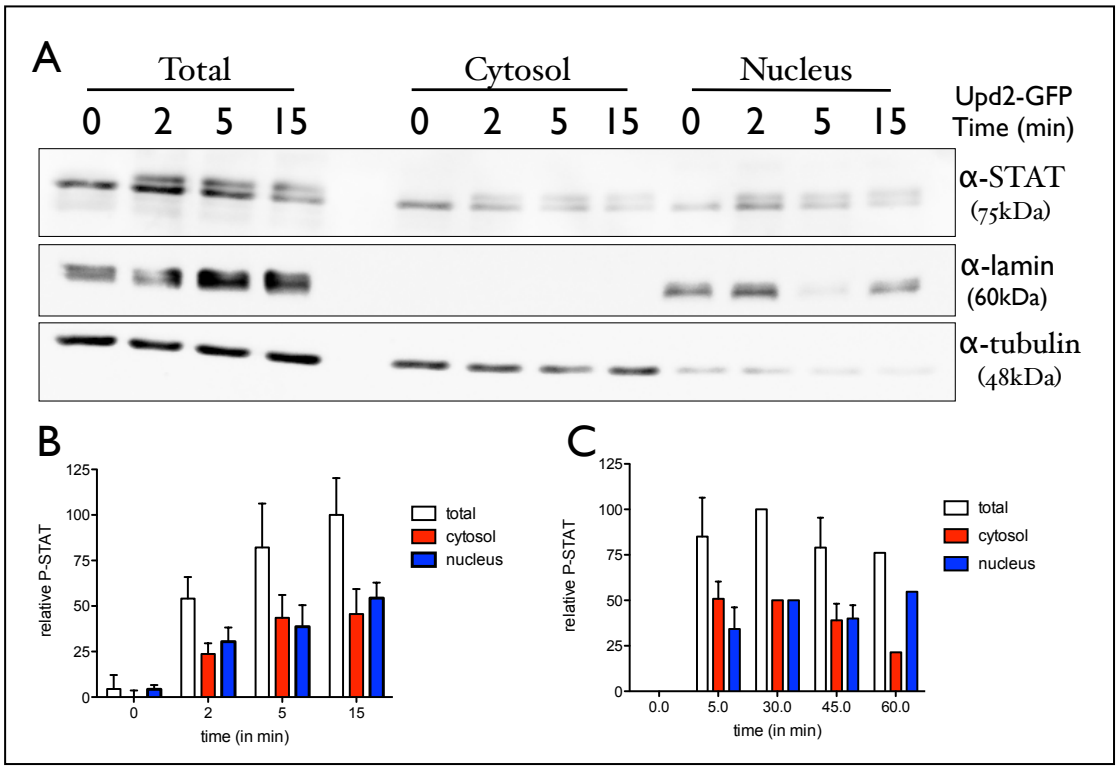

Figure 5.17: Cellular distribution of phosphorylated STAT92E

S2R$^+$ cells were incubated with 20nM Upd2-GFP for indicated time points at 25ºC. Total protein extracts (Total), the cytosolic fraction (Cytosol) and the nuclear fraction (Nucleus) were analysed by SDS-PAGE, the membrane was cut into sections and immunoblotted with anti-STAT92E (top), anti-lamin (middle) and anti-tubulin (bottom). A: Example of fractionation. B and C: Quantification of time dependent phosphorylated STAT92E (P-STAT), whereby the ratio of P-STAT92E to total STAT92E, normalised to the highest control sample, was plotted against time of activation with Upd2-GFP, error bars show standard error of the mean representing 2 independent experiments. B: short 15min time course. C: extended 60min time course (with one repeat only for 60 min).

5.5 Summary

In this final chapter I described the modulation of JAK/STAT transcription factor STAT92E. I focused mainly on the modification of STAT92E by phosphorylation. I showed that STAT92E is phosphorylated. Quantifying the phosphorylation induced bandshift abilities, I demonstrated that this phosphorylation is time-, ligand and receptor dependent. I did not detect any acetylation or sumoylation for STAT92E.

Investigating the role of Clathrin-mediated endocytosis, it seemed that STAT92E phosphorylation was controlled by early endocytic events, since a knockdown of AP2 or Clathrin enhanced the phosphorylation of the transcription factor. However, once the

receptor entered the cells and endocytosis was blocked at later stages, for instance by HRS knockdown, the phosphorylation of STAT92E occurred at normal levels.

To investigate this phenomenon closer I decided to use Phos-tag™ as an additive and enhancer of phosphorylated proteins in SDS-PAGE gels. STAT92E appeared to be differentially phosphorylated using the Phos-tag™ compound. Furthermore, I showed that AP2 or CHC knockdown resulted in an accumulation of PP-STAT92E.

To study the influence of AP2 on STAT92E phosphorylation further and to investigate novel modification sites I performed MS analysis of anti-STAT92E IPs. Thus, I could directly show that STAT92E was phosphorylated on its tyrosine on position 711 (Y-711). Surprisingly this phosphorylation also occurred in cells depleted of AP2.

In addition to STAT92E modification I also began to study the nuclear import of STAT92E and its phosphorylated form. Nevertheless, further experiments are necessary to evaluate the role of endocytosis and RasGAPs in this process.

CHAPTER 6. DISCUSSION

6.1 Summary of Findings

The overall aim of my PhD project was to understand how the endocytic pathway sets up signalosomes. These structures are defined as compartments or sub-domains within the trafficking pathway, which allow cell signalling to occur.

Within this work I investigated the role of Rab5 GEFs and endocytosis on JAK/STAT signalling. I showed that the knockdown of the Rab5 GEFs, RME-6 and Rabex5 influenced wing vein development differentially. Furthermore, I demonstrated that the JAK/STAT pathway was ectopically activated following knockdown of Rab5 GEFs. However, utilising *Drosophila* as a model system I was not able to find a suitable *in vivo* system to address whether endocytosis influences specific signalling pathways, thus setting up signalosomes. Therefore, I established *in vitro* assays to measure JAK/STAT signalling following activation of this pathway by the ligand, Upd2, in *Drosophila* tissue culture cells. I showed that pathway activation was regulated by endocytosis not only quantitatively, but also qualitatively. These qualitative differences drove me to address the question of the regulatory mechanism by which qualitative signalling occurred. I showed that STAT92E phosphorylation was altered when endocytosis was blocked early in the endocytic pathway.

We therefore can suggest a model in which novel ways of STAT92E regulation are responsible for differential signalling. This might occur due to post-translational modifications of the transcription factor while the receptor is travelling through the endocytic pathways. We speculate further that a novel regulator, which is associated with or controlled by the endocytic pathway might be responsible for the differential JAK/STAT pathway activity. Another hypothesis for the differential signalling is the requirement for co-factors, which enable STAT92E to differentially bind its targets. Naturally, the models are not mutually exclusive.

6.2 Are Rab5 GEFs involved in regulating signalling in Drosophila?

First, I set out to explore whether and how Rab5 GEFs influence *Drosophila* signalling pathways. Rab5 effectors enable Rab5 to act as a multifunctional protein and are

involved in numerous processes (Grosshans et al., 2006 and section 1.1.3). Rabs are targeted to membranes by their GEFs (Blumer et al., 2012), where spatially restricted activation can occur. It is feasible that Rab5 activators, GEFs, can also set up distinct platforms for specific functions (Semerdjieva et al., 2008). The tethering of vesicles to target membranes is mediated by an array of proteins, including EEA1 and SNAREs. As part of this complex the Rab5 GEF, Rabex5, activates Rab5 at a specific location. Rab5 then enables the turn over of PIs, recruiting EEA1 locally (McBride et al., 1999). Additionally, the interaction of Rabex5 and Rababtin-5 results in a Rab5 activating feedback, which is able to amplify Rab5 function (Horiuchi et al., 1997).

These examples show the diversity of Rab5, its activators and effectors. Importantly, the establishment of signalosomes can be achieved by a functional pool of Rab5.

The effect of APPL1, a Rab5 effector, in setting up signalosomes has been shown *in vivo* using zebrafish (Schenck et al., 2008). Unpublished data indicate that the Rab5 GEF, RME-6 establishes signalosomes for differential signalling of the RTK, Tie2 (Ferreira, et. al. in prep.).

The Smythe laboratory also showed that RME-6 was required to establish a functional pool of Rab5 for un-coating of Clathrin coated vesicles (Semerdjieva et al., 2008).

These results begged the question as to whether RME-6 and the other Rab5 GEFs might influence signalling in a whole organism by activating Rab5 locally and thus establishing functional platforms and signalosomes.

I tested the effect of Rab5 GEF knockdowns in *Drosophila melanogaster*. Since the fruit fly represents a model of lower complexity, I wanted to address whether Rab5 GEFs are able to establish membrane domains, by locally activating Rab5. In the first instance I investigated whether the individual GEFs had different effects on signalling. Using various assays analysing *Drosophila* at different developmental stages, I addressed the effect of the knockdown of Rab5 GEFs on the wing vein formation in adult flies, the migration of border cells in the oocyte as well as RTK signalling in embryos and whole adult flies.

Within these assays I predominantly used RNAi, which targeted the mRNA of the Rab5 GEFs for degradation. Ensuring spatially and temporal controlled knockdown I used the GAL4/UAS system to drive transcripts of dsRNA hairpins, which were then processed to generate siRNAs, triggering the degradation of homologous mRNAs.

6.2.1 Do Rab5 GEFs influence *Drosophila* developmental processes?

I wanted to perform structure-function analysis of Rabex5, Sprint and/or RME-6. I tried to identify robust phenotypes following knockdown of a Rab5 GEF *in vivo* with the aim to rescue such a phenotype by re-expressing wild type protein. This system would then allow me to assess the effects of mutant forms of the Rab5 GEF and identify the domains of the proteins, responsible for their roles in signalling. Therefore I searched for suitable assays in initial experiments.

6.2.1.1 Wing vein formation

Preliminary data showed that the loss of the different Rab5 GEFs induced distinct phenotypes in *D. melanogaster* wing vein formation (Zeidler and Smythe, unpublished). Within this work I aimed to explore the roles of Rab5 GEFs in more detail. I could confirm that the knockdown of RME-6 and Rabex5 induced additional veins and disrupted wing vein formation in the adult wing (Figure 3.3). The knockdown of the GEFs, Alsin and Sprint did not result in a deformation of the wing vein pattern. Importantly, the phenotypes occurring in RME-6 and Rabex5 depleted wings were different. RME-6 knockdown induced additional veins above the third longitudinal vein and posterior cross vein, whereas the knockdown of Rabex5 resulted in shorter posterior cross veins, which could not always connect L4 and L5 (Figure 3.3). Both RME-6 and Rabex5 knockdown similarly enhanced deltas at the end of longitudinal veins, L3 and L5.

Several signalling pathways, including EGFR, JAK/STAT, BMP and Notch signalling, control wing vein formation (Blair, 2007). Studies investigating the EGFR pathway and its regulators often use this wing vein formation to address the genetic interaction of EGFR and it regulators and the effect of the signalling components on the pathway (for example (Butchar et al., 2012; Hahn et al., 2013)). To further investigate the impact of Rab5 GEFs on specific signalling pathways, I compared the phenotypes, caused by GEF depletion within the wing with the effects of knockdowns of the EGFR signalling pathway. But unfortunately I was not able to dissect out parallels between the EGFR signalling and the Rab5 GEFs (Table 3.1).

It still remains unclear whether the effect of RME-6 is due to an influence of the RTK pathway by its RasGAP domain or due to modulation of the endocytic pathway due to its Rab5 GEF domain. The phenotypes occurring due to the depletion of RME-6 or Rabex5 and EGFR signalling components differ from each other, hence the question is

whether they would have arisen from the same pathways or whether they were a pleitropic effect.

The relatively mild phenotypes I observed, did not encourage me to undertake structure-function analysis of Rab5 GEFs within the wing. In addition the involvement of different developmental processes would not allow me to study a single signalling pathway within this system.

These mild phenotypes, however, also might suggest that the Rab5 GEFs are redundant and the activation of Rab5 might have occurred to an almost normal extent, since the wing vein formation was not greatly impaired, as would be the case if Rab5 would not functioning properly.

6.2.1.2 Border cell migration

Because the wing vein assay did not give a robust phenotype, I set out to find an assay (or assays) to undertake structure-function analysis of the GEFs, by looking at border cell migration (see section 3.2.2). Border cell migration requires the endocytic pathway, since it is impaired when overexpressing dominant negative forms of Shibire (in mammals Dynamin) or Rab5 (Assaker et al., 2010; Silver et al., 2005a). Sprint has been suggested to act as the GEF activating Rab5 enabling proper border cell migration and RTK signalling (Jekely et al., 2005).

I first looked at EGFR signalling, since Jekely et al (2005) suggested Sprint as a novel regulator for RTK signalling in border cell migration, by delaying border cell migration in a *sprint* null mutation (*sprint*^{6G1}), when EGFR or PVR was overexpressed (Jekely et al., 2005). In contrast, my data suggested that the absence of Sprint did not influence the ability of border cells to migrate across the egg chamber, even when EGFR was overexpressed.

One possible reason for this inconsistency could be the saturation of GAL4 proteins in the system. In contrast to the work of Jekely et al, I used flies carrying a *UAS-GFP* construct, which allowed me to follow their border cells. This additional UAS could have depleted the pool of available GAL4 necessary for the overexpression of EGFR. The receptor overexpression might not have been sufficient to induce the delay of border cell migration in a *sprint* mutant background, as seen in the Rorth laboratory.

As I set out to use this assay to undertake structure-function analysis of Sprint, and possibly the other Rab5 GEFs, I would need to introduce another UAS controlled protein (e.g. Sprint with its mutant forms). Therefore, I decided not to pursue this line of

research. This additional UAS might compete with the GAL4 protein pool, similarly to the UAS-GFP and could lead thus to a deletion of the effect caused by *sprint*^{6G1} as a result of insufficiently overexpressed EGFR.

In order to analyse a single signalling pathway, I overexpressed several signalling receptors and ligands (individually) in their wt and dominant negative forms within the border cell cluster.

Thus I found two signalling pathways, EGFR and Notch signalling, which influenced border cell migration when their dominant negative receptor or ligand were overexpressed, but the ectopic expression of the wt forms did not impair the migrating cells. Delta or EGFR overexpression seemed suitable systems to investigate the influence of Rab5 GEFs on signalling (section 3.2.2). Since the overexpression of EGFR was apparently insufficient to induce a delay in border cell migration in *sprint*^{6G1} background, the sensitisation of the system by overexpressing Delta could be used to study the effects Rab5 GEFs further.

By investigating the effect Htl its overexpression at 25ºC, suggests that the pathway is involved in egg chamber development, since almost half of the border cell clusters only migrate 50% along the anterior/posterior axis. Surprisingly, the overexpression of neither the wt at 29ºC nor the dominant negative Htl did not affect this process, which suggests that Htl does not play a role in border cell migration. Together with the low to very low expression levels of Htl and its ligands in the ovary suggests that this RTK does not play a role in border cell migration (Gelbart and Emmert, 2013).

In addition to early endocytic components such as Dynamin and Rab5, ectopic expression of the dominant negative form of Rab11, which characterises the recycling endosome, induced delays in the migration of border cells (Assaker et al., 2010). Interestingly, a Rab GAP (Evi5), deactivating Rab11, was shown to influence border cell migration, by maintaining active RTKs at the leading edge of the border cell cluster (Laflamme et al., 2012). Evi5 could thus establish a platform in recycling endosomes for signalling to occur. This data points towards the importance of the endocytic pathway during border cell migration. It is likely due to the endocytic control of various signalling pathways (Montell et al., 2012).

6.2.1.3 RTK signalling

Several different RTK signalling pathways ensure the coordinated development of not only the wing but also of the fly embryo. I investigated whether the *sprint* mutant allele,

spint^{6G1} had an effect of RTK signalling during embryonic development. Phosphorylated ERK is an indication of signalling by most if not all RTKs. *Drosophila* RKT receptors Torso, Btl, Htl, DER are activated during embryogenesis in a spatially and temporally controlled manner (Gabay et al., 1997). Staining embryos with a phospho-ERK specific antibody I assessed one endpoint of RTK signalling. Unfortunately, I could not detect any obvious differences from *spint*^{6G1} to wt embryos (Figure 3.11).

Time restrictions did not allow me to investigate the role of the other Rab5 GEFs on the phosphorylation of ERK in the embryo. However, I knocked down the GEFs individually in the whole fly and my data indicated that ERK is highly phosphorylated in adult flies depleted of Rabex5. This was consistent with published data (Xu et al., 2010; Yan et al., 2010).

ERK is phosphorylated through the MAP Kinase pathway, including Raf1 activity, Raf1 binds directly to and is activated by Ras. Rabex5 was shown to act indirectly on ERK phosphorylation, by preparing Ras, for degradation with its ubiquitin-ligase activity (Xu et al., 2010; Yan et al., 2010). Therefore, Rabex5 might also act upon the RTK signalling required for wing vein development, as discussed above. Furthermore, it would be interesting to ascertain where exactly ERK is phosphorylated within the developing embryo in a *Rabex5* mutant background as ERK is activated by a number of RTKs throughout the developing embryo (Gabay et al., 1997). This could enlighten whether this modulation of Ras affects all RTKs or only certain subsets within this model system, since in the mammalian system Ras ubiquitination by Rabex5 is isoform-specific (Xu et al., 2010), I postulate that Rabex5 might regulate only a very specific subset of RTK pathways. This would be in tune with the notion of signalosomes, trafficking islands set up by the endocytic pathway (Miaczynska and Bar-Sagi, 2010).

6.2.1.4 JAK/STAT ligand, Upd-induced eye overgrowth

I next addressed the influence of Rab5 GEFs in JAK/STAT signalling. This signalling pathway is also involved in the formation of wing veins and more importantly it was recently shown to be controlled by endocytosis (Devergne et al., 2007; Vidal et al., 2010). These publications and data presented here suggests that the endocytic pathway controls JAK/STAT signalling in a tissue specific manner, as discussed in section 6.4.1 in detail.

To examine the effect of Rab5 GEFs on JAK/STAT signalling *in vivo*, I used an assay in which the eye proliferates in an uncontrolled fashion due to the ectopic induction of

Upd activating JAK/STAT signalling (Bach et al., 2003; Mukherjee et al., 2006). Using this sensitised assay was more likely to show the effect of positive regulators of the JAK/STAT pathway. For instance the loss of one copy of STAT92E rescues the overgrowth phenotype (Figure 3.10; Bach et al., 2003 and Mukherjee et al., 2006). Negative regulators of the overgrowth need to act strongly on the signalling pathway to achieve an even further increase in eye size, making it a much less sensitive assay to detect negative regulators of the pathway. I used mutant flies or flies where individual Rab5 GEFs were knocked down by RNAi to investigate their influence of JAK/STAT signalling (Figure 3.10). If the endocytic pathway and thus Rab5 GEFs act as positive regulators within the fly eye tissue, this assay could possible enable me to address their influence well.

The loss of one copy of *Sprint* or *Rabex5* did not influence eye overgrowth. This was in the contrary to findings reported by Mukherjee et al 2005 (Mukherjee et al., 2006). They identified Sprint as a negative regulator of JAK/STAT, showing that the over-growth index rises, when one copy of the *sprint* allele was missing. Using a scoring scheme is always highly subjective, even though all scores were obtained blind – by two independent researchers, who did not know which genotype they scored at the time of scoring. It could well be that we did not score fly eyes as stringently as Mukherjee et al 2005. And even if we tried to use exactly the same experimental conditions, maybe the overexpression of Upd was slightly altered such that the effect of $sprint^{6G1}$ was not visible anymore. Additional to the mutant alleles of *sprint* and *rabex5*, I addressed the influence of the *Drosophila* Rab5 GEFs, by knockdown using dsRNA lines. The depletion of all tested Rab5 GEFs did not alter the Upd-induced eye overgrowth (Figure 3.10).

As this assay is slightly biased towards finding positive regulators I decided directly to investigate JAK/STAT signalling further using reporter assays *in vivo* and *in vitro.*

6.2.2 Rab5 GEFs influence ligand-independent JAK/STAT pathway activation *in vivo* and *in vitro*

Investigating the role of Rab5 GEFs I used *in vivo* and *in vitro* JAK/STAT reporters and analysed targets of the pathway (*in vitro* only). Thus I did not need to overexpress pathway components and hence avoiding possible mis-regulation of the pathway due to experimental design.

My data showed that the single knockdown of either Sprint, RME-6 or Rabex5 resulted in an ectopic activation of JAK/STAT signalling *in vivo* and /or *in vitro*. Measuring JAK/STAT activation with the same 10xSTAT reporter *in vivo* (10xSTAT-GFP) in the imaginal wing disc or *in vitro* (*10xSTATLuc*) in tissue culture cells, I observed induction of the pathway in the absence of the ligand. Interestingly, RME-6 and Sprint depletion caused JAK/STAT ligand-independent signalling *in vivo*, whereas *in vitro* the knockdown of Rabex5 and Sprint resulted in ligand-independent signalling. (Figure 3.7 & Figure 4.12). Furthermore, expression of the JAK/STAT target mRNA *Domeless* was enhanced significantly in mock-treated cells, when Rabex5 or Sprint was knocked down in $S2R^+$ cells (Figure 4.21 C. This phenomenon also occurred for weaker targets in this assay like *Wnt* or *Bazooka*, which showed higher expression in Sprint (Rabex5 knockdown affected only *Wnt*) knockdown samples, when not induced with Upd2-GFP (data not shown).

It was unlikely that the reporter construct is responsible for this ligand-independent signalling, since the same reporter was influenced in the same way by different GEFs depending on whether it was used *in vivo* or *in vitro*. However, the same Rab5 GEF (Rabex5 and Sprint) knockdown caused ligand-independent pathway activation measured by two independent reporters in the same system ($S2R^+$ cells), suggests that the cellular environment (within the developing wing or in $S2R^+$ cells) and not the used JAK/STAT signalling reporters, caused this ligand-independent signalling. Therefore it remains unclear as to the causes of the ligand-independent signalling.

It is possible that this ligand-independent signalling might be usually suppressed by Rab5 GEFs, for instance, by acting on receptor dimerisation. The receptor, Dome was shown to be able to dimerise independently of ligand (Brown et al., 2003). In addition, the heterodimerisation with the negative regulator Latran, a short non-signalling JAK/STAT receptor occurs without the ligand present (Kallio et al., 2010; Makki et al., 2010). Even though it was suggested that Latran does not influence the internalisation of Dome (Makki et al., 2010), it could be possible that the Rab5 GEFs enhance the association of Latran with Dome, influencing thus ligand-independent JAK/STAT signalling.

Apart from its role in the canonical JAK/STAT signalling, STAT92E has been reported to act in non-canonical signalling. For instance, un-stimulated, un-phosphorylated STAT92E stabilizes the heterochromatin protein 1 on heterochromatin and acts thus on an additional level to its function as a transcription factor on expression of JAK/STAT

targets (Shi et al., 2008). This function could cause ligand-independent pathway activation. I tested whether RME-6 knockdown influenced STAT92E phosphorylation. The knockdown of RME-6 did not seem to influence STAT92E phosphorylation, whether un-stimulated or after Upd2 incubation (Figure 5.9). However, RME-6 knockdown did not affect ligand-dependent or –independent JAK/STAT signalling *in vitro*, measuring activation with the *10xSTATLuc* reporter and target mRNA expression (Figure 4.12 & Figure 4.21), but only induced ligand-independent JAK/STAT pathway activation *in vivo*. Thus the influence of STAT92E phosphorylation on ligand independent signalling (or vice versa) still needs to be addressed *in vitro*.

6.2.2.1 Ligand-independent JAK/STAT signalling due to cross-talk with Ras?

JAK/STAT signalling was shown to crosstalk to the RTK pathway (Eulenfeld et al., 2012). One hypothesis for the ligand-independent JAK/STAT activation is that JAK/STAT might be activated by a Ras-mediated pathway. It was suggested that SOCS36E can suppress signalling not only through the JAK/STAT pathway, but also through Ras in *Drosophila* (Callus and Mathey-Prevot, 2002). In addition, a RasGAP, p120, transfers Ras into its inactive state. P120 cannot inactivate Ras, when bound to SOCS3 resulting in Ras activation (Cacalano et al., 2001).

The knockdown of Ras resulted in a failure to activate the JAK/STAT pathway and I could not observe any ligand -dependent or -independent activation above background (Figure 4.12). This indicates that Ras apparently acts upstream of the JAK/STAT signalling pathway.

The knockdown of RME-6/Sprint and or Sprint/Rabex5 cause ligand–independent activation *in vivo* and *in vitro* respectively. Since Rme-6 contains a Ras-GAP and Sprint a Ras binding domain, it was feasible that these domains might influence JAK/STAT signalling via Ras, (similar to p120) and be the cause of the observed ligand independent pathway activation. In addition, Rabex5 restricts Ras, by marking Ras with ubiquitin and preparing thus for degradation (Xu et al., 2010; Yan et al., 2010).

The double knockdown of the Rab5 GEFs with Ras mirrored the effect of Ras single knockdown, suggesting that there was no rescue of any residual Ras by the GEFs.

It is worth noting that the *ras* mutant allele and other RTK signalling components, like an Insulin receptor or EGFR did not have an effect on the Upd-induced eye overgrowth (Bach et al., 2003), suggesting that the JAK/STAT pathway does not crosstalk with Ras and RTK signalling within all tissues.

Further experiments would have to be undertaken to dissect precisely the cause of this activation. To find additional modifiers of this phenomenon cells could first be sensitised by knockdown of individual Rab5 GEFs (Rabex5 or Sprint) and then used to perform a genome-wide screen of dsRNA to search for modifiers of un-induced JAK/STAT activation, which do not influence ligand induced signalling. This could possibly find identify candidate proteins that are responsible for the ligand-independent JAK/STAT activation.

6.2.3 Creating a RME-6 knockout mutant

Because of the evidence that RME-6 may promote signalosome formation in mammalian cells (Ferreira et al., in prep), I wanted to address whether RME-6 is able to establish similar signalling domain in an *in vivo* system. The use of RNAi to deplete cells of proteins has many advantages, including the tissue controlled expression of the RNAi. Unfortunately, there was only one available RNAi transgenic line, enabling the conditional inactivation of RME-6. Using this line I observed a weak phenotype following RME-6 depletion in the wing vein, which was not sufficient to undertake structure-function analysis of RME-6.

Therefore I attempted to create a mutant for RME-6 in *Drosophila*. I used the ends out homologous recombineering strategy, as there were very little P-elements in the genomic region of RME-6 and this strategy would allow me a faster and more elegant way of creating the RME-6 knockout (Huang et al., 2008). Even though I used an improved ubiquitous driven GAL4 line to eliminate unmobilised donor and false positives (*ubiquitin-GAL4[3xP3-GFP]* from Baena-Lopez et al., 2013), I was not able to create a mutant for RME-6.

It is very unlikely that a homozygous RME-6 mutant is lethal, since a) its ubiquitous knockdown did not show any obvious phenotype affecting viability or fly-health and b) there is likely to be significant redundancy between the Rab5 GEFs; for instance although the single knockouts of Rabex5 or RME-6 impair endocytosis in C. elegans, only the double mutant worm is lethal (Sato et al., 2005). It is more likely that the two failed attempts to create the mutant are due to the donor construct. It may be that the homologous arms chosen did not allow for a highly efficient crossover, or the genomic region is densely packed with heterochromatin. A more efficient method of gene targeting was described recently and future efforts could increase recombination events by introducing double-stand breaks within the RME-6 region, by CRISPR *(*Clustered

Regularly Interspaced Short Palindromic Repeat) in addition to using a different donor construct (Baena-Lopez et al., 2013).

6.3 Regulation of JAK/STAT signalling by endocytosis

To study ligand uptake I could either use immunofluorescence and follow the GFP-tagged ligand directly as it was taken up by cells or I could measure internalised ligand bio-chemically with an enzyme linked immuno sorbent assay (ELISA).

The use of immunofluorescence has many advantages and is widely used in the investigation of endocytosis. It is a very direct method to show ligand uptake and its path through the endocytic pathway, and can be even applied to live cells and organisms (Toya et al. 2000). Additionally, it is visually appealing and often supports biochemical data. One could argue that unless an automated measuring system or elaborative quantification methods were used, findings can be influenced by the interpreter and thus misjudged. In the case of my project, inconsistent staining and high auto-fluorescence of *D. melanogaster* cells precluded the use of immunofluorescence.

Another advantage of the microscopy-based assays is the possibility of co-staining with endocytic markers like Rab5. It would thus be possible to determine which endocytic compartments are reached by the receptor and ligand, although the lack of high-quality antibodies in *Drosophila* reduces these possibilities greatly. The expression of tagged endocytic proteins could bypass this problem. Even though this could potentially distort the endocytic system, as for instance the overexpression of Rab5 causes enlarged early endosomes (Bucci et al., 1992).

Because of the difficulties with using immunofluorescence, I decided to use an ELISIA based assay to measure ligand-uptake in cells. The ELISA assay had several advantages: it was quick, more quantitative than the assessment by microscopy and allowed a greater number of samples to be processed at the same time. Since I measured the fused GFP, rather than Upd2 directly I could use commercially available antibodies for the detection of Upd2-GFP. On the other hand one could argue that measuring ligand uptake by ELISA is a rather indirect way of showing endocytic events, but performing a number of controls reduced the possibility of drawing false conclusions.

The use of immunofluorescence still displays big advantages and in future analysis of appropriate systems should be undertaken to visualise Upd2 uptake and its trafficking. This analysis of the endocytic pathway would indicate whether Upd2 is delivered to a

population of signalling endosomes, which have not been previously identified in flies. It would be intriguing to dissect, which particular markers characterise the *Drosophila* signalosomes, since the fly lacks EEA1 and APPL1, Rab5 effectors, which establish signalosomes in mammals (Beas et al., 2012; Schenck et al., 2008). Using tagged endocytic proteins could be a possibility to visualise distinct compartments, as exemplified by (Wendler et al., 2010).

6.3.1 Clathrin-mediated endocytosis of JAK/STAT

Using the ELSIA assay, I showed that the JAK/STAT ligand, Upd2 is internalised by Clathrin-mediated endocytosis. This was also previously suggested by immunofluorescence *in vitro* and *in vivo* (Devergne et al., 2007; Vidal et al., 2010).

Using dsRNA to knock down Clathrin or AP2, I could detect significantly less intracellular Upd2, however the levels of internal Upd2 still lay above the background levels, which were observed following Dome knockdown (Figure 4.6). The incomplete depletion of Clathrin and AP2 proteins after the knockdown could explain these residual uptake, since I detected approximately 25% *Clathrin* mRNA and 20% AP2 proteins remaining after the knockdown (Figure 4.7). On the other hand a Clathrin-independent uptake mechanism could also account for reduced Upd2 uptake, when I depleted cells of Clathrin or AP2, especially when considering that Clathrin-independent endocytosis is upregulated following inhibition of Clathrin-mediated endocytosis ((Damke et al., 1995)). Furthermore, endocytic studies of the mammalian JAK/STAT pathway indicated that interferon receptors are trafficked by both Clathrin-dependent and -independent endocytic pathways (Marchetti et al., 2006; Sadir et al., 2001).

The knockdown of the receptor, Dome resulted in a significant decrease of Upd2-GFP uptake (Figure 4.6). However, I could still detect a considerable amount of internal Upd2 in Dome depleted $S2R^{+}$ cells. This background ligand uptake was probably due to the incomplete knockdown of the receptor, which mRNA levels decreased down to approx 25% (Figure 4.7) and / or receptor-independent fluid phase uptake of Upd2.

6.4 Clathrin-mediated endocytosis controls JAK/STAT signalling

6.4.1 Endocytosis a negative or positive regulator of JAK/STAT signalling?

As discussed above and shown in Chapter Chapter 4 that JAK/STAT signalling is controlled by Clathrin-mediated endocytosis. The Upd2- dependent induction of a

10xSTATLuc reporter and JAK/STAT target gene expression of *SOCS36E* and *Domeless* was inhibited in $S2R^+$ cells depleted of Clathrin or AP2. Furthermore, the knockdown of an ESCRTI complex, TSG101, did not influence either luciferase or target gene expression. This suggests that JAK/STAT signalling is Clathrin-dependent and is active before reaching TSG101-dependent compartments. This indicates that the endocytic pathway represents a positive regulator of JAK/STAT signalling in $S2R^+$ cells.

This stands in contrast to published work from Vidal et al, 2010, which suggested endocytosis as a negative regulator of JAK/STAT signalling. That study showed, using a very similar approach, that knockdown of Clathrin resulted in an increase of pathway activation (Vidal et al., 2010). Their data included *in vivo* and *in vitro* knockdown studies, which stood in contrast to previous *in vivo* studies (Devergne et al., 2007). Devergne et al used Clathrin and Rab5 mutant clones within the egg chamber and suggested that the ligand-receptor complex needs to be internalised and trafficked to be able to signal. One could argue that using mutant clones distorts the cell fate of the fast developing oocyte cells so much that they lose their identity and a typical JAK/STAT responsive reporter (pointed-lacZ) fails to be induced by the ligand. However, I used the approach of dsRNA to interfere with trafficking and could, similarly to Devergne et al, not activate signalling when Clathrin-mediated endocytosis was blocked. Studies in mammalian cells suggest that the endocytic pathway controls the uptake of IFN receptors and JAK/STAT signalling (Claudinon et al., 2007) for a review. In general in most mammalian systems IFN receptors are restricted by endocytosis in the extent and duration of signalling (Marchetti et al., 2006).

In conclusion the JAK/STAT pathway is negatively or positively controlled by endocytosis. This seemingly controversy does not only apply to JAK/STAT signalling is not the only signalling pathway. Wnt and EGF signalling was both shown to be influenced in both directions by trafficking components (Chanut-Delalande et al., 2010; Gagliardi et al., 2008).

Variances between studies can be also illustrated by the two genome wide screens undertaken for JAK/STAT signalling. Indeed some regulators, such as SOCS36, were found in both screens, but given the number of identified modulators of JAK/STAT the overlap between the screens was surprisingly low. Similarly endocytic regulators such as Rab5 and TSG101 were identified by Muller et al but not in the Baeg et al screen. This suggests that these differences occur because different biological systems and

experimental set up were used. (Baeg et al., 2005; Muller et al., 2008; Muller et al., 2005).

This data supports the premise that the endocytic pathway regulates signalling depending on the cellular environment, that the cell is ultimately able to respond to its specific needs, which might differ dependent on the environment or developmental stage it is in (Chanut-Delalande et al., 2010).

Another argument to explain these differences is concerned with the different JAK/STAT reporters used. Since the studies described used an array of different, partly overlapping reporter sets, the methods of JAK/STAT signal detection were complementary rather than opposing each other. For instance I used the *10xSTATLuc* reporter similar to that of Vidal et al, 2010 *in vivo*. In addition to ectopically expressed reporters, this study also showed data from endogenous JAK/STAT pathway activation, by either looking at STAT92E nuclear localisation with an anti-STAT92E (Devergne et al., 2007; Silver et al., 2005a) or measuring mRNA levels of endogenous JAK/STAT targets (this study).

6.4.1.1 JAK/STAT transcriptional profiles

Several studies have measured JAK/STAT transcriptional targets under distinct circumstances, including overexpression of Upd, of a constitutively active kinase (Hop^{Tum}) or using a loss of function allele of Hop (Flaherty et al., 2009; Kwon et al., 2008; Terry et al., 2006; Wang et al., 2013). Both *Domeless* and *SOCS36E* were found as targets in germ-line stem cells in the testis, eye imaginal discs and in the brain (Bina et al., 2010; Flaherty et al., 2009; Terry et al., 2006; Wang et al., 2013), whereas *SOCS36E* alone was also upregulated in KC_{167} cells and whole third instar larvae (Bina et al., 2010; Kwon et al., 2008). Surprisingly, both *Domeless* and *SOCS36E* were upregulated in the brain upon Upd over-expression, but failed to be repressed in a Hop loss of function mutant, hence the authors suggested that they are not JAK/STAT targets (Wang et al., 2013).

There was surprisingly little overlap between the transcriptional profile induced by Upd either in KC_{167} cells *in vitro*, eye disc or testis (Bina et al., 2010; Flaherty et al., 2009; Terry et al., 2006). The big differences in the systems being analysed could explain this lack of commonality. However, all three studies identified *SOCS36E* and *Wnt4* as JAK/STAT targets, which I also found to be upregulated upon Upd2 treatment Figure

4.15. The endocytic regulation of *Wnt4* was not pursued since it was a weak target and was technically difficult to measure, because of its low expression.

The overexpression of Upd within the eye discs and testis stem cell niche however also induced *Domeless* expression, which was not induced in KC_{167} cells, but in $S2R^+$ tissue culture cells. *Net* on the other hand was identified as a target in KC_{167} and $S2R^+$ cells, but not in the testis. This suggests that the expression of JAK/STAT targets is highly dependent on its cellular environment, as also shown comprehensively for *Domeless* expression *in vivo* (Brown et al., 2001a).

The mRNA of endocytic components like Clathrin, Rab5 and Rab5 GEFs did not increase upon ligand stimulation (data not shown), which was consistent with the transcriptional profiling data from Bina, et al, 2010 and Flaherty et al, 2009. This is likely due to the fact that endocytic proteins are highly stable and are expressed independently of most changes in the cellular environment.

Importantly the studies are different in one other major aspect; they all looked at different developmental stages, cell types or tissue culture cell lines. This suggests that the regulation of JAK/STAT by endocytosis is complex and specific to the environment in which cells find themselves. This phenomenon is seen in other systems, too. Chanut-Delalande et al., 2010 report that the ESCRT-0 components HRS and STAM are required for EGF signalling in the pupal wing, but repress the EGFR pathway during embryogenesis (Chanut-Delalande et al., 2010).

6.4.2 STAT92E modulation by Clathrin-mediated endocytosis

In order to investigate the mechanism responsible for the endocytic control of JAK/STAT signalling, I analysed post-translational modifications of the transcription factor STAT92E. STAT92E is phosphorylated upon pathway activation. In Chapter 5 I showed that this occurs in a receptor- and ligand-dependent manner. STAT92E phosphorylation takes place on a highly conserved tyrosine at position 711 and shown to be crucial for STAT92E function (Ekas et al., 2010; Karsten et al., 2006; Yan et al., 1996).

6.4.2.1 Clathrin and AP2 depletion enhance STAT92E phosphorylation

JAK/STAT ligand uptake and signalling was controlled by Clathrin-mediated endocytosis. Surprisingly, although cells depleted of AP2 or Clathrin were unable to activate JAK/STAT signalling, STAT92E phosphorylation was enhanced (Figure 5.7), but transcription of both *10xSTATLuc* and endogenous targets was inhibited.

STAT92E is tyrosine phosphorylated at position 711. However, in cells expressing STAT92E with a tyrosine to phenylalanine mutation at position 711, an anti-phospho-tyrosine antibody was still able to detect a band corresponding to STAT92E (Ekas et al., 2010). This indicates there are other residues on STAT92E, which are tyrosine phosphorylated. Together with my data showing hyperphosphorylation of STAT92E in conditions where signalling is blocked, this suggests a model in which STAT92E is phosphorylated on additional sites (to Y-711), which subsequently inhibit STAT92E in its function as a transcription factor.

One can speculate that the trapping of the receptor on the cell surface induces merely a physical accumulation of components including the kinase and thus leading to increased phospho-STAT92E. Indeed Dome accumulates at the plasma membrane in *Clathrin* mutant tissues (Devergne et al., 2007). This hyper-phosphorylation of STAT92E might block its a) function as a transcription factor, b) DNA binding properties, or c) nuclear transport.

In mammalian tissue culture cells the INFAR was shown to by regulated by Clathrin-mediated endocytosis. Blocking the endocytic pathway resulted in a delay of downstream phosphorylation of the transcription factors, STAT1 and STAT2, as well as their nuclear enrichment. This was consistent with a block of JAK/STAT controlled luciferase activation in Clathrin-depleted mammalian cells. Interestingly, the same inhibition did not result in signal inhibition of INGR signalling, whose uptake was also regulated Clathrin-mediated endocytosis (Marchetti et al., 2006).

This suggested that INF receptors are not only endocytosed in distinct ways, but also their signalling occurs from different locations (IFNAR1 intercellularly and IFNGR1 from the plasma membrane). The *Drosophila* JAK/STAT signalling pathway only contains one signalling receptor. Interpreting my data I postulate hence that Clathrin-mediated endocytosis modulates the transcription factor, restricting thus signalling to Clathrin-dependent and internal compartments. For further discussion see also section 6.5.

6.4.2.2 Differential STAT92E phosphorylation?

To quantify phosphorylated STAT92E I took advantage of its bandshifting properties. Quantification is a main advantage of using the bandshift assay. I also exploited the existence of an SDS-PAGE gel additive, Phos-tag™, which binds to phosphorylated proteins causing them to decrease their mobility on SDS-PAGE gels. Using the Phos-

tag™ gels I detected additional bands for STAT92E (PP-STAT92E), corresponding to phosphorylated forms of the transcription factor (Figure 5.10 and Figure 5.11).

There is a small possibility that the bands seen on the Phos-tag™ gels could be artificial. It might be that both bands corresponded to STAT92E phosphorylated on the same residue and the two distinct forms occurred due to differential binding to the Phos-tag™ add-on. Alternatively, the P-STAT92E band could be due to the bandshift also seen on standard gels and the PP-STAT92E related to phosphorylated STAT92E bound to Phos-tag™.

At the same time the distinct forms could be due to differential phosphorylation. To test whether both bands correspond to tyrosine phosphorylation of STAT92E, anti-STAT92E IPs and subsequent analysis with an anti-phospho-tyrosine antibody could be performed. A more definite answer about the differential phosphorylation of STAT92E can be obtained by MS analysis. Within this analysis the Phos-tag™ technology could be applied as well, this would allow for an enhanced detection of phosphorylated peptides (Fila and Honys, 2012). Since I already was able to detect Y-711 phosphorylation, I expect the Phos-tag™ technology would further increase the signal.

6.4.2.3 Clathrin-mediated endocytosis modifies STAT92E phosphorylation, but not on Y-711

The detection of two distinct phosphorylated forms of STAT92E suggested that STAT92E was differentially phosphorylated. Preliminary experiments indicated that the effect of enhanced phosphorylation in Clathrin/AP2 depleted cells might be due to PP-STAT92E (Figure 5.12). Additional experiments are, nevertheless, essential to dissect these differences.

Most STATs are phosphorylated on serines as well as tyrosines. This serine residue is located in close proximity to the tyrosine on the C-terminus of the transcription factor and could be responsible for this additional form of phosphorylated STAT92E (Lim and Cao, 2006).

In order to fulfil its function the transcription factor, STAT92E is phosphorylated on a highly conserved tyrosine at position 711 (Yan et al., 2010). I was able to detect this phosphorylation directly by MS (section 5.3). Importantly, when AP2 was knocked down Y-711 was still phosphorylated. This finding might contradict at first glance the commonly accepted model that Y-711 phosphorylation on STAT92E is sufficient for transcriptional activation,. One possibility to explain the signal- inhibition, is that the

endocytic pathway causes an additional modification on the transcription factor, which leads to its inhibition (see below).

In mammalian cells, the endocytic pathway was shown to differentially modulate STAT phosphorylation (German et al., 2011; Marchetti et al., 2006). STAT3 is phosphorylated on the conserved tyrosine (in this case Y-705), but also on a serine closer to the C-terminus of the protein (S-727). This serine can be also found in STAT1 and STAT4, but does not appear to be conserved in *Drosophila* STAT92E. Interestingly, STAT phosphorylation on Ser727 was suggested to occur due to an interaction with the MAPK pathway and to take place at the late endosome (German et al., 2011).

6.5 Signalling from signalosomes

My analysis of JAK/STAT signalling not only showed that it is controlled by Clathrin-mediated endocytosis, but that there is differential signalling upon Upd2 stimulation in $S2R^+$ cells (Figure 6.1). Both, the *10xSTATLuc* reporter and the expression of the target genes, *SOCS36E* and *Domeless*, were Clathrin- and AP2-dependent. Furthermore, the knockdown of an ESCRTI complex component, TSG101, did not influence either luciferase or endogenous target expression. Importantly, I could detect differences in JAK/STAT signalling using these two readouts. The luciferase reporter activation was not influenced by a Rab5 knockdown, suggesting that signalling occurred prior to a Rab5 positive compartment. The mRNA of the JAK/STAT targets, *SOCS36E* and *Domeless*, on the other hand could not be induced by Upd2 in HRS depleted cells. HRS acts later on the endocytic pathway compared to Rab5 positive compartments, since it ensures the maturation of MVBs. Thus my data suggest that *SOCS36E* and *Domeless* mRNA is activated beyond a HRS dependent and Rab5 positive endocytic compartment. I therefore postulate a model in which JAK/STAT signalling occurs from and is regulated by signalosomes. This suggests that different specialised compartments of the endocytic pathway generate environments that are conductive to signalling by some but not all compartments.

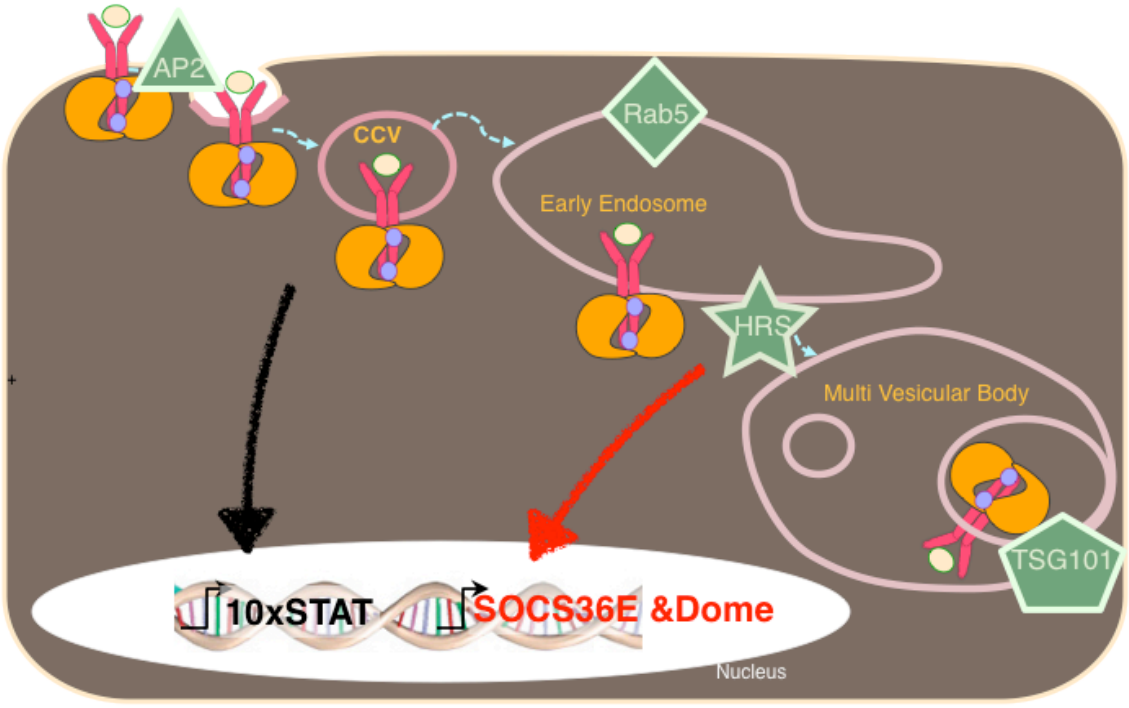

Figure 6.1: Model of differential signalling in *Drosophila* S2R$^+$ cells
The *10xSTATLuc* reporter and the expression of the target genes, *SOCS36E* and *Domeless*, were Clathrin- and AP2-dependent, but TSGS101, an ESCRTI complex component, did not influence either luciferase or endogenous target expression. The luciferase reporter activation was not influenced by a Rab5 knockdown, which acts prior HRS. The mRNA of the JAK/STAT targets, *SOCS36E* and *Domeless*, could not be induced by Upd2 after a HRS knockdown.

The first report of these signalosomes showed that EGFR trafficking was required to induce distinct signalling pathways. Endocytosis was blocked by overexpressing the dominant active form of Dynamin in mammalian tissue culture cells and after ligand treatment all tyrosine-phosphorylated proteins were immunoprecipitated. The immunoblot with the same antibody showed the occurrence of hyper- and hypophosphorylated proteins, suggesting thus distinct signalling outputs (Vieira et al., 1996). Even though EGFR pathway components are differentially phosphorylated, recent transcription profile analysis suggested that the endocytic pathway did not influence the transcriptional response of EGFR in HeLa cells (Brankatschk et al., 2012). My data is therefore one of the few reports showing differential gene activation.

The existence of signalling platforms was also shown *in vivo* directly using a zebra fish model demonstrating that APPL segregates differential Akt signalling (Schenck et al., 2008). However, not only RTK signalling is subjected to qualitative endocytic control also for instance the B-cell receptor was shown to be regulated by endocytosis.

Chatudevi et al showed in 2011 that the block of endocytosis led to a dysregulation of gene transcription (Chaturvedi et al., 2011).

Noticeably, data from (Devergne et al., 2007) showed that signalling occurs already from Clathrin-dependent structures and continues in Rab5-dependent compartments. In *clathrin* mutant cells a reduced JAK/STAT signal activation could be detected, Furthermore, *clathrin* mutant tissues showed a strong reduction on STAT92E nuclear accumulation. However in tissues lacking Rab5, small amounts of nuclear STAT92E was still detected. This suggested that JAK/STAT signalling occurs from the plasma membrane and it is partly reduced when the receptors enter the cell. Unfortunately they did not show the direct pathway signalling activation in both mutant tissues, but showed that signalling is impaired in *clathrin* mutant cells (Devergne et al., 2007). It would be of interest to analyse whether this signalling is not only quantitatively but also qualitatively regulated by investigating an array of JAK/STAT targets (see also 6.4.1.1)

STAT signalling platforms cannot only be set up by the endocytic pathway. Calnexin, an endoplasmic reticulum (ER) tethered chaperone is cleaved by Caspase-8 triggered by EGF. The cytosolic domain binds then to PIAS, an inhibitor of phosphorylated STAT3. However upon ER stress, Calnexin becomes Caspase insensitive and thus unable to enhance STAT3 signalling (Lakkaraju and van der Goot, 2013). This example illustrates that the novel / unknown regulators contribute to a complex network of signalling.

6.5.1.1 JAK/STAT missregulation/missactivation

During the analysis and discussion of JAK/STAT signalosomes, I was not able to compare directly cells depleted of Rab5 with both signalling outputs. The knockdown of Rab5 and other JAK/STAT regulators, namely Ptp61F and Hop resulted in a ligand independent JAK/STAT target activation (Figure 4.20). Hop as the JAK kinase and Ptp61F as a suggested phosphatase for STAT92E should have opposite effects; and indeed, using JAK/STAT luciferase reporters this could be shown *in vitro*. (Baeg et al., 2005; Muller et al., 2005).

Investigating JAK/STAT signalling by assaying mRNA targets I measured endogenous targets with an incredibly sensitive system. This is likely so sensitive that I can detect either dsRNA-induced cellular stress or responses due to the depletion of these essential proteins. Protein accumulation leading to stress in the endoplasmic reticulum was suggested to induce JAK/STAT transcription alteration, by modulating JAK2

phosphoylation and STAT5 DNA binding properties. However within this alteration SOCS protein levels remained unchanged (Flores-Morales et al., 2001).

Rab5 knockdown in particular is likely to manifest itself in the alteration in numerous (signalling) pathways. In a Rab5 depleted background a ligand independent pathway activation occurred, when measuring JAK/STAT endogenous targets. This signals were not observed within the *10xSTATLuc* assay. This suggested that the target assay measuring mRNA was more sensitive to changes in the cellular environment. Interestingly the expression of *gAlpha73B* and *Net* mRNA was increased when the receptor was depleted Figure 4.16, even in the mock-treated samples. This increased expression might be due to a similar response, caused by Dome knockdown and / or ligand treatment.

Since JNK is a major pathway regulating stress responses, further investigations could focus on this pathway to analyse the interaction between the JAK/STAT and JNK signalling. Indeed in the midgut it has been shown that JNK activation triggers Upd expression and thus JAK/STAT activation (Jiang et al., 2009).

A genome wide analysis of genes altered as a result of the knockdown of Rab5, Hop or Ptp61F also could provide insight in as to which pathways might have been influenced upon knockdown of these proteins.

6.5.2 STAT92E manipulation by signalosomes

Data presented here suggests that JAK/STAT signalling occurs from distinct signalling platforms within $S2R^{+}$ cells. Strikingly, I detected differences in JAK/STAT signalling depending on which transcriptional target I measured. The signalling measured by the *10xSTATLuc* was Rab5 independent (Figure 4.12), since a Rab5 knockdown did not influence the response to Upd2. Unfortunately, the knockdown of Rab5 caused a ligand independent increase of the *SOCS36E* and *Domeless* mRNA (as discussed above), therefore I was not able to address its influence on JAK/STAT targets directly. However, the knockdown of a later acting component, HRS, as part of the ESCRT-0 complex, resulted in a failure to activate JAK/STAT target gene expression upon ligand stimulation, thus stalling pathway activation. This suggests that the *10xSTATLuc* reporter is activated from an earlier compartment then the induction of *SOCS36E* and *Domeless* mRNA (Figure 6.1).

The strength of signalling is dependent on the ligand and the notion that weak signals can be effectively transmitted to the nucleus by the use of the endosomal compartments.

This was shown elegantly for the c-Met-activated STAT3 signal (Kermorgant and Parker, 2008). STAT3 is only activated weakly by HGF, whereas oncostatin M (OM) strongly induces STAT3 phosphorylation and nuclear translocation. However, when the endocytic pathway is blocked, HGF cannot trigger downstream signals anymore. Importantly, OM-induced STAT3 nuclear import still occurs, when endocytosis was blocked (Kermorgant and Parker, 2008). This is an example how the endocytic pathway provides the cell with a platform to separate and in this case enhance weak signals. It still remains to speculations as to how the cell can distinguish between two signals and act accordingly, as commented by (McShane and Zerial, 2008). However, we start to understand the mechanism of how differential signalling is regulated by the endocytic pathway.

Obtaining data, which indicates the establishment of signalosomes, opened up the question of the molecular mechanism. In section 6.4.2 and beyond I discuss my findings that $S2R^{+}$ cells depleted of Clathrin and AP2 abolish JAK/STAT activation, but still phosphorylate STAT92E on Y-711, and appear to have additional phosphorylation sites. Interestingly, this enhanced phosphorylation did not occur, when the trafficking pathway was blocked at later stages, by HRS depletion. The late inhibition of the endocytic pathway allowed normal *10xSTATLuc* signal activation, but on the other hand mRNA of JAK/STAT targets could not be induced. Since the enhanced phosphorylation was not evident under conditions when HRS was knocked down and *Domeless* and *SOCS36E* were not transcribed, this suggests that there must be another mechanism via yet unknown regulators or novel / additional modifications of STAT92E, which inhibits JAK/STAT signalling, when occurring from HRS dependent compartments. This proposes the model that STAT92E is regulated from the various endocytic compartments differently either via STAT92E modifications or the interaction with additional regulators allowing for distinct signal activation. Naturally, the possibilities are not mutually exclusive (Figure 6.2).

6.5.2.1 Putative STAT92E modifications

Studies to date have mostly investigated the influence by endocytosis on the functionally crucial tyrosine phosphorylation on the C-terminus of STATs (Bild et al., 2002; Kermorgant and Parker, 2008). However, there is a set of STAT modifications described, which could be responsible for the differential signalling I observed. Mammalian STAT5b was shown to be phosphorylated on a serine at position 193. This

phosphorylation resulted in a maximal Stat5b transcriptional activity. Furthermore, S-193 was constitutively phosphorylated in numerous malignant cells (Dephoure et al., 2008; Mitra et al., 2012; Olsen et al., 2010). This serine is conserved down to *Drosophila* and since the fruit flies can model malignant overgrowth of hematopoietic cells, it would be very interesting to investigate whether it could be phosphorylated in response to Upd2 and if it is responsible for tumour formation in flies (Luo et al., 1995).

Other modifications like sumoylation or acetylation can also regulate STAT92E. STAT92E was shown to be sumoylated on a non-conserved residue on the N-terminus of the protein, which inhibited signalling (Gronholm et al., 2010). A similar negative effect was seen in mammalian STAT1 and 5. However, this sumoylation occurred on the C-terminal end of the proteins and was not conserved down to *Drosophila* (Lim and Cao, 2006). This does not preclude its being sumoylated on another site.

The acetylation of STAT proteins has been shown under several different conditions, however the occurrence of this modification on STAT92E has yet to be observed (Korzus et al., 1998; Shankaranarayanan et al., 2001; Wang et al., 2005b; Wieczorek et al., 2012; Yuan et al., 2005).

Most of these modifications are found in mammalian cancer cells, where an up- or downregulation of JAK/STAT signalling occurred due to, for instance, the mutation of JAKs. Obviously, this could lead to artificial modifications, but importantly it indicates that these modifications have the potential to be implemented in the regulation of JAK/STAT signalling.

Mammalian STAT acetylation in general seems to enhance JAK/STAT signalling (Kramer, 2013). It would be interesting to see whether such modification is conserved down to *Drosophila* and if it could be responsible for differential signalling. Enok, a putative histone acetyltransferase was found in several JAK/STAT screens to positively regulate its signalling (Baeg et al., 2005; Kallio et al., 2010; Muller et al., 2005). Interestingly, cells depleted of Enok increased their JAK/STAT signalling upon stimulation with Upd, whereas the expression of a hyperactivated kinase (Hop^{tum}) caused a decrease in pathway activation (Kallio et al., 2010). This could reflect a missregulation of the JAK/STAT signalling as discussed in section 6.5.1.1. Furthermore, it also could indicate ligand-independent pathway activation (section 6.2.2)

Interestingly, there are a few reports suggesting various post-translational modifications that act as molecular switches to regulate STAT activity. Van Nguyen et al hypothesised that STAT1 sumoylation and acetylation have opposing effects, since they show that the

sumoylation of a residue close to the activating tyrosine can negatively influence acetylation (Van Nguyen et al., 2011). Furthermore, a switch between acetylation and phosphorylation of STAT1 was shown and the authors suggested it to act as a cycle to limit the duration of cytokine signalling (Kramer et al., 2009).

The effect and occurrence of methylation on a highly conserved arginine in the very N-terminus is still extensively discussed in the literature (Duong et al., 2004; Mowen et al., 2001; Stark and Darnell, 2012). Future analysis of STAT92E could add to this discussion. On one hand, due to the linear pathway and evolutionary position it could enlighten whether the methylation is essential or a later acquired modification used to fine-tune the complex mammalian pathway. On the other hand further studies of STAT92E will add a level of complexity into the regulation of JAK/STAT by implicating the endocytic cycle as a possible regulatory element.

The characterisation of STAT92E has progressed well within the last years. We know from structure function analysis that a methionine M-647 is responsible for DNA binding and the conserved Y-711 crucial for pathway activation (Karsten et al., 2006; Yan et al., 1996). These structure-function analyses used transfected tagged STAT92E carrying various point mutations. I showed that endogenous STAT92E band shifts on a SDS gel when phosphorylated. However neither Myc-, HA- nor GFP- tagged STAT92E transfected into $S2R^{+}$ cells performed a bandshift upon ligand treatment (data not shown). Thus, unfortunately, I could not use the bandshift ability of endogenous STAT92E to undertake similar structure function analysis of known and putative modification sites of STAT92E, addressing its observed increased phosphorylation.

6.5.3 Differential signalling due to distinct STAT binding sites?

The *10xSTATLuc* reporter used in this study consists of five tandem repeats of a 441-bp fragment found upstream of *SOCS36E*, containing two potential 3n STAT92E binding sites (TTCnnnGAA) (Baeg et al., 2005). This raises the concern, that the observed Clathrin-dependent, Rab5-independent signalling, with the observed differences to the target mRNA expression are due to an artefact of the reporter used, since the promoter of the luciferase in an artificially constructed sequence and does not truly represent an endogenous JAK/STAT target.

Even though the *10xSTATLuc* represents an artificial JAK/STAT target, my study shows that the endocytic pathway is able to distinguish at least two distinct targets (a.) the *10xSTATLuc* and b.) the mRNA of *SOCS36E* and *Domeless*). Although both

methods of measuring JAK/STAT activation use very similar 3n STAT binding sites, the differences in the number of binding sites and its surroundings could be sufficient for the distinct transcriptional activity, controlled by STAT92E, as suggested in this study.

My data suggests that STAT92E binding upon Upd2 simulation of the *10xSTATLuc* reporter is differentially regulated by the endocytic pathway. It is possible that STAT92E needs a co-transcription factor to activate certain targets. The induction of the JAK/STAT target, *Domeless*, for instance is dependent on the presence of the co-transcription factor Tinnman (Rivas et al., 2008). Nevertheless, the occurrence and/or action of such co-regulators could be still controlled by the endocytic pathway and further experiments are necessary to confirm these suggestions. Ultimately, it would be ideal to analyse transcriptional target activation, which is regulated by an AP2/Clathrin dependent, but Rab5 independent compartment.

The chosen targets *SOCS36E* and *Domeless* are controlled by two different STAT92E binding sites. Whereas SOCS36E expression is regulated by a 3n STAT binding site, *Domeless* mRNA is controlled by a 4n site (Muller et al., 2005; Rivas et al., 2008). These differences could be the key to activate subsets of genes under certain conditions, aided by the compartmentalisation of the pathway by endocytic structures. STAT92E binds more strongly to 3n sites (Rivas et al., 2008) and I observed stronger pathway activation for *SOCS36E* than for *Domeless* mRNA Figure 4.19. In addition in general expression of *SOCS36E* mRNA was less affected by the knockdown of regulatory proteins, like Clathrin or RacGAPs Figure 4.18 and Figure 4.22. Ideally more JAK/STAT targets containing 3n and 4n STAT binding sites should be addressed before a final conclusion can be made (see also 6.4.1.1).

As an alternative approach, an electrophoretic mobility shift assay (EMSA) analysis to address whether the endocytic knockdowns affect the ability of STAT92E to bind DNA could be performed. It would also be of interest to know whether STAT92E binds differentially to its 3n or 4n binding site, when activated from distinct endocytic compartments. Conversely, JAK/STAT targets identified by Bina et al 2010, did not seem to be influenced in their strength of activation/repression upon pathway stimulation neither by the number nor quality of their STAT92E binding sites (Bina et al., 2010).

6.5.4 Nuclear import

Once phosphorylated, STAT proteins have to shuttle into the nucleus in order to activate transcription. I investigated whether the nuclear import of STAT92E is regulated by endocytic events, by analysing nuclear and cytosolic cell fractions. With this I not only could investigate the cellular localisation of STAT, but also its phosphorylation state.

I showed in section 5.1.1, that STAT92E phosphorylation peaked after 30 min ligand stimulation and resulted subsequently in the decrease of phosphorylation (as discussed above). Phosphorylated STAT92E could be detected in the nuclear fraction, shortly after stimulation with Upd2-GFP, however, accumulation of phospho-STA92E only occurred after 60 min ligand stimulation (Figure 5.17). In addition to bio-chemical fractionation, I also investigated the translocation of STAT92E into the nucleus by microscopy. Preliminary microscopy experiments showed an enhanced signal of STAT92E in the nucleus only after 45 min continuous ligand simulation (data not shown).

This suggests that a continuous ligand stimulation of the JAK/STAT pathway is necessary to enrich phospho-STAT92E in the nucleus. Additionally it could reveal a time-dependent more efficient nuclear import. These preliminary data sets need additional repeats to allow to drawing concrete conclusions. Further analysis and even further extended time courses would be necessary to confirm this late accumulation of phospho-STAT92E in the nucleus.

By contrast, mammalian STAT translocates relatively quickly into the nucleus. Phosphorylated STAT6 for instance is enriched in the nucleus after only 15 minutes, interestingly this enrichment is suggested to be due to a decrease in nuclear export (Chen and Reich, 2010). It seems thus that nuclear accumulation of phospho-STAT92E requires more than 15 min. To support this statement more evidence needs to be collected.

A disadvantage of the fractionation protocol used is the possible precipitation of DNA bound proteins while preparing the whole cell lysates for analysis on the SDS PAGE gel. In order to investigate this, additional fractionation of the nuclear fraction in DNA bound and soluble components, would also address this how much phospho-STAT92E binds to DNA and could be used in the conjunction with Clathrin or AP2 knockdown. This displays an advantage of using the biochemical analysis of STAT92E translocation compared, for instance, to using microscopy and following thus the translocation of STAT92E into the nucleus. The additional fractionation of the nuclear fraction in DNA-

bound and soluble proteins could also provide further insight on STAT92E properties by endocytic components.

The translocation of phosphorylated STAT92E into the nucleus correlates with its activity. In cells transfected with the kinase, Hop, an increase in pathway activity is observed and most of P-STAT92E translocates into the nucleus (Karsten et al., 2006). Within this publication the detection of phosphorylated STAT92E by immunofluorescence was still possible. Unfortunately, the antibody detecting P-STAT92E is not available anymore. Although pathway activation and presumably STAT92E translocation is much stronger when overexpressing Hop (Karsten et al., 2006), instead of activating the pathway with its ligand (this study), the constant activation of the JAK/STAT pathway by transfecting the kinase, did not enable me to use this method of enhancing the translocation of STAT92E. Since I wanted to study early steps in endocytosis controlling JAK/STAT I relied on pathway stimulation by the ligand within a limited time frame. And even though nuclear translocation of STAT92E is an elegant way to study the JAK/STAT pathway, either very constant activation (transfection of Hop) or longer ligand exposure is necessary for this event to occur.

The block of JAK/STAT ligand internalisation, by overexpression of the dominant negative form of Shibire (Dynamin in mammals) blocked the nuclear translocation of STAT92E in the developing egg, suggesting thus endocytosis to be a positive regulator of JAK/STAT signalling (Silver et al., 2005b). Also growth factor-induced STAT3 nuclear translocation is inhibited when endocytosis was blocked by inhibitors or Clathrin was knocked down (Bild et al., 2002; Kermorgant and Parker, 2008).

These examples illustrate that nuclear import of STAT is often used to indicate JAK/STAT pathway activation (for instance (Devergne et al., 2007; Kermorgant and Parker, 2008). Nevertheless, especially within the study of Devergne et al 2007, this method was difficult to apply, since the total levels of STAT92E in follicle cells was strongly reduced in *clathrin* mutant clones and it becomes thus difficult to analyse STAT92E nuclear localisation (Devergne et al., 2007). However, the authors additionally addressed signalling with a JAK/STAT specific reporter (Devergne et al., 2007).

6.5.5 Novel regulators?

I wanted to explore what causes the differential signalling and enhanced phosphorylation by Domeless when endocytosis is inhibited. After a literature research

I decided on a few promising candidates, which were implicated with either JAK/STAT signalling control or the regulation of endocytosis.

My starting point was a JAK/STAT modifier screen which had suggested several regulators of STAT92E phosphorylation (Baeg et al., 2005). This study identified many transcription factors and proteins with (predicted) DNA binding properties, but also Ptp61, which altered Hop and STAT92E phosphorylation. It was interesting to investigate whether these kinases/phosphatases also alter endogenous phospho-STAT92E levels. The knockdown of Ptp61F, however, resulted in a ligand-independent increase of *SOCS36E* and *Domeless* mRNA Figure 4.20. We interpret these findings as a stress related response to the knockdown as discussed above.

The transcription factor Taf1 also gained my attention, since it negatively regulates the Upd-induced 10xSTAT92E reporter activity, whereas TotM-reporters are positively influenced by Taf1 (Kallio et al., 2010). Taf1 could act for instance as a co-tanscription factor for JAK/STAT signalling and thus enable differential signal activation.

Furthermore, Not4 a protein part of the Ccr4-Not complex and responsible for protein quality control was shown to be a regulator of JAK/STAT (Collart et al., 2013). It would be interesting to study, since it binds to STAT92E, but does not change its phosphorylation state (Baeg et al., 2005). However, Not4 knockdown was shown to decrease several JAK/STAT targets, including the *10xSTATLuc* reporter, *totA* and *totM* mRNA and controlled luciferase reporters, and also its over-expression increases stress response even independent of *E. coli* infection (Kallio et al., 2010). The model of action of Not4 is apparently independent of its Ring domain, which includes an E4-Ubiquitin ligase. This is further evidence that STAT ubiquitination does not play a major role in its regulation (as discussed in 5.3.6 & 6.5.2.1).

Since there was no evidence, to my knowledge, that these JAK/STAT regulators were controlled by or linked to the endocytic pathway, I wondered whether proteins, which are not transcription factors, were more likely to link the transcriptional output and STAT92E phosphorylation within the endocytic pathway. Therefore I focussed my attention on Myopic and RacGAPs.

6.5.5.1 Myopic

A good candidate to link endocytosis, phosphorylation and signal activation of STAT92E is the *D. melanogaster* protein Myopic, ortholog to the mammalian HD-PTP. It contains a Bro1-Domain, with which Myopic is able to bind to the ESCRT III

complex, and a tyrosine phosphatase domain. It was also found to negatively modulate both pathway activation and receptor dimerisation in two independent JAK/STAT cell-based RNAi screens (Wright and Fisher, personal communication).

Here, I show that Myopic knockdown blocks the activation of *Domeless* mRNA as a target, whereas *SOCS36E* mRNA expression is induced as normal (Figure 4.18). However, further investigations and repeats would be necessary to conclude a qualitative difference in signalling. Furthermore, the remaining Myopic protein concentration may have been still high enough to trigger only *SOCS36E*, but not *Domeless* mRNA induction upon Upd2-GFP incubation, since the *SOCS36E* mRNA response might be more sensitive to Upd2 and more robust in regards to the depletion of JAK/STAT regulators.

The depletion of Rab5 results in the increase of Dome protein levels (K. Fisher personal communication). Interestingly, Myopic knockdown also led to increased Dome. Furthermore, it was observed that Dome levels were more strongly increased when the pathway was activated by addition of pathway ligand (K. Fisher personal communication). Together with my data this indicates that increased receptor levels might lead to pathway inhibition. More experimental data and specifically repeats of these results using identical systems (cell types, duration and strength of stimulation ect.) are essential to confirm this model.

Myopic has previously been shown to regulate Toll, Hippo and EGFR signalling, whilst acting within the ESCRT machinery (Gilbert et al., 2011; Huang et al., 2010; Miura et al., 2008). The activity of the Hippo co-tanscription factor Yorkie for instance is regulated by Myopic via a mechanism involving direct binding and modulation of Yorkie endosomal association. Interestingly, Myopic mutant cells influenced only some Hippo pathway targets (Gilbert et al., 2011).

Differential target activation by myopic did not seem to depend on its phosphatase activity. In addition, other evidence suggest that Myopic's phosphatase domain is not functional. My results show no change in phosphorylation of STAT92E, when Myopic was knocked down, suggesting that it is not a substrate for the phosphatase Figure 5.8. It also has been demonstrated that its human ortholog, HD-PTP, has a functional form with an inactive phosphatase domain (Gingras et al., 2009) and biochemical analysis has shown very little phosphatase activity for Myopic (Chen et al., 2012) .

6.5.5.2 RacGAP and Tumbleweed

Another possible group of regulators of JAK/STAT signalosomes are RacGAPs. Even though the proteins are not regulated by or part of the endocytic pathway, publications from the Kitamura laboratory revealed a role of MgcRacGAP for the nuclear localisation and activation of STATs in a unique way (Kawashima et al., 2009; Kawashima et al., 2006). Hence I wondered about their role in *Drosophila* JAK/STAT signalling. The *Drosophila* homologue Rotund (or also RacGAP50C) does not contain the domain responsible for STAT import. A blast with this part of McgRacGAP however, found high sequence identities with Tumbleweed, one of 16 RacGAPs in *Drosophila*. Therefore, I decided to investigate the influence of both proteins in JAK/STAT signalling.

My preliminary data suggests a decrease in mRNA targets upon dsRNA knockdown, especially *Domeless* mRNA seem to be affected (Figure 4.22). This could be due to residual protein remaining after the knockdown and *SOCS36E* expression is less sensitive to levels of regulatory proteins. The phosphorylation of STAT92E however does not appear to be altered by either of these two RacGAPs (Figure 5.9). Experiments to address whether these factors also influence STAT92E nuclear import still need to be undertaken. It additionally would be of interest to address the role of RacGAPs *in vivo* in the JAK/STAT pathway, since Tumbleweed was shown to regulate EGFR and Wnt signalling during *Drosophila* development (Jones and Bejsovec, 2005; Sotillos and Campuzano, 2000).

6.5.6 Signalosomes *in vivo*

To analyse JAK/STAT signalosomes in detail, I would also like to include *in vivo* analysis of the signalling. The use of tissue culture cells has many advantages and I exploited them in the start of this project since I did not find an appropriate *in vivo* system at first. However, having established a scaffold, which demonstrates JAK/STAT signalosomes, I am confident my findings can be translated into an *in vivo* system.

Assays with cultured cells are easy to manipulate, especially I could control well when and for how long the ligand activates the pathway. Such a temporal restriction is more difficult to realise *in vivo*. However the fast developing embryo, could be an excellent model to study JAK/STAT signalling, since ligand expression is spatially and temporally controlled (Johnson et al., 2011). Using defined developmental stages several JAK/STAT targets have been studied (Rivas et al., 2008; Sotillos et al., 2010).

The endocytic control of the pigmentation protein, Yellow, by Megalin, a low-density lipoprotein receptor-related protein, was described recently to be regulated by endocytosis (Riedel et al., 2011). The question remained open of how is the endocytic pathway able to distinguish between distinct regions to ensure the melanisation of hairs only. Historically endocytosis in *Drosophila* was studied within the compound eye. The bride of sevenless (Boss) ligand is a transmembrane protein expressed on the surface of R8 photoreceptor cells in *Drosophila*. It binds to its receptor on neighbouring cells, where the ligand-receptor complex is endocytosed (Kohyama-Koganeya and Hirabayashi, 2010). A HRP-Boss chimera serves as a convenient tool for analysing endocytic traffic (Chang et al., 2004; Chang et al., 2002; Sunio et al., 1999).

An alternative to these *in vivo* studies would be consideration with *ex vivo* analysis of for instance Garland cells, which are nephrocyte type cells within the third instar larvae. Most *in vivo* assays would not allow me to control the ligand exposure precisely, temporally and spatially. However, their signalling processes are poorly investigated and ligand-receptor interactions have not been studied to a great extent (Chang et al., 2002; Chanut-Delalande et al., 2010; Kosaka and Ikeda, 1983; Vijayakrishnan et al., 2009).

6.6 Conclusion and future perspectives

Within this thesis I described how the block of early endocytosis by AP2 and Clathrin knockdown resulted in the failure to induce Upd2-dependent JAK/STAT signalling. I also demonstrated that the same block resulted in an enhanced STAT92E phosphorylation. Surprisingly STAT92E was phosphorylated on the functionally important Y-711, when AP2 was depleted. This led me to the conclusion that there was an additional regulation of STAT92E. This novel level of modification is quite likely due to phosphorylation, since I observed increased phosphorylated STAT92E, when AP2 was knocked down.

There are numerous reports describing the regulation and identifying novel regulators of JAK/STAT. Often the questions remain open of how are these modifiers regulated. One possibility of an additional level of regulation is the trafficking pathway. It provides the cell with platform for differential signalling, signalosomes. These signalosomes have been implemented for various signalling pathways.

Signalosomes were first described for EGFR signalling (Vieira et al., 1996) and ever since the number of pathways controlled by signalosomes has increased rapidly. Here I

present data, which indicates the existence of signalosomes for JAK/STAT signalling. I furthermore suggest that the transcription factor, STAT92E is differentially modified due course of the trafficking pathway, although this hypothesis needs additional evidences to pinpoint the molecular mechanism of signal regulation.

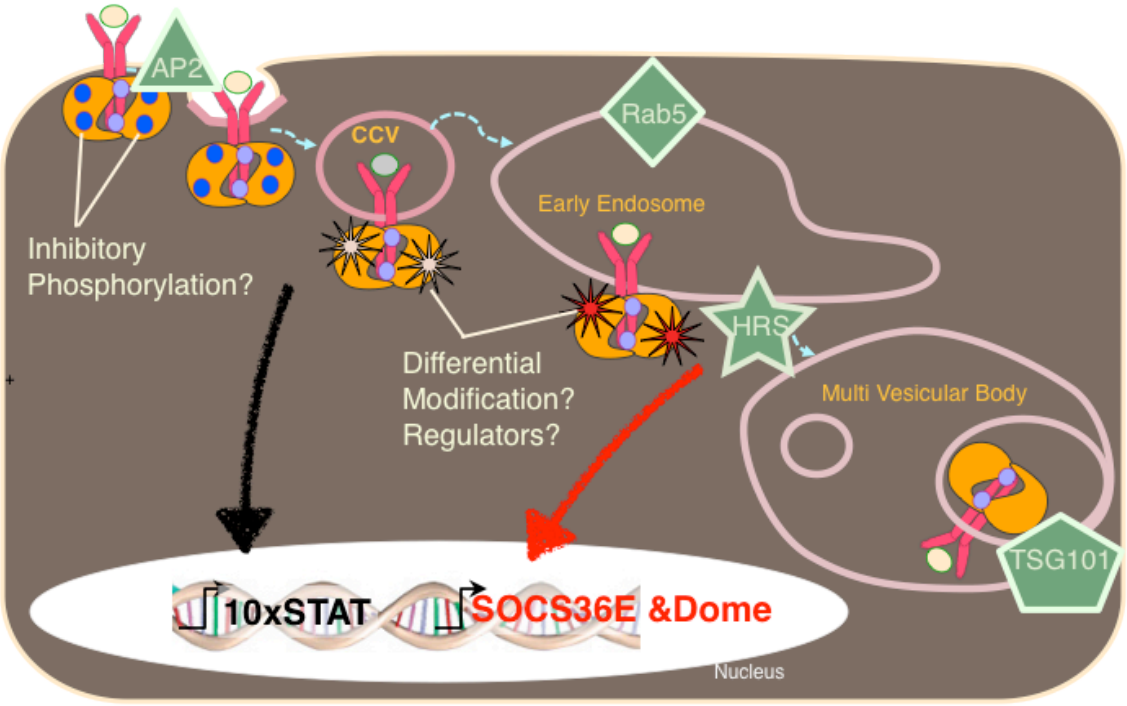

Figure 6.2: Model of JAK/STAT signalling and STAT92E modification

Here I propose that STAT is differentially modificated while travelling through the endocytic pathway, this could be either by phosphorylation or other post-translational modification or even additional binding partners. These modification(s) still remain to be identified.

There are two main focus points future research should address; on the one hand to extend the analysis of JAK/STAT targets, in order to draw a more comprehensive picture of the JAK/STAT signalosome, on the other hand to translate my findings into an *in vivo* system, thus we would be able to ascertain the functional impact of JAK/STAT signalosomes.

The JAK/STAT signalosome equips the cell with a mechanism to separate differential signals. This allows precise cellular responses to environmental changes. Within the developing egg for instance Upd is expressed in follicle cells in both the anterior and the posterior pole, however only anterior follicle cells allow the development of border cells and their migration to the oocyte. Not only JAK/STAT signalling ensures this specific

developmental process, but also other signalling pathways from the cellular environment. The endocytic pathway allows the cell to physically make compartments, which distinguish and activate subsets of signals, allowing it to respond specifically to a certain environment.

The understanding of these globally processes still remain very patchy, but understanding the fundamental processes behind the regulation by signalosomes allows us to draw models and drive research in more complex directions.

The knowledge of the influence of endocytic events of signalling can be implemented in the development of novel drugs, and more importantly of their delivery or place of action. It could be possible that thus cancer drugs, targeting the JAK/STAT pathway only act in the endocytic vesicles, since their pH is different from the rest of the cell. This would allow the block of only certain targets, which might reduce possible side effects and or increase the specificity of used drugs.

Unfortunately, we are still a long way away from the use of such specialised medication, but the basic understanding of pathways regulating signalling and thus JAK/STAT related cancers, helps us to start to grasp the immense complexity the natural system has provided us to control of signalling pathways to maintain a cellular homeostasis.

Abbreviations

AGC	automatic gain control
approx.	approximately
AP	adaptor protein
bp	base pair
CCP	Clathrin coated pit
CCV	Clathrin coated vesicle
cDNA	complementary Desoxynucleotidacid
CIP	calf intestine phosphatase
CM	conditioned medium
CRISPR	*c*lustered regularly interspaced short palindromic repeat
CORVET	class C core vacuole/endosome tethering factor
D. melanogaster	*Drosophila melanogaster*
DNA	desoxynucleotidacid
dsRNA	double stranded ribonucleic acid
DSS	disuccinimidyl suberate
E. coli	*Escherichia coli*
EEA1	early endosome antigen 1
ELISA	enzyme linked immunosorbent assay
EDT	electron transfer dissociation
EDTA	ethylene diamine tetraacetic acid
EGF(R)	epidermal growth factor (receptor)
EGTA	ethylene glycol tetraacetic acid
EMSA	electrophoretic mobility shift assay
ESCRT	endosomal sorting complexes required for transport
et. al.	et alia (latin for: and others)
g	gravity
GAP	GTPase-activating proteins
Gα	G-coupled α receptor
GEEC	GPI-AP-enriched early endosomal compartments
GDI	GDP dissociation inhibitor
GFP	green fluoresent protein
GTP	guanysyltriphophate
GEF	GTP exchange factor
h	hour
HEPES	4-(2-hydroxyethyl)-1-piperazineethanesulfonic acid
HGF	hepatocyte growth factor
HOPS	homotypic fusion and vacuole protein sorting
HPLC	high pressure liquid chromatography
ILV	intraluminal vesicles
IFNAR1	interferon alpha receptor 1
IFNGR1	interferon gamma receptor 1

IP	Immunopreciptiation
IPTG	Isopropyl β-D-1-thiogalactopyranoside
k	kilo
LB	Luria-Bertain
mAb	monoclonal antibody
MAPK	mitogen-activated protein kinase
min	minutes
mRNA	messenger ribonucleic acid
MS	mass spectrometry
MVB	multivesicular bodies
NLS	nuclear localisation signal
NSF	N-ethylmaleimide sensitive factor
O/N	over night
OM	oncostatin M
ODxxx	optical density at xxx nm
PAGE	polyacryl amin gel electrophoresis
PBS	phosphorsalinebuffer
PCR	polymerase chain reaction
pcv	posterior cross vein
phospho-STAT92E	phosphorylated STAT92E
P-STAT92E	phosphorylated STAT92E
PI3K	phosphatidylinositol 3-kinase
PI5P	phosphatidylinositol 5-phosphatase
PtdIns	phosphatidylinositol
qPCR	quantitative polymerase chain reaction
RKT	receptor tyrosine kinase
rpm	rounds per minute
RT	room temperature
SCT	supernatant collection tube
SDS	Sodium Dodecyl Sulfate
sec	seconds
SNARE	soluble NSF attachment protein receptor
SUMO	small ubiquitin-like modifier
TEMED	N-N-N'-N'' tetra methyl ethylene diamin
TGN	trans-Golgi network
Tris	Trishydroxymethylaminoethan
V	volts
v/v	volume / volume
w/v	weight / volume
wt	wild type
10xSTATLuc	10xSTAT luciferase

References

Aït-Slimane T1, Galmes R, Trugnan G, Maurice M., 2009, Basolateral internalization of GPI-anchored proteins occurs via a clathrin-independent flotillin-dependent pathway in polarized hepatic cells. Mol Biol Cell. 20(17):3792-800.

Agaisse, H., and N. Perrimon, 2004, The roles of JAK/STAT signaling in Drosophila immune responses: Immunological Reviews, v. 198, p. 72-82.

Agaisse, H., U. M. Petersen, M. Boutros, B. Mathey-Prevot, and N. Perrimon, 2003, Signaling role of hemocytes in Drosophila JAK/STAT-dependent response to septic injury: Developmental Cell, v. 5, p. 441-450.

Aguet, F. o., C. N. Antonescu, M. Mettlen, S. L. Schmid, and G. Danuser, 2013, Advances in Analysis of Low Signal-to-Noise Images Link Dynamin and AP2 to the Functions of an Endocytic Checkpoint: Developmental Cell, v. 26, p. 279-291.

Ait-Slimane, T., R. Galmes, G. Trugnan, and M. Maurice, 2009, Basolateral internalization of GPI-anchored proteins occurs via a clathrin-independent flotillin-dependent pathway in polarized hepatic cells: Molecular Biology of the Cell, v. 20, p. 3792-3800.

Alonso, V. n., and P. A. Friedman, 2013, Minireview: ubiquitination-regulated G protein-coupled receptor signaling and trafficking: Molecular endocrinology (Baltimore, Md.), v. 27, p. 558-572.

Amaddii, M., M. Meister, A. Banning, A. Tomasovic, J. Mooz, K. Rajalingam, and R. Tikkanen, 2012, Flotillin-1/reggie-2 protein plays dual role in activation of receptor-tyrosine kinase/mitogen-activated protein kinase signaling: The Journal of Biological Chemistry, v. 287, p. 7265-7278.

Arbouzova, N. I., E. A. Bach, and M. P. Zeidler, 2006, Ken & Barbie Selectively Regulates the Expression of a Subset of JAK/STAT Pathway Target Genes: Current Biology, v. 16, p. 80-88.

Arbouzova, N. I., and M. P. Zeidler, 2006, JAK/STAT signalling in Drosophila: insights into conserved regulatory and cellular functions: Development, v. 133, p. 2605-2616.

Assaker, G., D. Ramel, S. K. Wculek, M. Gonz√°lez-Gait√°n, and G. Emery, 2010, Spatial restriction of receptor tyrosine kinase activity through a polarized endocytic cycle controls border cell migration: Proceedings of the National Academy of Sciences, v. 107, p. 22558-22563.

Avraham, R., and Y. Yarden, 2011, Feedback regulation of EGFR signalling: decision making by early and delayed loops: Nature reviews. Molecular cell biology, v. 12, p. 104-117.

Babst, M., D. J. Katzmann, W. B. Snyder, B. Wendland, and S. D. Emr, 2002, Endosome-associated complex, ESCRT-II, recruits transport machinery for protein sorting at the multivesicular body: Developmental Cell, v. 3, p. 283-289.

Bach, E. A., L. A. Ekas, A. Ayala-Camargo, M. S. Flaherty, H. Lee, N. Perrimon, and G.-H. Baeg, 2007, GFP reporters detect the activation of the Drosophila JAK/STAT pathway in vivo: Gene expression patterns: GEP, v. 7, p. 323-331.

Bach, E. A., S. Vincent, M. P. Zeidler, and N. Perrimon, 2003, A sensitized genetic screen to identify novel regulators and components of the Drosophila janus

kinase/signal transducer and activator of transcription pathway: Genetics, v. 165, p. 1149-1166.
Bache, K. G., A. Brech, A. Mehlum, and H. Stenmark, 2003, Hrs regulates multivesicular body formation via ESCRT recruitment to endosomes: The Journal of Cell Biology, v. 162, p. 435-442.
Bache, K. G., T. Slagsvold, A. Cabezas, K. R. Rosendal, C. Raiborg, and H. Stenmark, 2004, The growth-regulatory protein HCRP1/hVps37A is a subunit of mammalian ESCRT-I and mediates receptor down-regulation: Molecular Biology of the Cell, v. 15, p. 4337-4346.
Bache, K. G., S. Stuffers, L. Maler√∏d, T. Slagsvold, C. Raiborg, D. Lechardeur, S. b. W√§lchli, G. L. Lukacs, A. Brech, and H. Stenmark, 2006, The ESCRT-III subunit hVps24 is required for degradation but not silencing of the epidermal growth factor receptor: Molecular Biology of the Cell, v. 17, p. 2513-2523.
Baeg, G.-H., R. Zhou, and N. Perrimon, 2005, Genome-wide RNAi analysis of JAK/STAT signaling components in Drosophila: Genes & Development, v. 19, p. 1861-1870.
Baena-Lopez, L. A., C. Alexandre, A. Mitchell, L. Pasakarnis, and J.-P. Vincent, 2013, Accelerated homologous recombination and subsequent genome modification in Drosophila: Development, v. 140, p. 4818-4825.
Balaji, K., and J. Colicelli, 2012, RIN1 regulates cell migration through RAB5 GTPases and ABL tyrosine kinases: Communicative & integrative biology, v. 6.
Balaji, K., C. Mooser, C. M. Janson, J. M. Bliss, H. Hojjat, and J. Colicelli, 2013, RIN1 orchestrates the activation of RAB5 GTPases and ABL tyrosine kinases to determine the fate of EGFR: Journal of Cell Science, v. 125, p. 5887-5896.
Banninger, G., and N. C. Reich, 2004, STAT2 nuclear trafficking: The Journal of Biological Chemistry, v. 279, p. 39199-39206.
Barbieri, M. A., C. Kong, P.-I. Chen, B. F. Horazdovsky, and P. D. Stahl, 2003, The SRC homology 2 domain of Rin1 mediates its binding to the epidermal growth factor receptor and regulates receptor endocytosis: The Journal of Biological Chemistry, v. 278, p. 32027-32036.
Barr, F., and D. G. Lambright, 2010, Rab GEFs and GAPs: Current Opinion in Cell Biology, v. 22, p. 461-470.
Bazan JF., 1990, Haemopoietic receptors and helical cytokines. Immunol Today. V 11(10):350-4.
Beas, A. O., V. Taupin, C. Teodorof, L. T. Nguyen, M. Garcia-Marcos, and M. G. Farquhar, 2012, Galphas promotes EEA1 endosome maturation and shuts down proliferative signaling through interaction with GIV (Girdin): Molecular Biology of the Cell, v. 23, p. 4623-4634.
Bild, A. H., J. Turkson, and R. Jove, 2002, Cytoplasmic transport of Stat3 by receptor-mediated endocytosis: EMBO J, v. 21, p. 3255-3263.
Bina, S., V. M. Wright, K. H. Fisher, M. Milo, and M. P. Zeidler, 2010, Transcriptional targets of Drosophila JAK/STAT pathway signalling as effectors of haematopoietic tumour formation: EMBO reports, v. 11, p. 201-207.
Binari, R., and N. Perrimon, 1994, Stripe-specific regulation of pair-rule genes by hopscotch, a putative Jak family tyrosine kinase in Drosophila: Genes & Development, v. 8, p. 300-312.

Blair, S. S., 2007, Wing Vein Patterning in Drosophila and the Analysis of Intercellular Signaling: Annual Review of Cell and Developmental Biology, v. 23, p. 293-319.

Blouin, C. d. M., and C. Lamaze, 2013, Interferon Gamma Receptor: The Beginning of the Journey: Frontiers in Immunology, v. 4.

Blumer, J., J. Rey, L. Dehmelt, T. Mazel, Y.-W. Wu, P. Bastiaens, R. S. Goody, and A. Itzen, 2012, RabGEFs are a major determinant for specific Rab membrane targeting: The Journal of Cell Biology, v. 200, p. 287-300.

Bonifacino JS1, Traub LM., 2003 Signals for sorting of transmembrane proteins to endosomes and lysosomes. Annu Rev Biochem. v ;72:395-447.

Boudny, V., and J. Kovarik, 2002, JAK/STAT signaling pathways and cancer. Janus kinases/signal transducers and activators of transcription: Neoplasma, v. 49, p. 349-355.

Brankatschk, B., S. P. Wichert, S. D. Johnson, O. Schaad, M. J. Rossner, and J. Gruenberg, 2012, Regulation of the EGF transcriptional response by endocytic sorting: Science Signaling, v. 5.

Brodsky, F. M., 2012, Diversity of Clathrin Function: New Tricks for an Old Protein: Annual Review of Cell and Developmental Biology, v. 28, p. 309-336.

Brown, S., N. Hu, and J. C. Hombr√≠a, 2001a, Identification of the first invertebrate interleukin JAK/STAT receptor, the Drosophila gene domeless: Current Biology: CB, v. 11, p. 1700-1705.

Brown, S., N. Hu, and J. C.-G. Hombr√≠a, 2003, Novel level of signalling control in the JAK/STAT pathway revealed by in situ visualisation of protein-protein interaction during Drosophila: Development, v. 130, p. 3077-3084.

Brown, S., N. Hu, and J. C.-G. Hombr*f*±ÃÅa, 2001b, Identification of the first invertebrate interleukin JAK/STAT receptor, the Drosophila gene domeless: Current Biology, v. 11, p. 1700-1705.

Bucci, C., R. G. Parton, I. H. Mather, H. Stunnenberg, K. Simons, B. Hoflack, and M. Zerial, 1992, The small GTPase rab5 functions as a regulatory factor in the early endocytic pathway: Cell, v. 70, p. 715-728.

Butchar, J. P., D. Cain, S. N. Manivannan, A. D. McCue, L. Bonanno, S. Halula, S. Truesdell, C. L. Austin, T. L. Jacobsen, and A. Simcox, 2012, New Negative Feedback Regulators of Egfr Signaling in Drosophila: Genetics, v. 191, p. 1213-1226.

Cacalano, N. A., D. Sanden, and J. A. Johnston, 2001, Tyrosine-phosphorylated SOCS-3 inhibits STAT activation but binds to p120 RasGAP and activates Ras: Nature Cell Biology, v. 3, p. 460-465.

Cai, H., H. Shim, C. Lai, C. Xie, X. Lin, W. J. Yang, and J. Chandran, 2008, ALS2/alsin knockout mice and motor neuron diseases: Neuro-degenerative diseases, v. 5, p. 359-366.

Callus, B. A., and B. Mathey-Prevot, 2002, SOCS36E, a novel Drosophila SOCS protein, suppresses JAK/STAT and EGF-R signalling in the imaginal wing disc: Oncogene, v. 21, p. 4812-4821.

Carbone CJ1, Zheng H, Bhattacharya S, Lewis JR, Reiter AM, Henthorn P, Zhang ZY, Baker DP, Ukkiramapandian R, Bence KK, Fuchs SY., 2012, Protein tyrosine phosphatase 1B is a key regulator of IFNAR1 endocytosis and a target for antiviral therapies. Proc Natl Acad Sci U S A. v 20;109(47):19226-31.

Cardenas, A. M., and F. D. Marengo, 2012, Rapid endocytosis and vesicle recycling in neuroendocrine cells: Cellular and molecular neurobiology, v. 30, p. 1365-1370.
Carney, D. S., B. A. Davies, and B. F. Horazdovsky, 2006, Vps9 domain-containing proteins: activators of Rab5 GTPases from yeast to neurons: Trends in Cell Biology, v. 16, p. 27-35.
Chadda, R., M. T. Howes, S. J. Plowman, J. F. Hancock, R. G. Parton, and S. Mayor, 2007, Cholesterol-sensitive Cdc42 activation regulates actin polymerization for endocytosis via the GEEC pathway: Traffic (Copenhagen, Denmark), v. 8, p. 702-717.
Chang, H. C., M. Hull, and I. Mellman, 2004, The J-domain protein Rme-8 interacts with Hsc70 to control clathrin-dependent endocytosis in Drosophila: The Journal of Cell Biology, v. 164, p. 1055-1064.
Chang, H. C., S. L. Newmyer, M. J. Hull, M. Ebersold, S. L. Schmid, and I. Mellman, 2002, Hsc70 is required for endocytosis and clathrin function in Drosophila: The Journal of Cell Biology, v. 159, p. 477-487.
Chanut-Delalande, H. l. n., A. C. Jung, M. M. Baer, L. Lin, F. o. Payre, and M. Affolter, 2010, The Hrs/Stam Complex Acts as a Positive and Negative Regulator of RTK Signaling during Drosophila Development: PLoS ONE, v. 5.
Chaturvedi, A., R. Martz, D. Dorward, M. Waisberg, and S. K. Pierce, 2011, Endocytosed BCRs sequentially regulate MAPK and Akt signaling pathways from intracellular compartments: Nature immunology, v. 12, p. 1119-1126.
Chavrier, P., R. G. Parton, H. P. Hauri, K. Simons, and M. Zerial, 1990, Localization of low molecular weight GTP binding proteins to exocytic and endocytic compartments: Cell, v. 62, p. 317-329.
Chen, D.-Y., M.-Y. Li, S.-Y. Wu, Y.-L. Lin, S.-P. Tsai, P.-L. Lai, Y.-T. Lin, J.-C. Kuo, T.-C. Meng, and G.-C. Chen, 2012, The Bro1-domain-containing protein Myopic/HDPTP coordinates with Rab4 to regulate cell adhesion and migration: Journal of Cell Science, v. 125, p. 4841-4852.
Chen, H.-C., and N. C. Reich, 2010, Live Cell Imaging Reveals Continuous STAT6 Nuclear Trafficking: The Journal of Immunology, v. 185, p. 64-70.
Chen, X., U. Vinkemeier, Y. Zhao, D. Jeruzalmi, J. E. Darnell, Jr., and J. Kuriyan, 1998, Crystal structure of a tyrosine phosphorylated STAT-1 dimer bound to DNA: Cell, v. 93, p. 827-839.
Christoforidis, S., H. M. McBride, R. D. Burgoyne, and M. Zerial, 1999a, The Rab5 effector EEA1 is a core component of endosome docking: Nature, v. 397, p. 621-625.
Christoforidis, S., M. Miaczynska, K. Ashman, M. Wilm, L. Zhao, S.-C. Yip, M. D. Waterfield, J. M. Backer, and M. Zerial, 1999b, Phosphatidylinositol-3-OH kinases are Rab5 effectors: Nat Cell Biol, v. 1, p. 249-252.
Christoforidis, S., and M. Zerial, 2000, Purification and Identification of Novel Rab Effectors Using Affinity Chromatography: Methods, v. 20, p. 403-410.
Cimica, V., H.-C. Chen, J. K. Iyer, and N. C. Reich, 2011, Dynamics of the STAT3 Transcription Factor: Nuclear Import Dependent on Ran and Importin-?: PLoS ONE, v. 6.
Clague, M. J., and S. Urbe, 2001, Ubiquitin: Same Molecule, Different Degradation Pathways: Cell, v. 143, p. 682-685.

Claudinon, J., M.-N. l. Monier, and C. Lamaze, 2007, Interfering with interferon receptor sorting and trafficking: Impact on signaling: Biochimie, v. 89, p. 735-743.

Cocucci, E., F. o. Aguet, S. Boulant, and T. Kirchhausen, 2012, The first five seconds in the life of a clathrin-coated pit: Cell, v. 150, p. 495-507.

Collart, M. A., O. O. Panasenko, and S. I. Nikolaev, 2013, The Not3/5 subunit of the Ccr4-Not complex: A central regulator of gene expression that integrates signals between the cytoplasm and the nucleus in eukaryotic cells: Cellular Signalling, v. 25, p. 743-751.

Constantinescu SN, Huang LJ, Nam H, Lodish HF., 2001, The erythropoietin receptor cytosolic juxtamembrane domain contains an essential, precisely oriented, hydrophobic motif. Mol Cell. v 7(2):377-85.

Couturier C1, Jockers R., 2003, Activation of the leptin receptor by a ligand-induced conformational change of constitutive receptor dimers. J Biol Chem. v 18;278(29):26604-1

Croker, B. A., H. Kiu, and S. E. Nicholson, 2008, SOCS regulation of the JAK/STAT signalling pathway: Seminars in Cell & Developmental Biology, v. 19, p. 414-422.

Dagil R, Knudsen MJ, Olsen JG, O'Shea C, Franzmann M, Goffin V, Teilum K, Breinholt J, Kragelund BB., 2012, The WSXWS motif in cytokine receptors is a molecular switch involved in receptor activation: insight from structures of the prolactin receptor. Structure. v 8;20(2):270-82.

Damke, H., T. Baba, A. M. van der Bliek, and S. L. Schmid, 1995, Clathrin-independent pinocytosis is induced in cells overexpressing a temperature-sensitive mutant of dynamin: The Journal of Cell Biology, v. 131, p. 69-80.

Daub, H., J. V. Olsen, M. Bairlein, F. Gnad, F. S. Oppermann, R. K√∂rner, Z. n. Greff, G. r. K√©ri, O. Stemmann, and M. Mann, 2008, Kinase-selective enrichment enables quantitative phosphoproteomics of the kinome across the cell cycle: Molecular cell, v. 31, p. 438-448.

de Renzis, S., B. S√∂nnichsen, and M. Zerial, 2002, Divalent Rab effectors regulate the sub-compartmental organization and sorting of early endosomes: Nature Cell Biology, v. 4, p. 124-133.

Decker, T., and P. Kovarik, 1999, Transcription factor activity of STAT proteins: structural requirements and regulation by phosphorylation and interacting proteins: Cellular and Molecular Life Sciences: CMLS, v. 55, p. 1535-1546.

Dephoure, N., C. Zhou, J. Villén, S. A. Beausoleil, C. E. Bakalarski, S. J. Elledge, and S. P. Gygi, 2008, A quantitative atlas of mitotic phosphorylation: Proceedings of the National Academy of Sciences, v. 105, p. 10762-10767.

Devergne, O., C. Ghiglione, and S. Noselli, 2007, The endocytic control of JAK/STAT signalling in Drosophila: J Cell Sci, v. 120, p. 3457-3464.

Dietzl, G., D. Chen, F. Schnorrer, K.-C. Su, Y. Barinova, M. Fellner, B. Gasser, K. Kinsey, S. Oppel, S. Scheiblauer, A. Couto, V. Marra, K. Keleman, and B. J. Dickson, 2007, A genome-wide transgenic RNAi library for conditional gene inactivation in Drosophila: Nature, v. 448, p. 151-156.

Dirac-Svejstrup, A. B., T. Sumizawa, and S. R. Pfeffer, 1997, Identification of a GDI displacement factor that releases endosomal Rab GTPases from Rab-GDI: The EMBO Journal, v. 16, p. 465-472.

Donaldson, J. G., N. Porat-Shliom, and L. A. Cohen, 2009, Clathrin-independent endocytosis: A unique platform for cell signaling and PM remodeling: Cellular Signalling, v. 21, p. 1-6.

Doppler, H., and P. Storz, Regulation of VASP by phosphorylation: Consequences for cell migration: Cell adhesion & migration, v. 7.

Dubois, L., M. Lecourtois, C. Alexandre, E. Hirst, and J. P. Vincent, 2001, Regulated endocytic routing modulates wingless signaling in Drosophila embryos: Cell, v. 105, p. 613-624.

Duchek, P., K. Somogyi, G. J√©kely, S. Beccari, and P. R√∏rth, 2001, Guidance of cell migration by the Drosophila PDGF/VEGF receptor: Cell, v. 107, p. 17-26.

Duong, F. H. T., M. Filipowicz, M. Tripodi, N. La Monica, and M. H. Heim, 2004, Hepatitis C virus inhibits interferon signaling through up-regulation of protein phosphatase 2A: Gastroenterology, v. 126, p. 263-277.

Ehret, G. B., P. Reichenbach, U. Schindler, C. M. Horvath, S. Fritz, M. Nabholz, and P. Bucher, 2001, DNA binding specificity of different STAT proteins. Comparison of in vitro specificity with natural target sites: The Journal of Biological Chemistry, v. 276, p. 6675-6688.

Ekas, L. A., T. J. Cardozo, M. S. Flaherty, E. A. McMillan, F. C. Gonsalves, and E. A. Bach, 2010, Characterization of a dominant-active STAT that promotes tumorigenesis in Drosophila: Developmental Biology, v. 344, p. 621-636.

Endo, T., A. Sasaki, M. Minoguchi, A. Joo, and A. Yoshimura, 2003, CIS1 interacts with the Y532 of the prolactin receptor and suppresses prolactin-dependent STAT5 activation: Journal of biochemistry, v. 133, p. 109-113.

Eulenfeld, R., A. Dittrich, C. Khouri, P. J. Muller, B. Mutze, A. Wolf, and F. Schaper, 2012, Interleukin-6 signalling: More than Jaks and STATs: European Journal of Cell Biology, v. 91, p. 486-495.

Fabrowski, P., A. S. Necakov, S. Mumbauer, E. Loeser, A. Reversi, S. Streichan, J. A. G. Briggs, and S. De Renzis, 2013, Tubular endocytosis drives remodelling of the apical surface during epithelial morphogenesis in Drosophila: Nature Communications, v. 4.

Faini, M., R. Beck, F. T. Wieland, and J. A. G. Briggs, 2013, Vesicle coats: structure, function, and general principles of assembly: Trends in Cell Biology, v. 23, p. 279-288.

Ferreira, F., M. Foley, A. Cooke, M. Cunningham, G. Smith, R. Woolley, G. Henderson, E. Kelly, S. Mundell, and E. Smythe, 2012, Endocytosis of G protein-coupled receptors is regulated by clathrin light chain phosphorylation: Current Biology: CB, v. 22, p. 1361-1370.

Fila, J., and D. Honys, 2012, Enrichment techniques employed in phosphoproteomics: Amino acids, v. 43, p. 1025-1047.

Flaherty, M. S., J. Zavadil, L. A. Ekas, and E. A. Bach, 2009, Genome-wide expression profiling in the Drosophila eye reveals unexpected repression of notch signaling by the JAK/STAT pathway: Developmental Dynamics, v. 238, p. 2235-2253.

Flores-Morales, A., L. Fern√°ndez, E. Rico-Bautista, A. Umana, C. Negr√≠n, J. G. Zhang, and G. Norstedt, 2001, Endoplasmic reticulum stress prolongs GH-induced Janus kinase (JAK2)/signal transducer and activator of transcription (STAT5) signaling pathway: Molecular endocrinology (Baltimore, Md.), v. 15, p. 1471-1483.

Friedbichler, K., A. Hoelbl, G. Li, K. D. Bunting, V. Sexl, F. Gouilleux, and R. Moriggl, 2011, Serine phosphorylation of the Stat5a C-terminus is a driving force for transformation: Frontiers in bioscience (Landmark edition), v. 16, p. 3043-3056.

Gabay, L., R. Seger, and B. Z. Shilo, 1997, MAP kinase in situ activation atlas during Drosophila embryogenesis: Development, v. 124, p. 3535-3541.

Gagliardi, M., E. Piddini, and J.-P. Vincent, 2008, Endocytosis: A Positive or a Negative Influence on Wnt Signalling?: Traffic, v. 9, p. 1-9.

Galvis, A., V. Balmaceda, H. Giambini, A. Conde, Z. Villasana, M. W. Fornes, and M. A. Barbieri, 2009, Inhibition of early endosome fusion by Rab5-binding defective Ras interference 1 mutants: Archives of Biochemistry and Biophysics, v. 482, p. 83-95.

Gasteiger, E., A. Gattiker, C. Hoogland, I. Ivanyi, R. D. Appel, and A. Bairoch, 2003, ExPASy: The proteomics server for in-depth protein knowledge and analysis: Nucleic acids research, v. 31, p. 3784-3788.

Gelbart, W. M., and D. B. Emmert, 2013, FlyBase High Throughput Expression Pattern Data.

German, C. L., B. M. Sauer, and C. L. Howe, 2011, The STAT3 beacon: IL-6 recurrently activates STAT 3 from endosomal structures: Experimental Cell Research, v. 317, p. 1955-1969.

Ghiglione, C., O. Devergne, E. Georgenthum, F. Carball√®s, C. M√©dioni, D. Cerezo, and S. p. Noselli, 2002, The Drosophila cytokine receptor Domeless controls border cell migration and epithelial polarization during oogenesis: Development, v. 129, p. 5437-5447.

Gilbert, M. M., M. Tipping, A. Veraksa, and K. H. Moberg, 2011, A Screen for Conditional Growth Suppressor Genes Identifies the Drosophila Homolog of HD-PTP as a Regulator of the Oncoprotein Yorkie: Developmental Cell, v. 20, p. 700-712.

Gilbert, M. M., B. K. Weaver, J. P. Gergen, and N. C. Reich, 2005, A novel functional activator of the Drosophila JAK/STAT pathway, unpaired2, is revealed by an in vivo reporter of pathway activation: Mechanisms of Development, v. 122, p. 939-948.

Gingras, M.-C., Y. L. Zhang, D. Kharitidi, A. J. Barr, S. Knapp, M. L. Tremblay, and A. Pause, 2009, HD-PTP Is a Catalytically Inactive Tyrosine Phosphatase Due to a Conserved Divergence in Its Phosphatase Domain: PLoS ONE, v. 4.

Goh, L. K., F. Huang, W. Kim, S. Gygi, and A. Sorkin, 2010, Multiple mechanisms collectively regulate clathrin-mediated endocytosis of the epidermal growth factor receptor: The Journal of Cell Biology, v. 189, p. 871-883.

Gouilleux, F., H. Wakao, M. Mundt, and B. Groner, 1994, Prolactin induces phosphorylation of Tyr694 of Stat5 (MGF), a prerequisite for DNA binding and induction of transcription: The EMBO Journal, v. 13, p. 4361-4369.

Grammont, M., and K. D. Irvine, 2001, fringe and Notch specify polar cell fate during Drosophila oogenesis: Development (Cambridge, England), v. 128, p. 2243-2253.

Grant SL, Begley CG., 1999, The oncostatin M signalling pathway: reversing the neoplastic phenotype? Mol Med Today. V 5(9):406-12.

Gronholm, J., D. Ungureanu, S. Vanhatupa, M. Ramet, and O. Silvennoinen, 2010, Sumoylation of Drosophila transcription factor STAT92E: Journal of innate immunity, v. 2, p. 618-624.

Grosshans, B. L., D. Ortiz, and P. Novick, 2006, Rabs and their effectors: Achieving specificity in membrane traffic: Proceedings of the National Academy of Sciences, v. 103, p. 11821-11827.

Hadano, S., C. K. Hand, H. Osuga, Y. Yanagisawa, A. Otomo, R. S. Devon, N. Miyamoto, J. Showguchi-Miyata, Y. Okada, R. Singaraja, D. A. Figlewicz, T. Kwiatkowski, B. A. Hosler, T. Sagie, J. Skaug, J. Nasir, R. H. Brown, S. W. Scherer, G. A. Rouleau, M. R. Hayden, and J. E. Ikeda, 2001, A gene encoding a putative GTPase regulator is mutated in familial amyotrophic lateral sclerosis 2: Nature Genetics, v. 29, p. 166-173.

Hahn, I., B. Fuss, A. Peters, T. Werner, A. Sieberg, D. Gosejacob, and M. Hoch, 2013, The Drosophila Arf GEF Steppke controls MAPK activation in EGFR signaling: Journal of Cell Science, v. 126, p. 2470-2479.

Hanahan, D., and R. A. Weinberg, 2011, Hallmarks of Cancer: The Next Generation: Cell, v. 144, p. 646-674.

Hanson, P. I., and A. Cashikar, 2012, Multivesicular Body Morphogenesis: Annual Review of Cell and Developmental Biology, v. 28, p. 337-362.

Harir, N., C. Pecquet, M. Kerenyi, K. Sonneck, B. Kovacic, R. Nyga, M. Brevet, I. Dhennin, V. Gouilleux-Gruart, H. Beug, P. Valent, K. Lassoued, R. Moriggl, and F. Gouilleux, 2007, Constitutive activation of Stat5 promotes its cytoplasmic localization and association with PI3-kinase in myeloid leukemias: Blood, v. 109, p. 1678-1686.

Harrison, D. A., P. E. McCoon, R. Binari, M. Gilman, and N. Perrimon, 1998, Drosophila unpaired encodes a secreted protein that activates the JAK signaling pathway: Genes & Development, v. 12, p. 3252-3263.

Hazan-Halevy, I., D. Harris, Z. Liu, J. Liu, P. Li, X. Chen, S. Shanker, A. Ferrajoli, M. J. Keating, and Z. Estrov, 2010, STAT3 is constitutively phosphorylated on serine 727 residues, binds DNA, and activates transcription in CLL cells: Blood, v. 115, p. 2852-2863.

Heldin, C. H., 1995, Dimerization of cell surface receptors in signal transduction: Cell, v. 80, p. 213-223.

Henry, A. G., J. N. Hislop, J. Grove, K. Thorn, M. Marsh, and M. von Zastrow, 2012, Regulation of Endocytic Clathrin Dynamics by Cargo Ubiquitination: Developmental Cell, v. 23, p. 519-532.

Hirst, J., C. Irving, and G. H. H. Borner, 2013, Adaptor protein complexes AP-4 and AP-5: new players in endosomal trafficking and progressive spastic paraplegia: Traffic (Copenhagen, Denmark), v. 14, p. 153-164.

Hombria, J. C.-G., S. Brown, S. Hader, and M. P. Zeidler, 2005, Characterisation of Upd2, a Drosophila JAK/STAT pathway ligand: Developmental Biology, v. 288, p. 420-433.

Honing, S., D. Ricotta, M. Krauss, K. Spate, B. Spolaore, A. Motley, M. Robinson, C. Robinson, V. Haucke, and D. J. Owen, 2005, Phosphatidylinositol-(4,5)-bisphosphate regulates sorting signal recognition by the clathrin-associated adaptor complex AP2: Molecular Cell, v. 18, p. 519-531.

Hopkins, C. R., 1983, Intracellular routing of transferrin and transferrin receptors in epidermoid carcinoma A431 cells: Cell, v. 35, p. 321-330.

Horiuchi, H., R. Lipp√©, H. M. McBride, M. Rubino, P. Woodman, H. Stenmark, V. Rybin, M. Wilm, K. Ashman, M. Mann, and M. Zerial, 1997, A Novel Rab5 GDP/GTP Exchange Factor Complexed to Rabaptin-5 Links Nucleotide Exchange to Effector Recruitment and Function: Cell, v. 90, p. 1149-1159.

Hou, X. S., M. B. Melnick, and N. Perrimon, 1996, marelle Acts Downstream of the Drosophila HOP/JAK Kinase and Encodes a Protein Similar to the Mammalian STATs: Cell, v. 84, p. 411-419.

Howe, C. L., 2005, Modeling the signaling endosome hypothesis: Why a drive to the nucleus is better than a (random) walk: Theoretical Biology and Medical Modelling, v. 2.

Hu, H., M. Milstein, J. M. Bliss, M. Thai, G. Malhotra, L. C. Huynh, and J. Colicelli, 2008, Integration of Transforming Growth Factor {beta} and RAS Signaling Silences a RAB5 Guanine Nucleotide Exchange Factor and Enhances Growth Factor-Directed Cell Migration: Mol. Cell. Biol., v. 28, p. 1573-1583.

Huang, F., L. K. Goh, and A. Sorkin, 2007, EGF receptor ubiquitination is not necessary for its internalization: Proceedings of the National Academy of Sciences of the United States of America, v. 104, p. 16904-16909.

Huang, F., A. Khvorova, W. Marshall, and A. Sorkin, 2004, Analysis of clathrin-mediated endocytosis of epidermal growth factor receptor by RNA interference: The Journal of Biological Chemistry, v. 279, p. 16657-16661.

Huang, F., D. Kirkpatrick, X. Jiang, S. Gygi, and A. Sorkin, 2006, Differential regulation of EGF receptor internalization and degradation by multiubiquitination within the kinase domain: Molecular Cell, v. 21, p. 737-748.

Huang, H.-R., Z. J. Chen, S. Kunes, G.-D. Chang, and T. Maniatis, 2010, Endocytic pathway is required for Drosophila Toll innate immune signaling: Proceedings of the National Academy of Sciences, v. 107, p. 8322-8327.

Huang, J., W. Zhou, A. M. Watson, Y.-N. Jan, and Y. Hong, 2008, Efficient Ends-Out Gene Targeting In Drosophila: Genetics, v. 180, p. 703-707.

Huang, L., C. Q. Pan, B. Li, L. Tucker-Kellogg, B. Tidor, Y. Chen, and B. C. Low, 2011, Simulating EGFR-ERK Signaling Control by Scaffold Proteins KSR and MP1 Reveals Differential Ligand-Sensitivity Co-Regulated by Cbl-CIN85 and Endophilin: PLoS ONE, v. 6.

Hunker, C. M., A. Galvis, M. L. Veisaga, and M. A. Barbieri, 2006a, Rin1 is a negative regulator of the IL3 receptor signal transduction pathways: Anticancer Research, v. 26, p. 905-916.

Hunker, C. M., H. Giambini, A. Galvis, J. Hall, I. Kruk, M. L. Veisaga, and M. A. Barbieri, 2006b, Rin1 regulates insulin receptor signal transduction pathways: Experimental Cell Research, v. 312, p. 1106-1118.

Huotari, J., and A. Helenius, 2011, Endosome maturation: The EMBO Journal, v. 30, p. 3481-3500.

Igaki, T., J. C. Pastor-Pareja, H. Aonuma, M. Miura, and T. Xu, 2009, Intrinsic Tumor Suppression and Epithelial Maintenance by Endocytic Activation of Eiger/TNF Signaling in Drosophila: Developmental Cell, v. 16, p. 458-465.

Ihle, J. N., 1995, The Janus protein tyrosine kinases in hematopoietic cytokine signaling: Seminars in immunology, v. 7, p. 247-254.

Imami, K., N. Sugiyama, Y. Kyono, M. Tomita, and Y. Ishihama, 2008, Automated Phosphoproteome Analysis for Cultured Cancer Cells by Two-Dimensional NanoLC-MS Using a Calcined Titania/C18 Biphasic Column: Analytical Sciences, v. 24, p. 161-166.

Incardona, J. P., J. Gruenberg, and H. Roelink, 2002, Sonic hedgehog induces the segregation of patched and smoothened in endosomes: Current Biology: CB, v. 12, p. 983-995.

Jekely, G., and P. Rorth, 2003, Hrs mediates downregulation of multiple signalling receptors in Drosophila: EMBO Reports, v. 4, p. 1163-1168.

Jekely, G., H.-H. Sung, C. M. Luque, and P. Rorth, 2005, Regulators of Endocytosis Maintain Localized Receptor Tyrosine Kinase Signaling in Guided Migration: Developmental Cell, v. 9, p. 197-207.

Jiang, H., P. H. Patel, A. Kohlmaier, M. O. Grenley, D. G. McEwen, and B. A. Edgar, 2009, Cytokine/Jak/Stat Signaling Mediates Regeneration and Homeostasis in the Drosophila Midgut: Cell, v. 137, p. 1343-1355.

Jiang, X., and A. Sorkin, 2003, Epidermal Growth Factor Receptor Internalization through Clathrin-Coated Pits Requires Cbl RING Finger and Proline-Rich Domains But Not Receptor Polyubiquitylation: Traffic, v. 4, p. 529-543.

Jin, E. J., C.-C. Chan, E. Agi, S. Cherry, E. Hanacik, M. Buszczak, and P. R. Hiesinger, 2012, Similarities of Drosophila rab GTPases Based on Expression Profiling: Completion and Analysis of the rab-Gal4 Kit: PLoS ONE, v. 7.

Johnson, A. N., M. H. Mokalled, T. N. Haden, and E. N. Olson, 2011, JAK/Stat signaling regulates heart precursor diversification in Drosophila: Development, v. 138, p. 4627-4638.

Johnstone, K., R. E. Wells, D. Strutt, and M. P. Zeidler, 2013, Localised JAK/STAT Pathway Activation Is Required for Drosophila Wing Hinge Development: PLoS ONE, v. 8.

Jones, W. M., and A. Bejsovec, 2005, RacGap50C Negatively Regulates Wingless Pathway Activity During Drosophila Embryonic Development: Genetics, v. 169, p. 2075-2086.

Jones, W. M., A. T. Chao, M. Zavortink, R. Saint, and A. Bejsovec, 2010, Cytokinesis proteins Tum and Pav have a nuclear role in Wnt regulation: Journal of Cell Science, v. 123, p. 2179-2189.

Kallio, J., H. Myllym√§ki, J. Gr√∂nholm, M. Armstrong, L.-M. Vanha-aho, L. M√§kinen, O. Silvennoinen, S. Valanne, and M. R√§met, 2010, Eye transformer is a negative regulator of Drosophila JAK/STAT signaling: The FASEB Journal, v. 24, p. 4467-4479.

Kametaka, S., and S. Waguri, 2012, Visualization of TGN-endosome trafficking in mammalian and Drosophila cells: Methods in enzymology, v. 504, p. 255-271.

Karsten, P., I. Plischke, N. Perrimon, and M. P. Zeidler, 2006, Mutational analysis reveals separable DNA binding and trans-activation of Drosophila STAT92E: Cellular Signalling, v. 18, p. 819-829.

Katzmann, D. J., C. J. Stefan, M. Babst, and S. D. Emr, 2003, Vps27 recruits ESCRT machinery to endosomes during MVB sorting: The Journal of Cell Biology, v. 162, p. 413-423.

Kawashima, T., Y. C. Bao, Y. Minoshima, Y. Nomura, T. Hatori, T. Hori, T. Fukagawa, T. Fukada, N. Takahashi, T. Nosaka, M. Inoue, T. Sato, M. Kukimoto-Niino, M. Shirouzu, S. Yokoyama, and T. Kitamura, 2009, A Rac GTPase-Activating Protein, MgcRacGAP, Is a Nuclear Localizing Signal-Containing Nuclear Chaperone in the Activation of STAT Transcription Factors: Molecular and Cellular Biology, v. 29, p. 1796-1813.

Kawashima, T., Y. C. Bao, Y. Nomura, Y. Moon, Y. Tonozuka, Y. Minoshima, T. Hatori, A. Tsuchiya, M. Kiyono, T. Nosaka, H. Nakajima, D. A. Williams, and T. Kitamura, 2006, Rac1 and a GTPase-activating protein, MgcRacGAP, are

required for nuclear translocation of STAT transcription factors: The Journal of Cell Biology, v. 175, p. 937-946.
Kelly, B. T., and D. J. Owen, 2011, Endocytic sorting of transmembrane protein cargo: Current Opinion in Cell Biology, v. 23, p. 404-412.
Kermorgant, S. p., and P. J. Parker, 2008, Receptor trafficking controls weak signal delivery: a strategy used by c-Met for STAT3 nuclear accumulation: The Journal of Cell Biology, v. 182, p. 855-863.
Kinouchi, K., A. Ichihara, and H. Itoh, 2011, Functional characterization of (pro)renin receptor in association with V-ATPase: Frontiers in bioscience (Landmark edition), v. 16, p. 3216-3223.
Kittler JT1, Chen G, Kukhtina V, Vahedi-Faridi A, Gu Z, Tretter V, Smith KR, McAinsh K, Arancibia-Carcamo IL, Saenger W, Haucke V, Yan Z, Moss SJ, 2008, Regulation of synaptic inhibition by phospho-dependent binding of the AP2 complex to a YECL motif in the GABAA receptor gamma2 subunit. Proc Natl Acad Sci U S A. 2008 Mar 4;105(9):3616-21.
Kohyama-Koganeya, A., and Y. Hirabayashi, 2010, The Drosophila 7-pass transmembrane glycoprotein BOSS and metabolic regulation: What Drosophila can teach us about human energy metabolism: Methods in enzymology, v. 480, p. 525-538.
Komada, M., and N. Kitamura, 2001, Hrs and Hbp: Possible Regulators of Endocytosis and Exocytosis: Biochemical and Biophysical Research Communications, v. 281, p. 1065-1069.
Komada, M., R. Masaki, A. Yamamoto, and N. Kitamura, 1997, Hrs, a tyrosine kinase substrate with a conserved double zinc finger domain, is localized to the cytoplasmic surface of early endosomes: The Journal of Biological Chemistry, v. 272, p. 20538-20544.
Komyod, W., U.-M. Bauer, P. C. Heinrich, S. Haan, and I. Behrmann, 2005, Are STATS arginine-methylated?: The Journal of Biological Chemistry, v. 280, p. 21700-21705.
Korzus, E., J. Torchia, D. W. Rose, L. Xu, R. Kurokawa, E. M. McInerney, T. M. Mullen, C. K. Glass, and M. G. Rosenfeld, 1998, Transcription factor-specific requirements for coactivators and their acetyltransferase functions: Science (New York, N.Y.), v. 279, p. 703-707.
Kosaka, T., and K. Ikeda, 1983, Reversible blockage of membrane retrieval and endocytosis in the garland cell of the temperature-sensitive mutant of Drosophila melanogaster, shibirets1: The Journal of Cell Biology, v. 97, p. 499-507.
Kramer, O. H., 2013, Acetylation of Endogenous STAT Proteins, Springer.
Kramer, O. H., D. Baus, S. K. Knauer, S. Stein, E. Jager, R. H. Stauber, M. Grez, E. Pfitzner, and T. Heinzel, 2006, Acetylation of Stat1 modulates NF-kappaB activity: Genes & Development, v. 20, p. 473-485.
Kramer, O. H., S. K. Knauer, G. Greiner, E. Jandt, S. Reichardt, K.-H. Gohrs, R. H. Stauber, F. D. Buhmer, and T. Heinzel, 2009, A phosphorylation-acetylation switch regulates STAT1 signaling: Genes & Development, v. 23, p. 223-235.
Kramer, O. H., and R. Moriggl, 2012, Acetylation and sumoylation control STAT5 activation antagonistically: JAK-STAT, v. 1, p. 203-207.
Krzemien, J., L. Dubois, R. Makki, M. Meister, A. Vincent, and M. Crozatier, 2007, Control of blood cell homeostasis in Drosophila larvae by the posterior signalling centre: Nature, v. 446, p. 325-328.

Kwon, S. Y., H. Xiao, B. P. Glover, R. Tjian, C. Wu, and P. Badenhorst, 2008, The nucleosome remodeling factor (NURF) regulates genes involved in Drosophila innate immunity: Developmental Biology, v. 316, p. 538-547.

Laflamme, C., G. Assaker, D. Ramel, J. F. Dorn, D. She, P. S. Maddox, and G. Emery, 2012, Evi5 promotes collective cell migration through its Rab-GAP activity: The Journal of Cell Biology, v. 198, p. 57-67.

Lakhan, S. E., S. Sabharanjak, and A. De, 2009, Endocytosis of glycosylphosphatidylinositol-anchored proteins: Journal of biomedical science, v. 16.

Lakkaraju, A. K. K., and F. G. van der Goot, 2013, Calnexin Controls the STAT3-Mediated Transcriptional Response to EGF: Molecular Cell, v. 51, p. 386-396.

Lanzetti, L., A. Palamidessi, L. Areces, G. Scita, and P. P. Di Fiore, 2004, Rab5 is a signalling GTPase involved in actin remodelling by receptor tyrosine kinases: Nature, v. 429, p. 309-314.

Lavens, D., T. Montoye, J. Piessevaux, L. Zabeau, J. l. Vandekerckhove, K. Gevaert, W. Becker, S. Eyckerman, and J. Tavernier, 2006, A complex interaction pattern of CIS and SOCS2 with the leptin receptor: Journal of Cell Science, v. 119, p. 2214-2224.

Levkowitz, G., H. Waterman, E. Zamir, Z. Kam, S. Oved, W. Y. Langdon, L. Beguinot, B. Geiger, and Y. Yarden, 1998, c-Cbl/Sli-1 regulates endocytic sorting and ubiquitination of the epidermal growth factor receptor: Genes & Development, v. 12, p. 3663-3674.

Lim, C. P., and X. Cao, 2006, Structure, function, and regulation of STAT proteins: Molecular BioSystems, v. 2, p. 536-550.

Lim, J. P., and P. A. Gleeson, 2011, Macropinocytosis: an endocytic pathway for internalising large gulps: Immunology and cell biology, v. 89, p. 836-843.

Linossi, E. M., J. J. Babon, D. J. Hilton, and S. E. Nicholson, 2013, Suppression of cytokine signaling: the SOCS perspective: Cytokine & Growth Factor Reviews, v. 24, p. 241-248.

Linossi, E. M., and S. E. Nicholson, 2012, The SOCS box-adapting proteins for ubiquitination and proteasomal degradation: IUBMB life, v. 64, p. 316-323.

Lippe, R., M. Miaczynska, V. Rybin, A. Runge, and M. Zerial, 2001, Functional Synergy between Rab5 Effector Rabaptin-5 and Exchange Factor Rabex-5 When Physically Associated in a Complex: Mol. Biol. Cell, v. 12, p. 2219-2228.

Liu, L., K. M. McBride, and N. C. Reich, 2005, STAT3 nuclear import is independent of tyrosine phosphorylation and mediated by importin-?3: Proceedings of the National Academy of Sciences of the United States of America, v. 102, p. 8150-8155.

Lloyd, T. E., R. Atkinson, M. N. Wu, Y. Zhou, G. Pennetta, and H. J. Bellen, 2002, Hrs Regulates Endosome Membrane Invagination and Tyrosine Kinase Receptor Signaling in Drosophila: Cell, v. 108, p. 261-269.

Lodhi, I. J., D. Bridges, S.-H. Chiang, Y. Zhang, A. Cheng, L. M. Geletka, L. S. Weisman, and A. R. Saltiel, 2008, Insulin Stimulates Phosphatidylinositol 3-Phosphate Production via the Activation of Rab5: Mol. Biol. Cell, v. 19, p. 2718-2728.

Lodhi, I. J., S.-H. Chiang, L. Chang, D. Vollenweider, R. T. Watson, M. Inoue, J. E. Pessin, and A. R. Saltiel, 2007, Gapex-5, a Rab31 guanine nucleotide

exchange factor that regulates Glut4 trafficking in adipocytes: Cell Metabolism, v. 5, p. 59-72.
Lu, H., and D. Bilder, 2005, Endocytic control of epithelial polarity and proliferation in Drosophila: Nat Cell Biol, v. 7, p. 1232-1239.
Lunde, K., B. Biehs, U. Nauber, and E. Bier, 1998, The knirps and knirps-related genes organize development of the second wing vein in Drosophila: Development (Cambridge, England), v. 125, p. 4145-4154.
Luo, H., W. P. Hanratty, and C. R. Dearolf, 1995, An amino acid substitution in the Drosophila hopTum-l Jak kinase causes leukemia-like hematopoietic defects: The EMBO Journal, v. 14, p. 1412-1420.
Ma, L., J.-s. Gao, Y. Guan, X. Shi, H. Zhang, M. K. Ayrapetov, Z. Zhang, L. Xu, Y.-M. Hyun, M. Kim, S. Zhuang, and Y. E. Chin, 2010, Acetylation modulates prolactin receptor dimerization: Proceedings of the National Academy of Sciences of the United States of America, v. 107, p. 19314-19319.
Makki, R., M. Meister, D. Pennetier, J.-M. Ubeda, A. Braun, V. Daburon, J. Krzemie≈Ñ, H.-M. Bourbon, R. Zhou, A. Vincent, and M. l. Crozatier, 2010, A Short Receptor Downregulates JAK/STAT Signalling to Control the Drosophila Cellular Immune Response: PLoS Biol, v. 8.
Mao, Y., Y. Shang, V. C. Pham, J. A. Ernst, J. R. Lill, S. J. Scales, and J. Zha, 2011, Polyubiquitination of insulin-like growth factor I receptor (IGF-IR) activation loop promotes antibody-induced receptor internalization and down-regulation: The Journal of Biological Chemistry, v. 286, p. 41852-41861.
Marchetti, M., M.-N. Monier, A. Fradagrada, K. Mitchell, F. Baychelier, P. Eid, L. Johannes, and C. Lamaze, 2006, Stat-mediated Signaling Induced by Type I and Type II Interferons (IFNs) Is Differentially Controlled through Lipid Microdomain Association and Clathrin-dependent Endocytosis of IFN Receptors: Molecular Biology of the Cell, v. 17, p. 2896-2909.
Marquez, R. M., M. A. Singer, N. T. Takaesu, W. R. Waldrip, Y. Kraytsberg, and S. J. Newfeld, 2001, Transgenic Analysis of the Smad Family of TGF-Œ≤ Signal Transducers in Drosophila melanogaster Suggests New Roles and New Interactions Between Family Members: Genetics, v. 157, p. 1639-1648.
Matsui, Y., A. Kikuchi, S. Araki, Y. Hata, J. Kondo, Y. Teranishi, and Y. Takai, 1990, Molecular cloning and characterization of a novel type of regulatory protein (GDI) for smg p25A, a ras p21-like GTP-binding protein: Molecular and Cellular Biology, v. 10, p. 4116-4122.
Mattera, R., C. N. Arighi, R. Lodge, M. Zerial, and J. S. Bonifacino, 2003, Divalent interaction of the GGAs with the Rabaptin-5-Rabex-5 complex: EMBO J, v. 22, p. 78-88.
Mattera, R., and J. S. Bonifacino, 2008, Ubiquitin binding and conjugation regulate the recruitment of Rabex-5 to early endosomes: EMBO J, v. 27, p. 2484-2494.
Maurel-Zaffran, C., J. Pradel, and Y. Graba, 2010, Reiterative use of signalling pathways controls multiple cellular events during Drosophila posterior spiracle organogenesis: Developmental Biology, v. 343, p. 18-27.
Mayya, V., D. H. Lundgren, S.-I. Hwang, K. Rezaul, L. Wu, J. K. Eng, V. Rodionov, and D. K. Han, 2009, Quantitative phosphoproteomic analysis of T cell receptor signaling reveals system-wide modulation of protein-protein interactions: Science signaling, v. 2.

McBride, H. M., V. Rybin, C. Murphy, A. Giner, R. Teasdale, and M. Zerial, 1999, Oligomeric Complexes Link Rab5 Effectors with NSF and Drive Membrane Fusion via Interactions between EEA1 and Syntaxin 13: Cell, v. 98, p. 377-386.

McBride, K. M., G. Banninger, C. McDonald, and N. C. Reich, 2002, Regulated nuclear import of the STAT1 transcription factor by direct binding of importin-?: The EMBO Journal, v. 21, p. 1754-1763.

McDonald, C., and N. C. Reich, 1999, Cooperation of the transcriptional coactivators CBP and p300 with Stat6: Journal of interferon & cytokine research: the official journal of the International Society for Interferon and Cytokine Research, v. 19, p. 711-722.

McMahon, H. T., and E. Boucrot, 2011, Molecular mechanism and physiological functions of clathrin-mediated endocytosis: Nature reviews. Molecular cell biology, v. 12, p. 517-533.

McShane, M. P., and M. Zerial, 2008, Survival of the weakest: signaling aided by endosomes: The Journal of Cell Biology, v. 182, p. 823-825.

Meissner, T., E. Krause, I. L√∂dige, and U. Vinkemeier, 2004, Arginine methylation of STAT1: a reassessment: Cell, v. 119, p. 587-589.

Mendez, J., and B. Stillman, 2000, Chromatin association of human origin recognition complex, cdc6, and minichromosome maintenance proteins during the cell cycle: assembly of prereplication complexes in late mitosis: Molecular and cellular biology, v. 20, p. 8602-8612.

Meyer, T., A. Begitt, I. Lodige, M. v. Rossum, and U. Vinkemeier, 2002, Constitutive and IFN-?-induced nuclear import of STAT1 proceed through independent pathways: The EMBO Journal, v. 21, p. 344-354.

Miaczynska, M., and D. Bar-Sagi, 2010, Signaling endosomes: seeing is believing: Current Opinion in Cell Biology, v. 22, p. 535-540.

Miaczynska, M., S. Christoforidis, A. Giner, A. Shevchenko, S. Uttenweiler-Joseph, B. Habermann, M. Wilm, R. G. Parton, and M. Zerial, 2004, APPL Proteins Link Rab5 to Nuclear Signal Transduction via an Endosomal Compartment: Cell, v. 116, p. 445-456.

Mitra, A., J. A. Ross, G. Rodriguez, Z. S. Nagy, H. L. Wilson, and R. A. Kirken, 2012, Signal Transducer and Activator of Transcription 5b (Stat5b) Serine 193 Is a Novel Cytokine-induced Phospho-regulatory Site That Is Constitutively Activated in Primary Hematopoietic Malignancies: Journal of Biological Chemistry, v. 287, p. 16596-16608.

Miura, G. I., J.-Y. Roignant, M. Wassef, and J. E. Treisman, 2008, Myopic acts in the endocytic pathway to enhance signaling by the Drosophila EGF receptor: Development (Cambridge, England), v. 135, p. 1913-1922.

Miyazawa K, Bäckström G, Leppänen O, Persson C, Wernstedt C, Hellman U, Heldin CH, Ostman A., 1998, Role of immunoglobulin-like domains 2-4 of the platelet-derived growth factor alpha-receptor in ligand-receptor complex assembly. J Biol Chem. v 25;273(39):25495-502.

Moberg, K. H., S. Schelble, S. K. Burdick, and I. K. Hariharan, 2005, Mutations in erupted, the Drosophila Ortholog of Mammalian Tumor Susceptibility Gene 101, Elicit Non-Cell-Autonomous Overgrowth: Developmental Cell, v. 9, p. 699-710.

Mohr, A., N. Chatain, T. s. Domoszlai, N. Rinis, M. Sommerauer, M. Vogt, and G. Muller-Newen, 2012, Dynamics and non-canonical aspects of JAK/STAT signalling: European Journal of Cell Biology, v. 91, p. 524-532.

Montell, D. J., 2003, Border-cell migration: the race is on: Nature Reviews Molecular Cell Biology, v. 4, p. 13-24.

Montell, D. J., W. H. Yoon, and M. Starz-Gaiano, 2012, Group choreography: mechanisms orchestrating the collective movement of border cells: Nature reviews. Molecular cell biology, v. 13, p. 631-645.

Morrison, H. A., H. Dionne, T. E. Rusten, A. Brech, W. W. Fisher, B. D. Pfeiffer, S. E. Celniker, H. Stenmark, and D. Bilder, 2008, Regulation of Early Endosomal Entry by the Drosophila Tumor Suppressors Rabenosyn and Vps45: Mol. Biol. Cell, v. 19, p. 4167-4176.

Mottola, G., A.-K. Classen, M. Gonz√°lez-Gait√°n, S. Eaton, and M. Zerial, 2010, A novel function for the Rab5 effector Rabenosyn-5 in planar cell polarity: Development, v. 137, p. 2353-2364.

Mowen, K. A., J. Tang, W. Zhu, B. T. Schurter, K. Shuai, H. R. Herschman, and M. David, 2001, Arginine methylation of STAT1 modulates IFNalpha/beta-induced transcription: Cell, v. 104, p. 731-741.

Mukherjee, T., 2005, Chaacterization of the role of Drosophila JAK/STAT signalling in cellular proliferation: Dissertation.

Mukherjee, T., J. C.-G. Hombria, and M. P. Zeidler, 2005, Opposing roles for Drosophila JAK//STAT signalling during cellular proliferation, v. 24, p. 2503-2511.

Mukherjee, T., U. Sch√§fer, and M. P. Zeidler, 2006, Identification of Drosophila genes modulating Janus kinase/signal transducer and activator of transcription signal transduction: Genetics, v. 172, p. 1683-1697.

Muller, P., M. Boutros, and M. P. Zeidler, 2008, Identification of JAK/STAT pathway regulators,ÄîInsights from RNAi screens: Seminars in Cell & Developmental Biology, v. 19, p. 360-369.

Muller, P., D. Kuttenkeuler, V. Gesellchen, M. P. Zeidler, and M. Boutros, 2005, Identification of JAK/STAT signalling components by genome-wide RNA interference: Nature, v. 436, p. 871-875.

Muller, P., D. Pugazhendhi, and M. P. Zeidler, 2012, Modulation of human JAK-STAT pathway signaling by functionally conserved regulators: JAK-STAT, v. 1, p. 34-43.

Murray, J. T., C. Panaretou, H. Stenmark, M. Miaczynska, and J. M. Backer, 2002, Role of Rab5 in the recruitment of hVps34/p150 to the early endosome: Traffic (Copenhagen, Denmark), v. 3, p. 416-427.

Nada, S., A. Hondo, A. Kasai, M. Koike, K. Saito, Y. Uchiyama, and M. Okada, 2009, The novel lipid raft adaptor p18 controls endosome dynamics by anchoring the MEK,ÄìERK pathway to late endosomes: The EMBO Journal, v. 28, p. 477-489.

Naslavsky, N., M. Boehm, P. S. Backlund, Jr., and S. Caplan, 2004, Rabenosyn-5 and EHD1 interact and sequentially regulate protein recycling to the plasma membrane: Molecular Biology of the Cell, v. 15, p. 2410-2422.

Navaroli, D. M., K. D. Bellve, C. Standley, L. M. Lifshitz, J. Cardia, D. Lambright, D. Leonard, K. E. Fogarty, and S. Corvera, 2012, Rabenosyn-5 defines the fate of the transferrin receptor following clathrin-mediated endocytosis:

Proceedings of the National Academy of Sciences of the United States of America, v. 109, p. E471-E480.
Nazarewicz, R. R., G. Salazar, N. Patrushev, A. S. Martin, L. Hilenski, S. Xiong, and R. W. Alexander, 2010, Early Endosomal Antigen 1 (EEA1) Is an Obligate Scaffold for Angiotensin II-induced, PKC- -dependent Akt Activation in Endosomes: Journal of Biological Chemistry, v. 286, p. 2886-2895.
Neuman-Silberberg, F. S., and T. Sch√ºpbach, 1996, The Drosophila TGF-[alpha]-like protein Gurken: expression and cellular localization during Drosophila oogenesis: Mechanisms of Development, v. 59, p. 105-113.
Nielsen, E., S. Christoforidis, S. Uttenweiler-Joseph, M. Miaczynska, F. Dewitte, M. Wilm, B. Hoflack, and M. Zerial, 2000, Rabenosyn-5, a Novel Rab5 Effector, Is Complexed with hVPS45 and Recruited to Endosomes through a FYVE Finger Domain: J. Cell Biol., v. 151, p. 601-612.
Okutani, Y., A. Kitanaka, T. Tanaka, H. Kamano, H. Ohnishi, Y. Kubota, T. Ishida, and J. Takahara, 2001, Src directly tyrosine-phosphorylates STAT5 on its activation site and is involved in erythropoietin-induced signaling pathway: Oncogene, v. 20, p. 6643-6650.
Olsen, J. V., M. Vermeulen, A. Santamaria, C. Kumar, M. L. Miller, L. J. Jensen, F. Gnad, J. Cox, T. S. Jensen, E. A. Nigg, S. Brunak, and M. Mann, 2010, Quantitative Phosphoproteomics Reveals Widespread Full Phosphorylation Site Occupancy During Mitosis: Science Signaling, v. 3, p. ra3-ra3.
Otomo, A., S. Hadano, T. Okada, H. Mizumura, R. Kunita, H. Nishijima, J. Showguchi-Miyata, Y. Yanagisawa, E. Kohiki, E. Suga, M. Yasuda, H. Osuga, T. Nishimoto, S. Narumiya, and J.-E. Ikeda, 2003, ALS2, a novel guanine nucleotide exchange factor for the small GTPase Rab5, is implicated in endosomal dynamics: Hum. Mol. Genet., v. 12, p. 1671-1687.
Palfy, M., A. Rem√©nyi, and T. Korcsmaros, 2012, Endosomal crosstalk: meeting points for signaling pathways: Trends in Cell Biology, v. 22, p. 447-456.
Pelkmans, L., E. Fava, H. Grabner, M. Hannus, B. Habermann, E. Krausz, and M. Zerial, 2005, Genome-wide analysis of human kinases in clathrin- and caveolae/raft-mediated endocytosis: Nature, v. 436, p. 78-86.
Pennock, S., and Z. Wang, 2003, Stimulation of Cell Proliferation by Endosomal Epidermal Growth Factor Receptor As Revealed through Two Distinct Phases of Signaling: Molecular and Cellular Biology, v. 23, p. 5803-5815.
Pfeffer, S. R., 2013, Rab GTPase regulation of membrane identity: Current Opinion in Cell Biology, v. 25, p. 414-419.
Pons, V. r., P.-P. Luyet, E. Morel, L. Abrami, F. G. van der Goot, R. G. Parton, and J. Gruenberg, 2008, Hrs and SNX3 Functions in Sorting and Membrane Invagination within Multivesicular Bodies: PLoS Biol, v. 6.
Poteryaev, D., S. Datta, K. Ackema, M. Zerial, and A. Spang, 2010, Identification of the Switch in Early-to-Late Endosome Transition: Cell, v. 141, p. 497-508.
Prior, I. A., and J. F. Hancock, 2013, Ras trafficking, localization and compartmentalized signalling: Seminars in Cell & Developmental Biology, v. 23, p. 145-153.
Puri, C., D. Tosoni, R. Comai, A. Rabellino, D. Segat, F. Caneva, P. Luzzi, P. P. Di Fiore, and C. Tacchetti, 2005, Relationships between EGFR Signaling-competent and Endocytosis-competent Membrane Microdomains: Mol. Biol. Cell, v. 16, p. 2704-2718.

Puthenveedu, M. A., and M. von Zastrow, 2006, Cargo Regulates Clathrin-Coated Pit Dynamics: Cell, v. 127, p. 113-124.

Radtke S1, Hermanns HM, Haan C, Schmitz-Van De Leur H, Gascan H, Heinrich PC, Behrmann I., 2002, Novel role of Janus kinase 1 in the regulation of oncostatin M receptor surface expression. J Biol Chem. v 29;277(13):11297-305.

Ragimbeau J1, Dondi E, Alcover A, Eid P, Uzé G, Pellegrini S., 2003, The tyrosine kinase Tyk2 controls IFNAR1 cell surface expression. EMBO J. v 3;22(3):537-47.

Rahajeng, J., S. Caplan, and N. Naslavsky, 2010, Common and distinct roles for the binding partners Rabenosyn-5 and Vps45 in the regulation of endocytic trafficking in mammalian cells: Experimental Cell Research, v. 316, p. 859-874.

Raiborg, C., J. r. Wesche, L. Maler√∏d, and H. Stenmark, 2006, Flat clathrin coats on endosomes mediate degradative protein sorting by scaffolding Hrs in dynamic microdomains: Journal of Cell Science, v. 119, p. 2414-2424.

Rajan, A., and N. Perrimon, 2012, Drosophila Cytokine Unpaired 2 Regulates Physiological Homeostasis by Remotely Controlling Insulin Secretion: Cell, v. 151, p. 123-137.

Ramanathan, H. N., G. Zhang, and Y. Ye, 2013, Monoubiquitination of EEA1 regulates endosome fusion and trafficking: Cell & Bioscience, v. 3.

Ray, S., I. Boldogh, and A. R. Brasier, 2005, STAT3 NH2-terminal acetylation is activated by the hepatic acute-phase response and required for IL-6 induction of angiotensinogen: Gastroenterology, v. 129, p. 1616-1632.

Reider, A., and B. Wendland, 2011, Endocytic adaptors ‚Äì social networking at the plasma membrane: Journal of Cell Science, v. 124, p. 1613-1622.

Riedel, F., D. Vorkel, and S. Eaton, 2011, Megalin-dependent Yellow endocytosis restricts melanization in the Drosophila cuticle: Development, v. 138, p. 149-158.

Rink, J., E. Ghigo, Y. Kalaidzidis, and M. Zerial, 2005, Rab Conversion as a Mechanism of Progression from Early to Late Endosomes: Cell, v. 122, p. 735-749.

Rivas, M. a. L., L. Cobreros, M. P. Zeidler, and J. C.-G. Hombr√≠a, 2008, Plasticity of Drosophila Stat DNA binding shows an evolutionary basis for Stat transcription factor preferences: EMBO Reports, v. 9, p. 1114-1120.

Roy, S., B. Wyse, and J. F. Hancock, 2002, H-Ras Signaling and K-Ras Signaling Are Differentially Dependent on Endocytosis: Molecular and Cellular Biology, v. 22, p. 5128-5140.

Royle, S. J., 2012, The role of clathrin in mitotic spindle organisation: Journal of Cell Science, v. 125, p. 19-28.

Ruohola, H., K. A. Bremer, D. Baker, J. R. Swedlow, L. Y. Jan, and Y. N. Jan, 1991, Role of neurogenic genes in establishment of follicle cell fate and oocyte polarity during oogenesis in Drosophila: Cell, v. 66, p. 433-449.

Sadir, R., A. Lambert, H. Lortat-Jacob, and G. Morel, 2001, Caveolae and clathrin-coated vesicles: two possible internalization pathways for IFN-gamma and IFN-gamma receptor: Cytokine, v. 14, p. 19-26.

Sambrook, and Russell, 2002, Molecular cloning: a laboratory manual: Cold Spring Harbor, NY: Cold Spring Harbor Laboratory Press.

Sato, M., K. Sato, P. Fonarev, C.-J. Huang, W. Liou, and B. D. Grant, 2005, Caenorhabditis elegans RME-6 is a novel regulator of RAB-5 at the clathrin-coated pit: Nat Cell Biol, v. 7, p. 559-569.

Schenck, A., L. Goto-Silva, C. Collinet, M. Rhinn, A. Giner, B. Habermann, M. Brand, and M. Zerial, 2008, The Endosomal Protein Appl1 Mediates Akt Substrate Specificity and Cell Survival in Vertebrate Development: Cell, v. 133, p. 486-497.

Schnatwinkel, C., S. Christoforidis, M. R. Lindsay, S. Uttenweiler-Joseph, M. Wilm, R. G. Parton, and M. Zerial, 2004, The Rab5 effector Rabankyrin-5 regulates and coordinates different endocytic mechanisms: PLoS biology, v. 2.

Schober, M., I. Rebay, and N. Perrimon, 2005, Function of the ETS transcription factor Yan in border cell migration: Development, v. 132, p. 3493-3504.

Schroeder, F., H. Huang, A. L. McIntosh, B. P. Atshaves, G. G. Martin, and A. B. Kier, 2010, Caveolin, sterol carrier protein-2, membrane cholesterol-rich microdomains and intracellular cholesterol trafficking: Sub-cellular biochemistry, v. 51, p. 279-318.

Segev, N., 2001, Ypt and Rab GTPases: insight into functions through novel interactions: Current Opinion in Cell Biology, v. 13, p. 500-511.

Seidel, H. M., L. H. Milocco, P. Lamb, J. E. Darnell, Jr., R. B. Stein, and J. Rosen, 1995, Spacing of palindromic half sites as a determinant of selective STAT (signal transducers and activators of transcription) DNA binding and transcriptional activity: Proceedings of the National Academy of Sciences of the United States of America, v. 92, p. 3041-3045.

Sekimoto, T., N. Imamoto, K. Nakajima, T. Hirano, and Y. Yoneda, 1997, Extracellular signal-dependent nuclear import of Stat1 is mediated by nuclear pore-targeting complex formation with NPI-1, but not Rch1: The EMBO Journal, v. 16, p. 7067-7077.

Semerdjieva, S., B. Shortt, E. Maxwell, S. Singh, P. Fonarev, J. Hansen, G. Schiavo, B. D. Grant, and E. Smythe, 2008, Coordinated regulation of AP2 uncoating from clathrin-coated vesicles by rab5 and hRME-6: J. Cell Biol., v. 183, p. 499-511.

Seubert N, Royer Y, Staerk J, Kubatzky KF, Moucadel V, Krishnakumar S, Smith SO, Constantinescu SN., 2003, Active and inactive orientations of the transmembrane and cytosolic domains of the erythropoietin receptor dimer. Mol Cell. v 12(5):1239-50.

Shankaranarayanan, P., P. Chaitidis, H. K√ºhn, and S. Nigam, 2001, Acetylation by histone acetyltransferase CREB-binding protein/p300 of STAT6 is required for transcriptional activation of the 15-lipoxygenase-1 gene: The Journal of Biological Chemistry, v. 276, p. 42753-42760.

Shi, S., K. Larson, D. Guo, S. J. Lim, P. Dutta, S.-J. Yan, and W. X. Li, 2008, Drosophila STAT is required for directly maintaining HP1 localization and heterochromatin stability: Nat Cell Biol, v. 10, p. 489-496.

Shin, H.-W., M. Hayashi, S. Christoforidis, S. Lacas-Gervais, S. Hoepfner, M. R. Wenk, J. Modregger, S. Uttenweiler-Joseph, M. Wilm, A. Nystuen, W. N. Frankel, M. Solimena, P. De Camilli, and M. Zerial, 2005, An enzymatic cascade of Rab5 effectors regulates phosphoinositide turnover in the endocytic pathway: The Journal of Cell Biology, v. 170, p. 607-618.

Shin, H. Y., and N. C. Reich, 2013, Dynamic trafficking of STAT5 depends on an unconventional nuclear localization signal: Journal of Cell Science, v. 126, p. 3333-3343.
Sigismund, S., E. Argenzio, D. Tosoni, E. Cavallaro, S. Polo, and P. P. Di Fiore, 2008, Clathrin-Mediated Internalization Is Essential for Sustained EGFR Signaling but Dispensable for Degradation: Developmental Cell, v. 15, p. 209-219.
Silver, D. L., R. G. Erika, and D. J. Montell, 2005a, Requirement for JAK/STAT signaling throughout border cell migration in Drosophila: Development, v. 132, p. 3483-3492.
Silver, D. L., E. R. Geisbrecht, and D. J. Montell, 2005b, Requirement for JAK/STAT signaling throughout border cell migration in Drosophila: Development, v. 132, p. 3483-3492.
Silver, D. L., and D. J. Montell, 2001, Paracrine Signaling through the JAK/STAT Pathway Activates Invasive Behavior of Ovarian Epithelial Cells in Drosophila: Cell, v. 107, p. 831-841.
Sivars, U., D. Aivazian, and S. R. Pfeffer, 2003, Yip3 catalyses the dissociation of endosomal Rab-GDI complexes: Nature, v. 425, p. 856-859.
Solinger, J. A., and A. Spang, 2013, Tethering complexes in the endocytic pathway: CORVET and HOPS: FEBS Journal, v. 280, p. 2743-2757.
Solis, G. P., A.-M. L√ºchtenborg, and V. L. Katanaev, 2013, Wnt secretion and gradient formation: International journal of molecular sciences, v. 14, p. 5130-5145.
Sorkin, A., and L. K. Goh, 2008, Endocytosis and intracellular trafficking of ErbBs: Experimental cell research, v. 314, p. 3093-3106.
Sorkin, A., and M. von Zastrow, 2009, Endocytosis and signalling: intertwining molecular networks: Nat Rev Mol Cell Biol, v. 10, p. 609-622.
Sotillos, S., and S. Campuzano, 2000, DRacGAP, a novel Drosophila gene, inhibits EGFR/Ras signalling in the developing imaginal wing disc: Development, v. 127, p. 5427-5438.
Sotillos, S., J. M. Espinosa-Vazquez, F. Foglia, N. Hu, and J. C.-G. Hombria, 2010, An efficient approach to isolate STAT regulated enhancers uncovers STAT92E fundamental role in Drosophila tracheal development: Developmental Biology, v. 340, p. 571-582.
Stang, E., F. y. D. Blystad, M. Kazazic, V. Bertelsen, T. Brodahl, C. Raiborg, H. Stenmark, and I. H. Madshus, 2004, Cbl-dependent Ubiquitination Is Required for Progression of EGF Receptors into Clathrin-coated Pits: Molecular Biology of the Cell, v. 15, p. 3591-3604.
Staerk J1, Defour JP, Pecquet C, Leroy E, Antoine-Poirel H, Brett I, Itaya M, Smith SO, Vainchenker W, Constantinescu SN., 2011, Orientation-specific signalling by thrombopoietin receptor dimers., EMBO J. v 2;30(21):4398-413.
Stark, G. R., and J. E. Darnell, Jr., 2012, The JAK-STAT pathway at twenty: Immunity, v. 36, p. 503-514.
Stec, W., O. Vidal, and M. P. Zeidler, 2013, Drosophila SOCS36E negatively regulates JAK/STAT pathway signaling via two separable mechanisms: Molecular Biology of the Cell, v. 24, p. 3000-3009.
Stec, W. J., and M. P. Zeidler, 2011, Drosophila SOCS Proteins: Journal of signal transduction, v. 2011.

Stenmark, H., 2009, Rab GTPases as coordinators of vesicle traffic: Nat Rev Mol Cell Biol, v. 10, p. 513-525.
Stenmark, H., G. Vitale, O. Ullrich, and M. Zerial, 1995, Rabaptin-5 is a direct effector of the small GTPase Rab5 in endocytic membrane fusion: Cell, v. 83, p. 423-432.
Stern, K. A., G. D. Visser Smit, T. L. Place, S. Winistorfer, R. C. Piper, and N. L. Lill, 2007, Epidermal Growth Factor Receptor Fate Is Controlled by Hrs Tyrosine Phosphorylation Sites That Regulate Hrs Degradation: Molecular and Cellular Biology, v. 27, p. 888-898.
Strutt, D., 2009, Gradients and the specification of planar polarity in the insect cuticle: Cold Spring Harbor perspectives in biology, v. 1.
Suh, H.-Y., D.-W. Lee, K.-H. Lee, B. Ku, S.-J. Choi, J.-S. Woo, Y.-G. Kim, and B.-H. Oh, 2010, Structural insights into the dual nucleotide exchange and GDI displacement activity of SidM/DrrA: The EMBO Journal, v. 29, p. 496-504.
Sunio, A., A. B. Metcalf, and H. Kr√§mer, 1999, Genetic Dissection of Endocytic Trafficking inDrosophila Using a Horseradish Peroxidase-Bride of Sevenless Chimera: hook Is Required for Normal Maturation of Multivesicular Endosomes: Molecular Biology of the Cell, v. 10, p. 847-859.
Swaminathan G1, Varghese B, Fuchs SY., 2008, Regulation of prolactin receptor levels and activity in breast cancer. J Mammary Gland Biol Neoplasia. v 13(1):81-91.
Tall, G. G., M. A. Barbieri, P. D. Stahl, and B. F. Horazdovsky, 2001, Ras-activated endocytosis is mediated by the Rab5 guanine nucleotide exchange activity of RIN1: Developmental Cell, v. 1, p. 73-82.
Tang, X., J.-S. Gao, Y.-j. Guan, K. E. McLane, Z.-L. Yuan, B. Ramratnam, and Y. E. Chin, 2007, Acetylation-Dependent Signal Transduction for Type I Interferon Receptor: Cell, v. 131, p. 93-105.
Teis, D., N. Taub, R. Kurzbauer, D. Hilber, M. E. d. Araujo, M. Erlacher, M. Offterdinger, A. Villunger, S. Geley, G. Bohn, C. Klein, M. W. Hess, and L. A. Huber, 2006, p14,ÄìMP1-MEK1 signaling regulates endosomal traffic and cellular proliferation during tissue homeostasis: The Journal of Cell Biology, v. 175, p. 861-868.
Terry, N. A., N. Tulina, E. Matunis, and S. DiNardo, 2006, Novel regulators revealed by profiling Drosophila testis stem cells within their niche: Developmental Biology, v. 294, p. 246-257.
Thomas, C., and D. Strutt, 2013, Rabaptin-5 and Rabex-5 are neoplastic tumour suppressor genes that interact to modulate Rab5 dynamics in Drosophila melanogaster: Developmental Biology.
Thoreau E, Petridou B, Kelly PA, Djiane J, Mornon JP., 1991, Structural symmetry of the extracellular domain of the cytokine/growth hormone/prolactin receptor family and interferon receptors revealed by hydrophobic cluster analysis. FEBS Lett. v 22;282(1):26-31.
Timmermann A1, Küster A, Kurth I, Heinrich PC, Müller-Newen G., 2002, A functional role of the membrane-proximal extracellular domains of the signal transducer gp130 in heterodimerization with the leukemia inhibitory factor receptor.
Eur J Biochem. v 269(11):2716-26.
Tonozuka, Y., Y. Minoshima, Y. C. Bao, Y. Moon, Y. Tsubono, T. Hatori, H. Nakajima, T. Nosaka, T. Kawashima, and T. Kitamura, 2004, A GTPase-activating

protein binds STAT3 and is required for IL-6,Äìinduced STAT3 activation and for differentiation of a leukemic cell line: Blood, v. 104, p. 3550-3557.
Topp, J. D., N. W. Gray, R. D. Gerard, and B. F. Horazdovsky, 2004, Alsin is a Rab5 and Rac1 guanine nucleotide exchange factor: The Journal of Biological Chemistry, v. 279, p. 24612-24623.
Toya, M., Y. Iida, and A. Sugimoto, Imaging of mitotic spindle dynamics in Caenorhabditis elegans embryos: Methods in cell biology, v. 97, p. 359-372.
Tuan, R. S., Lo, C. W. , 2000, Developmental Biology Protocols: Volume III: Humana Press.
Ullrich, O., S. Reinsch, S. Urb√©, M. Zerial, and R. G. Parton, 1996, Rab11 regulates recycling through the pericentriolar recycling endosome: The Journal of Cell Biology, v. 135, p. 913-924.
Ungureanu, D., S. Vanhatupa, J. Gr√∂nholm, J. J. Palvimo, and O. Silvennoinen, 2005, SUMO-1 conjugation selectively modulates STAT1-mediated gene responses: Blood, v. 106, p. 224-226.
Urbe, S., I. G. Mills, H. Stenmark, N. Kitamura, and M. J. Clague, 2000, Endosomal Localization and Receptor Dynamics Determine Tyrosine Phosphorylation of Hepatocyte Growth Factor-Regulated Tyrosine Kinase Substrate: Molecular and Cellular Biology, v. 20, p. 7685-7692.
Vaccari, T., T. E. Rusten, L. Menut, I. P. Nezis, A. Brech, H. Stenmark, and D. Bilder, 2009, Comparative analysis of ESCRT-I, ESCRT-II and ESCRT-III function in Drosophila by efficient isolation of ESCRT mutants: Journal of Cell Science, v. 122, p. 2413-2423.
van der Sluijs, P., M. Hull, P. Webster, P. M√¢le, B. Goud, and I. Mellman, 1992, The small GTP-binding protein rab4 controls an early sorting event on the endocytic pathway: Cell, v. 70, p. 729-740.
Van Nguyen, T., P. Angkasekwinai, H. Dou, F.-M. Lin, L.-S. Lu, J. Cheng, Y. E. Chin, C. Dong, and E. T. H. Yeh, 2011, SUMO-specific protease 1 is critical for early lymphoid development through regulation of STAT5 activation: Molecular Cell, v. 45, p. 210-221.
Varsano, T., M. Q. Dong, I. Niesman, H. Gacula, X. Lou, T. Ma, J. R. Testa, J. R. Yates, and M. G. Farquhar, 2006, GIPC Is Recruited by APPL to Peripheral TrkA Endosomes and Regulates TrkA Trafficking and Signaling: Molecular and Cellular Biology, v. 26, p. 8942-8952.
Vidal, O. M., W. Stec, N. Bausek, E. Smythe, and M. P. Zeidler, 2010, Negative regulation of Drosophila JAK-STAT signalling by endocytic trafficking: J Cell Sci, v. 123, p. 3457-3466.
Vieira, A. V., C. Lamaze, and S. L. Schmid, 1996, Control of EGF receptor signaling by clathrin-mediated endocytosis: Science, v. 274, p. 2086-2089.
Vijayakrishnan, N., S. E. Phillips, and K. Broadie, 2009, Drosophila Rolling Blackout Displays Lipase Domain-Dependent and -Independent Endocytic Functions Downstream of Dynamin: Traffic, v. 11, p. 1567-1578.
Vollmer P1, Oppmann B, Voltz N, Fischer M, Rose-John S., 1999, A role for the immunoglobulin-like domain of the human IL-6 receptor. Intracellular protein transport and shedding, Eur J Biochem. v 263(2):438-46.
von Zastrow, M., and A. Sorkin, 2007, Signaling on the endocytic pathway: Current Opinion in Cell Biology, v. 19, p. 436-445.

Wang, H., X. Chen, T. He, Y. Zhou, and H. Luo, 2013, Evidence for Tissue-Specific JAK/STAT Target Genes in Drosophila Optic Lobe Development: Genetics, v. 195, p. 1291-1306.
Wang, Q., G. Villeneuve, and Z. Wang, 2005a, Control of epidermal growth factor receptor endocytosis by receptor dimerization, rather than receptor kinase activation: EMBO Reports, v. 6, p. 942-948.
Wang, R., P. Cherukuri, and J. Luo, 2005b, Activation of Stat3 sequence-specific DNA binding and transcription by p300/CREB-binding protein-mediated acetylation: The Journal of Biological Chemistry, v. 280, p. 11528-11534.
Wang, X., J. C. Adam, and D. Montell, 2007, Spatially localized Kuzbanian required for specific activation of Notch during border cell migration: Developmental Biology, v. 301, p. 532-540.
Wang, Y., S. Pennock, X. Chen, and Z. Wang, 2002, Endosomal Signaling of Epidermal Growth Factor Receptor Stimulates Signal Transduction Pathways Leading to Cell Survival: Molecular and Cellular Biology, v. 22, p. 7279-7290.
Weber, C., T. B. Schreiber, and H. Daub, 2011, Dual phosphoproteomics and chemical proteomics analysis of erlotinib and gefitinib interference in acute myeloid leukemia cells: Journal of proteomics, v. 75, p. 1343-1356.
Wendler, F., A. K. Gillingham, R. Sinka, C. Rosa-Ferreira, D. E. Gordon, X. Franch-Marro, A. A. Peden, J.-P. Vincent, and S. Munro, 2010, A genome-wide RNA interference screen identifies two novel components of the metazoan secretory pathway: The EMBO Journal, v. 29, p. 304-314.
White, I. J., L. M. Bailey, M. R. Aghakhani, S. E. Moss, and C. E. Futter, 2006, EGF stimulates annexin 1-dependent inward vesiculation in a multivesicular endosome subpopulation: EMBO J, v. 25, p. 1-12.
Wieczorek, M., T. Ginter, P. Brand, T. Heinzel, and O. H. Kramer, 2012, Acetylation modulates the STAT signaling code: Cytokine & Growth Factor Reviews, v. 23, p. 293-305.
Wilkins, M. R., I. Lindskog, E. Gasteiger, A. Bairoch, J. C. Sanchez, D. F. Hochstrasser, and R. D. Appel, 1997, Detailed peptide characterization using PEPTIDEMASS--a World-Wide-Web-accessible tool: Electrophoresis, v. 18, p. 403-408.
Wollert, T., and J. H. Hurley, 2010, Molecular mechanism of multivesicular body biogenesis by ESCRT complexes: Nature, v. 464, p. 864-869.
Wölfler A, Irandoust M, Meenhuis A, Gits J, Roovers O, Touw IP., 2009, Site-specific ubiquitination determines lysosomal sorting and signal attenuation of the granulocyte colony-stimulating factor receptor. Traffic. v 10(8):1168-79.
Wright, V. M., K. L. Vogt, E. Smythe, and M. P. Zeidler, 2011, Differential activities of the Drosophila JAK/STAT pathway ligands Upd, Upd2 and Upd3: Cellular Signalling, v. 23, p. 920-927.
Wu, C., C. F. Lai, and W. C. Mobley, 2001, Nerve growth factor activates persistent Rap1 signaling in endosomes: The Journal of neuroscience: the official journal of the Society for Neuroscience, v. 21, p. 5406-5416.
Wu, P., P. Wee, J. Jiang, X. Chen, and Z. Wang, 2012, Differential regulation of transcription factors by location-specific EGF receptor signaling via a spatio-temporal interplay of ERK activation: PLoS ONE, v. 7.

Xu, D., and C.-K. Qu, 2008, Protein tyrosine phosphatases in the JAK/STAT pathway: Frontiers in bioscience: a journal and virtual library, v. 13, p. 4925-4932.

Xu, L., V. Lubkov, L. J. Taylor, and D. Bar-Sagi, 2010, Feedback Regulation of Ras Signaling by Rabex-5-Mediated Ubiquitination: Current Biology, v. 20, p. 1372-1377.

Yan, H., M. Jahanshahi, E. A. Horvath, H.-Y. Liu, and C. M. Pfleger, 2010, Rabex-5 Ubiquitin Ligase Activity Restricts Ras Signaling to Establish Pathway Homeostasis in Drosophila: Current Biology, v. 20, p. 1378-1382.

Yan, R., S. Small, C. Desplan, C. R. Dearolf, and J. E. Darnell, Jr., 1996, Identification of a Stat gene that functions in Drosophila development: Cell, v. 84, p. 421-430.

Yang, X.-J., and C.-M. Chiang, 2013, Sumoylation in gene regulation, human disease, and therapeutic action: F1000prime reports, v. 5.

Yu, A., J.-F. o. Rual, K. Tamai, Y. Harada, M. Vidal, X. He, and T. Kirchhausen, 2007, Association of Dishevelled with the Clathrin AP-2 Adaptor Is Required for Frizzled Endocytosis and Planar Cell Polarity Signaling: Developmental Cell, v. 12, p. 129-141.

Yuan, Z.-L., Y.-J. Guan, D. Chatterjee, and Y. E. Chin, 2005, Stat3 dimerization regulated by reversible acetylation of a single lysine residue: Science (New York, N.Y.), v. 307, p. 269-273.

Zavortink, M., N. Contreras, T. Addy, A. Bejsovec, and R. Saint, 2005, Tum/RacGAP50C provides a critical link between anaphase microtubules and the assembly of the contractile ring in Drosophila melanogaster: Journal of Cell Science, v. 118, p. 5381-5392.

Zeng, R., Y. Aoki, M. Yoshida, K.-i. Arai, and S. Watanabe, 2002, Stat5B shuttles between cytoplasm and nucleus in a cytokine-dependent and -independent manner: Journal of immunology (Baltimore, Md.: 1950), v. 168, p. 4567-4575.

Zerial, M., and H. McBride, 2001, Rab proteins as membrane organizers: Nat Rev Mol Cell Biol, v. 2, p. 107-117.

Zhang, J., C. Reiling, J. B. Reinecke, I. Prislan, L. A. Marky, P. L. Sorgen, N. Naslavsky, and S. Caplan, 2012, Rabankyrin-5 interacts with EHD1 and Vps26 to regulate endocytic trafficking and retromer function: Traffic (Copenhagen, Denmark), v. 13, p. 745-757.

Zheng, J., W.-H. Shen, T.-J. Lu, Y. Zhou, Q. Chen, Z. Wang, T. Xiang, Y.-C. Zhu, C. Zhang, S. Duan, and Z.-Q. Xiong, 2008, Clathrin-dependent Endocytosis Is Required for TrkB-dependent Akt-mediated Neuronal Protection and Dendritic Growth: Journal of Biological Chemistry, v. 283, p. 13280-13288.

Zhong, Z., Z. Wen, and J. E. Darnell, Jr., 1994, Stat3: a STAT family member activated by tyrosine phosphorylation in response to epidermal growth factor and interleukin-6: Science (New York, N.Y.), v. 264, p. 95-98.

Zhu, H., Z. Liang, and G. Li, 2009, Rabex-5 Is a Rab22 Effector and Mediates a Rab22-Rab5 Signaling Cascade in Endocytosis, v. 20, p. 4720-4729.

Zhu, H., G. Zhu, J. Liu, Z. Liang, X. C. Zhang, and G. Li, 2007, Rabaptin-5-independent Membrane Targeting and Rab5 Activation by Rabex-5 in the Cell: Mol. Biol. Cell, v. 18, p. 4119-4128.

Zhuang, S., 2013, Regulation of STAT signaling by acetylation: Cellular Signalling, v. 25, p. 1924-1931.

Zoncu, R., R. M. Perera, D. M. Balkin, M. Pirruccello, D. Toomre, and P. D. Camilli, 2009, A Phosphoinositide Switch Controls the Maturation and Signaling Properties of APPL Endosomes: Cell, v. 136, p. 1110-1121.